R/V Mirai MR23-06C Cruise Report (MR23-Fujiwara)

Arctic Challenge for Sustainability II (ArCS II)

Arctic Ocean, Bering Sea, and North Pacific
25 August – 4 October 2023

Japan Agency for Marine-Earth Science and Technology (JAMSTEC)

Contents

1. Cruise Summary

1.1. Cruise Information

I. Cruise ID: MR23-06C (MR23-Fujiwara)

II. Name of vessel: R/V Mirai

III. Title of project: Arctic Challenge for Sustainability II (ArCSII)

IV. Title of cruise: Observation cruise of ArCSII

V. Chief Scientist: Amane Fujiwara [Japan Agency for Marine-Earth Science and Technology]

VI. Cruise period: Aug 25 (Shimizu, Shizuoka, Japan) –Oct 4, 2023 (Dutch Harbor, AK, USA)

VII. Ports of departure: Shimizu/ call: Dutch Harbor / arrival: Dutch Harbor

VIII. Research area: North Pacific, Bering Sea, Arctic Ocean

IX. Research map

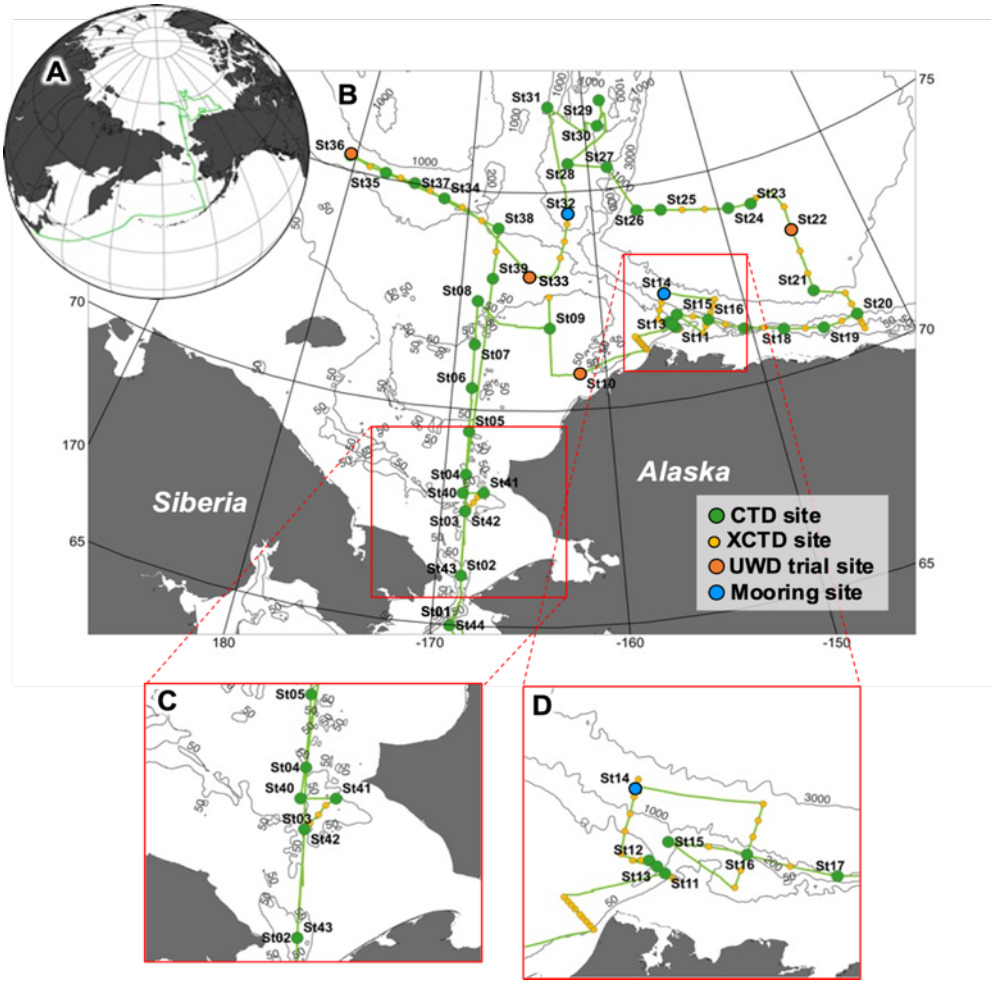

Figure 1-1. (A) Map of the entire cruise track, (B) close research area of the Chukchi Sea, the Beaufort Sea and the East Siberian Sea, and enlarged research area (C) around the Bering Strait

and (D) Point Barrow. Green dots indicate stations where we conducted observations using Conductivity-Temperature-Depth (CTD) sensors with water sampling bottles, plankton nets, sediment core sampling, and bio-optical instruments. Blue dots represent sediment trap mooring sites. Yellow dots reveal where we collected hydrographic data using eXpendable Conductivity-Temperature-Depth (XCTD) sensor. Orange dots are trial sites for the underwater drone.

1.2. Objectives

On the basis of our previous observations and theoretical considerations, we have come to realize that the Arctic Ocean plays an important role in global climate changes. The objectives of this cruise are as follows:

a. To quantify on-going changes in ocean, atmosphere, and ecosystem, which are related to the recent Arctic warming and sea ice reduction.
b. To clarify important processes and interactions among atmosphere, ocean, and ecosystem behind Arctic changes, and their effects on human society.
c. To collect data to provide accurate projections and environmental assessments for stakeholders so that they can make appropriate decisions on the sustainable development of the Arctic region.

1.3. Overview

We conducted meteorological and hydrographic surveys including marine biogeochemical samplings in the Pacific sector of the Arctic Ocean, the northern Bering Sea and the North Pacific Ocean on board the R/V Mirai from 28 August to 5 October 2023 under the framework of the Arctic Challenge for Sustainability II (ArCS II) Project (Figure 1-2). The research areas included the EEZ and the territorial sea of the USA. The observational activities consisted of CTD (Conductivity-Temperature-Depth)/LADCP (Lowered Acoustic Doppler Current Profiler)/water samplings, XCTD (eXpendable Conductivity-Temperature-Depth), ocean microstructure measurements, wave and surface drifting buoy deployments, bio-optical measurements, zooplankton net samplings, sediment samplings, incubation experiments, ship-board ocean current and surface water monitoring, meteorological measurements and samplings, aerosol observations, trials of an in-water drone, satellite observations, doppler radar, sea ice radar, sea bottom topography, gravity, and magnetic field measurements, and mooring and sediment trap recoveries and deployments (Figure 1-2).

In this cruise, we had 101 oceanographic stations (44 CTD and 57 XCTD stations) including 44 water sampling site, 37 zooplankton net sites, 10 sediment sampling sites, 18 sites for drifting buoy launches, 2 sites for recoveries and deployments of hydrographic and sediment trap moorings. We also had 48 sondes launch and 27 flight for flying drone for the meteorological and

atmospheric observations. Continuous meteorological and oceanographic observations/samplings were carried out on the cruise track. We conducted the trial of an in-water drone, which is designed for oceanographic observation including under the sea ice (see section 3.2). These missions were successfully completed thanks to great efforts made by the captain, ice pilot, officers, crews, and all the participants in this cruise (Photo 2-1). We would like to express our sincere appreciation to the United States Department of State and the Alaska Fisheries Science Center of the NOAA National Marine Fisheries Service of the Department of Commerce of the United States for allowing us to conduct observations in the areas under their jurisdictions. Based on the data obtained in this cruise, we will be able to shed light on the Arctic change and its controlling factors and will contribute to global climate change studies.

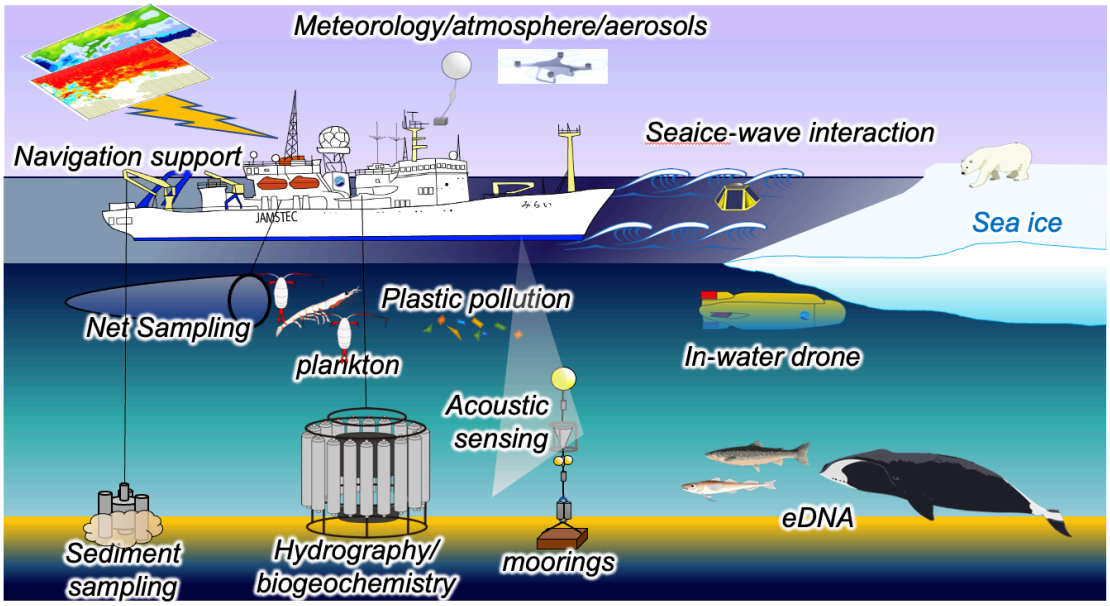

Figure 1-2: A schematic of the observational activities during MR23-06C (MR23-Fujiwara) cruise.

2. Research Proposal and Science Party

2.1 Title of proposal/Representative Personnel

1. Observational study of the Arctic environmental changes: Pacific-Arctic interaction, biogeochemical transport, mixing and marine ecosystem/Amane Fujiwara (JAMSTEC)
2. Research and development of under-ice observation technology/Hiroshi Yoshida (JAMSTEC)
3. Quantification of the microplastic inventory in the waters of the western Arctic Ocean and microplastic influx from the Pacific Ocean/Takahito Ikenoue (JAMSTEC)
4. Changes in clouds and aerosols over the ice-free Arctic Ocean/Kasutoshi Sato (National Institute of Polar Research, Japan)
5. Possibility of the expanding distribution in plankton and fishes associated with sea ice reduction in the Pacific sector of the Arctic Ocean/Kohei Matsuno (Hokkaido University)
6. Observation of air-sea-wave-ice interaction over the Pacific Arctic region/Tsubasa Kodaira (The University of Tokyo)
7. Investigating the physical and ecophysiological basis of fall phytoplankton blooms in the Chukchi and Beaufort seas/Colin Kremer (University of Connecticut)
8. Nitrogen Fixation in a Changing Arctic Ocean An Overlooked Source of Nitrogen/Lisa von Friesen (University of Copenhagen)
9. Exploring microplankton interactions and their functional roles in a changing Arctic/Eva Siliva Lopes (Interdisciplinary Centre of Marine and Environmental Research)
10. Determining the contribution of siphonophores to mesopelagic backscatter in the Arctic/Alix Rommel (University of St. Andrews)
11. Better understanding of climate-driven changes of biogeochemical dynamics in the western Arctic Ocean via R/V Mirai 2023 Cruise A perspective of stable carbon isotope/Zhangxian Ouyang (University of Delaware)
12. Temporal variations of the carbonate chemical components in the Arctic Ocean within summertime/Manami Tozawa (Hokkaido University)
13. Observation of water vapor isotopic ratios/Park Hotaek (JAMSTEC)
14. Observation of atmospheric greenhouse gases and related species in the North Pacific region/Yasunori Tohjima (National Institute for Environmental Studies)

2.2. Science Party

Table 2-1. List of onboard participants

Name	Affliation	Occupation
FUJIWARA Amane	JAMSTEC	Chief Scientist/ Research Scientist
HATTA Mariko	JAMSTEC	2nd chief Scientist/ Research Scientist
ONODERA Jonaotaro	JAMSTEC	3rd chief Scientist/ Senior Scientist
KIMURA Satoshi	JAMSTEC	Research Scientist
ZHANG Yuanxin	JAMSTEC	Postdoctoral Researcher
FUKAI Yuri	JAMSTEC	Postdoctoral Researcher
HOSODA Nanami	JAMSTEC/Hokkaido University	Research Assistant
KOSHI Yuri	JAMSTEC/The University of Tokyo	Research Assistant
YOSHIDA Hiroshi	JAMSTEC	Principal Scientist
TANAKA Kiyotaka	JAMSTEC	Project Senior Research Technician
SUGESAWA Makoto	JAMSTEC	Research Assistant
ZHAO Shiye	JAMSTEC	Research Scientist
SATO Kazutoshi	National Institute of Polar Reseach	Assistant Professor
INOUE Jun	National Institute of Polar Reseach	Assosiate Professor
TAKAHASHI Kazu	The Graduate University for Advanced Studies	Graduate Student
KODAIRA Tsubasa	The University of Tokyo	Lecturer
MATSUNO Kohei	Hokkaido University	Assistant Professor
KAWAKAMI Tatsuya	Hokkaido University	Postdoctoral Researcher
LOPES Eva Silva	Interdisciplinary Centre of Marine and Environmental Research	Graduate Student
DONG Bo	University of Delaware	Graduate Student
ROMMEL Alix Claire Maria	University of St Andrews	Graduate Student
VON FRIESEN Lisa Winberg	University of Copenhagen	Postdoctoral Researcher
HAGEN Stine Zander	University of Copenhagen	Graduate Student
LARSON Hannah	University of Connecticut	Graduate Student
SNIDER David Duke	Martech Polar	Ice Pilot
OYAMA Ryo	Nippon Marine Enterprises	Chief Technical Staff
YOSHIDA Kazuho	Nippon Marine Enterprises	Technical Staff
OGAWA Satomi	Nippon Marine Enterprises	Technical Staff
SUGIMOTO Yohei	Nippon Marine Enterprises	Technical Staff
FUJIKI Nagisa	Marine Works Japan	Chief Technical Staff
HASHIMUKAI Takayuki	Marine Works Japan	Technical Staff
ORUI Masahiro	Marine Works Japan	Technical Staff
USHIROMURA Hiroki	Marine Works Japan	Technical Staff
YODA Aine	Marine Works Japan	Technical Staff
FUJIOKA Riho	Marine Works Japan	Technical Staff
ODA Yuta	Marine Works Japan	Technical Staff
ARIGA Shiori	Marine Works Japan	Technical Staff
NAKAMURA Tomoki	Marine Works Japan	Technical Staff
NAKATOMI Nobuyuki	Marine Works Japan	Technical Staff
AMIKURA Shintaro	Marine Works Japan	Technical Staff

Table 2-2. List of crew member

Name	Rank/Ratings
INOUE Haruhiko	Master
CHIBA Masato	Chief Officer
EGASHIRA Takeshi	1st Officer
TSUJI Akihisa	Jr.1st Officer
KANAYAMA Keiji	2nd Officer
HIASA Yuri	3rd Officer
FUNAE Koji	Chief Engineer
TAKAHASHI Jun	1st Engineer
MIKAMI Ryuzo	2nd Engineer
TAKEYA Genta	3rd Engineer
INOUE Yoichi	Chief Radio Operator
KUDO Kazuyoshi	Boatswain
SATO Tsuyoshi	Quarter Master
ISHII Yukito	Quarter Master
KOMATA Shuji	Quarter Master
TAMOTSU Hideaki	Quarter Master
OKUBO Hideyuki	Quarter Master
SHIMPO Satoshi	Quarter Master
TANIKAWA Masaya	Quarter Master
UEHARA Shohei	Quarter Master
OISHI Yuki	Sailor
TERASAKI Iori	Sailor
TANIGUCHI Daisuke	No.1 Oiler
ANDO Kazuya	Oiler
WATANABE Takuya	Oiler
UCHIYAMA Tsuyoshi	Assistant Oiler
MARUYAMA Kyotaro	Assistant Oiler
FUJIURA Eima	Assistant Oiler
ONOUE Tatsunari	Chief Steward
ASANO Toshiyuki	Steward
SUGIYAMA Masaru	Steward
OKUMURA Kenichi	Steward
MURAKAMI Kanjuro	Steward
HANGAI Yuta	Steward

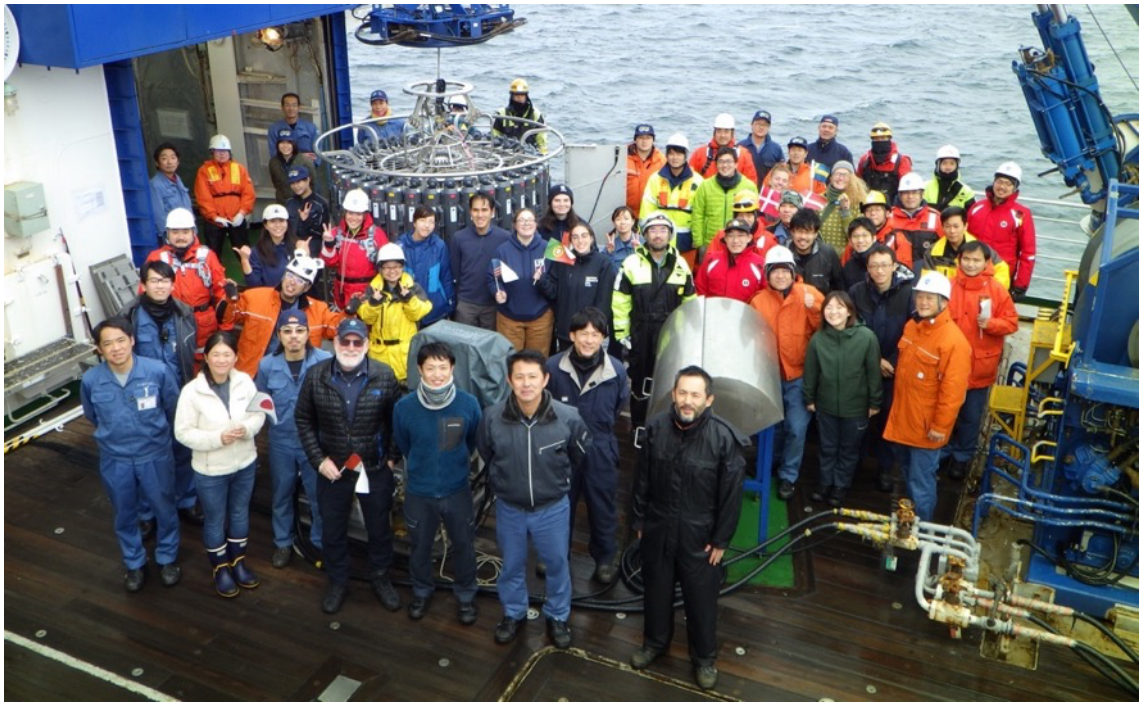

Photo 2-1. Group photo of the MR23-06C cruise.

3. Research/Development Activities

3.1. Observational study of the Arctic environmental changes: Pacific-Arctic interaction, biogeochemical transport, mixing and marine ecosystem

3.1.1. Meteorological Observations

3.1.1.I. Surface Meteorological Observations

(1) Responsible personnel

Amane Fujiwara	JAMSTEC -PI
Ryo Oyama	NME (Nippon Marine Enterprises, Ltd.)
Kazuho Yoshida	NME
Satomi Ogawa	NME
Yohei Sugimoto	NME
Yoichi Inoue	MIRAI Crew

(2) Purpose, background

Surface meteorological parameters are observed as a basic dataset of the meteorology. These parameters provide the temporal variation of the meteorological condition surrounding the ship.

(3) Activities

Observation period: 25 Aug. 2023- 04 Oct. 2023 (UTC)

(4) Methods, instruments

i) Instruments and methods

In this cruise, the two systems for the observation were used.

1) MIRAI Surface Meteorological (SMet) system

Instruments of SMet system are listed in Table 3.1.1.I-1. Data were collected and processed by KOAC-7800 weather data processor made by Koshin-Denki, Japan. The data set consists of 6 seconds averaged data.

Table 3.1.1.I-1: Instruments and installation locations of SMet system

Sensors	Type	Manufacturer	Location (altitude from surface)
Anemometer	KS-5900	Koshin Denki, Japan	Foremast (25 m)
Tair/RH	HMP155	Vaisala, Finland	Compass deck (21 m)
with aspirated radiation shield	43408 Gill	R.M. Young, U.S.A.	starboard and port side

Thermometer: SST	RFN2-0	Koshin Denki, Japan	4th deck (-1m, inlet -5m) Captain deck (13 m)
Barometer	Model-370	Setra System, U.S.A.	Weather observation room
Capacitive rain gauge	50202	R. M. Young, U.S.A.	Compass deck (19 m)
Optical rai gauge	ORG-815DS	Osi, USA	Compass deck (19 m)
Radiometer (short wave)	MS-802	Eko Seiki, Japan	Radar mast (28 m)
Radiometer (long wave)	MS-202	Eko Seiki, Japan	Radar mast (28 m)
Wave height meter	WM-2	Tsurumi-seiki, Japan	Bow (10 m) Stern (8m)

2) Shipboard Oceanographic and Atmospheric Radiation (SOAR) measurement system

SOAR system designed by BNL (Brookhaven National Laboratory, USA) consists of major five parts.

a. Analog meteorological data sampling with CR1000 logger manufactured by Campbell Scientific Inc. Canada – wind pressure, and rainfall (by a capacitive rain gauge) measurement.
b. Digital meteorological data sampling from individual sensors - air temperature, relative humidity and precipitation (by optical rain gauge (ORG)) measurement.
c. Radiation data sampling with CR1000X logger manufactured by Campbell Inc. and radiometers with ventilation unit manufactured by Hukseflux Thermal Sensors B.V. Netherlands – short and long wave downward radiation measurement.
d. Photosynthetically Available Radiation (PAR) sensor manufactured by Biospherical Instruments Inc. (USA) - PAR measurement.
e. Scientific Computer System (SCS) developed by NOAA (National Oceanic and Atmospheric Administration, USA) - centralized data acquisition and logging of all data sets.

SCS recorded radiation, air temperature, relative humidity, CR1000 and ORG data. SCS composed Event data (JamMet) from these data and ship's navigation data every 6 seconds. Instruments and their locations are listed in Table 3.1.1-I-2.

Table 3.1.1.I-2: Instruments and installation locations of SOAR system

Sensors (Meteorological)	Type	Manufacturer	Location (altitude from surface)

Anemometer	05106	R.M. Young, USA	Foremast (25 m)
Barometer with pressure port	PTB210 61002 Gill	VAISALA, Finland R.M. Young, USA	Foremast (23 m)
Rain gauge	50202	R.M. Young, USA	Foremast (24 m)
Tair/RH with aspirated radiation shield	HMP155 43408 Gill	VAISALA, Finland R.M. Young, USA	Foremast (23 m)
Optical rain gauge	ORG-815DR	Osi, USA	Foremast (24 m)

Sensors (Radiation)	Type	Manufacturer	Location *
Radiometer (short wave) with ventilation unit	SR20 VU01	Hukseflux Thermal Sensors B.V., Netherlands	Foremast (25 m)
Radiometer (long wave) with ventilation unit	IR20 VU01	Hukseflux Thermal Sensors B.V., Netherlands	Foremast (25 m)

Sensor (PAR&UV)	Type	Manufacturer	Location (altitude from surface)
PAR&UV sensor	PUV-510	Biospherical Instrum ents Inc., USA	Navigation deck (18m)

For the quality control as post processing, we checked the following sensors, before and after the cruise.

a. Young Rain gauge (SMet and SOAR)
   Inspect of the linearity of output value from the rain gauge sensor to change Input value by adding fixed quantity of test water.
b. Barometer (SMet and SOAR)
   Comparison with the portable barometer value, PTB220, VAISALA
c. Thermometer (air temperature and relative humidity) (SMet and SOAR)
   Comparison with the portable thermometer value, HM70, VAISALA

ii) Parameters

1) SMet system measured parameters are listed in Table 3.1.1-I-3.
2) SOAR system measured parameters are listed in Table 3.1.1-I -4.

Table3.1.1.I-3: Parameters of MIRAI SMet system

Parameter	Units	Remarks
1 Latitude	degree	
2 Longitude	degree	
3 Ship's speed	knot	MIRAI log
4 Ship's heading	degree	MIRAI gyro
5 Relative wind speed	m/s	6sec./10min. averaged
6 Relative wind direction	degree	6sec./10min. averaged
7 True wind speed	m/s	6sec./10min. averaged
8 True wind direction	degree	6sec./10min. averaged
9 Barometric pressure	hPa	adjusted to sea surface level 6sec. averaged
10 Air temperature (starboard)	degC	6sec. averaged
11 Air temperature (port)	degC	6sec. averaged
12 Dewpoint temperature (starboard)	degC	6sec. averaged
13 Dewpoint temperature (port)	degC	6sec. averaged
14 Relative humidity (starboard)	%	6sec. averaged
15 Relative humidity (port)	%	6sec. averaged
16 Sea surface temperature	degC	6sec. averaged
17 Precipitation intensity (optical rain gauge)	mm/hr	hourly accumulation
18 Precipitation (capacitive rain gauge)	mm/hr	hourly accumulation
19 Downwelling shortwave radiation	W/m^2	6sec. averaged
20 Downwelling infra-red radiation	W/m^2	6sec. averaged
21 Significant wave height (bow)	m	hourly
22 Significant wave height (stern)	m	hourly
23 Significant wave period (bow)	second	hourly
24 Significant wave period (stern)	second	hourly

Table 3.1.1.I-4: Parameters of SOAR system (JamMet)

Parameter	Units	Remarks
1 Latitude	degree	
2 Longitude	degree	
3 SOG	knot	
4 COG	degree	
5 Relative wind speed	m/s	

6 Relative wind direction	degree	
7 Barometric pressure	hPa	
8 Air temperature	degC	
9 Relative humidity	%	
10 Precipitation intensity (optical rain gauge)	mm/hr	
11 Precipitation (capacitive rain gauge)	mm/hr	reset at 50 mm
12 Down welling shortwave radiation	W/m^2	
13 Down welling infra-red radiation	W/m^2	
14 Defuse irradiance	W/m^2	
15 “SeaSnake” raw data	mV	
16 SSST (SeaSnake)	degC	
17 PAR	$microE/cm^2/sec$	
18 UV 305 nm	$microW/cm^2/nm$	
19 UV 320 nm	$microW/cm^2/nm$	
20 UV 340 nm	$microW/cm^2/nm$	
21 UV 380 nm	$microW/cm^2/nm$	

(5) Results, Future Plans, Lists

i) Result

Figure. 3.1.1.I-1. shows the time series of the following parameters;

Wind (SOAR)

Air temperature (SMet)

Relative humidity (SMet)

Precipitation (SOAR, ORG)

Short / Long wave radiation (SOAR)

Pressure (SMet)

Sea surface temperature (SMet)

Significant wave height (SMet)

ii) Data archives

These data obtained in this cruise will be submitted to the Data Management Group of JAMSTEC, and will be opened to the public via “Data Research System for Whole Cruise Information in JAMSTEC (DARWIN)” in JAMSTEC web site.

<http://www.godac.jamstec.go.jp/darwin/e>

iii) Remarks (Time in UTC)

a) The following periods, Sea surface temperature of SMet data were available.

07:06 25 Aug. 2023 - 00:00 03 Sep. 2023

17:00 05 Sep. 2023 - 23:30 02 Oct. 2023

b) The following periods, increasing of SMet capacitive rain gauge data were invalid due to MF/HF radio transmission.

04:55 25 Aug. 2023 - 05:04 25 Aug.

08:11 27 Aug. 2023 - 08:12 27 Aug.

01:19 02 Sep. 2023

00:43 25 Sep. 2023

01:12 25 Sep. 2023

17:33 29 Sep. 2023 - 17:34 29 Sep.

c) The following period, SMet wind speed/direction data were invalid due to system maintenance.

03:04 18 Sep. 2023 - 03:15 18 Sep. 2023

d) The following period, SMet wind speed/direction were measured by the vane anemometer on the foremast.

03:16 18 Sep. 2023 - 04 Oct. 2023 (End of Cruise)

e) The following periods, the wave data were invalid.

02:00 05 Sep. 2023 - 03:53 05 Sep. 2023

23:00 14 Sep. 2023 - 01:55 15 Sep. 2023

f) The following period, SOAR PAR data acquisition was suspended due to system trouble.

05:04 25 Aug. 2023 - 10:17 25 Aug.

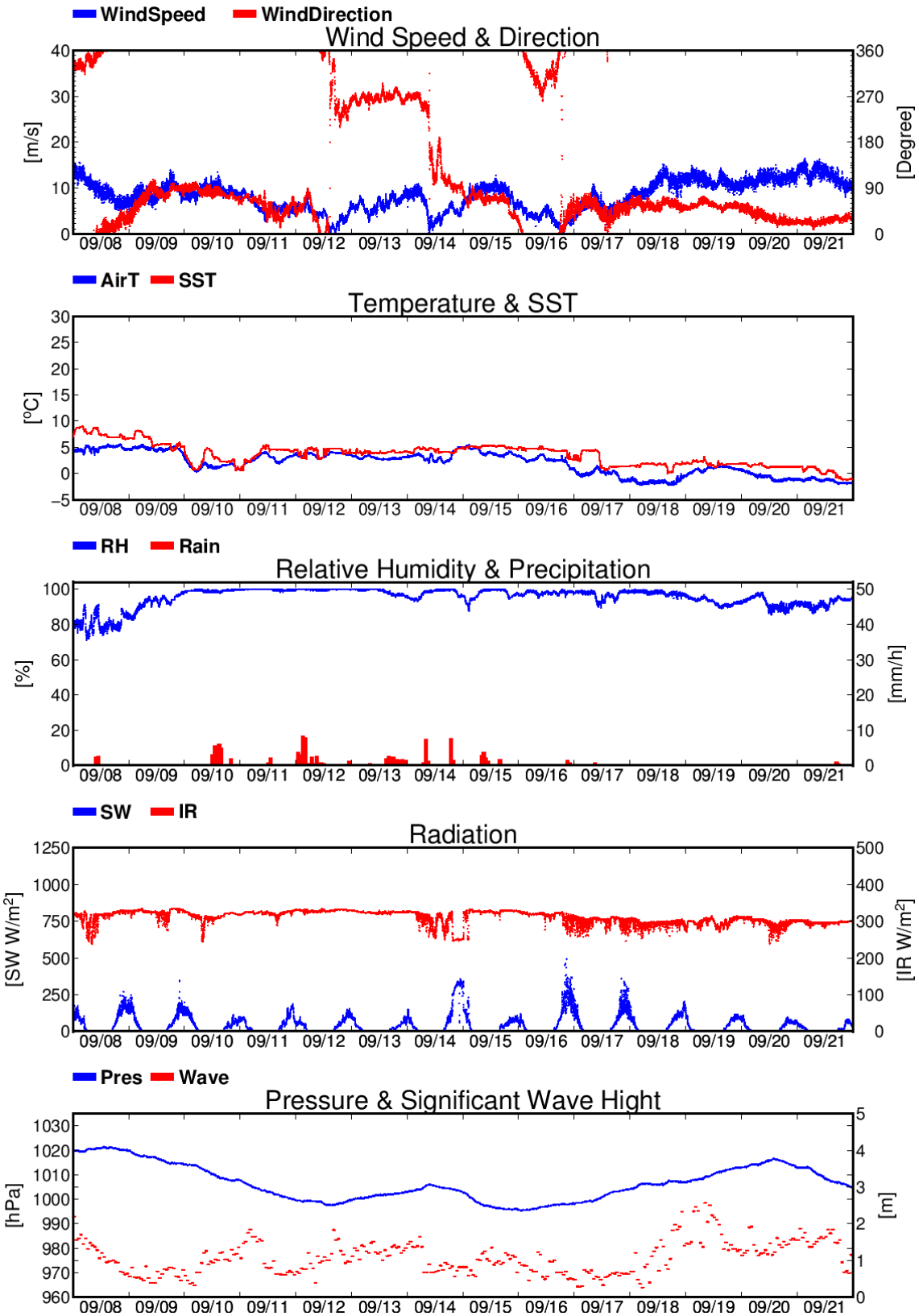

Figure 3.1.1.I-1: Time series of surface meteorological parameters during this cruise

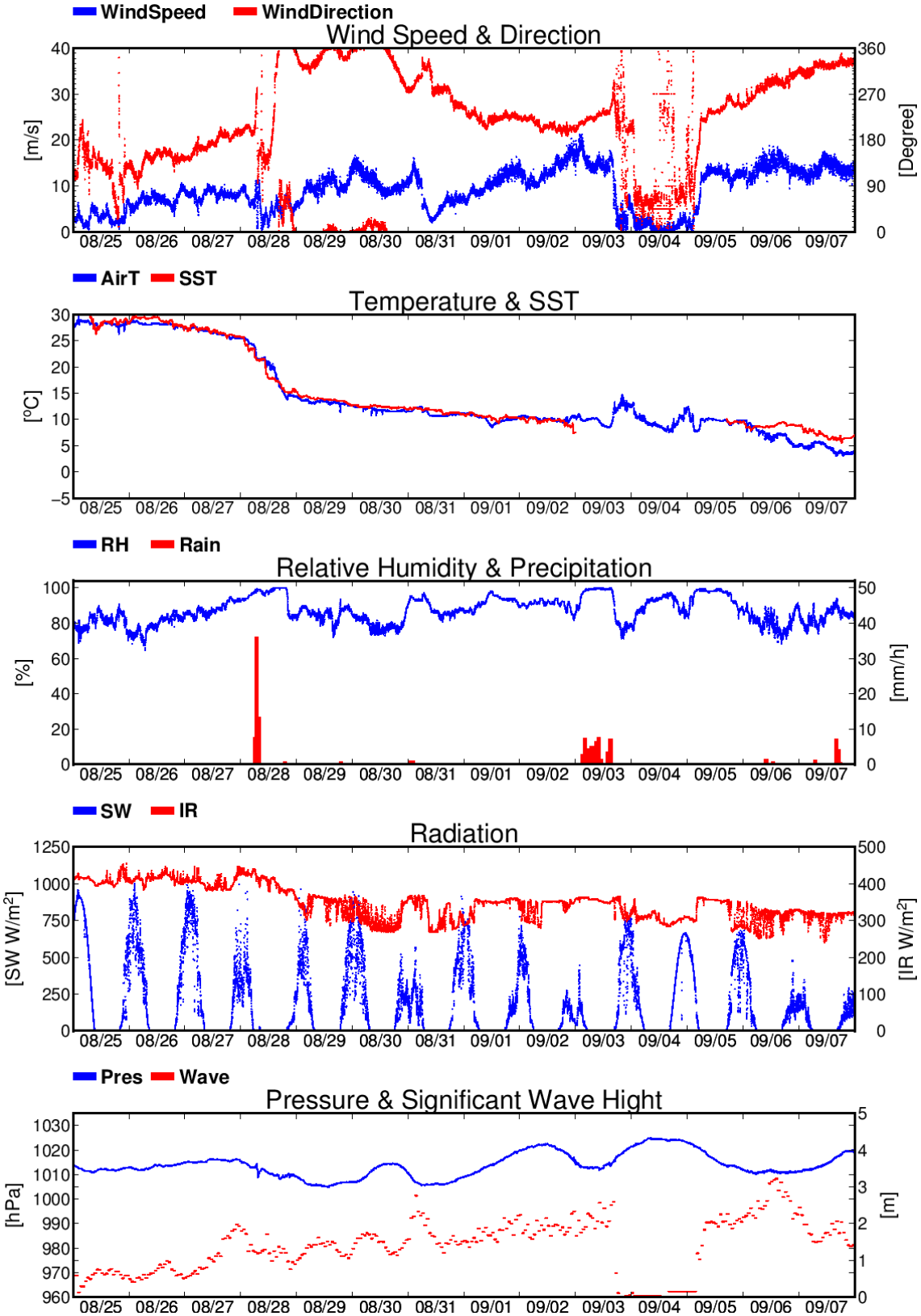

Figure 3.1.1.I-1: (Continued)

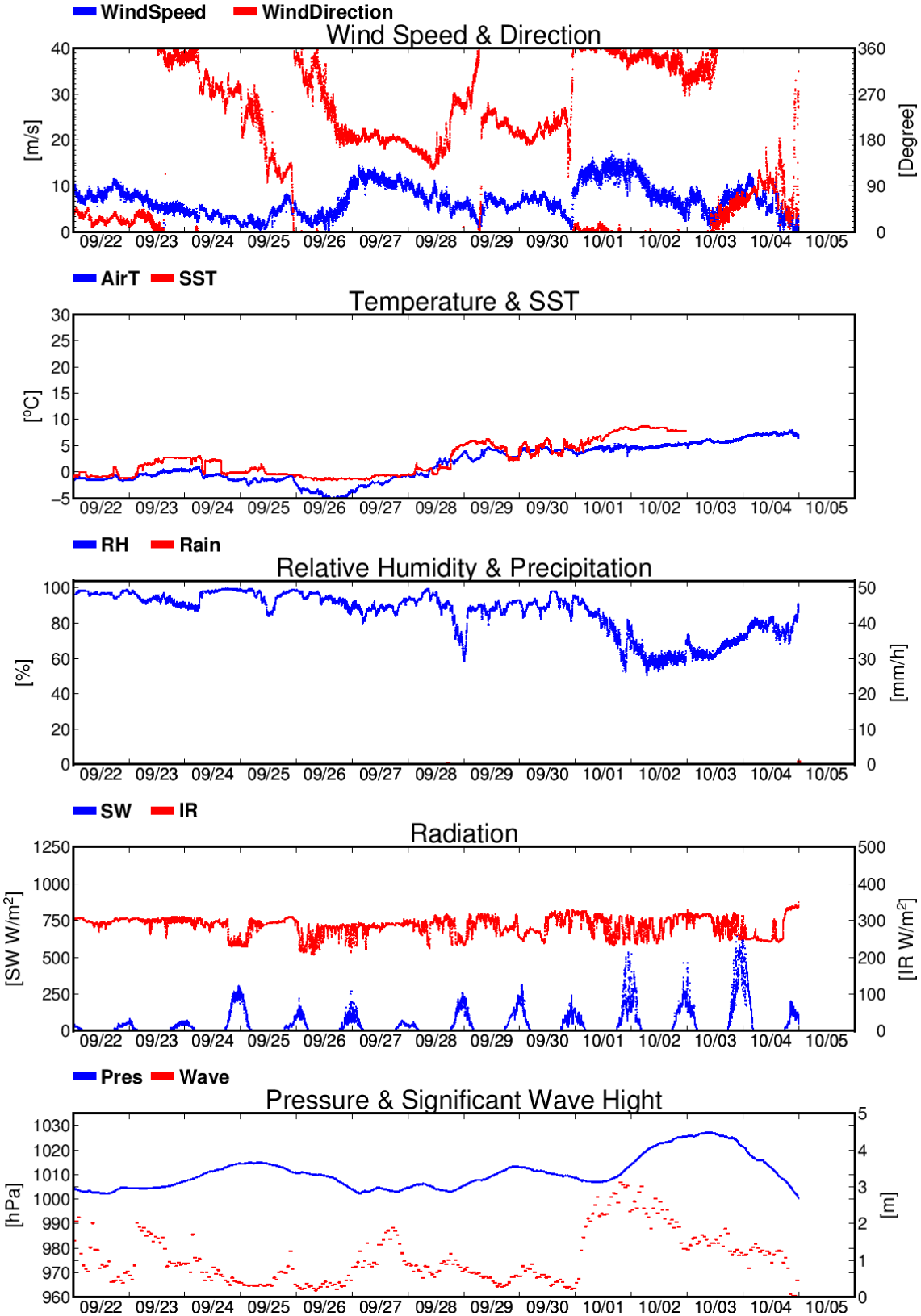

Figure 3.1.1.I-1: (Continued)

3.1.1.II. Ceilometer (CL51)

(1) Responsible personnel

Amane Fujiwara	JAMSTEC -PI
Ryo Oyama	NME (Nippon Marine Enterprises, Ltd.)
Kazuho Yoshida	NME
Satomi Ogawa	NME
Yohei Sugimoto	NME
Yoichi Inoue	MIRAI Crew

(2) Purpose, background

The information of cloud base height and the liquid water amount around cloud base is important to understand the process on formation of the cloud. As one of the methods to measure them, the ceilometer observation was carried out.

(3) Activities

Observation period: 25 Aug. 2023 - 04 Oct. 2023

(4) Methods, instruments

Cloud base height and backscatter profile were observed by ceilometer (CL51, VAISALA, Finland). The measurement configurations are shown in Table 3.1.1-II-1. On the archive dataset, cloud base height and backscatter profile are recorded with the resolution of 10 m.

Table 3.1.1.II-1: The measurement configurations

Property	Description
Laser source	Indium Gallium Arsenide (InGaAs) Diode
Transmitting center wavelength	910±10 nm at 25 degC
Transmitting average power	19.5 mW
Repetition rate	6.5 kHz
Detector	Silicon avalanche photodiode (APD)
Responsibility at 905 nm	65 A/W
Cloud detection range	0 ~ 13 km
Measurement range	0 ~ 15 km
Resolution	10 m in full range
Sampling rate	36 sec.
Sky Condition	Cloudiness in octas (0 ~ 9) 0 Sky Clear 1 Few 3 Scattered 5-7 Broken 8 Overcast 9 Vertical Visibility

(5) Results, Future Plans, Lists

i) Results

Figure 3.1.1.II-1 shows the time-series of the lowest, second and third cloud base height during the cruise.

ii) Data archives

These data obtained in this cruise will be submitted to the Data Management Group of JAMSTEC, and will be opened to the public via “Data Research System for Whole Cruise Information in JAMSTEC (DARWIN)” in JAMSTEC web site.

< http://www.godac.jamstec.go.jp/darwin/e >

iii) Remarks (Times in UTC)

Window cleaning

19:41 31 Aug. 2023

01:15 02 Sep. 2023

17:30 21 Sep. 2023

21:39 23 Sep. 2023

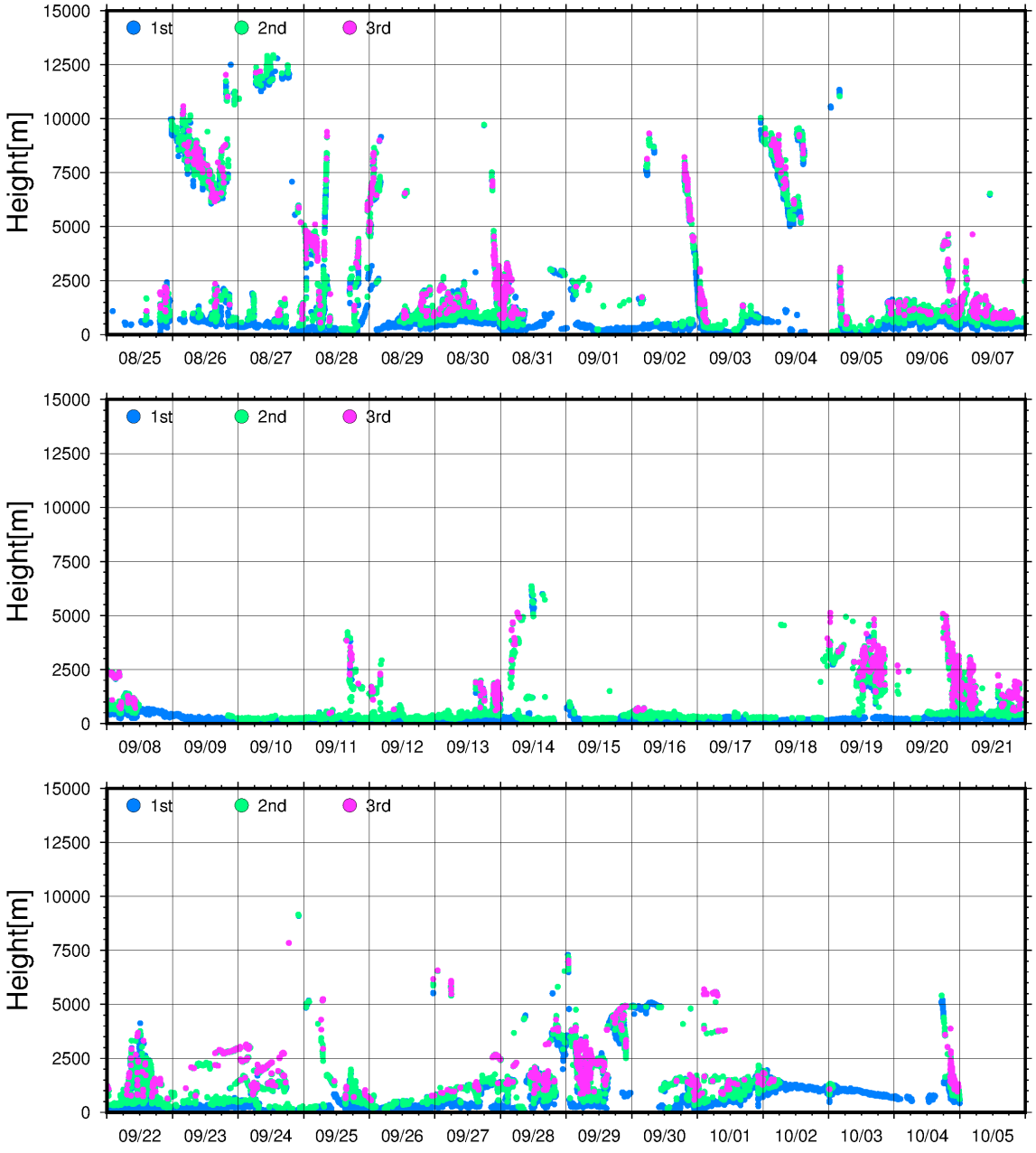

Figure 3.1.1.II-1: Time series of cloud base height during this cruise

3.1.2. Physical Oceanographic observations

3.1.2.I. CTD cast and water sampling

(1) Responsible personnel

Amane Fujiwara	(JAMSTEC)	(Principal Investigator)
Aine Yoda	(MWJ)	(Operation Leader)
Riho Fujioka	(MWJ)	
Takayuki Hashimukai	(MWJ)	
Hiroki Ushiromura	(MWJ)	
Satoshi Kimura	(JAMSTEC)	
Yuri Koshi	(JAMSTEC)	

(2) Purpose, background

The CTDO2/water sampling measurements were conducted to obtain vertical profiles of seawater properties by sensors and water sampling.

(3) Activities

During the MR23-06C cruise, 51 casts of CTD were carried out. Date, time and locations of the CTD casts are listed in Table 3.1.2.I-1.

Table 3.1.2.I-1 MR23-06C CTD cast table

MR23-06C CTD cast table

Stnnbr	Castno	Date(UTC)	Time(UTC)		BottomPosition		Depth	Wire	HT Above	Max	Max	CTD	Remark
		(mmddyy)	Start	End	Latitude	Longitude	(m)	Out (m)	Bottom (m)	Depth	Pressure	Filename	
001	001	090723	21:08	21:33	65-00.03N	169-04.83W	50.3	36.8	6.1	43.6	44.0	001M001	
002	001	090823	06:47	07:14	66-10.18N	168-39.99W	54.7	-	5.2	49.5	50.0	002M001	forget to record Wire Out
003	001	090823	16:54	17:15	67-39.57N	168-40.12W	49.9	40.2	5.5	43.6	44.0	003M001	
003	002	090823	18:30	18:56	67-39.89N	168-39.90W	49.7	40.8	5.4	43.6	44.0	003M002	
004	001	090923	00:34	01:00	68-30.09N	168-45.05W	53.3	43.6	5.2	47.5	48.0	004M001	
005	001	090923	06:36	07:02	69-30.00N	168-44.96W	51.3	-	5.3	45.5	46.0	005M001	SOJ trouble
006	001	090923	16:13	16:34	70-30.04N	168-45.28W	38.7	30.0	5.5	32.7	33.0	006M001	
007	001	090923	22:57	23:19	71-30.12N	168-45.29W	48.7	37.1	4.6	43.5	44.0	007M001	
008	001	091023	04:42	05:09	72-30.00N	168-45.02W	58.8	50.5	5.6	52.4	53.0	008M001	
009	001	091023	16:37	16:59	71-54.02N	163-38.51W	41.0	32.0	4.6	35.6	36.0	009M001	
010	001	091123	21:35	21:56	70-50.49N	161-42.97W	44.4	35.1	5.0	38.6	39.0	010M001	
011	001	091223	16:06	16:33	71-39.58N	155-01.27W	98.0	90.2	4.7	93.0	94.0	011M001	
012	001	091223	20:42	21:14	71-48.04N	155-23.10W	149.0	140.0	6.1	142.5	144.0	012M001	
013	001	091223	23:58	00:50	71-44.10N	155-11.92W	303.0	295.0	5.5	296.7	300.0	013M001	
014	001	091323	19:38	20:00	72-28.32N	155-24.43W	1987.0	96.8	-	99.9	101.0	014M001	
014	002	091323	21:07	23:02	72-28.06N	155-23.85W	1978.0	1966.9	9.8	1963.2	1993.0	014M002	
015	001	091423	16:16	17:12	71-56.35N	154-46.36W	476.0	460.0	9.4	461.7	467.0	015M001	
016	001	091423	22:10	22:47	71-41.41N	152-42.96W	208.0	201.0	5.0	202.8	205.0	016M001	
017	001	091523	03:33	04:27	71-18.68N	150-28.54W	382.0	359.8	9.8	360.0	364.0	017M001	
018	001	091523	16:39	17:03	71-03.91N	147-56.43W	80.0	68.5	4.6	72.2	73.0	018M001	
019	001	091523	22:11	22:46	70-48.99N	145-25.04W	186.0	176.6	5.6	179.1	181.0	019M001	
020	001	091623	04:10	04:33	70-50.94N	143-03.23W	1201.0	146.5	-	148.4	150.0	020M001	
020	002	091623	05:53	07:24	70-50.95N	143-03.18W	1201.0	1189.8	11.3	1187.3	1203.0	020M002	
021	001	091723	03:23	03:49	71-41.37N	145-12.08W	3338.0	96.1	-	99.0	100.0	021M001	
021	002	091723	04:56	07:29	71-41.39N	145-11.96W	3338.0	3326.0	8.0	3317.9	3379.0	021M002	
022	001	091723	22:44	01:20	73-09.97N	145-09.81W	3603.0	3591.7	9.1	3583.5	3652.0	022M001	
023	001	091823	22:29	23:26	74-00.82N	147-27.72W	3775.0	491.9	-	496.2	502.0	023M001	
024	001	091923	05:04	07:08	74-03.62N	149-14.89W	3814.0	3817.3	9.4	3801.2	3876.0	024M001	
025	001	091923	21:34	22:00	74-21.59N	154-30.02W	3854.0	145.0	-	148.4	150.0	025M001	
025	002	091923	23:12	01:59	74-21.62N	154-29.89W	3853.0	3842.2	10.0	3835.1	3911.0	025M002	
026	001	092023	04:58	06:58	74-26.10N	156-24.97W	3859.0	3841.6	10.4	3834.1	3910.0	026M001	
027	001	092023	21:12	22:36	75-29.99N	158-22.62W	1333.0	1317.0	10.9	1320.8	1339.0	027M001	
028	001	092123	05:17	06:35	75-38.64N	161-44.73W	893.0	867.5	13.5	869.0	880.0	028M001	
029	001	092123	19:48	19:56	77-02.17N	158-22.46W	1570.0	24.8	-	30.7	31.0	029M001	
029	002	092123	20:53	22:22	77-02.39N	158-22.15W	1544.0	1541.7	11.6	1538.9	1561.0	029M002	
030	001	092223	02:47	04:20	76-27.58N	158-49.30W	1400.0	1384.4	10.6	1379.7	1399.0	030M001	
031	001	092223	21:47	22:05	76-56.96N	163-21.83W	1839.0	96.5	-	98.9	100.0	031M001	
031	002	092223	23:19	01:18	76-57.02N	163-18.60W	1999.0	1987.5	11.0	1981.4	2012.0	031M002	
032	001	092323	21:13	21:27	74-30.51N	161-56.68W	1665.0	97.0	-	98.9	100.0	032M001	
032	002	092323	23:19	01:03	74-30.92N	162-01.71W	1643.0	1632.5	9.9	1628.4	1652.0	032M002	
034	001	092523	16:21	17:11	74-46.01N	172-03.79W	321.0	308.2	10.0	310.5	314.0	034M001	
035	001	092623	04:51	05:49	75-07.78N	177-13.70W	408.0	395.8	10.5	396.4	401.0	035M001	
036	001	092723	00:01	01:15	75-19.70N	179-29.15E	604.0	589.1	10.3	590.9	598.0	036M001	
037	001	092723	18:15	19:06	75-01.09N	174-40.52W	287.0	274.3	6.0	280.9	284.0	037M001	
038	001	092823	06:26	07:21	74-10.77N	167-30.61W	251.0	242.9	4.7	245.3	248.0	038M001	
039	001	092823	16:51	17:16	73-01.70N	167-45.48W	66.6	58.6	5.4	60.4	61.0	039M001	
040	001	092923	21:32	21:58	68-04.53N	168-52.03W	59.1	49.2	5.3	52.5	53.0	040M001	
041	001	093023	01:55	02:23	68-06.00N	167-39.99W	52.8	44.8	5.0	47.5	48.0	041M001	
042	001	093023	05:44	06:11	67-39.58N	168-40.07W	49.6	41.5	5.8	43.6	44.0	042M001	
043	001	093023	16:48	17:10	66-10.19N	168-39.83W	55.1	46.9	5.2	49.5	50.0	043M001	
044	001	093023	23:41	00:02	64-59.95N	169-04.74W	50.0	41.2	4.7	44.6	45.0	044M001	

(4) Methods, instruments

Winch and cable

Traction winch system (3.0 ton) (Dynacon, Inc., Bryan, Texas, USA)

Armored cable (φ = 9.53 mm) (Rochester Wire & Cable, LLC, Culpeper, Virginia, USA)

Compact underwater slip ring swivel (Hanayuu Co., Ltd., Shizuoka, Japan)

CTD: SBE911plus CTD system

Deck unit: SBE11plus (Sea-Bird Scientific, Washington, USA)

Serial no. 11P54451-0872

Frame and water sampler

460 kg stainless steel frame for 36-position 12-L water sample bottles with an aluminum rectangular fin (54 × 90 cm) to resist frame's rotation

36-position carousel water sampler, SBE 32 (Sea-Bird Scientific, Washington, USA)
Serial no. 3221746-0278

12-L sample bottle, model OTE 110 (OceanTest Equipment, Inc., Fort Lauderdale, Florida, USA) (No TEFLON coating)
12-L Niskin-X water sample bottle, model 1010X, General Oceanic, Inc., Miami, Florida, USA (No TEFLON coating)
Bottle number 1 to 36 were fitted with Viton O-rings

Underwater unit

Pressure sensor, SBE 9plus (Sea-Bird Scientific, Washington, USA)
Serial no. 09P54451-1027 (117457) (calibration date: Jun 09, 2022)

Temperature sensor
Deep standard reference thermometer, SBE 35, (Sea-Bird Scientific, Washington, USA)
Serial no. 53 (calibration date: Jun 26, 2023)
Primary, SBE SBE 3Plus (Sea-Bird Scientific, Washington, USA)
Serial no. 032730 (calibration date: Apr 11, 2023)
Secondary, SBE 3F (Sea-Bird Scientific, Washington, USA)
Serial no. 035737 (calibration date: Nov 05, 2022)

Conductivity sensor
Primary, SBE 4C (Sea-Bird Scientific, Washington, USA)
Serial no. 042435 (calibration date: Sep 02, 2022)
Secondary, SBE 4C (Sea-Bird Scientific, Washington, USA)
Serial no. 041206 (calibration date: Mar 21, 2023)

Dissolved oxygen sensor
Primary, RINKO III (JFE Advantech Co., Ltd., Hyogo, Japan)
Serial no. 0287, Sensing foil no. 163011(calibration date: May 11, 2023)
Secondary, SBE 43 (Sea-Bird Scientific, Washington, USA)
Serial no. 432211 (calibration date: Dec 20, 2022)

Chlorophyll Fluorometer (Seapoint Sensors Inc., New Hampshire, USA)
Serial no. 3618, Gain: 10X (0-15 ug/L)

Transmissometer, C-Star, (WET Labs, Inc., Philomath, Oregon, USA)
Serial no. 1363DR (calibration date: Sep 19, 2021)

PAR sensor, PAR-Log ICSW (Sea-Bird Scientific, Washington, USA)
Serial no. 2201 (calibration date: Dec 16, 2021)

Ultraviolet fluorometer (Seapoint Sensors Inc., New Hampshire, USA)
Serial no. 6246, Gain setting: 30X (0-50 QSU)

Nitrate sensor (Satlantic Inc.,)
Serial no. 1613 (calibration date: Aug 31, 2023)

Altimeter, PSA-916T (Teledyne Benthos, Inc.)
Serial no. 1100

Pump, SBE 5T (Sea-Bird Scientific, Washington, USA)
Primary serial no. 055816
Secondary serial no. 054598

Bottom contact switch (Sea-Bird Scientific, Washington, USA)

Software

Data acquisition software, SEASAVE-Win32, version 7.26.7.121
Data processing software, SBEDataProcessing-Win32, version 7.26.7.129 and some original modules

Data Collection

The CTD system was powered on at least 20 minutes in advance of the data acquisition to stabilize the pressure sensor. The data was acquired at least two minutes before and after the CTD cast to collect atmospheric pressure data on the ship's deck.

The CTD package was lowered into the water from the starboard side and held 10 m beneath the surface to activate the pump. After the pump was activated, the package was lifted to the

surface and lowered at a rate of 1.0 m/s to 200 m then the package was stopped to operate the heave compensator of the crane. The package was lowered again at a rate of 1.0 m/s to the bottom, except for the deeper casts, where it was lowered at 1.2 m/s after it passed the depths where vertical gradient of water properties was large. For the up cast, the package was lifted at a rate of 1.2 m/s except for bottle firing stops.

As a rule, the bottle was fired after waiting from the stop for more than 30 seconds and the package was stayed at least 5 seconds for measurement of the SBE 35 at each bottle firing stops. For depths where vertical gradient of water properties was expected to be large (from surface thermocline), the bottle was fired after waiting from the stop fir 60 seconds to changing the water between inside and outside of the bottle. If multiple bottles were to be fired at the same water sampling layer, it was waited more than 8 seconds before firing the next bottle to allow SBE35 to process data. At 200 m from the surface, the package was stopped to stop the heave compensator of the crane.

・Parameters

Pressure, Temperature, Salinity, Dissolved Oxygen, Beam Transmission, Fluorescence, Photosynthetically Active Radiation, Chromophoric Dissolved Organic Matter (CDOM), Altimeter Height (100 m range)

・Data Processing

The procedure in processing of the obtained CTD data is herein described. In these processes, a utility software, SBE Data Processing-Win32 (ver.7.26.7.129) and some original modules were used.

(The process in order)

DATCNV converted the binary raw data to engineering unit data. DATCNV also extracts bottle information where scans were marked with the bottle confirm bit during acquisition. The scan duration to be included in bottle file was set to 4.4 seconds, and the offset was set to 0.0 seconds. The hysteresis correction for the SBE 43 data (voltage) was applied for both profile and bottle information data.

TCORP (original module) corrected the pressure sensitivity of the temperature (SBE3) sensor. -2.11007877e-08 (degC/dbar) for S/N2730 (t090C)

RINKOCOR (original module) corrected the time dependent, pressure induced effect (hysteresis) of the RINKOIII profile data.

RINKOCORROS (original module) corrected the time dependent, pressure induced effect (hysteresis) of the RINKOIII bottle information data by using the hysteresis corrected profile data.

BOTTLESUM created a summary of the bottle data. The data were averaged over 4.4 seconds.

ALIGNCTD aligned parameter data in time, relative to pressure to ensure that all calculations were made using measurements from the same parcel of water.

For an SBE 9plus with TC-ducted temperature and conductivity sensors and a 3000-rpm pump, the typical lag of temperature to pressure is 0 second and lag of conductivity relative to temperature is 0.073 seconds. The Deck Unit was programmed to advance conductivity relative to pressure so conductivity alignment in ALIGNCTD was not needed. Dissolved oxygen data are systematically delayed with respect to pressure mainly because of the long time constant of the dissolved oxygen sensor and of an additional delay from the transit time of water in the pumped pluming line. This delay was compensated by 5 seconds advancing dissolved oxygen sensor (SBE43) output (dissolved oxygen voltage) relative to the temperature data. Delay of the RINKOIII data was also compensated by 1 second advancing sensor output (voltage) relative to the temperature data. Delay of the transmissometer data was also compensated by 2 seconds advancing sensor output (voltage) relative to the temperature data.

WILDEDIT marked extreme outliers in the data files. The first pass of WILDEDIT obtained the accurate estimate of the true standard deviation of the data. The data were read in blocks of 1000 scans. Data greater than 10 standard deviations were flagged. The second pass computed a standard deviation over the same 1000 scans excluding the flagged values. Values greater than 20 standard deviations were marked bad. This process was applied to pressure, depth, temperature (primary and secondary), conductivity (primary and secondary), and dissolved oxygen voltage (SBE43).

CELLTM used a recursive filter to remove conductivity cell thermal mass effects from the measured conductivity. Typical values for SBE 9plus with TC duct and 3000 rpm pump which were 0.03 for thermal anomaly amplitude alpha and 7.0 for the time constant 1/beta were used.

FILTER performed a low-pass filter on pressure and depth with a time constant of 0.15 second.

In order to produce zero phase lag (no time shift) the filter runs forward first then backward.

WFILTER performed as a median filter to remove spikes in transmissometer data, fluorometer data, nitrate data, and ultraviolet fluorometer data. A median value was determined by 49 scans of the window. The window length is specified as 73 scans for nitrate data.

SECTIONU (original module of SECTION) selected a time span of data based on scan number in order to reduce a file size. The minimum number was set to be the starting time when the CTD package was beneath the sea-surface after activation of the pump. The maximum number was set to be the end time when the depth of the package was 1 dbar below the surface. The minimum and maximum numbers were automatically calculated in the module.

LOOPEDIT marked scans where the CTD was moving less than the minimum velocity of 0.0 m/s (traveling backwards due to ship roll).

DESPIKE (original module) removed spikes of the data. A median and mean absolute deviation was calculated in 1-dbar pressure bins for both down and up cast, excluding the flagged values. Values greater than 4 mean absolute deviations from the median were marked bad for each bin. This process was performed twice for temperature, conductivity and RINKOIII output.

DERIVE was used to compute dissolved oxygen (SBE43), salinity, potential temperature, and sigma-theta.

BINAVG averaged the data into 1 decibar pressure bins and1 sec time bins.

BOTTOMCUT (original module) deleted the deepest pressure bin when the averaged scan number of the deepest bin was smaller than the average scan number of the bin just above.

SPLIT was used to split data into down cast and up cast.

(5) Results, Future Plans, Lists

During this cruise, we judged presence or absence of noise, spike or shift in the obtained hydro-cast data. At station 031cast 2, CTD water sampler stopped at 250 dbar, and went down to 400db. After that we sampled at 400 dbar as usual. Bottle flags of sample bottles that were took from Bottom to 250db were flagged 7.

Definitions of these problems

(1) noise; Beam Transmission: station 014 cast 1, down cast 205dbar – 617dbar

(2) spike; Salinity: station 003 cast 1, down cast 23dbar

station 003 cast 2, down cast 26dbar

station 040 cast 1, down cast 5dbar

station 042 cast 1, down cast 24dbar

Dissolved Oxygen: station 016 cast 1, down cast 127dbar

Beam Transmission: station 026 cast 1, down cast 20dbar – 21dbar

Fluorescence: station 003 cast 2, down cast 23dbar

(3) shift; continuous data under trend to collect values deviated from accurate ones.

・Problems Encountered

At station 006 cast 1, station 012 cast 1, station 014 cast 2, station 016 cast 1, station 019cast 1, there was leak of the water sample bottle because the bottom cap of the bottle did not close correctly for the bottle model OTE 110 (Ocean Test Equipment, Inc.).

・Data archive

These data obtained in this cruise will be submitted to the Data Management Group of JAMSTEC, and will be opened to the public via “Data Research System for Whole Cruise Information in JAMSTEC (DARWIN)” in JAMSTEC web site.

3.1.2.II. XCTD

(1) Responsible personnel

Fujiwara Amane	JAMSTEC -PI
Ryo Oyama	NME (Nippon Marine Enterprises, Ltd.)
Kazuho Yoshida	NME
Satomi Ogawa	NME
Yohei Sugimoto	NME
Yoichi Inoue	MIRAI Crew

(2) Purpose, background

To obtain vertical profiles of sea water conductivity, temperature and salinity.

(3) Activities

Observation period : 11 Sep. 2023 – 30 Sep. 2023 (UTC)

(4) Methods, instruments

i) Instruments & methods

We observed vertical profiles of sea water temperature and salinity measured by XCTD-1N probes manufactured by Tsurumi-Seiki Co. (TSK). The electric signal from the probe was converted by MK-150N (TSK), and was recorded by AL-12B software (Ver.1.6.4, TSK).

ii) Parameters

The ranges and accuracies of parameters measured by the XCTD (eXpendable Conductivity, Temperature & Depth profiler) are as follows; Parameter Range Accuracy Conductivity 0 ~ 60 [mS/cm] +/- 0.03 [mS/cm] Temperature -2 ~ 35 [deg-C] +/- 0.02 [deg-C] Depth 0 ~ 1000 [m] 5 [m] or 2 [%] (either of them is major)

(5) Results, Future Plans, Lists

i) Lists

We launched 57 probes by using the automatic launcher. The all XCTD observation log is shown in Table 3.1.2.II-1.

Table 3.1.2.II-1: XCTD observation log

No.	Station ID	File Name	Date [YYYY/MM/DD]	Time [hh:mm]	Latitude [deg]	Longitude [deg]	Depth [m]
1	WaveBuoy1	202309110013	2023/09/11	00:14	72-36.7486N	163-38.6729W	53

2	DBO-5_01	202309120733	2023/09/12	07:35	71-14.8181N	157-10.0208W	47
3	DBO-5_02	202309120752	2023/09/12	07:54	71-17.2786N	157-14.7590W	56
4	DBO-5_03	202309120809	2023/09/12	08:11	71-19.7748N	157-19.8513W	89
5	DBO-5_04	202309120827	2023/09/12	08:29	71-22.3027N	157-24.9675W	109
6	DBO-5_05	202309120841	2023/09/12	08:41	71-24.1109N	157-28.6237W	124
7	DBO-5_06	202309120902	2023/09/12	09:04	71-27.2895N	157-34.9661W	112
8	DBO-5_07	202309120920	2023/09/12	09:21	71-29.8075N	157-40.1267W	85
9	DBO-5_08	202309120936	2023/09/12	09:38	71-32.2136N	157-45.2027W	72
10	DBO-5_09	202309120953	2023/09/12	09:54	71-34.6757N	157-50.3529W	65
11	X011	202309121849	2023/09/12	18:51	71-35.5356N	154-48.9935W	39
12	X012	202309121915	2023/09/12	19:17	71-37.8551N	154-54.8999W	56
13	X013	202309121947	2023/09/12	19:48	71-42.1104N	155-05.9483W	179
14	X014	202309122016	2023/09/12	20:17	71-45.9474N	155-17.0449W	205
15	X015	202309122201	2023/09/12	22:03	71-48.9694N	155-36.0909W	118
16	X016	202309122226	2023/09/12	22:27	71-49.5001N	155-50.1275W	89
17	NBC_01	202309130336	2023/09/13	03:38	71-53.9958N	156-07.2075W	75
18	NBC_02	202309130442	2023/09/13	04:44	72-05.9908N	155-54.8589W	210
19	NBC_03	202309130533	2023/09/13	05:34	72-14.9945N	155-41.3083W	720
20	NBC_04	202309130627	2023/09/13	06:28	72-23.9999N	155-29.4761W	1470
21	NBC_05	202309130723	2023/09/13	07:25	72-32.9939N	155-17.3536W	2330
22	X022	202309140545	2023/09/14	05:46	72-06.7499N	151-57.7529W	2613
23	X023	202309140644	2023/09/14	06:45	71-58.4000N	152-12.3386W	2076
24	X024	202309140733	2023/09/14	07:35	71-50.2227N	152-27.2014W	1221
25	X025	202309140915	2023/09/14	09:17	71-33.5576N	152-59.0044W	58
26	X026	202309141006	2023/09/14	10:08	71-24.9153N	153-14.3374W	59
27	X027	202309141948	2023/09/14	19:49	71-49.7871N	153-42.2393W	175
28	X028	202309150117	2023/09/15	01:17	71-29.9532N	151-38.8188W	985
29	X029	202309150703	2023/09/15	07:05	71-12.9006N	149-12.5909W	269
30	X030	202309151951	2023/09/15	19:53	70-55.8596N	146-35.5318W	291
31	X031	202309160125	2023/09/16	01:26	70-49.1451N	144-10.3326W	539
32	X032	202309160816	2023/09/16	08:17	70-42.6028N	143-01.5022W	539
33	X033	202309160851	2023/09/16	08:52	70-35.8912N	142-59.1645W	263
34	X034	202309160930	2023/09/16	09:32	70-28.6197N	142-57.0228W	59
35	X035	202309162149	2023/09/16	21:50	71-06.0347N	143-08.6763W	2271
36	X036	202309162345	2023/09/16	23:45	71-23.1967N	143-15.6439W	2981

37	X037	202309170942	2023/09/17	09:43	72-06.2816N	145-09.6103W	3352
38	X038	202309171232	2023/09/17	12:34	72-38.4595N	145-07.8095W	3473
39	X039	202309180447	2023/09/18	04:48	72-42.6759N	145-04.8255W	3699
40	X040	202309182003	2023/09/18	20:03	74-06.2133N	146-55.0620W	3767
41	X041	202309182123	2023/09/18	21:27	74-03.7403N	147-11.0261W	3772
42	X042	202309190949	2023/09/19	09:50	74-10.1943N	151-04.1750W	3839
43	X043	202309191215	2023/09/19	12:16	74-16.0817N	152-49.2142W	3852
44	X044	202309231440	2023/09/23	14:41	74-32.2548N	161-56.9085W	1690
45	X045	202309240338	2023/09/24	03:40	74-16.2041N	162-04.1503W	1312
46	X046	202309240539	2023/09/24	05:41	73-52.8627N	162-20.4001W	276
47	X047	202309240735	2023/09/24	07:37	73-30.3023N	162-43.0024W	154
48	X048	202309241859	2023/09/24	19:00	73-05.1713N	164-51.3580W	68
49	X049	202309250845	2023/09/25	08:46	74-20.3966N	168-52.6106W	180
50	X050	202309251118	2023/09/25	11:19	74-36.5911N	170-31.7025W	214
51	X051	202309260816	2023/09/26	08:17	75-11.3935N	178-40.7880W	571
52	X052	202309270904	2023/09/27	09:05	75-04.8076N	175-55.8290W	272
53	X053	202309272107	2023/09/27	21:08	74-53.9131N	173-18.7764W	320
54	X054	202309281032	2023/09/28	10:34	73-39.0081N	167-36.7514W	147
55	X055	202309300319	2023/09/30	03:20	68-00.0487N	167-59.9905W	54
56	X056	202309300408	2023/09/30	04:10	67-52.0538N	168-13.5088W	58
57	X057	202309300457	2023/09/30	04:59	67-45.0028N	168-29.9974W	50

ii) Data archives

These data obtained in this cruise will be submitted to the Data Management Group of JAMSTEC, and will be opened to the public via “Data Research System for Whole Cruise Information in JAMSTEC (DARWIN)” in JAMSTEC web site.

<http://www.godac.jamstec.go.jp/darwin/e>

3.1.2.III. Shipboard ADCP

(1) Responsible personnel

Fujiwara Amane	JAMSTEC -PI
Ryo Oyama	NME (Nippon Marine Enterprises, Ltd.)
Kazuho Yoshida	NME
Satomi Ogawa	NME
Yohei Sugimoto	NME
Yoichi Inoue	MIRAI Crew

(2) Purpose, background

To obtain continuous measurement data of the current profile along the ship's track.

(3) Activities

Observation periods : 25 Aug. 2023 – 3 Sep. 2023, 5 Sep. 2023 – 1st. Oct. 2023 (UTC)

(4) Methods, instruments

Upper ocean current measurements were made during this cruise, using the hull-mounted Acoustic Doppler Current Profiler (ADCP) system. For most of its operation, the instrument was configured for water-tracking mode. Bottom-tracking mode, interleaved bottom-ping with water-ping, was made to get the calibration data for evaluating transducer misalignment angle in the shallow water. The system consists of following components;

1. R/V MIRAI has installed the Ocean Surveyor for vessel-mount ADCP (frequency 76.8 kHz; Teledyne RD Instruments, USA). It has a phased-array transducer with single ceramic assembly and creates 4 acoustic beams electronically. We mounted the transducer head rotated to a ship-relative angle of 45 degrees azimuth from the keel.
2. For heading source, we use ship's gyro compass (Tokyo Keiki, Japan), continuously providing heading to the ADCP system directory. Additionally, we have Inertial Navigation Unit (Phins, Ixblue, France) which provide high-precision heading, attitude information, pitch and roll. They are stored in ".N2R" data files with a time stamp.
3. Differential GNSS system (StarPack-D, Fugro, Netherlands) providing precise ship's position.
4. We used VmDas software version 1.50.19(TRDI) for data acquisition.

5. To synchronize time stamp of ping with Computer time, the clock of the logging computer is adjusted to GPS time server by using NTP (Network Time Protocol).
6. Fresh water is charged in the sea chest to prevent bio fouling at transducer face.
7. The sound speed at the transducer does affect the vertical bin mapping and vertical velocity measurement, and that is calculated from temperature, salinity (constant value; 35.0 PSU) and depth (6.5 m; transducer depth) by equation in Medwin (1975).

Data were configured for “8 m” layer intervals starting about 23m below sea surface. Data were recorded every ping as raw ensemble data (.ENR). Additionally, 15 seconds averaged data were recorded as short-term average (.STA). 300 seconds averaged data were long-term average (.LTA), respectively.

Major acquisition parameters for the measurement, Direct Command, are shown in Table 3.1.2.III-1.

Table 3.1.2.III-1: Major parameters

Bottom-Track Commands	
BP = 001	Pings per Ensemble (almost less than 1,300m depth)
Environmental Sensor Commands	
EA = 04500	Heading Alignment (1/100 deg)
ED = 00065	Transducer Depth (0 - 65535 dm)
EF = +001	Pitch/Roll Divisor/Multiplier (pos/neg) [1/99 - 99]
EH = 00000	Heading (1/100 deg)
ES = 35	Salinity (0-40 pp thousand)
EX = 00000	Coordinate Transform (Xform:Type; Tilts; 3Bm; Map)
EZ = 10200010	Sensor Source (C; D; H; P; R; S; T; U)
C (1): Sound velocity calculates using ED, ES, ET (temp.)	
D (0): Manual ED	
H (2): External synchro	
P (0), R (0): Manual EP, ER (0 degree)	
S (0): Manual ES	
T (1): Internal transducer sensor	
U (0): Manual EU	
EV = 0	Heading Bias (1/100 deg)
Timing Commands	
TE = 00:00:02.00	Time per Ensemble (hrs:min:sec.sec/100)
TP = 00:02.00	Time per Ping (min:sec.sec/100)

Water-Track Commands

WA = 255	False Target Threshold (Max) (0-255 count)
WC = 120	Low Correlation Threshold (0-255)
WD = 111 100 000	Data Out (V; C; A; PG; St; Vsum; Vsum^2; #G; P0)
WE = 1000	Error Velocity Threshold (0-5000 mm/s)
WF = 0800	Blank After Transmit (cm)
WN = 100	Number of depth cells (1-128)
WP = 00001	Pings per Ensemble (0-16384)
WS = 800	Depth Cell Size (cm)
WV = 0390	Radial Ambiguity Velocity (cm/s)

(5) Results, Future Plans, Lists

i) Results

Figures 3.1.2.III-1. show the current velocity at 18th to 21st. September.

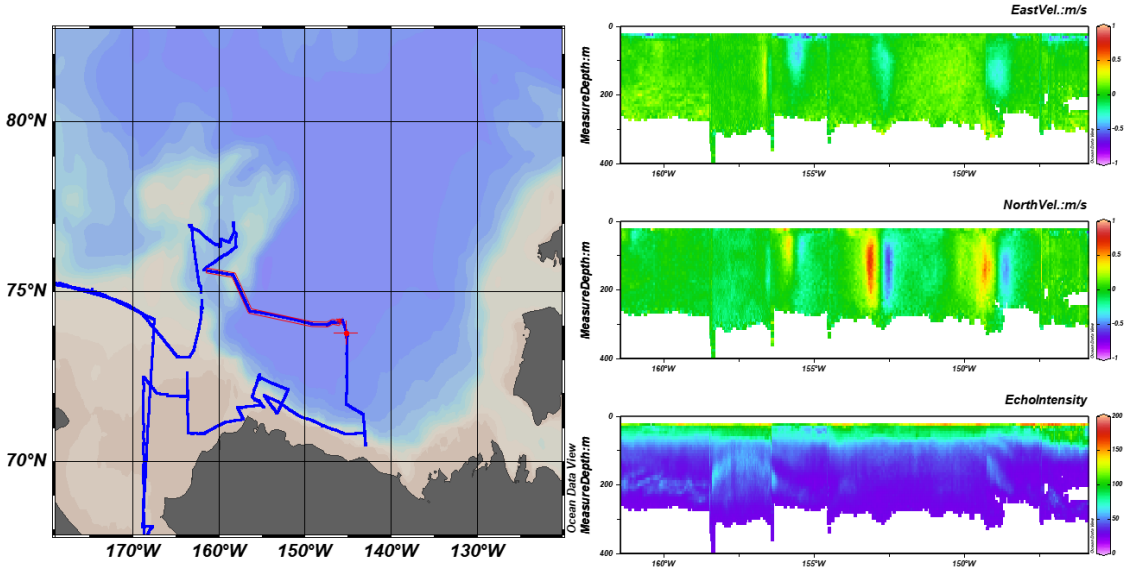

Figure 3.1.2.III-1. The current velocity at 18th to 21st. September.

ii) Data archives

These data obtained in this cruise will be submitted to the Data Management Group of JAMSTEC, and will be opened to the public via “Data Research System for Whole Cruise Information in JAMSTEC (DARWIN)” in JAMSTEC web site.

< http://www.godac.jamstec.go.jp/darwin/e >

3.1.2.IV. Moorings

(1) Responsible personnel

Jonaotaro Onodera JAMSTEC - Principal Investigator
Motoyo Itoh* JAMSTEC
Yuichiro Tanaka* AIST
Atsushi Suzuki* AIST
Katsunori Kimoto* JAMSTEC
Eiji Watanabe* JAMSTEC
Takuhei Shiozaki* Tokyo Univ. AORI
Hiroki Ushiromura as the leader of technical team for mooring operation of MWJ
Ryo Oyama as the leader for SSBL acoustic survey team of NME
(Yoshida, K., Ogawa, S., and Sugimoto, Y.).
*: onshore members

(2) Purpose, background

- To understand lateral transportation of shelf-origin matter to basin with physical oceanographic condition from northern off Barrow Canyon to the Chukchi Borderland.
- To monitor hydrographic condition regarding to ocean acidification and warming.
- To investigate biodiversity in the study region.

(3) Activities

- Recovery of time-series sediment trap mooring “NBC22t” off the north of Barrow Canyon.
- Deployment of time-series sediment trap mooring “NAP23t” in the southern Northwind Abyssal Plain.

(4) Methods, instruments

<Methods>

Acoustic communication of releasers to be deployed were examined in the Bering Sea (53°46.85’N 177°07.96’E, 3911 m water depth) on Aug. 31, 2023. The releasers were mounted on CTD frame, and it was tested at 1000 m depth using ship’s acoustic ranging system. Just before recovery operation of the mooring NBC22t, the ship passed away over the mooring NBC22t to examine whether the newly mounted acoustic system on the ship (water column image data: WCI) can detect the present state of the mooring equipment (some of them with mooring frame is handy size).

For the deployment sensors, log file or photograph of configuration process were taken. Sample cups of sediment trap were filled-with filtered sea water taken at 1000 m depth in the southwestern Canada Basin in the previous *Mirai* cruise. The water contains formalin (5 v/v%) and sodium hydroborate for pH adjustment (pH ~8.2). The time-series sediment trap was scheduled with 14-days interval from 00:00 of September 25, 2023 to 00:00 of Jan. 1, 2024 (UTC), and then 13-days interval to 00:00 of September 4, 2024. The battery of acoustic releasers is for two-years deployment. All serial numbers of deploying equipment and connection of all parts were checked just before the deployment and/or during the deployment operation. Mooring deployment started from the throw-in of the top buoy into water. The ranging and determination of mooring position was conducted by NME technical staff with ship's acoustic system.

Safety briefing by chief officer was conducted for all related staffs working on stern deck, just before the start of mooring operations. The deck work was conducted by crew and MWJ technicians. All staffs working on stern deck worn floating jackets, hard hat, safety shoes, and gloves. The "A" frame and capstan winch was applied for the mooring operation. Just in case, dragging tools, which are composed of hooks, weights, chains, shackles, TRITON wires and ropes, were loaded on the ship for mooring recovery.

<Instruments>
All instruments on the recovered and the deployed moorings are listed in Tables 3.1.2.IV-1 and -2. The designs of recovered and deployed mooring are shown in Figures 3.1.2.IV-1, -2, and -3. The all required procedure for export/reimport control at the Shimizu custom was performed by the Suzuyo, Co. Ltd.

(5) Results
The test of acoustic communication and releasing hook was successful for the Benthos 865A releaser at 1000 m depth. The Nichiyu LGC releaser at 1000 m responded to call, but the deck unit could not detect the response for the ranging probably due to ship's noise. The ranging by the Nichiyu LGC releaser was successful at 500 m depth.

The WCI data of NBC22t was successfully taken (Figure 3.1.2.IV -4). The WCI which shows strong acoustic signals in water column well corresponded to depths of each moored equipment from the top buoy to the deeper sediment trap at ~1000 m of NBC22t. The double releasers moored at ~1975 m and the sinker were uncertain in the obtained WCI. However, it might be due to the configuration of the WCI system at that time.

The recovery operation for NBC22t started from acoustic communication between ship's transducer and the transducer of acoustic releaser on 6:00 of Sep. 13 (SMT). The deployed releaser of Benthos 865A was enabled, and the release command was transmitted from 680 m away (horizontal distance). The release was successful at once of sending the release command. The crew went to the drifting top buoy with ship's zodiac to connect a rope from the *Mirai*'s stern. The rope was spooled on deck, and the mooring equipment was recovered on deck from the top buoy to the acoustic releasers (Table 3.1.2.IV-1). All of sediment trap samples were successfully retrieved (Figure 3.1.2.IV-5). Hydrographic data from the moored sensors were successfully recovered.

Deployment started from the throw-in of the top buoy. The ship went forward with slow speed (~1.0knot). Before the dropping sinker, the slow towing of mooring continued until the ship reaches at the planned target position of the mooring. Deepening and vanish of buoys from sea surface was confirmed, and then reaching of sinker at the seafloor was confirmed by ship's acoustic ranging system. The mooring position was determined using SSBL and transducer of Benthos 865A releaser. The acoustic response of Nichiyu releaser was also confirmed. The water depth was determined by the depth value of the mooring position in MBES topography map. The position, water depth, top depth, and recovery plan (season and ship) of the NAP23t will be noticed to AOOS and related persons in the world.

Regarding to the mooring activity, total of 60L water was sampled at 1000m depth of CTD Station 24. This is to be used for treatment of the recovered samples and pH-adjusted formalin sea water for next sediment-trap deployment in 2024.

Table 3.1.2.IV-1. Summary on the recovery of NBC22t on September 13, 2023 (UTC).

NBC22t Coordinates: 72°28.3689'N 155°24.1670'W, Water depth: 2004 m	
Transmitting the enable command of releaser Benthos 865A (S/N 1078) (860 m away from NBC22t position, relative direction 3°) #1 (No response) #2 (No response) #3 Confirmation of response from the releaser	 14:02 14:04 14:06 14:07
Transmission of the release command for Benthos 865A (680 m away from NBC22t position, relative direction 3°)	15:29
Weather Condition: rain Air Temp. 2.6°C, Atmospheric Press. 1002.0hPa, Wind Direction 271°, Wind Speed 7.3 m/s, SST 4.1°C, Wave 1.5 m, Current 0.8 knot, Curr. Dir. 145°	15:30
Zodiac boat on water	16:14
Connection of ship's rope to top buoy by clue on zodiac	16:27

Recovered Mooring Instruments

Item#	Type	Model	Serial Number	Time
1	Float Ice profiler CT DO Multi-Exciter PAR Iridium Beacon LED Flasher	MN-IP123 IPS-5 A7CT2-USB ARO-USB MFL50W-USB DEFI2-L MMI-513-32000 MMF-523-12000	ASL-SFFC-01 51123 0274 131 19 0F5I016 H01-001 J01-001	16:48
2	Transponder Floats	XT6001-17'' Benthos 17'' x4	75683 -	16:48
3	CT	SBE37SM	13677	16:52
4	Float	30inch steel	-	16:55
5	CT	SBE37SM	13678	17:00
6	ADCP	WHS-300	1563	17:04
7	CT DO pH	SBE37SM ARO-USB SPS-14	15456 136 390262005	17:05
8	Floats	Benthos 17'' x5	-	17:13
9	Logger ├ ADCP ├ Pressure ├ DO └ CO2	SeaGuard I DCS4520IW 4117E 4330IW CO2	1889	17:17
10	Sediment trap CT Turbidity Pressure	SMD26S-6000 A7CT-USB ACLW- DEFI2-D	26S034 613 0261 0C0N009	17:23
11	ADCP	Aquadopp DW	15193	17:27
12	Floats	Benthos 17'' x5	-	17:47
13	Sediment Trap	SMD26S-6000	26S035	18:00
14	Floats	Benthos 17'' x5	-	18:34
15	Releaser Releaser	Benthos 865A Nichiyu LGC	1078 0078	18:34
End of recovery operation at 72°27.8286'N 155°24.0040'W				18:34

Table 3.1.2.IV-2. Summary on the deployment of NAP23t on September 23, 2022 (UTC).

NAP23t Planned Coordinates: 74°31.37' N 161°55.88' W Water Depth: 1685 m	
Start of mooring deployment (74°30.8844'N 162°00.1230'W, 1658 m water depth)	16:23 (UTC)
Weather Condition: cloudy (horizon was clearly seen) Air temp. 0.1°C, Atmospheric pressure 1005.1hPa, Wind direction 334°, Wind speed 5.7 m/s, SST 2.8°C, Current direction 280.4°, Current speed 1.1 knot	

Time of instruments and anchor in water				
Item#	Type	Model	Serial Number	Time
1	Float Ice profiler CT DO Multi-Exciter PAR Iridium Beacon LED Flasher		ASL-SFFC-01 IPS-5 A7CT2-USB ARO-USB MFL50W-USB DEFI2-L MMI-513-32000 MMF-523-12000	16:25
2	Floats	Benthos 17'' x5	-	16:25
3	CT	SBE37SM	6934	16:29
4	Float	Steel 30''	-	16:30
5	CT	SBE37SM	8858	16:35
6	ADCP	WH-300 (w/ BT)	15385	16:37
7	CT DO pH	SBE37SM ARO-USB SPS-14Ti +Battery Unit	8860 0135 40306167001	16:42
8	Float	Benthos 17'' x5	-	16:48
9	Logger ├ ADCP ├ Pressure ├ DO └ CO2	SeaGuard II DCS4520IW 4117E 4330IW CO2	1958	16:53
10	Sediment trap CT	SMD26S-6000 A7CT-USB	26S032 0626	17:01
11	Floats	Benthos 17'' x5	-	17:30
12	Sediment trap	SMD26S-6000	26S033	17:44
13	Floats	Benthos 17'' x5	-	18:14
14	Releaser Releaser Pressure	Benthos 865A Nichiyu LGC DEFI2-D2XHG	537 0021 0F5H001	18:14
15	Anchor (72°28.259'N 155°24.824'W, 1995 m)	1000kg in air	-	18:32

Confirmation of anchor arrival at sea floor			18:45
Releaser ranging (Item#14)			
Depth: 1948 m, 1950 m, 1951 m (865A)		537	~19:05
Communication with Nichiyu LGC (no ranging)		0021	19:07
SSBL transponder survey for Benthos 865A			
Position	74°31.3753'N 161°56.5362'W		
Water Depth	1685 m (SeaBeam depth of the position)		
Estimated Top-buoy Depth	35 m		

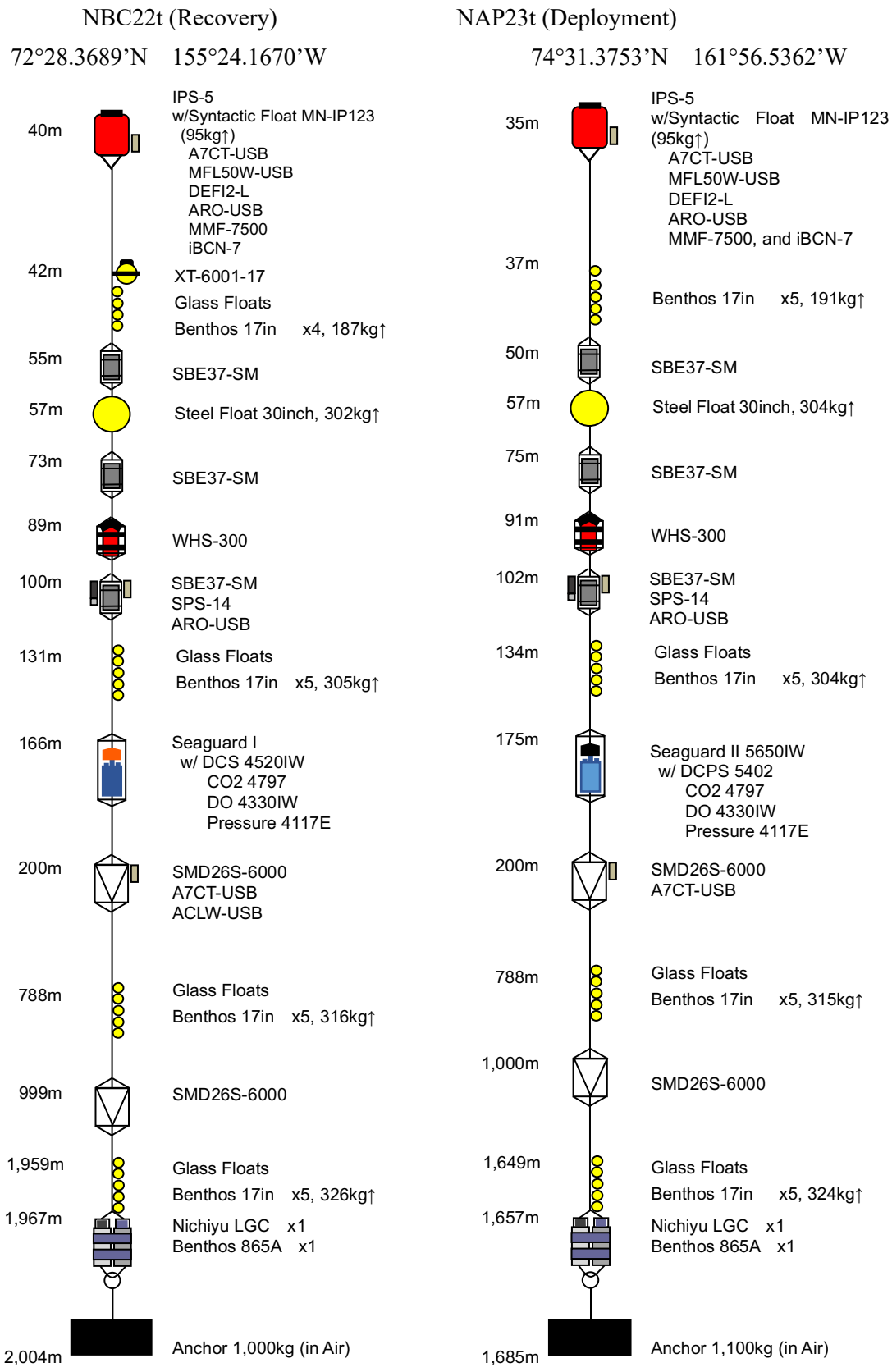

Figure 3.1.2.IV-1. The summary of mooring design for NBC22t and NAP23t.

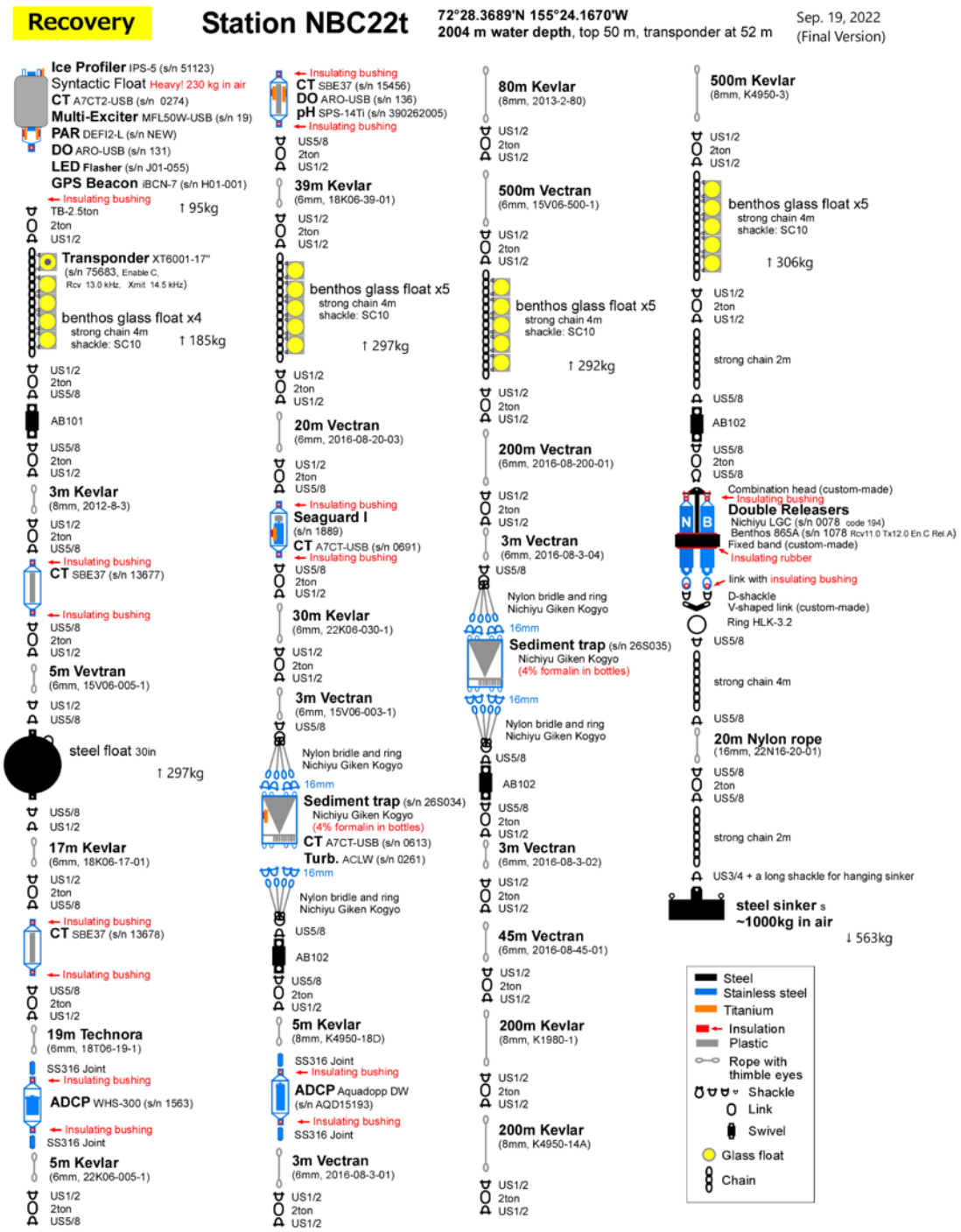

Figure 3.1.2.IV-2. The diagram of the sediment trap mooing NBC22t for recovery.

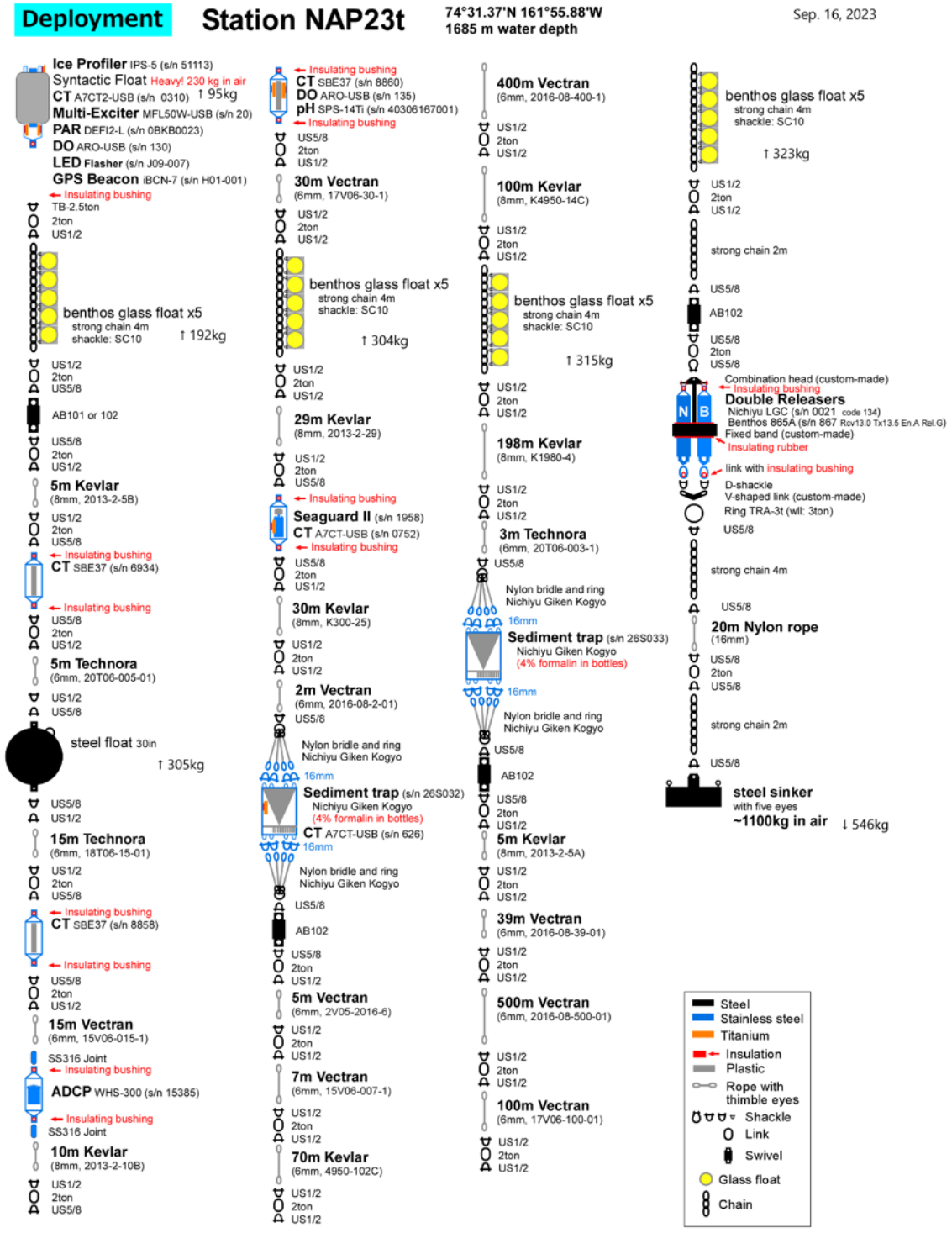

Figure 3.1.2.IV-3. The diagram of the sediment trap mooing NAP23t for deployment.

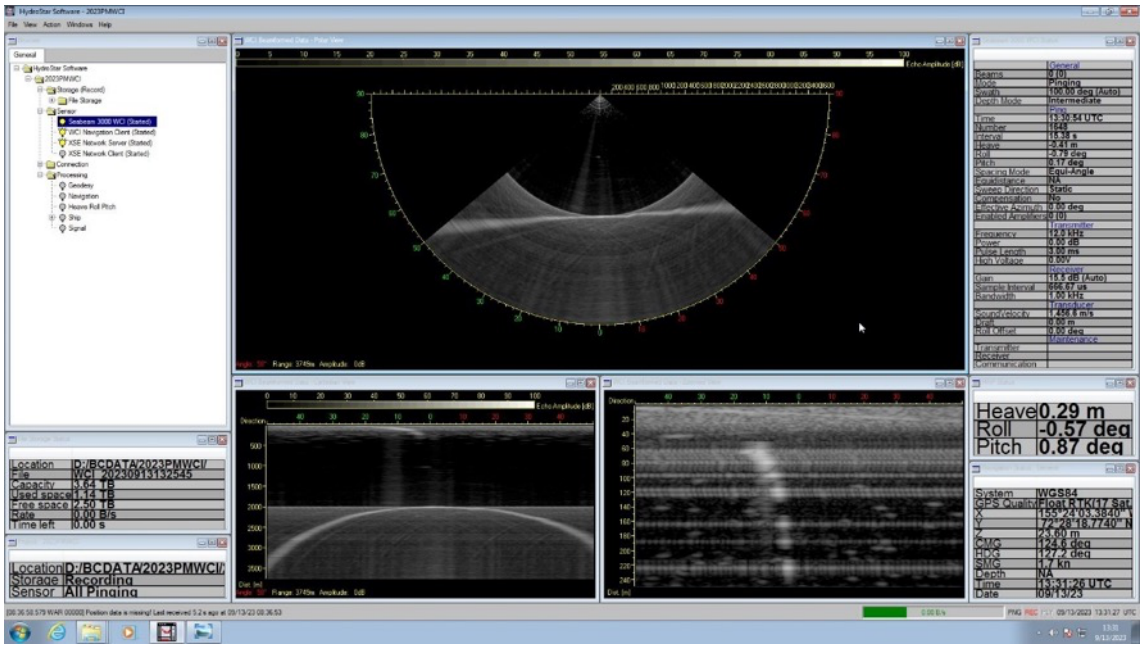

Figure 3.1.2.IV-4. The water column image by ship's acoustic system just above the mooring NBC22t. The top buoy and other moored equipment at nearly planned depths, and the tilting of upper part of the mooring by subsurface current are observed from the right-bottom image.

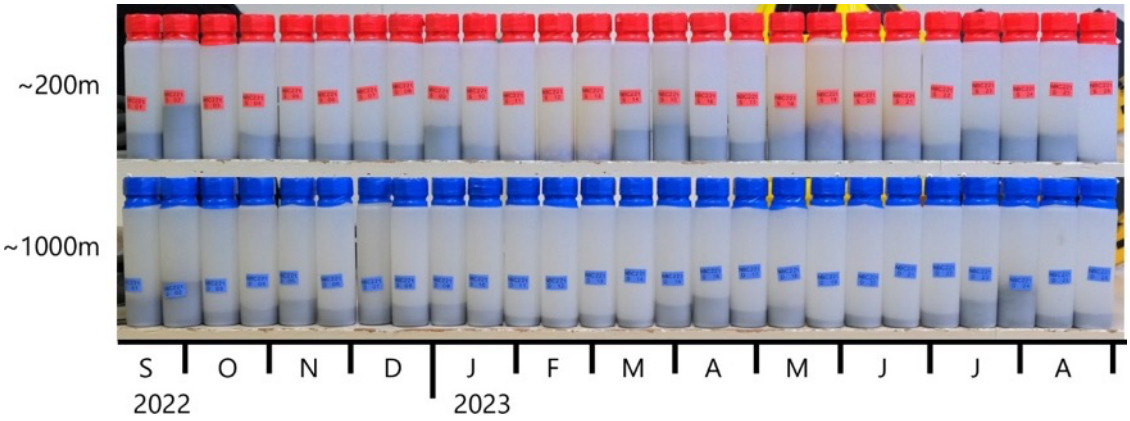

Figure 3.1.2.IV-5. The photograph of retrieved sediment-trap sample bottles from September 2022 through August 2023.

3.1.2.V. Salinity and seawater density

(1) Personnel

Hiroshi UCHIDA (JAMSTEC RIGC)

Amane FUJIWARA (JAMSTEC RIGC)

(2) Objective

The objective of this study is to collect bottle sampled salinity and density data to calibrate the CTD and thermo-salinograph salinity data and the refractive index density sensor data and to evaluate the algorithm to estimate Absolute Salinity anomaly provided along with TEOS-10 (IOC et al., 2010). Seawater samples for trace metal casts were also measured.

(3) Instruments and method

(3.1) Salinity

Salinity measurement was conducted basically based on the method by Kawano (2010) with modification of the time drift correction method (Uchida et al., 2020). Materials used in this cruise are as follows:

Standard Seawater: IAPSO Standard Seawater, Ocean Scientific International Ltd., Hampshire, UK

Batch P166

Salinometer: Autosal model 8400B; Guildline Instruments, Ltd., Ontario, Canada

Serial no. 62556

A peristaltic-type sample intake pump: Ocean Scientific International Ltd.

Thermometers: PRT model 1502A, Fluke Co., Everett, Washington, USA

Serial no. B81549 (for monitoring the bath temperature)

Serial no. B78466 (for monitoring the room temperature)

Stabilized power supply: model PCR1000LE, Kikusui Electronics Co., Japan

Serial no. XH004198

Data acquisition software: Vs8400B, Virtual Systems Co., Japan

Version 1.05T, Rev.02

Sample bottles:

100-mL polypropylene bottle with a degassing packaging aluminum bag (for CTD water sampling)

100-mL aluminum bottle (for thermo-salinograph and trace metal sampling)

Secondary Standard Seawater: Multiparametric Standard Seawater, KANSO TECHNOS Co., Ltd.

Lot PRE20

Ultra-pure water: Milli-Q water, Millipore, Billerica, Masachusetts, USA

Sub-standard seawater: Surface seawater collected in the cruise MR19-04 by filtering with a 0.20 μm pore capsule cartridge filter, ADVANTEC, Toyo Roshi Kaisha Ltd., Japan

Detergent: 2% neutral detergent, SCAT 20X-N, Dai-ichi Kogyo Seiyaku Co., Ltd., Japan

The collected water samples were stored in a refrigerated room (about 4 °C) in the R/V Mirai until measurements, and the water samples were measured on the R/V Mirai cruise MR23-07 (from October 7th to 27th, 2023).

The bath temperature of the salinometer was set to 24 °C. The salinometer was standardized only at the previous cruise (MR23-05 Leg 1) by using the IAPSO Standard Seawater (SSW). The standardization dial was set to 600 for serial no. 62556 and never changed during the cruise. The mean ± SD of the STANDBY and ZERO was 5126.5 ± 0.7 and 0.00000 ± 0.00000, respectively. The mean ± SD of the ambient room temperature was 23.4±0.5 °C, while that of the bath temperature was 23.9994±0.0007 °C.

The double conductivity ratios measured by the salinometer were used to calculate Practical Salinity using the algorithm for Practical Salinity Scale 1978 (IOC et al., 2010). A constant temperature of 24 °C was used in the calculation instead of using the measured bath temperature.

The measurement cell of the salinometer was rinsed with ultra-pure water and 2% neutral detergent after each day of measurement, and the electrode in the cell was soaked in the neutral detergent until next day of measurement.

Ultra-pure water and the IAPSO SSW were measured at the beginning and the end of each day of measurement (for samples of 1 to 3 stations). Sub-standard seawater was measured every about 10 samples to monitor stability of the salinometer during each day of measurement.

Correction factors of the salinometer were estimated from the mean Practical Salinity value of the SSW measurements and the certified Practical Salinity value for each day (see cruise report of MR23-07). The measured Practical Salinities for the water samples were corrected by using the correction factors. The standard deviation of the IAPSO SSW measurements was 0.0002 in Practical Salinity after the time drift correction. The mean ± SD of the ultra-pure water measurements was –0.00006±0.00012.

A total of 3 bottles of MSSW PRE20 was measured and the mean ± SD was 34.2771 ± 0.0000 in Practical Salinity.

(3.2) Seawater density

Seawater density for water samples was measured with a vibrating-tube density meter (DMA 5000M [serial no. 80570578], Anton-Paar GmbH, Graz, Austria) with a sample changer (Xsample

122 [serial no. 8548492], Anton-Paar GmbH). The sample changer was used to load samples automatically from up to forty-eight 12-mL glass vials.

The water samples collected for Practical Salinity measurement were measured by taking the water sample into a 12-mL glass vial for each bottle just before Practical Salinity measurement. The glass vial was sealed with Parafilm M (Pechiney Plastic Packaging, Inc., Menasha, Wisconsin, USA) immediately after filling. Densities of the samples were measured at 20 °C by the density meter.

The density meter was initially calibrated on the previous cruise (MR23-05 leg 2) by measuring air and pure water according to the instrument manual. However, measured density for the IAPSO Standard Seawater deviates from density of TEOS-10 calculated from practical salinity and composition of seawater, probably due to non-linearity of the density meter (Uchida et al., 2011). The non-linearity can be corrected by measuring a reference sample simultaneously as:

$$\rho_{corr} = \rho - (\rho_{ref} - \rho_{ref\_true}) + c\,(\rho - \rho_{ref\_true}),$$

where ρ_{corr} is the corrected density of the sample, ρ is measured density of the sample, ρ_{ref} is measured density of the reference, ρ_{ref_true} is true density of the reference, and c is non-linearity correction factor.

Time drift of the density meter was monitored by periodically measuring the density of ultra-pure water (Milli-Q water, Millipore, Billerica, Massachusetts, USA) produced on the R/V Mirai and pure water (Pure Water [water hardness 0], Ako Kasei Co. Ltd., Ako Hygo, Japan) made from seawater collected from a depth of 344 m off Muroto, Kochi, Japan, by filtering twice with a reverse osmosis membrane. In addition, Pure Water was deionized using ion exchange resin (Pure Maker, Sanei Corp., Arao, Kumamoto, Japan) conducted on 6 October 2019 and stored in a 2-L PET bottle at room temperature. Practical Salinity measured in the cruise ranged from –0.0003 to 0.0001 for the Milli-Q water and was 0.0002 for the Pure Water. The true density at 20 ºC of the Pure Water was estimated to be 998.2074 kg m^{-3} from the isotopic composition (δD = –3.4 ‰, $\delta^{18}O$ = –1.3 ‰) and International Association for the Properties of Water and Steam (IAPWS)-95 standard.

The non-linearity factor is estimated to be 0.000411 for the density meter (serial no. 80570578). In this cruise, the non-linearity and time drift of the density meter was monitored by periodically measuring the density of the IAPSO Standard Seawater (batch P166). True density at 20 °C for the batch P166 is estimated to be 1024.7638 kg/m^3 from Practical Salinity and composition changes of Standard Seawater using TEOS-10 (see Uchida et al., 2023). Average with standard deviation for the 104 measurements of the batch P166 was 1024.7639±0.0016 kg/m^3.

A total of 3 bottles of Multiparametric Standard Seawater (MSSW, KANSO TECHNOS Co.,

Ltd.) was also measured and the mean ± SD was 1024.2202 ± 0.0004 kg/m^3.

(4) Results

Absolute Salinity (also called density salinity, "DNSSAL") can be back calculated from the measured density and temperature (20 °C) with TEOS-10. A total of 83 pairs of replicate salinity samples and 81 pairs of replicate density samples were obtained for the CTD water sampling and the SD of the replicate sample measurements were as follows:

For pressure < 700 dbar

0.0036 for Practical Salinity (PSS-78) (n = 72)

0.0039 for Absolute Salinity (g/kg) (n = 70)

For pressure ≧ 700 dbar

0.0004 for Practical Salinity (PSS-78) (n = 11)

0.0016 for Absolute Salinity (g/kg) (n = 11)

The measured Absolute Salinity anomalies (δS_A) are shown in Figure below.

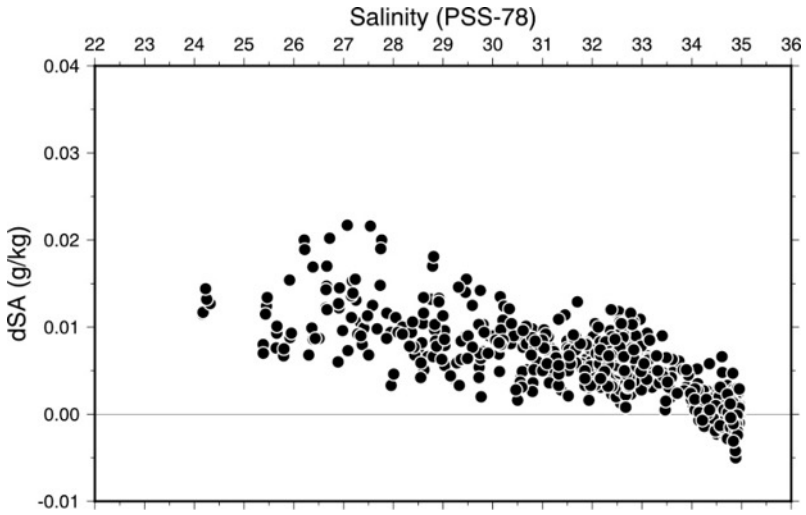

Figure 3.1.2.V-1. Absolute Salinity anomaly (δS_A) plotted against Practical Salinity.

(5) References

IOC, SCOR and IAPSO (2010): The international thermodynamic equation of seawater – 2010: Calculation and use of thermodynamic properties. Intergovernmental Oceanographic Commission, Manuals and Guides No. 56, UNESCO (English), 196 pp.

Kawano, T. (2010): Salinity. The GO-SHIP Repeat Hydrography Manual: A collection of Expert Reports and Guidelines, IOCCP Report No. 14, ICPO Publication Series No. 134, Version 1.

Pawlowicz, R., D.G. Wright and F. J. Millero (2011): The effects of biogeochemical processes on

ocean conductivity/salinity/density relationships and the characterization of real seawater. Ocean Science, 7, 363-387.

Uchida, H., T. Kawano, M. Aoyama and A. Murata (2011): Absolute salinity measurements of standard seawaters for conductivity and nutrients. La mer, 49, 237-244.

Uchida, H., T. Kawano, T. Nakano, M. Wakita, T. Tanaka and S. Tanihara (2020): An updated batch-to-batch correction for IAPSO standard seawater. J. Atmos. Oceanic Technol., 37, 1507-1520, doi:10.1175/JTECH-D-19-0184.1.

Uchida, H., M. Wakita, A. Makabe, and A. Murata (2023): Changes of the composition of International Association for the Physical and Sciences of the Ocean standard seawater. In: Murata A. Cheong C., editors. Chemical reference materials of ocean science: history, production, certification and current status.

(6) Data archive

These obtained data will be submitted to JAMSTEC Data Management Group (DMG).

3.1.2.VI. Sea Ice Radar

(1) Responsible personnel

Amane Fujiwara	JAMSTEC -PI
Ryo Oyama	NME (Nippon Marine Enterprises, Ltd.)
Kazuho Yoshida	NME
Satomi Ogawa	NME
Yohei Sugimoto	NME
Yoichi Inoue	MIRAI Crew

(2) Purpose, background

In the sea ice areas, marine radar provides an important tool for the detection of sea ice and icebergs. It is importance to monitor the sea ice daily and produce ice forecasts to assist ship traffic and other marine operations. In order to select route optimally, ice condition prediction technology is necessary, and image information of ice-sea radar is used for constructing a route selection algorithm.

(3) Activities

Observation period: 07 Sep. 2023- 30 Sep. 2023 (UTC)

(4) Methods, instruments

R/V MIRAI is equipped with an Ice Navigation Radar, “sigma S6 Ice Navigator (Rutter Inc.)”. The ice navigation radar, the analog signal from the x-band radar is converted by a modular radar interface and displayed as a digital video image. The sea ice radar is equipped with a screen capture function and saves at arbitrary time intervals.

(5) Results, Future Plans, Lists

i) Result

Figure x-x-x shows an image of sea ice from Sea ice radar.

ii) Data archives

These data obtained in this cruise will be submitted to the Data Management Group of JAMSTEC, and will be opened to the public via “Data Research System for Whole Cruise Information in JAMSTEC (DARWIN)” in JAMSTEC web site.

< http://www.godac.jamstec.go.jp/darwin/e >

3.1.3. Biogeochemical Observations

3.1.3.I. Dissolved Oxygen

(Descriptions for research activities, such as:

(1) Responsible personnel

Amane Fujiwara (JAMSTEC): Principal Investiator

Masahiro Orui (MWJ): Operation Leader

Tomoki Nakamura (MWJ)

Shintaro Amikura (MWJ)

(2) Objective

Determination of dissolved oxygen in seawater by Winkler titration.

(3) Parameters

Dissolved Oxygen

(4) Instruments and Methods

Following procedure is based on the Winkler method (Dickson, 1996; Culberson, 1991).

a. Instruments

Burette for sodium thiosulfate and potassium iodate;

Automatic piston burette (APB-510, APB-610 and APB-620) manufactured by Kyoto Electronics Manufacturing Co., Ltd. / 10 cm^3 of titration vessel

Detector;

Automatic photometric titrator (DOT-15X) manufactured by Kimoto Electric Co., Ltd.

Software;

DOT15X_Terminal Ver. 1.3.1

b. Reagents

Pickling Reagent I: Manganese(II) chloride solution (3 mol dm^{-3})

Pickling Reagent II:

Sodium hydroxide (8 mol dm^{-3}) / Sodium iodide solution (4 mol dm^{-3})

Sulfuric acid solution (5 mol dm^{-3})

Sodium thiosulfate (0.025 mol dm^{-3})

Potassium iodate (0.001667 mol dm^{-3})

c. Sampling

Seawater samples were collected with Niskin bottle attached to the CTD/Carousel Water Sampling System (CTD system). Seawater for oxygen measurement was transferred from the bottle to a volume calibrated flask (ca. 100 cm^3), and three times volume of the flask was overflowed. Temperature was simulteneously measured by digital thermometer during the overflowing. After transfering the sample, two reagent solutions (Reagent I and II) of 1 cm^3 each were added immediately and the stopper was inserted carefully into the flask. The sample flask was then shaken vigorously to mix the contents and to disperse the precipitate finely throughout. After the precipitate has settled at least halfway down the flask, the flask was shaken again vigorously to disperse the precipitate. The sample flasks containing pickled samples were stored in a laboratory until they were titrated.

d. Sample measurement

For over two hours after the re-shaking, the pickled samples were measured on board. Sulfuric acid solution with its volume of 1 cm^3 and a magnetic stirrer bar were put into the sample flask and the sample was stirred. The samples were titrated by sodium thiosulfate solution whose morality was determined by potassium iodate solution. Temperature of sodium thiosulfate during titration was recorded by a digital thermometer. Dissolved oxygen concentration (μmol kg^{-1}) was calculated by sample temperature during seawater sampling, salinity of the sensor on CTD system, flask volume, and titrated volume of sodium thiosulfate solution without the blank. During this cruise, 2 sets of the titration apparatus were used.

e. Standardization and determination of the blank

Concentration of sodium thiosulfate titrant was determined by potassium iodate solution. Pure potassium iodate was dried in an oven at 130 ºC, and 1.7835 g of it was dissolved in deionized water and diluted to final weight of 5 kg in a flask. After 10 cm^3 of the standard potassium iodate solution was added to an another flask using a volume-calibrated dispenser, 90 cm^3 of deionized water, 1 cm^3 of sulfuric acid solution, and 1 cm^3 of pickling reagent solution II and I were added in order. Amount of titrated volume of sodium thiosulfate for this diluted standard potassium iodate solution (usually 5 times measurements average) gave the morality of sodium thiosulfate titrant.

The oxygen in the pickling reagents I (1 cm^3) and II (1 cm^3) was assumed to be 7.6×10^{-8} mol (Murray et al., 1968). The blank due to other than oxygen was determined as follows. First, 1 and 2 cm^3 of the standard potassium iodate solution were added to each

flask using a calibrated dispenser. Then 100 cm^3 of deionized water, 1 cm^3 of sulfuric acid solution, 1 cm^3 of pickling II reagent solution, and same volume of pickling I reagent solution were added into the flask in order. The blank was determined by difference between the first (1 cm^3 of potassium iodate) titrated volume of the sodium thiosulfate and the second (2 cm^3 of potassium iodate) one. The titrations were conducted for 3 times and their average was used as the blank value.

(5) Results

a. Standardization and determination of the blank

Table 3.1.3.I-1 shows results of the standardization and the blank determination during this cruise.

Table 3.1.3.I-1 Results of the standardization and the blank determinations during cruise

Date (yyyy/mm/dd)	Potassium iodate ID	Sodium thiosulfate ID	DOT-15X (No.9)		DOT-15X (No.10)		Stations
			E.P. (cm^3)	Blank (cm^3)	E.P. (cm^3)	Blank (cm^3)	
2023/08/27	K23A01	T-22K	3.949	0.002	3.948	-0.003	
2023/09/03	K23A02	T-22K	3.946	0.002	3.947	-0.001	001
2023/09/08	K23A03	T-22K	3.946	0.001	3.947	0.000	002,003,004,005, 006,007, 008, 009, 010
2023/09/11	K23A04	T-22K	3.946	0.000	3.946	-0.002	011,012,013,014
2023/09/14	K23A05	T-22K	3.947	0.000	3.947	-0.001	015,016,017,018, 019,020,021,022, 023
2023/9/19	K23A06	T-22K	3.946	0.000	3.945	0.001	025,027,028,029, 030
2023/09/22	K23A07	T-22K	3.946	0.002	3.947	0.000	
2023/09/22	K23A07	T-22J	3.915	-0.001	3.913	-0.002	031,032,034,035, 036
2023/09/27	K23A08	T-22J	3.915	0.002	3.911	-0.002	037,038,039
2023/09/29	K23A09	T-22J	3.917	0.004	3.912	-0.001	040,041,042,043, 044
2023/10/01	K23A10	T-22J	3.918	0.003	3.911	0.002	

b. Repeatability of sample measurement

Replicate samples were taken at every CTD casts. The standard deviation of the replicate measurement (Dickson et al., 2007) was 0.47 μmol kg^{-1} (n=57).

(6) References

Culberson, C. H. (1991). *Dissolved Oxygen.* WHPO Publication 91-1.

Dickson, A. G. (1996). Determination of dissolved oxygen in sea water by Winkler titration. In *WOCE Operations Manual*, Part 3.1.3 Operations & Methods, WHP Office Report WHPO 91-1.

Dickson, A. G., Sabine, C. L., & Christian, J. R.(Eds.), (2007). *Guide to best practices for ocean CO_2 measurements, PICES Special Publication 3*: North Pacific Marine Science Organization.

Murray, C. N., Riley, J. P., & Wilson, T. R. S. (1968). The solubility of oxygen in Winklerreagents used for the determination of dissolved oxygen. *Deep Sea Res.*, 15, 237-238.

3.1.3.II. Nutrients

(1) Personnel

Mariko HATTA (JAMSTEC): Principal Investigator
Yuta ODA (MWJ): Operation Leader
Shiori ARIGA (MWJ)
Nobuyuki NAKATOMI (MWJ)

(2) Objectives

The objective of this document is to show the present status of the nutrient concentrations during the R/V Mirai MR23-06C cruise (EXPOCODE: 49NZ20230825) in the Arctic Ocean, and then evaluate the comparability of this obtained data set during this cruise using the certified reference materials of the nutrients in seawater.

(3) Parameters

The parameters are nitrate, nitrite, silicate, phosphate and ammonia in seawater.

(4) Instruments and methods

(4.1) Analytical detail using QuAAtro 39-J systems (BL TEC K.K.)

The analytical platform was replaced from QuAAtro 2-HR to QuAAtro 39 in March 2021. However, since this replacement, the several issues for the QuAAtro 39 system were reported (e.g. unexpected drift issue for the phosphate and the silicate determinations, unusual damage pump cover, see previous cruise report MR21-05C). In July 2022, in order to improve those issue and the analytical precisions, (1) their pumps were replaced from the 13-tube pump (model number: 166+B214-01, BL TEC K.K.) to the 14-tube pump (model number: TRA+B014-02, BL TEC K.K.), (2) their motor brackets were replaced to the new type that is a stainless model (model number: Motor-Braket-01-Rev-1 and Motor-Braket-02-Rev-1, BL TEC K.K.), and (3) their light source units were fixed firmly in order to reduce vibration. This modified system now calls “QuAAtro 39-J”.

Nitrate + nitrite and nitrite were analyzed by the following methodology that was modified from the original method of Grasshoff (1976). The flow diagrams were shown in Figure 3.1.3.II-1 for nitrate + nitrite and Figure 3.1.3.II-2 for nitrite. For the nitrate + nitrite analysis, the samples were mixed with the alkaline buffer (Imidazole) and then the mixture was pushed through a cadmium coil which was coated with a metallic copper. This step was conducted due to the reduction from nitrate to nitrite in the sample, which allowed us to determine nitrate + nitrite in the seawater sample. For the nitrite analysis, the sample was mixed with reagents without this

reduction step. In the flow system, the seawater sample with or without the reduction step was mixed with an acidic sulfanilamide reagent through a mixing coil to produce a diazonium ion. And then, the mixture was mixed with the N-1-naphthylethylenediamine dihydrochloride (NED) to produce a red azo dye. The azo dye compound was injected into the spectrophotometric detection to monitor the signal at 545 nm. Thus, for the nitrite analysis, the sample was determined without passing through the Cd coil. Nitrate was computed by the difference between nitrate+nitrite concentration and nitrite concentration.

The silicate method is analogous to that described for phosphate (see below). The method is essentially that of Grasshoff et al. (1999). The flow diagrams were shown in Figure 3.1.3.II-3. Silicomolybdic acid compound was first formed by mixing silicate in the sample with the molybdic acid. The silicomolybdic acid compound was then reduced to silicomolybdous acid, "molybdenum blue," using L-ascorbic acid as the reductant. And then the signal was monitored at 630 nm.

The methodology for the phosphate analysis is a modified procedure of Murphy and Riley (1962). The flow diagrams were shown in Figure 3.1.3.II-4. Molybdic acid was added to the seawater sample to form the phosphomolybdic acid compound, and then it was reduced to phosphomolybdous acid compound using L-ascorbic acid as the reductant. And then the signal was monitored at 880 nm.

The ammonia in seawater was determined using the flow diagrams shown in Figure 3.1.3.II-5. The sample was mixed with an alkaline solution containing EDTA, which ammonia as gas state was formed from seawater. The ammonia (gas) is absorbed in a sulfuric acid by way of 0.5 μm pore-size membrane filter (ADVANTEC PTFE) at the dialyzer attached to the analytical system. And then the ammonia absorbed in sulfuric acid was determined by coupling with phenol and hypochlorite to form indophenols blue, and the signal was determined at 630 nm.

The details of a modification of analytical methods for four parameters, nitrate, nitrite, silicate and phosphate, are also compatible with the methods described in the nutrients section in the new GO-SHIP repeat hydrography nutrients manual (Becker et al., 2019). This manual is a revised version of the GO-SHIP repeat hydrography nutrients manual (Hydes et al., 2010). The analytical method of ammonium is compatible with the determination of ammonia in seawater using a vaporization membrane permeability method (Kimura, 2000).

(4.2) Nitrate + Nitrite reagents

50 % Triton solution

50 mL of Triton® X-100 (CAS No. 9002-93-1) was mixed with 50 mL of ethanol (99.5 %).

Imidazole (buffer), 0.06 M (0.4 % w/v)

Dissolved 4 g of imidazole (CAS No. 288-32-4) in 1000 mL ultra-pure water, and then added 2 mL of hydrogen chloride (CAS No. 7647-01-0). After mixing, 1 mL of the 50 % Triton solution was added.

Sulfanilamide, 0.06 M (1 % w/v) in 1.2 M HCl

Dissolved 10 g of 4-aminobenzenesulfonamide (CAS No. 63-74-1) in 900 mL of ultra-pure water, and then add 100 mL of hydrogen chloride (CAS No. 7647-01-0). After mixing, 2 mL of the 50 % Triton solution was added.

NED, 0.004 M (0.1 % w/v)

Dissolved 1 g of N-(1-naphthalenyl)-1, 2-ethanediamine dihydrochloride (CAS No. 1465-25-4) in 1000 mL of ultra-pure water and then added 10 mL of hydrogen chloride (CAS No. 7647-01-0). After mixing, 1 mL of the 50 % Triton solution was added. This reagent was stored in a dark bottle.

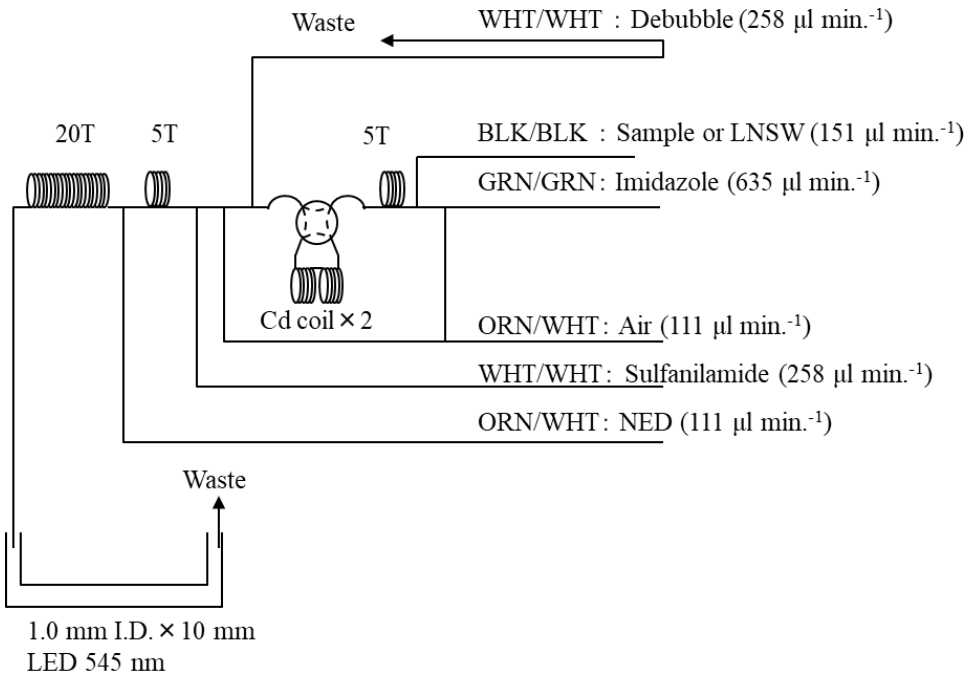

Figure 3.1.3.II-1 NO_3+NO_2 (1ch.) flow diagram.

(4.3) Nitrite reagents

50 % Triton solution

50 mL of Triton® X-100 (CAS No. 9002-93-1) was mixed with 50 mL of ethanol (99.5 %).

Sulfanilamide, 0.06 M (1 % w/v) in 1.2 M HCl

Dissolved 10 g of 4-aminobenzenesulfonamide (CAS No. 63-74-1) in 900 mL of ultra-pure water, and then added 100 mL of hydrogen chloride (CAS No. 7647-01-0). After mixing, 2 mL of the 50 % Triton solution was added.

NED, 0.004 M (0.1 % w/v)

Dissolved 1 g of N-(1-naphthalenyl)-1, 2-ethanediamine dihydrochloride (CAS No. 1465-25-4) in 1000 mL of ultra-pure water and then added 10 mL of hydrogen chloride (CAS No. 7647-01-0). After mixing, 1 mL of the 50 % Triton solution was added. This reagent was stored in a dark bottle.

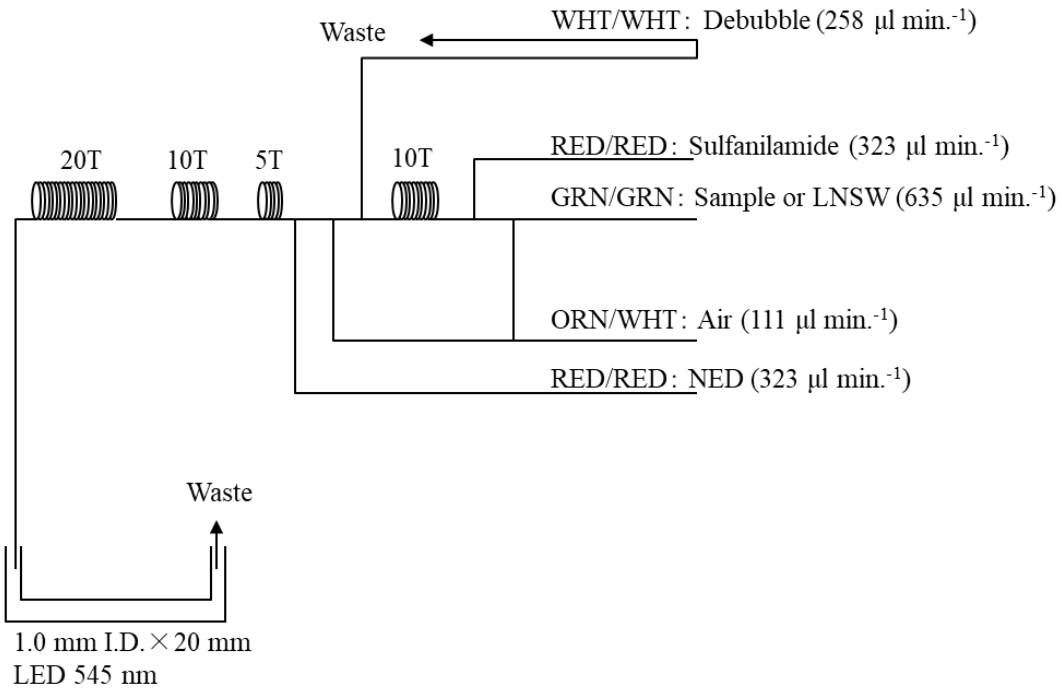

Figure 3.1.3.II-2 NO_2 (2ch.) flow diagram.

(4.4) Silicate reagents

15 % Sodium dodecyl sulfate solution

75 g of sodium dodecyl sulfate (CAS No. 151-21-3) was mixed with 425 mL of ultra-pure water.

Molybdic acid, 0.03 M (1 % w/v)

Dissolved 7.5 g of sodium molybdate dihydrate (CAS No. 10102-40-6) in 980 mL ultra-pure water, and then added 12 mL of 4.5M sulfuric acid. After mixing, 20 mL of the 15 % sodium dodecyl sulfate solution was added. Note that the amount of sulfuric acid was reduced from the

previous report (MR19-03C) since we have modified the method of Grasshoff et al. (1999).

Oxalic acid, 0.6 M (5 % w/v)

Dissolved 50 g of oxalic acid (CAS No. 144-62-7) in 950 mL of ultra-pure water.

Ascorbic acid, 0.01 M (3 % w/v)

Dissolved 2.5 g of L-ascorbic acid (CAS No. 50-81-7) in 100 mL of ultra-pure water. This reagent was freshly prepared every day.

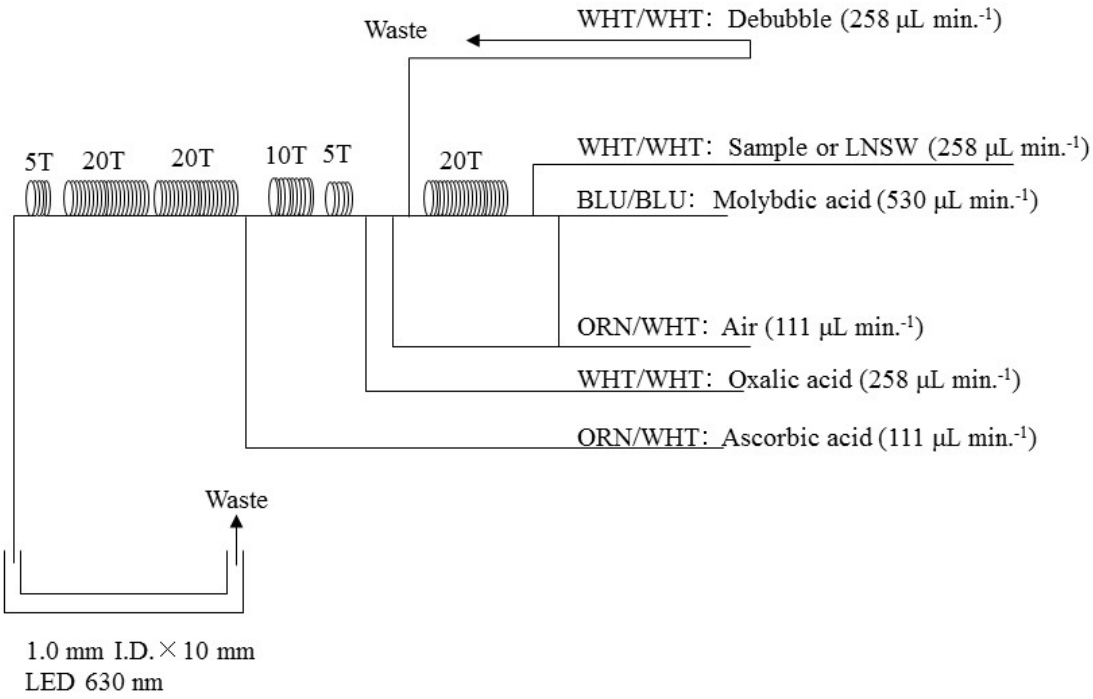

Figure 3.1.3.II-3 SiO_2 (3ch.) flow diagram.

(4.5) Phosphate reagents

15 % Sodium dodecyl sulfate solution

75 g of sodium dodecyl sulfate (CAS No. 151-21-3) was mixed with 425 mL of ultra-pure water.

Stock molybdate solution, 0.03 M (0.8 % w/v)

Dissolved 8 g of sodium molybdate dihydrate (CAS No. 10102-40-6) and 0.17 g of antimony potassium tartrate trihydrate (CAS No. 28300-74-5) in 950 mL of ultra-pure water, and then added 50 mL of sulfuric acid (CAS No. 7664-93-9).

PO4 color reagent

Dissolved 1.2 g of L-ascorbic acid (CAS No. 50-81-7) in 150 mL of the stock molybdate solution. After mixing, 3 mL of the 15 % sodium dodecyl sulfate solution was added. This reagent was freshly prepared before every measurement.

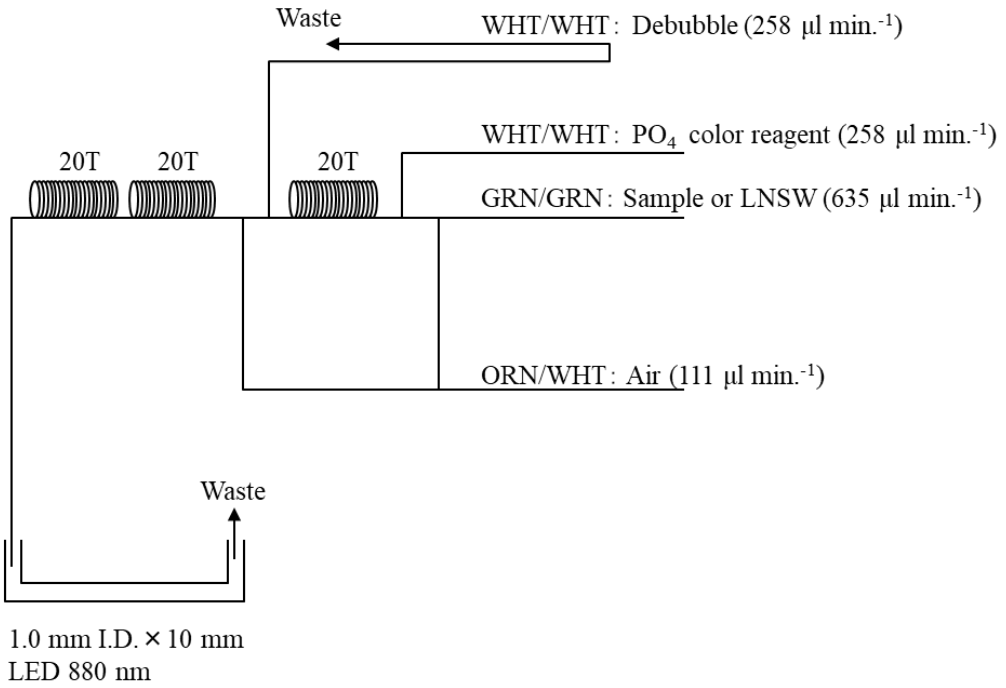

Figure3.1.3.II-4 PO_4 (4ch.) flow diagram.

(4.6) Ammonia reagents

30 % Triton solution

30 mL of Triton® X-100 (CAS No. 9002-93-1) was mixed with 70 mL of ultra-pure water.

EDTA

Dissolved 41 g of tetrasodium; 2-[2-[bis(carboxylatomethyl)amino]ethyl-(carboxylatemethyl)amino]acetate; tetrahydrate (CAS No. 13235-36-4) and 2 g of boric acid (CAS No. 10043-35-3) in 200 mL of ultra-pure water. After mixing, 1 mL of the 30 % Triton solution was added. This reagent is prepared every week.

NaOH liquid

Dissolved 1.5 g of sodium hydroxide (CAS No. 1310-73-2) and 16 g of tetrasodium; 2-[2-[bis(carboxylatomethyl)amino]ethyl-(carboxylatomethyl)amino]acetate; tetrahydrate (CAS

No. 13235-36-4) in 100 mL of ultra-pure water. This reagent was prepared every week. Note that we reduced the amount of sodium hydroxide from 5 g to 1.5 g because pH of C standard solutions has been lowered 1 pH unit due to the change of recipe of B standards solution (the details of those standard solutions, see 7.2.4).

Stock nitroprusside

Dissolved 0.25 g of sodium nitroferricyanide dihydrate (CAS No. 13755-38-9) in 100 mL of ultra-pure water, and then added 0.2 mL of 1M sulfuric acid. Stored in a dark bottle and prepared every month.

Nitroprusside solution

Added 4 mL of the stock nitroprusside and 4 mL of 1M sulfuric acid in 500 mL of ultra-pure water. After mixing, 2 mL of the 30 % Triton solution was added. This reagent was stored in a dark bottle and prepared every 2 or 3 days.

Alkaline phenol

Dissolved 10 g of phenol (CAS No. 108-95-2), 5 g of sodium hydroxide (CAS No. 1310-73-2) and 2 g of sodium citrate dihydrate (CAS No. 6132-04-3) in 200 mL of ultra-pure water. Stored in a dark bottle and prepared every week.

NaClO solution

Mixed 3 mL of sodium hypochlorite (CAS No. 7681-52-9) in 47 mL of ultra-pure water. Stored in a dark bottle and fleshly prepared before every measurement. This reagent needs to be 0.3 % available chlorine.

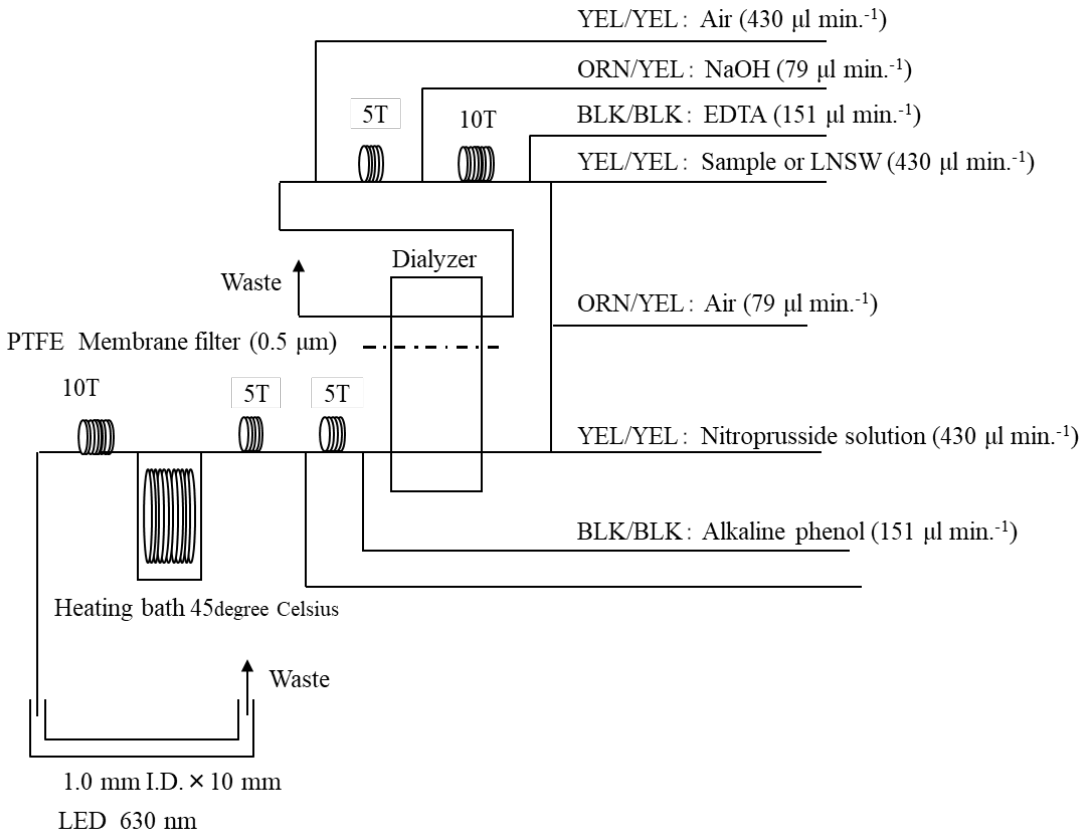

Figure 3.1.3.II-5 NH_4 (5ch.) flow diagram.

(4.7) Sampling procedures

Sampling for the nutrient samples was conducted right after the sampling for other parameters (oxygen, salinity and trace gases). Samples were collected into two new 10 mL polyacrylates vials without any sample drawing tube that is usually used for the oxygen samples. Each vial was rinsed three times before filling and then was sealed without any head space immediately after the collection. The vials were put into a water bath that was adjusted to the ambient temperature at 20.0 ± 0.2 degree Celsius, for more than 30 minutes to keep the constant temperature of samples before measuring. When the transmissometer signal (Xmiss) of the sample was less than 95 % or confirmed the presence of particles in the vial, we basically carried out centrifuging the sample by using a centrifuge (type: CN-820, Hsiang Tai). The conditions of the centrifuge were set at about 3400 rpm for 2.5 minutes. The treated samples were listed in Table 3.1.3.II-1.

No transfer from the vial to another container was made and the vials were placed on an autosampler tray directly. Samples were analyzed within 24 hours after collection.

(4.8) Data processing

Raw data from QuAAtro 39-J were treated as follows:

- Checked if there were any baseline shifts.

- Checked the shape of each peak and positions of peak values. If necessary, a change was made for the positions of peak values.

- Conducted carry-over correction and baseline drift correction followed by sensitivity correction to apply to the peak height of each sample.

- Conducted baseline correction and sensitivity correction using linear regression.

- Using the salinity (Bottle SAL) and the laboratory room temperature (20 degree Celsius), the density of each sample was calculated. The obtained density was used to calculate the final nutrient concentration with the unit of μmol kg^{-1}.

- Calibration curves to obtain the nutrient concentrations were assumed second-order equations.

(4.9) Summary of nutrients analysis

Total of the 25 runs were conducted to obtain the values for the samples that collected by 41 casts at 41 stations during this cruise. Note that re-calculation for ammonia analysis has been done at Stn.29 cast 2 (run serial: 14), Stn.30 cast 1 (run serial: 14), Stn.31 cast 2 (run serial: 16), Stn.32 cast 2 (run serial: 17), Stn.34 cast 1(run serial: 18), Stn.43 cast 1 (run serial: 25) and Stn.44 cast 1 (run serial: 25) due to significant error of baseline correction protocol. The total number of the seawater samples were 595. For each sample depth, the duplicate of each were collected. The sampling locations for the nutrients was shown in Figure 3.1.3.II-6.

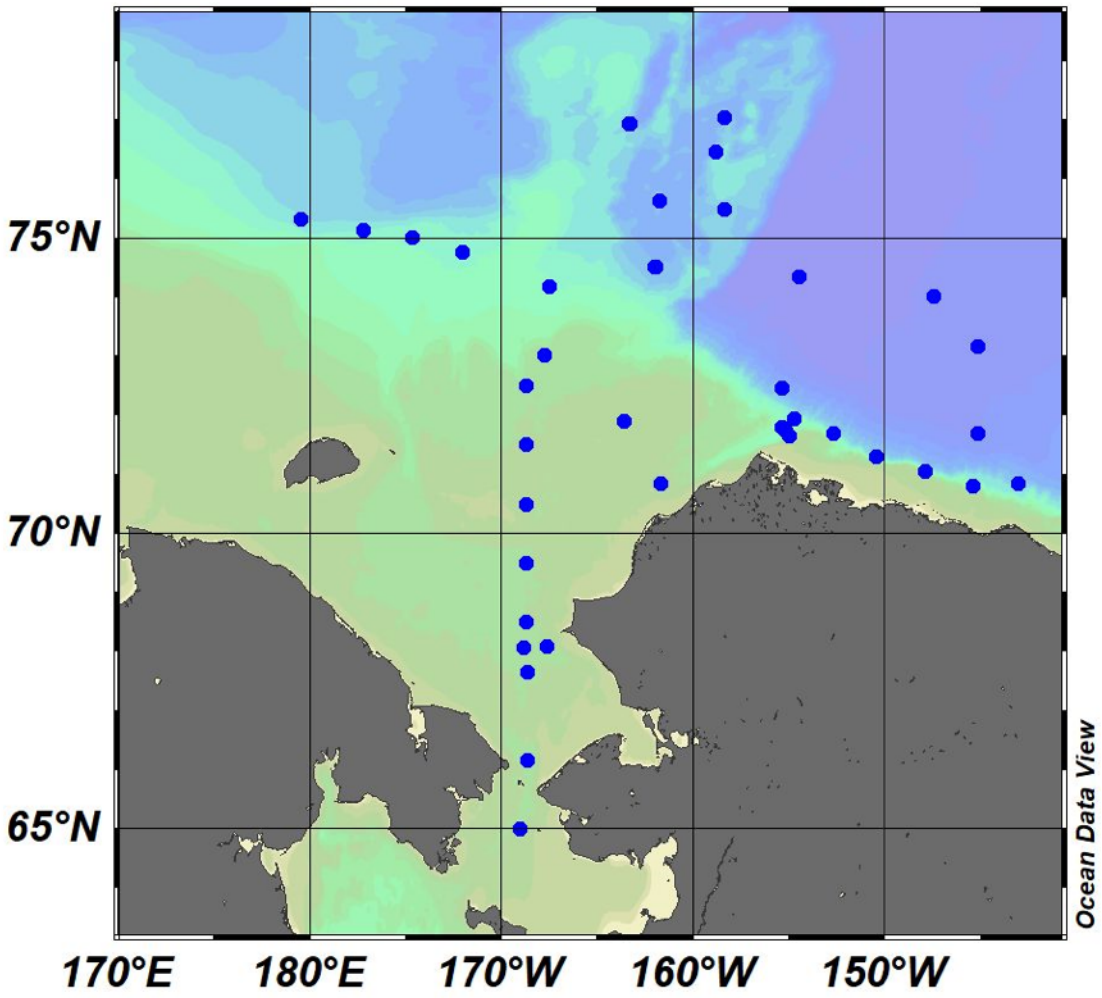

Figure 3.1.3.II-6 Sampling positions of nutrients sample.

Table 3.1.3.II-1 Centrifuged samples

Station	Cast	Bottle	Depth (dbar)	Trans (%)
1	1	28	40.1	81.547
1	1	1	44.4	80.318
2	1	0	0.0	-
2	1	32	5.3	89.457
2	1	31	10.4	90.186
2	1	29	30.5	94.105
2	1	28	40.7	94.379
2	1	1	49.6	90.460
3	2	35	23.0	91.604
3	2	29	30.2	76.254
3	2	28	40.0	59.649
3	2	1	44.2	55.905
4	1	0	0.0	-
4	1	32	5.1	88.081
4	1	31	9.9	88.335
4	1	30	20.1	89.011
4	1	35	21.2	89.426
4	1	29	30.1	81.533
4	1	28	40.1	69.507
4	1	1	47.9	64.294
5	1	0	0.0	-
5	1	32	4.8	93.152
5	1	31	10.0	93.209
5	1	35	15.9	94.323
5	1	28	39.9	80.602
5	1	1	46.1	64.389
6	1	30	20.3	94.635
6	1	35	23.3	93.305
6	1	29	30.0	74.303
6	1	1	33.2	75.040
7	1	29	29.9	93.820
7	1	28	39.9	86.855
7	1	1	43.4	81.388
8	1	35	27.0	93.059
8	1	29	30.1	94.600
8	1	28	40.1	80.562
8	1	27	50.1	79.847
8	1	1	53.2	80.020
9	1	35	18.0	90.639
9	1	30	20.2	92.379
9	1	29	30.4	82.060
9	1	1	35.3	77.530
10	1	35	26.2	88.298
10	1	29	30.5	81.944
10	1	1	38.9	77.908
11	1	0	0.0	-
11	1	33	4.9	80.204
11	1	32	9.9	79.099
11	1	35	13.2	87.528
11	1	29	29.7	90.626
11	1	28	40.3	94.868
11	1	27	50.1	89.677
11	1	26	76.0	82.175
11	1	1	93.6	74.609
12	1	0	0.0	-
12	1	33	5.5	88.461
12	1	32	10.0	88.584
12	1	35	12.2	88.139
12	1	30	20.4	94.675
12	1	29	30.5	92.075
12	1	28	40.8	94.740
12	1	27	50.1	91.775
12	1	26	75.5	93.310
12	1	25	100.3	92.631
12	1	24	125.6	90.744
12	1	1	143.9	86.924

Station	Cast	Bottle	Depth (dbar)	Trans (%)
13	1	0	0.0	-
13	1	33	5.4	93.153
13	1	35	8.1	93.692
13	1	32	10.8	94.588
13	1	23	150.0	90.922
13	1	22	175.8	92.913
13	1	21	200.5	83.061
13	1	20	225.4	79.687
13	1	19	251.9	78.536
13	1	1	300.3	74.441
13	1	34	300.5	73.663
14	2	0	0.0	-
14	2	34	5.1	94.784
14	2	36	16.9	92.564
14	2	32	20.7	92.115
15	1	36	14.9	94.168
15	1	27	125.2	93.984
15	1	26	149.9	93.668
15	1	20	399.9	90.065
15	1	1	466.8	89.556
16	1	0	0.0	-
16	1	35	5.0	88.924
16	1	36	6.9	88.871
16	1	34	10.1	90.180
16	1	32	29.7	93.487
16	1	30	50.0	91.757
16	1	29	75.0	90.820
16	1	28	100.3	87.822
16	1	27	125.4	87.113
16	1	26	150.1	87.692
16	1	25	175.1	90.351
16	1	1	204.6	90.362
17	1	22	250.1	92.951
17	1	21	299.6	90.988
17	1	1	363.8	89.498
19	1	1	181.2	94.840
20	2	36	14.8	93.698
20	2	33	20.1	90.235
31	2	32	30.1	91.895
32	2	27	125.2	94.542
37	1	33	20.6	94.529
38	1	1	245.1	94.631
39	1	36	18.3	93.144
39	1	33	20.3	94.899
39	1	32	30.4	86.113
39	1	31	40.3	85.568
39	1	1	61.2	88.641
40	1	0	0.0	-
40	1	35	5.3	89.857
40	1	34	10.6	89.331
40	1	36	14.6	91.304
40	1	33	20.5	90.748
40	1	32	30.3	92.158
40	1	31	40.2	65.271
40	1	30	49.8	56.836
40	1	1	52.5	51.944
41	1	0	0.0	-
41	1	35	5.0	82.882
41	1	34	10.1	89.312
41	1	32	30.0	77.319
41	1	31	40.2	76.563
41	1	1	47.6	75.525
42	1	0	0.0	-
42	1	35	5.2	89.183
42	1	34	10.3	91.699
42	1	36	18.1	93.600

Station	Cast	Bottle	Depth (dbar)	Trans (%)
42	1	33	19.9	89.729
42	1	32	30.0	77.918
42	1	31	40.0	65.519
42	1	1	44.3	63.790
43	1	0	0.0	-
43	1	35	5.1	85.915
43	1	34	10.3	86.637
43	1	36	15.2	86.238
43	1	33	20.3	85.730
43	1	32	30.0	85.179

Station	Cast	Bottle	Depth (dbar)	Trans (%)
43	1	31	40.1	86.126
43	1	1	49.8	85.839
44	1	0	0.0	-
44	1	35	5.0	90.460
44	1	34	10.1	90.576
44	1	33	20.4	90.784
44	1	32	30.3	91.936
44	1	31	40.3	84.356
44	1	1	44.5	79.090

(5) Station list

The sampling stations were listed as shown in Table 3.1.3.II-2.

Table 3.1.3.II-2 List of stations

Station	Cast	Date (UTC)	Position*		Depth (m)
		(mmddyy)	Latitude	Longitude	
001	1	090723	65-00.04N	-16-04.84E	50
002	1	090823	66-10.18N	-16-40.01E	55
003	2	090823	67-39.89N	-16-39.91E	50
004	1	090923	68-30.10N	-16-45.05E	53
005	1	090923	69-30.01N	-16-44.96E	51
006	1	090923	70-30.04N	-16-45.28E	39
007	1	090923	71-30.13N	-16-00.00E	49
008	1	091023	72-30.01N	-16-45.03E	59
009	1	091023	71-54.03N	-16-38.51E	41
010	1	091123	70-50.49N	-16-42.98E	44
011	1	091223	71-39.58N	-15-01.28E	98
012	1	091223	71-48.04N	-15-00.00E	149
013	1	091323	71-00.00N	-15-00.00E	303
014	2	091323	72-28.07N	-15-23.85E	1978
015	1	091423	71-56.36N	-15-46.36E	476
016	1	091423	71-41.41N	-15-42.97E	208
017	1	091523	71-18.68N	-15-28.55E	382
018	1	091523	71-03.91N	-14-56.44E	80
019	1	091523	70-49.00N	-14-25.04E	186
020	2	091623	70-50.96N	-14-03.19E	1201
021	2	091723	71-41.39N	-14-11.96E	3338
022	1	091723	73-09.97N	-14-09.82E	3603

023	1	091823	74-00.83N	-14-27.73E	3775
025	2	092023	74-21.62N	-15-29.90E	3853
027	1	092023	75-00.45N	-15-00.00E	1333
028	1	092123	75-38.65N	-16-44.74E	893
029	2	092123	77-02.39N	-15-22.16E	1544
030	1	092223	76-27.58N	-15-49.30E	1400
031	2	092223	76-57.03N	-16-18.61E	1999
032	2	092323	74-30.93N	-16-01.72E	1643
034	1	092523	74-46.01N	-17-03.79E	321
035	1	092623	75-07.78N	-17-13.71E	408
036	1	092723	75-19.71N	179-29.15E	604
037	1	092723	75-01.09N	-17-40.53E	287
038	1	092823	74-10.78N	-16-30.62E	251
039	1	092823	73-01.71N	-16-45.49E	67
040	1	092923	68-04.54N	-16-52.03E	59
041	1	093023	68-00.41N	-16-40.00E	53
042	1	093023	67-39.59N	-16-40.07E	50
043	1	093023	66-00.04N	-16-00.00E	55
044	1	093023	64-59.96N	-16-00.00E	50

* Position indicates latitude and longitude where CTD reached maximum depth at the cast.

(6) Certified Reference Material of nutrients in seawater

KANSO certified reference materials (CRMs, Lot: CQ, CR, CJ, CP) were used to ensure the comparability and traceability of nutrient measurements during this cruise. The details of CRMs are shown below.

Production

KANSO CRMs for inorganic nutrients in seawater were produced by KANSO Co.,Ltd. This CRM has been produced using autoclaved natural seawater based on the quality control system under ISO Guide 34 (JIS Q 0034).

KANSO Co.,Ltd. has been accredited under the Accreditation System of the National Institute of Technology and Evaluation (ASNITE) as a CRM producer since 2011. (Accreditation No.: ASNITE 0052 R)

Property value assignment

The certified values were the arithmetic means of the results of 30 bottles from each batch

(measured in duplicates) analyzed by both KANSO Co.,Ltd. and Japan Agency for Marine-Earth Science and Technology (JAMSTEC) using the colorimetric method (continuous flow analysis, CFA, method). The salinity of the calibration standards solution to obtain each calibration curve was adjusted to the salinity of the used CRMs within ± 0.5.

Metrological Traceability

Each certified value of nitrate, nitrite, and phosphate of KANSO CRMs was calibrated using one of the Japan Calibration Service System (JCSS) standard solutions for each nitrate ion, nitrite ion, and phosphate ion. JCSS standard solutions were calibrated using the secondary solution of JCSS for each of these ions. The secondary solution of JCSS was calibrated using the specified primary solution produced by Chemicals Evaluation and Research Institute (CERI), Japan. CERI-specified primary solutions were calibrated using the National Metrology Institute of Japan (NMIJ) primary standards solution of nitrate ions, nitrite ions and phosphate ions, respectively.

The certified value of silicate of KANSO CRM except for CRM lot CJ was calibrated using a newly established silicon standards solution named “exp64” produced by JAMSTEC and KANSO and Lot. AA produced by KANSO. This silicon standard solution was produced by a dissolution technique with an alkaline solution. The mass fraction of Si in the produced solution was calibrated based on NMIJ CRM 3645-a Si standard solution by a technology consulting system of the National Institute of Advanced Industrial Science and Technology (AIST), and this value is traceable to the International System of Units (SI). The reported silicate value of CRM lot CJ was determined by silicon standard solution 1000 mg L^{-1} provided by Merck, Lot HC54715536, which is traceable to the National Institute of Standards and Technology (NIST) silicon standard reference material (SRM) 3150.

The certified values of nitrate, nitrite, and phosphate of KASNO CRM are thus traceable to the SI through the unbroken chain of calibrations, JCSS, CERI and NMIJ solutions as stated above, each having stated uncertainties. The certified values of silicate of KANSO CRM are traceable to the SI through the unbroken chain of calibrations, NMIJ CRM 3645-a Si standard solution, having stated uncertainties.

As stated in the certificate of NMIJ CRMs, each certified value of dissolved silica, nitrate ions, and nitrite ions was determined by more than one method using one of NIST SRM of silicon standard solution and NMIJ primary standards solution of nitrate ions and nitrite ions. The concentration of phosphate ions as stated information value in the certificate was determined NMIJ primary standards solution of phosphate ions. Those values in the certificate of NMIJ CRMs are traceable to the SI.

One of the analytical methods used for certification of NMIJ CRM for nitrate ions, nitrite

ions, phosphate ions and dissolved silica was a colorimetric method (continuous mode and batch mode). The colorimetric method is the same as the analytical method (continuous mode only) used for certification of KANSO CRM. For certification of dissolved silica, exclusion chromatography/isotope dilution-inductively coupled plasma mass spectrometry and ion exclusion chromatography with post-column detection was used. For certification of nitrate ions, ion chromatography by direct analysis and ion chromatography after halogen-ion separation was used. For certification of nitrite ions, ion chromatography by direct analysis was used.

NMIJ CRMs were analyzed at the time of certification process for CRM and the results were confirmed within expanded uncertainty stated in the certificate of NMIJ CRMs.

(6.1) CRM for this cruise

19 sets of CRM lots CQ, CR, CJ, and CP were used, which almost cover a range of nutrients concentrations in the Arctic Ocean.

Each CRM's serial number was randomly selected. The CRM bottles were stored at a room named "BIOCHEMICAL LABORATORY" on the ship, where the temperature was maintained around 19.13 degree Celsius – 22.29 degree Celsius.

(6.2) CRM concentration

Nutrients concentrations for the CRM lots CQ, CR, CJ, and CP were shown in Table 3.1.3.II-3.

Table 3.1.3.II-3 Certified concentration and the uncertainty (k=2) of CRMs.

unit: μmol kg^{-1}

Lot	Nitrate	Nitrite*	Silicate	Phosphate	Ammonia**
CQ	0.06 ± 0.03	0.074 ± 0.070	2.20 ± 0.07	0.030 ± 0.009	1.76
CR	5.46 ± 0.16	0.975 ± 0.070	14.00 ± 0.3	0.394 ± 0.014	0.95
CJ	16.20 ± 0.20	0.053 ± 0.007	38.50 ± 0.40	1.190 ± 0.020	0.77
CP	24.8 ± 0.3	0.318 ± 0.070	61.1 ± 0.3	1.753 ± 0.018	0.87

* For Nitrite concentration, there is a trend that the value has been increased 0.004 ± 0.002 μmol kg^{-1} per year. Nitrite concentration values were determined in June 2023.

**Ammonia values are all reference value. The values of CQ and CR were reported by KANSO. The other reported values were determined by JAMSTEC.

(7) Nutrients standards

(7.1) Volumetric laboratory-ware of in-house standards

All volumetric glassware and polymethylpentene (PMP)-ware used were gravimetrically

calibrated. Plastic volumetric flasks were gravimetrically calibrated at the water temperature of use within 1 K at around 20 degree Celsius.

(7.1.1) Volumetric flasks

Volumetric flasks of Class quality (Class A) are used because their nominal tolerances are 0.05 % or less over the size ranges likely to be used in this work. Since Class A flasks are made of borosilicate glass, the standard solutions were transferred to plastic bottles as quickly as possible after the solutions were made up to volume and well mixed in order to prevent the excessive dissolution of silicate from the glass. PMP volumetric flasks were gravimetrically calibrated and used only within 1.3 K of the calibration temperature.

The computation of volume contained by the glass flasks at various temperatures other than the calibration temperatures were conducted by using the coefficient of linear expansion of borosilicate crown glass.

The coefficient of cubical expansion of each glass and PMP volumetric flask was determined by actual measurement in 2023. The coefficient of cubical expansion of glass volumetric flask (SHIBATA HARIO) was 0.00000975 to 0.0000172 K^{-1} and that of PMP volumetric flask (NALGEN PMP) was 0.00038 to 0.00042 K^{-1}. The weights obtained in the calibration weightings were corrected for the density of water and air buoyancy.

(7.1.2) Pipettes

All glass pipettes have nominal calibration tolerances of 0.1 % or better. These were gravimetrically calibrated to verify and improve upon this nominal tolerance.

(7.2) Reagents, general considerations

(7.2.1) Specifications

For nitrate standard, “potassium nitrate 99.995 suprapur®” provided by Merck, Batch B1983565, CAS No. 7757-79-1, was used.

For nitrite standard solution, we used a nitrite ion standard solution (NO_2^- 1000) provided by Wako, Lot TPH2043, Code. No. 146-06453. This standard solution was certified by Wako using the ion chromatography method. Calibration result is 1004 mg L^{-1} at 20 degree Celsius. Expanded uncertainty of calibration (k=2) is 0.8 % for the calibration result.

For the silicate standard solution, we used Si standard solution Lot. AA which was produced by alkali fusion technique from 5N SiO_2 powder produced by KANSO. The mass fraction of Si in the Lot. AA solution was calibrated based on NMIJ CRM 3645-a03 Si standard solution.

For phosphate standard, we used a potassium dihydrogen phosphate anhydrous 99.995

suprapur®" provided by Merck, Batch B2015508, CAS No.: 7778-77-0.

For ammonia standard, ammonium chloride (CRM 3011-a) provided by NMIJ, CAS No. 12125-02-9 was used. The purity of this standard was reported as >99.9 % by the manufacture. Expanded uncertainty of calibration (k=2) was 0.026 %.

(7.2.2) Ultra-pure water

Ultra-pure water (Milli-Q water) freshly drawn was used for the preparation of reagents, standard solutions and for measurements of the reagent and the system blanks.

(7.2.3) Low nutrients seawater (LNSW)

Surface water having low nutrient concentration was taken and filtered using a 0.20 μm pore capsule cartridge filter around 13N and 136E during the MR21-03 cruise in June 2021. Obtained seawater was drained into multiple 20 L Cubitainer (flexible containers) and stored in a cardboard box.

The concentrations of each nutrient in LNSW were measured in June 2020. The averaged nutrient values in the LNSW were 0.01 μmol L^{-1} for nitrate, 0.003 μmol L^{-1} for nitrite, 1.08 μmol L^{-1} for silicate, 0.075 μmol L^{-1} for phosphate and 0.01 μmol L^{-1} for ammonia. The concentrations of nitrate, nitrite and ammonia were lower than the detection limit as stated in Chapter (8.5).

(7.2.4) Concentrations of nutrients for A, D, B and C standards

Concentrations of nutrients for A, D, B and C standards were adjusted as shown in Table 3.1.3.II-4.

We used the KANSO Si standard solution for A standard of silicate, which doesn't need to be neutralized by the hydrochloric acid. B standard was diluted from A standard with the following recipes shown in Table 3.1.3.II-5. In order to match the salinity and the density of the stock solution (B standard) to the LNSW, during this dilution step, 15.00 g of sodium chloride powder was dissolved in B standard, and then the final volume was adjusted to 500 mL.

The C standard solution was prepared in the LNSW following the recipes shown in Table 3.1.3.II-6. All volumetric laboratory tools were calibrated prior the cruise as stated in chapter (7.1). Then the actual concentrations of nutrients in each fresh standard solution were calculated based on the solution temperature, together with the determined factors of volumetric laboratory wares.

The calibration curves for each run for nitrate, nitrite, silicate and phosphate were obtained using 6 levels, C-1, C-2, C-3, C-4, C-6 and C-7. For ammonia, that was obtained using 3 levels, C-1, C-5, C-7. C-2, C-3, C-4 and C-6 were the CRM of nutrients in seawater, C-5 and C-7 were diluting using the B standard solution, and C-1 was LNSW.

The D standard solutions were made to calculate the reduction rate of Cd coil. The D

standard was diluted from the A standard solution into the pure water.

Table 3.1.3.II-4 Nominal concentrations of nutrients for A, D, B and C standards.

unit: μmol L^{-1}

	A	B	D	C-1	C-2	C-3	C-4	C-5	C-6	C-7
NO_3	22500	675	900	LNSW	CQ	CR	CJ	-	CP	40.5
NO_2	21800	26	870	LNSW	CQ	CR	CJ	-	CP	1.57
SiO_2	35500	1420		LNSW	CQ	CR	CJ	-	CP	85
PO_4	6000	60		LNSW	CQ	CR	CJ	-	CP	3.6
NH_4	4000	160		LNSW	-	-	-	4.8	-	9.6

Table 3.1.3.II-5 B standard recipes. The final volume was 500 mL.

	A Std.
NO_3	15 mL
NO_2*	15 mL
SiO_2	20 mL
PO_4	5 mL
NH_4	20 mL

*NO2 was D standard solution which was diluted from A standard.

Table 3.1.3.II-6 Working calibration standard recipes. The final volume was 500 mL.

C Std.	B Std.
C-5	15 mL
C-7	30 mL

(7.2.5) Renewal of in-house standard solutions

In-house standard solutions as stated in paragraph (7.2.4) were remade by each “renewal time” shown in Table 3.1.3.II-7(a) to (c).

Table 3.1.3.II-7(a) Timing of renewal of in-house standards.

NO_3, NO_2, SiO_2, PO_4, NH_4	Renewal time

A-1 Std. (NO_3)	maximum a month
A-2 Std. (NO_2)	commercial prepared solution
A-3 Std. (SiO_2)	commercial prepared solution
A-4 Std. (PO_4)	maximum a month
A-5 Std. (NH_4)	maximum a month
D-1 Std.	maximum 8 days
D-2 Std.	maximum 8 days
B Std. (mixture of A-1, D-2, A-3, A-4 and A-5 std.)	maximum 8 days

Table 3.1.3.II-7(b) Timing of renewal of working calibration standards.

Working standards	Renewal time
C Std. (diluted from B Std.)	every 24 hours

Table 3.1.3.II-7(c) Timing of renewal of in-house standards for reduction estimation.

Reduction estimation	Renewal time
36 μM NO_3 (diluted D-1 Std.)	when C Std. renewed
35 μM NO_2 (diluted D-2 Std.)	when C Std. renewed

(8) Quality control

(8.1) The precision of the nutrient analyses during the cruise

The highest standard solution (C-7) was repeatedly determined every 5 to 15 samples to obtain the analytical precision of the nutrient analyses during this cruise. During each run, the total number of the C-7 determination was 5-13 times depending on the run. Each run, we obtained the analytical precision based on this C-7 results, shown in Figures 3.1.3.II-7 to3.1.3.II-11. In this cruise, there was total 25 runs. The analytical precisions were less than 0.2 % for nitrate, silicate, and phosphate.

The overall precisions throughout this cruise were calculated based on the analytical precisions obtained from all of the runs, and shown in Table 3.1.3.II-8. During this cruise, overall median precisions were 0.09 % for nitrate, 0.14 % for nitrite, 0.11 % for silicate, 0.10 % for phosphate and 0.38 % for ammonia, respectively. The overall median precision for each parameter during this cruise was comparable to the previously published the precisions during the R/V Mirai cruises conducted in 2009 - 2022.

Table 3.1.3.II-8 Summary of overall precision based on the replicate analyses (*k*=1)

	Nitrate CV %	Nitrite CV %	Silicate CV %	Phosphate CV %	Ammonia CV %
Median	0.09	0.14	0.11	0.10	0.38
Mean	0.09	0.13	0.11	0.10	0.40
Maximum	0.14	0.20	0.19	0.15	0.73
Minimum	0.05	0.06	0.06	0.04	0.15
n	25	25	25	24	24

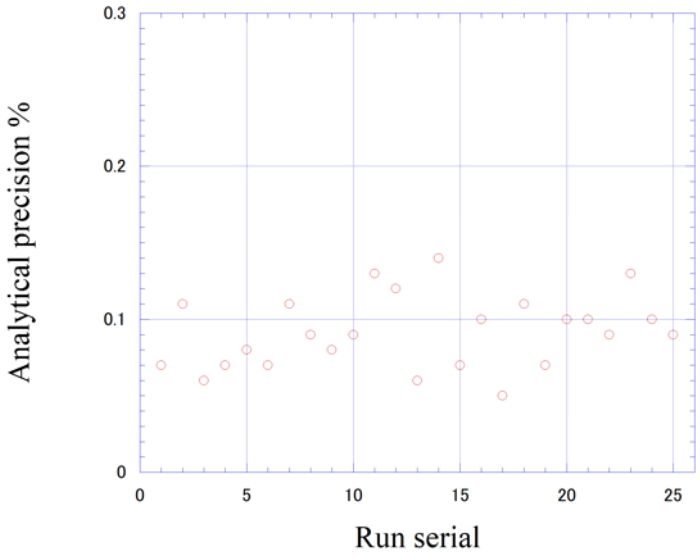

Figure 3.1.3.II-7 Time series of precision of nitrate in this cruise.

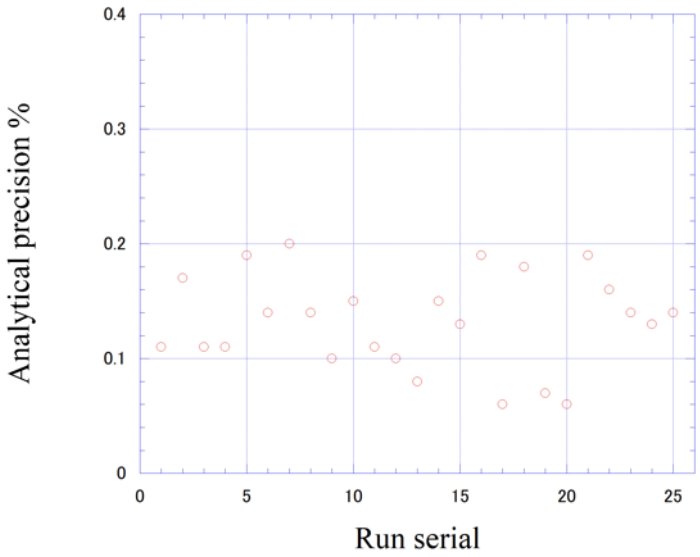

Figure 3.1.3.II-8 same as 3.1.3.II-7 but for nitrite.

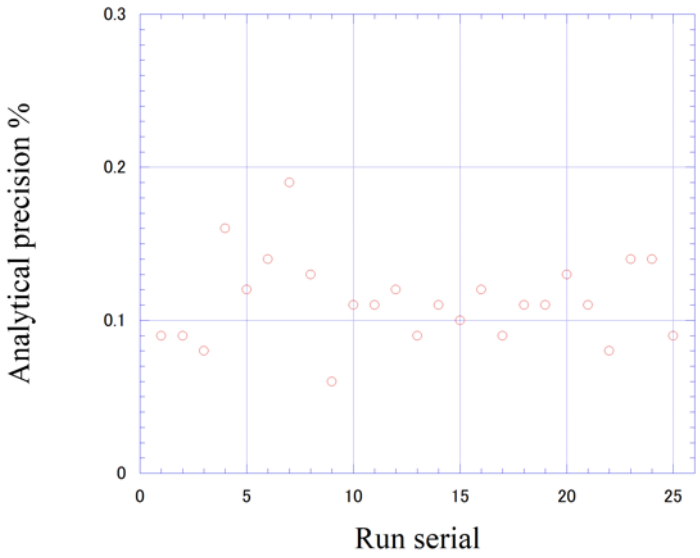

Figure 3.1.3.II-9 same as 3.1.3.II-7 but for silicate.

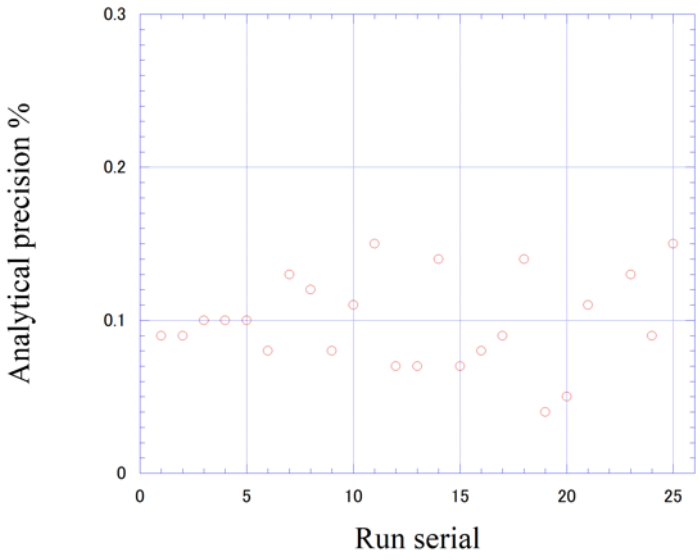

Figure 3.1.3.II-10 same as 3.1.3.II-7 but for phosphate.

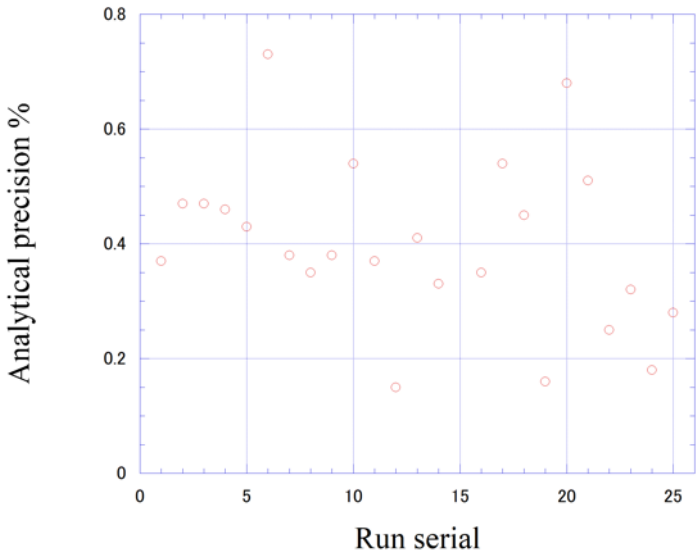

Figure 3.1.3.II-11 same as 3.1.3.II-7 but for ammonia.

(8.2) CRM lot. CP measurement during this cruise

CRM lot. CP was measured every run to evaluate the comparability throughout the cruise. All of the results of the lot. CP during this cruise were shown in Figures 3.1.3.II-12 to 3.1.3.II-16. All of the measured concentrations of CRM lot. CP was within the uncertainty of certified values for nitrate, nitrite, silicate and phosphate. The reported CRM values were shown in Table 3.1.3.II-3.

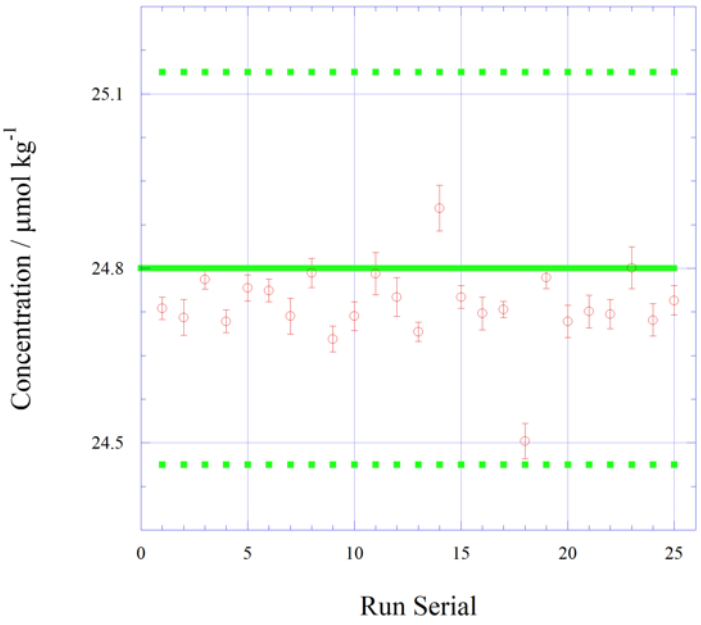

Figure 3.1.3.II-12 Time series of CRM-CP of nitrate in this cruise. Solid green line is certified nitrate concentration of CRM and broken green line show uncertainty of certified value at k=2.

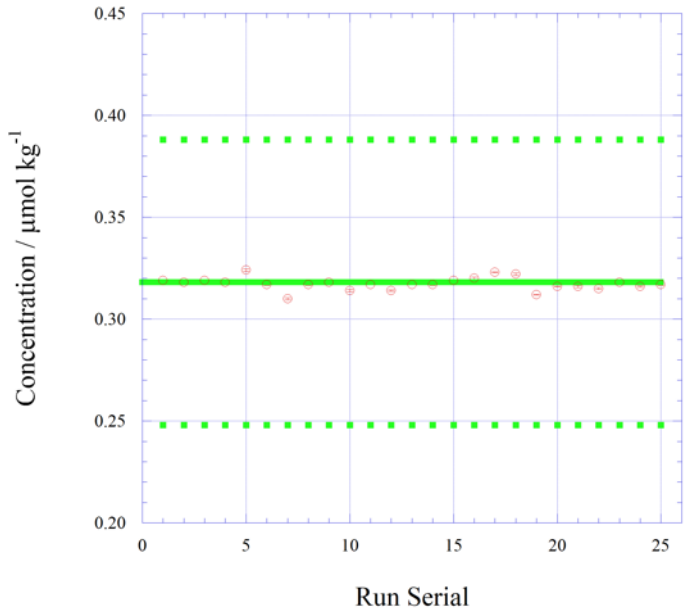

Figure 3.1.3.II-13 Same as Figure 3.1.3.II-12, but for nitrite.

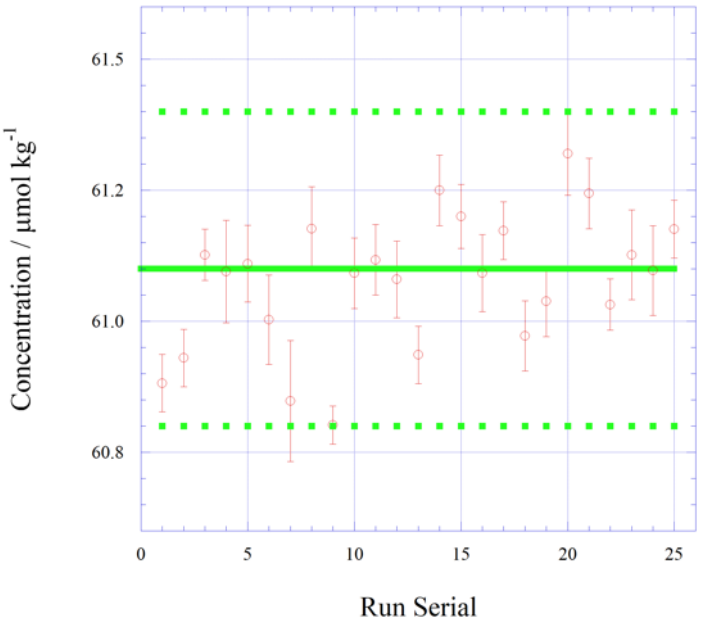

Figure 3.1.3.II-14 Same as Figure 3.1.3.II-12, but for silicate.

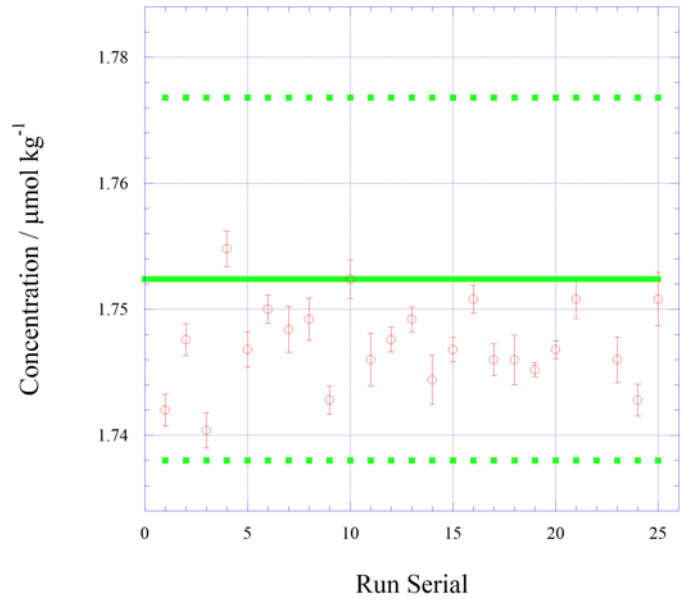

Figure 3.1.3.II-15 Same as Figure 3.1.3.II-12, but for phosphate.

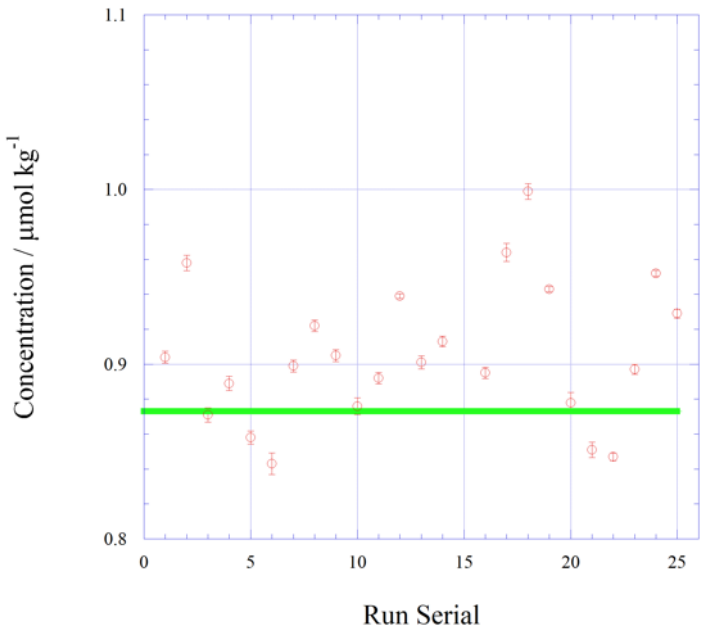

Figure 3.1.3.II-16 Time series of CRM-CP of ammonia in this cruise. Solid green line is reference value for ammonia concentration of CRM-CP.

(8.3) Carryover

We also summarized the magnitudes of carry over throughout the cruise. In order to evaluate carryover in each run, we performed C-7 determinations, followed by two consecutive runs of the LNSW solution. The difference from LNSW-1 to LNSW-2 was obtained and used for this “carryover” evaluation. The Carryover (%) was obtained from the following equation.

Carryover (%) = (LNSW-1 – LNSW-2) / (C-7 – LNSW-2) * 100 (%)

The summary of the carryover (%) was shown in Table 3.1.3.II-9 and Figure 3.1.3.II-17 to 3.1.3.II-21. Overall results were low % of carryover (<0.2 % for nitrite and phosphate; <0.3 % for nitrate and silicate; <1 % for ammonia), but occasionally we detected slightly higher carryover (%) for ammonia measurement, and it might have affected the obtained values of CRM, more detail is stated in Chapter (9).

Table 3.1.3.II-9 Summary of carryover throughout this cruise.

	Nitrate %	Nitrite %	Silicate %	Phosphate %	Ammonia %
Median	0.22	0.15	0.25	0.14	0.86
Mean	0.22	0.16	0.24	0.15	0.99
Maximum	0.25	0.42	0.34	0.32	1.81
Minimum	0.17	0.00	0.16	0.02	0.62
n	25	25	25	25	25

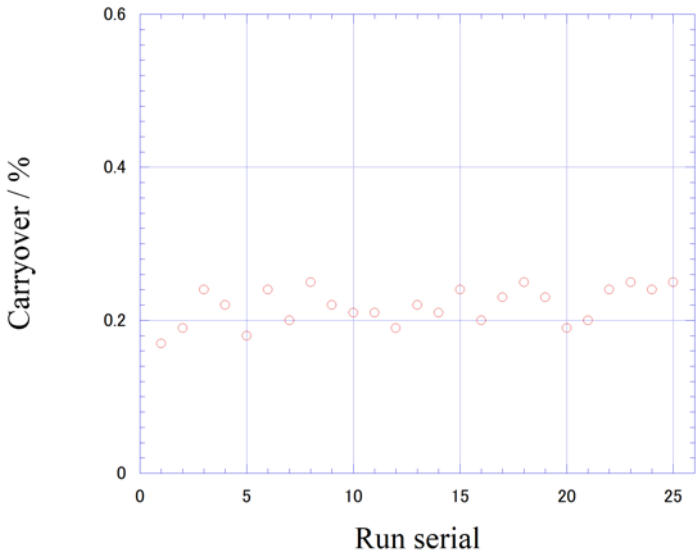

Figure 3.1.3.II-17 Time series of carryover of nitrate in MR23-06C.

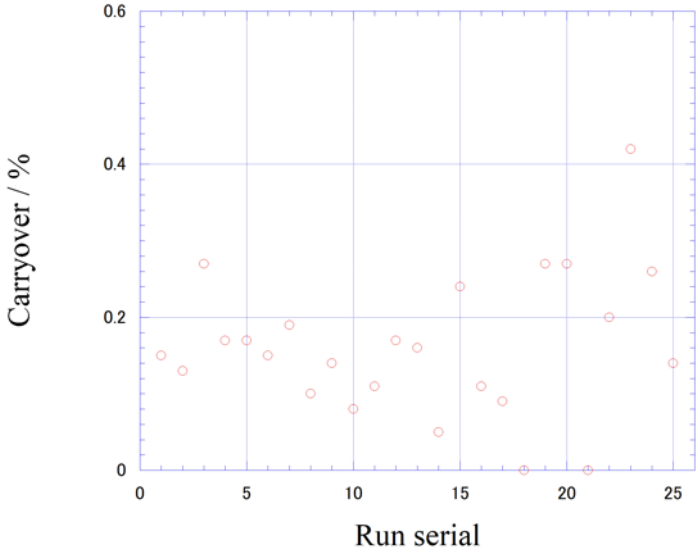

Figure 3.1.3.II-18 same as 3.1.3.II-17 but for nitrite.

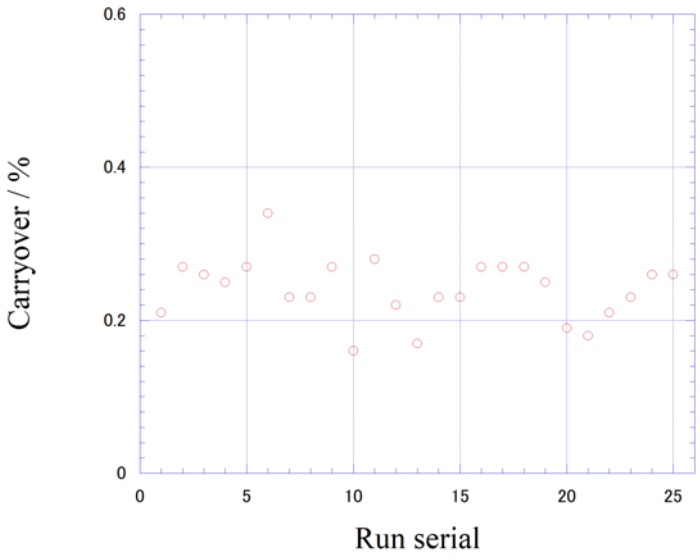

Figure 3.1.3.II-19 same as 3.1.3.II-17 but for silicate

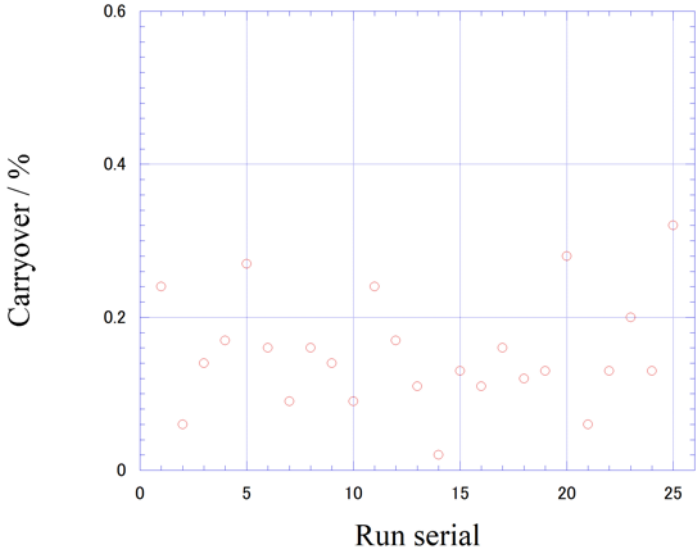

Figure 3.1.3.II-20 same as 3.1.3.II-17 but for phosphate.

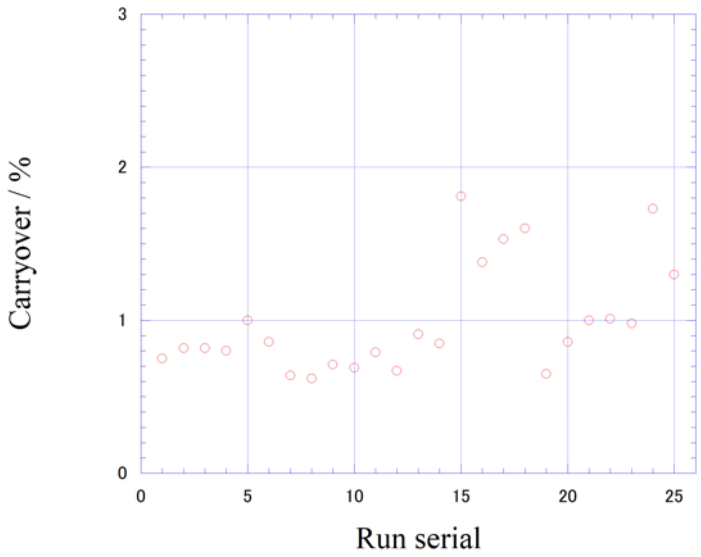

Figure 3.1.3.II-21 same as 3.1.3.II-17 but for ammonia.

(8.4) Estimation of uncertainty of nitrate, silicate, phosphate, nitrite and ammonia concentrations

Empirical equations, eq. (1), (2) and (3) to estimate the uncertainty of measurement of nitrate, silicate and phosphate were obtained based on 25 measurements of 19 sets of CRMs (Table 3.1.3.II-3). These empirical equations are as follows, respectively.

Nitrate Concentration C_{NO3} in μmol kg^{-1}:

Uncertainty of measurement of nitrate (%) = 0.19581+ 1.10120 * (1 / C_{NO3}) --- (1)

where C_{NO3} is nitrate concentration of sample.

Silicate Concentration C_{SiO2} in μmol kg^{-1}:

Uncertainty of measurement of silicate (%) = 0.20654 + 2.25950 * (1 / C_{SiO2}) --- (2)

where C_{SiO2} is silicate concentration of sample.

Phosphate Concentration C_{PO4} in μmol kg^{-1}:

Uncertainty of measurement of phosphate (%) = –0.029888 + 0.35848 * (1 / C_{PO4}) --- (3)

where C_{PO4} is phosphate concentration of sample.

Empirical equations, eq. (4) and (5) to estimate the uncertainty of measurement of nitrite and ammonia were obtained based on duplicate measurements of the samples.

Nitrite Concentration C_{NO2} in µmol kg^{-1}:

Uncertainty of measurement of nitrite (%) =

$$-0.32649 + 0.25813 * (1 / C_{NO2}) - 0.00025314 * (1 / C_{NO2}) * (1 / C_{NO2}) \quad \text{--- (4)}$$

where C_{NO2} is nitrite concentration of sample.

Ammonia Concentration C_{NH4} in µmol kg^{-1}:

Uncertainty of measurement of ammonia (%) =

$$0.54214 + 1.3367 * (1 / C_{NH4}) - 0.023133 * (1 / C_{NH4}) * (1 / C_{NH4}) \quad \text{-- (5)}$$

where C_{NH4} is ammonia concentration of sample.

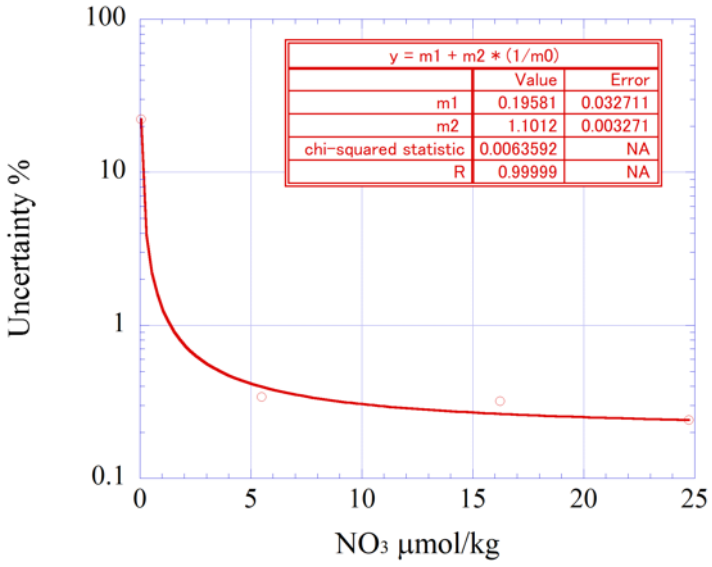

Figure 3.1.3.II-22 Estimation of uncertainty for nitrate.

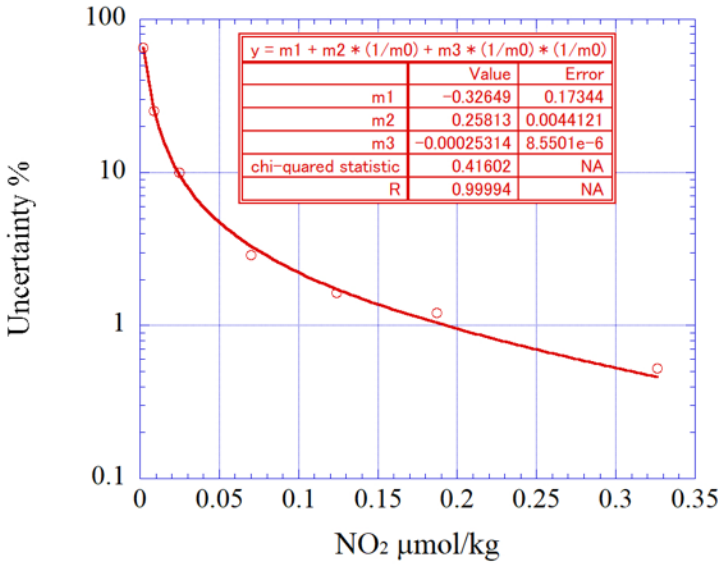

Figure 3.1.3.II-23 Estimation of uncertainty for nitrite.

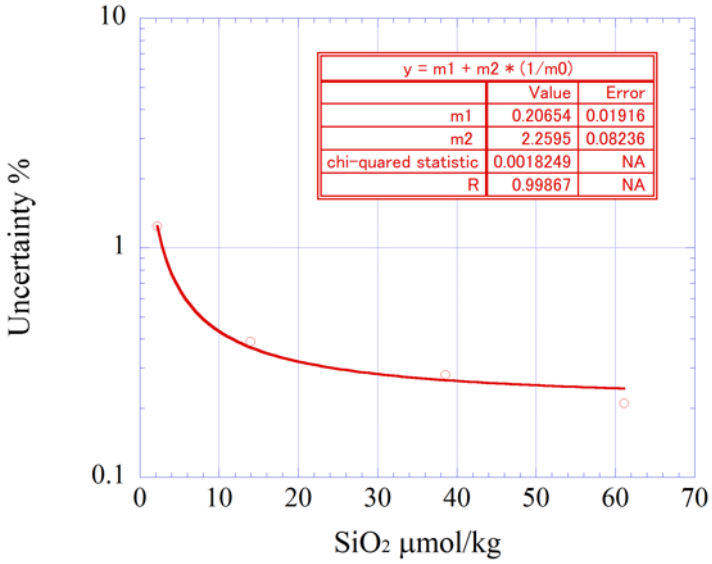

Figure 3.1.3.II-24 Estimation of uncertainty for silicate.

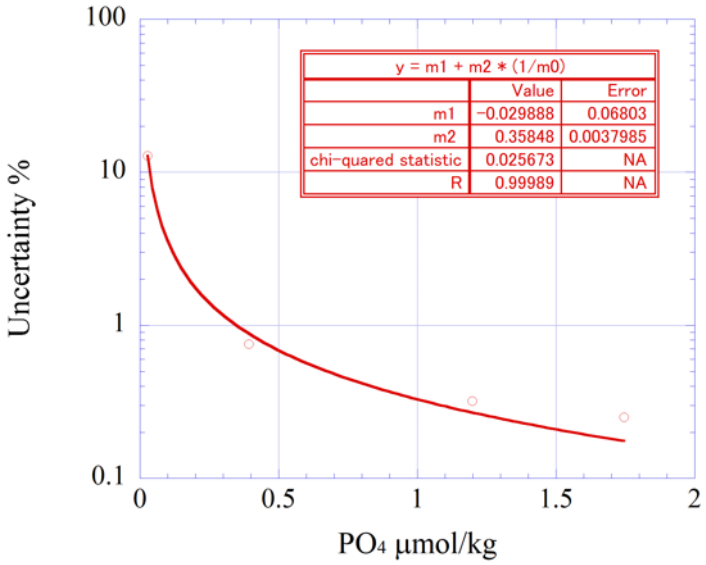

Figure 3.1.3.II-25 Estimation of uncertainty for phosphate.

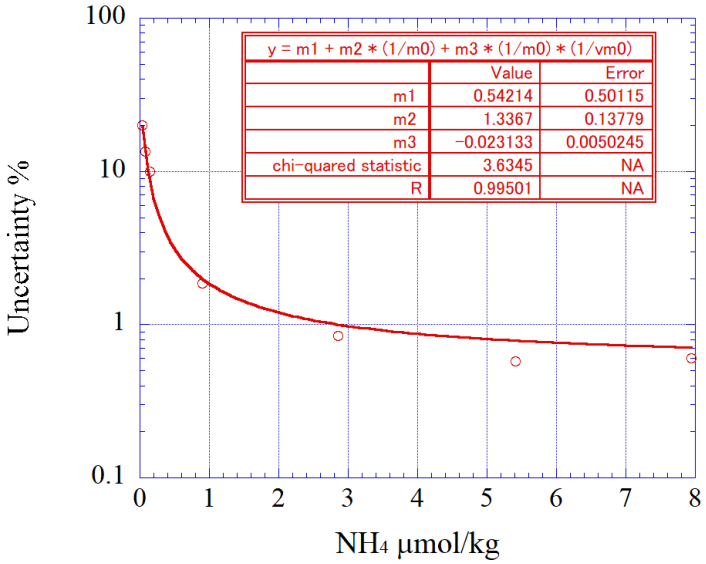

Figure 3.1.3.II-26 Estimation of uncertainty for ammonia.

(8.5) Detection limit and quantitative determination of nutrients analyses during the cruise

The LNSW was determined every 5 to 15 samples to obtain detection limit of the nutrient

analyses during this cruise. During each run, the total number of the LNSW determination was 7-15 times depending on the run. The detection limit was calculated based on the LNSW results obtained from all the runs by the following equation.

Detection limit = 3 * standard deviation of repeated measurement of LNSW

The summary of the detection limit was shown in Table 3.1.3.II-10. During this cruise, the detection limit is 0.01 μmol kg^{-1} for nitrate, 0.003 μmol kg^{-1} for nitrite, 0.05 μmol kg^{-1} for silicate, 0.005 μmol kg^{-1} for phosphate and 0.02 μmol kg^{-1} for ammonia, respectively.

The quantitative determination of nutrient analyses is the concentration of which uncertainty is 33 % in the empirical equations, eq. (1) to (5) in chapter (8.4). The summary of quantitative determination was shown in Table 3.1.3.II-10. During in this cruise, the quantitative determination was 0.03 μmol kg^{-1} for nitrate, 0.010 μmol kg^{-1} for nitrite, 0.07 μmol kg^{-1} for silicate, 0.011 μmol kg^{-1} for phosphate and 0.20 μmol kg^{-1} for ammonia, respectively.

Replicate samples were taken at all of the layers. The summary of average and standard deviation of the difference between each pair of analysis was shown in Table 3.1.3.II-11. During this cruise, average of the difference between each pair of analyses were 0.01 μmol kg^{-1} for nitrate, 0.003 μmol kg^{-1} for nitrite, 0.05 μmol kg^{-1} for silicate, 0.004 μmol kg^{-1} for phosphate and 0.02 μmol kg^{-1} for ammonia, respectively. Standard deviation of the difference between each pair of analyses were 0.01 μmol kg^{-1} for nitrate, 0.003 μmol kg^{-1} for nitrite, 0.05 μmol kg^{-1} for silicate, 0.004 μmol kg^{-1} for phosphate and 0.02 μmol kg^{-1} for ammonia, respectively.

Table 3.1.3.II-10 Summary of detection limit and quantitative determination.

	Nitrate μmol kg^{-1}	Nitrite μmol kg^{-1}	Silicate μmol kg^{-1}	Phosphate μmol kg^{-1}	Ammonia μmol kg^{-1}
Detection limit	0.01	0.003	0.05	0.005	0.02
Quantitative determination	0.03	0.010	0.07	0.011	0.20

Table 3.1.3.II-11 Summary of average and standard deviation of the difference between each pair of analysis.

	Nitrate μmol kg^{-1}	Nitrite μmol kg^{-1}	Silicate μmol kg^{-1}	Phosphate μmol kg^{-1}	Ammonia μmol kg^{-1}
Average	0.01	0.003	0.05	0.004	0.02
Standard deviation	0.01	0.003	0.05	0.004	0.02

n	595	584	595	590	583

(9) Problems and our actions/solutions

Overall obtained result of the CRM for ammonia measurements (CQ: 1.81 ± 0.03 μmol kg^{-1}; CR: 1.00 ± 0.03 μmol kg^{-1}) was within the uncertainty range of the reported reference values (CQ: 1.76 ± 0.07 μmol kg^{-1}; CR: 0.95 ± 0.15 μmol kg^{-1}, KANSO). However, some results exceeded the uncertainty range slightly but significantly (Figure 3.1.3.II-27, 3.1.3.II-28). It might be because the ammonium value in CRM becomes higher over the storage period due to the lack of refrigeration. Moreover, we observed that the analysis date for those measurements indicated a slightly increased Carryover %. it became apparent that there was a possibility of an error, resulting in an overestimated carryover effect on the baseline value. As a result, we have re-calculated the baseline values for the specified dates (Run serials: 14, 16, 17, 18, and 25).

The current analysis of ammonia determination consists of three standard calibration points (7.2.4), and in order to improve the quantitative determination at low values, an additional lower calibration point should be added in future work.

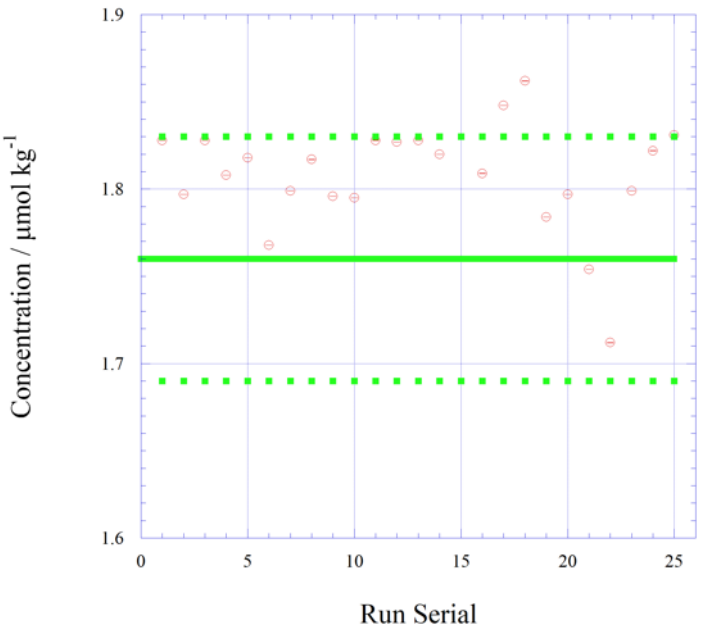

Figure 3.1.3.II-27 Time series of CRM-CQ of ammonia in this cruise. Solid green line is referenced ammonia concentration of CRM and broken green line show uncertainty of referenced value at k=2.

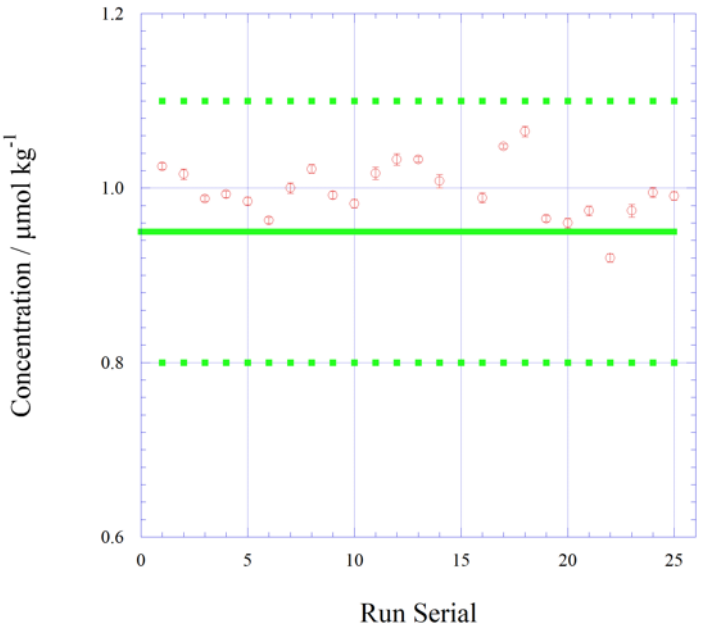

Figure 3.1.3.II-28 Time series of CRM-CR of ammonia in this cruise. Solid green line is referenced ammonia concentration of CRM and broken green line show uncertainty of referenced value at k=2.

(10) List of reagents

List of reagents is shown in Table 3.1.3.II-12.

Table 3.1.3.II-12 List of reagent in this cruise.

IUPAC name	CAS Number	Formula	Compound Name	Manufacture	Grade
4-Aminobenzenesulfonamide	63-74-1	$C_6H_8N_2O_2S$	Sulfanilamide	FUJIFILM Wako Pure Chemical Corporation	JIS Special Grade
Ammonium chloride	12125-02-9	NH_4Cl	Ammonium Chloride	FUJIFILM Wako Pure Chemical Corporation	JIS Special Grade
Antimony potassium tartrate trihydrate	28300-74-5	$K_2(SbC_4H_2O_6)_2 \cdot 3H_2O$	Bis[(+)-tartrato]diantimonate(III) Dipotassium Trihydrate	FUJIFILM Wako Pure Chemical Corporation	JIS Special Grade
Boric acid	10043-35-3	H_3BO_3	Boric Acid	FUJIFILM Wako Pure Chemical Corporation	JIS Special Grade
Hydrogen chloride	7647-01-0	HCl	Hydrochloric Acid	FUJIFILM Wako Pure Chemical Corporation	JIS Special Grade
Imidazole	288-32-4	$C_3H_4N_2$	Imidazole	FUJIFILM Wako Pure Chemical Corporation	JIS Special Grade
L-Ascorbic acid	50-81-7	$C_6H_8O_6$	L-Ascorbic Acid	FUJIFILM Wako Pure Chemical Corporation	JIS Special Grade
N-(1-Naphthalenyl)-1,2-ethanediamine, dihydrochloride	1465-25-4	$C_{12}H_{16}Cl_2N_2$	N-1-Naphthylethylenediamine Dihydrochloride	FUJIFILM Wako Pure Chemical Corporation	for Nitrogen Oxides Analysis
Oxalic acid	144-62-7	$C_2H_2O_4$	Oxalic Acid	FUJIFILM Wako Pure Chemical Corporation	Wako Special Grade
Phenol	108-95-2	C_6H_6O	Phenol	FUJIFILM Wako Pure Chemical Corporation	JIS Special Grade
Potassium nitrate	7757-79-1	KNO_3	Potassium Nitrate	Merck KGaA	Suprapur®
Potassium dihydrogen phosphate	7778-77-0	KH_2PO_4	Potassium dihydrogen phosphate anhydrous	Merck KGaA	Suprapur®
Sodium chloride	7647-14-5	NaCl	Sodium Chloride	FUJIFILM Wako Pure Chemical Corporation	TraceSure®
Sodium citrate dihydrate	6132-04-3	$Na_3C_6H_5O_7 \cdot 2H_2O$	Trisodium Citrate Dihydrate	FUJIFILM Wako Pure Chemical Corporation	JIS Special Grade
Sodium dodecyl sulfate	151-21-3	$C_{12}H_{25}NaO_4S$	Sodium Dodecyl Sulfate	FUJIFILM Wako Pure Chemical Corporation	for Biochemistry
Sodium hydroxide	1310-73-2	NaOH	Sodium Hydroxide for Nitrogen Compounds Analysis	FUJIFILM Wako Pure Chemical Corporation	for Nitrogen Analysis
Sodium hypochlorite	7681-52-9	NaClO	Sodium Hypochlorite Solution	Kanto Chemical co., Inc.	Extra pure
Sodium molybdate dihydrate	10102-40-6	$Na_2MoO_4 \cdot 2H_2O$	Disodium Molybdate(VI) Dihydrate	FUJIFILM Wako Pure Chemical Corporation	JIS Special Grade
Sodium nitroferricyanide dihydrate	13755-38-9	$Na_2[Fe(CN)_5NO] \cdot 2H_2O$	Sodium Pentacyanonitrosylferrate(III) Dihydrate	FUJIFILM Wako Pure Chemical Corporation	JIS Special Grade
Sulfuric acid	7664-93-9	H_2SO_4	Sulfuric Acid	FUJIFILM Wako Pure Chemical Corporation	JIS Special Grade
tetrasodium;2-[2-[bis(carboxylatomethyl)amino]ethyl-(carboxylatomethyl)amino]acetate;tetrahydrate	13235-36-4	$C_{10}H_{12}N_2Na_4O_8 \cdot 4H_2O$	Ethylenediamine-N,N,N',N'-tetraacetic Acid Tetrasodium Salt Tetrahydrate (4NA)	Dojindo Molecular Technologies, Inc.	-
Synonyms: t-Octylphenoxypolyethoxyethanol 4-(1,1,3,3-Tetramethylbutyl)phenyl-polyethylene glycol Polyethylene glycol tert-octylphenyl ether	9002-93-1	$(C_2H_4O)_nC_{14}H_{22}O$	Triton®X-100	MP Biomedicals, Inc.	-

(11) Data archives

These data obtained in this cruise will be submitted to the Data Management Group of JAMSTEC, and will be opened to the public via “Data Research System for Whole Cruise Information in JAMSTEC (DARWIN)” in JAMSTEC web site.

<http://www.godac.jamstec.go.jp/darwin/e>

(12) References

Becker, S., Aoyama, M., Malcolm E., Woodward, S., Bakker, K., Coverly, S., Mahaffey, C., Tanhua, T., (2019) The precise and accurate determination of dissolved inorganic nutrients in seawater, using Continuous Flow Analysis methods, n: The GO-SHIP Repeat Hydrography Manual: A Collection of Expert Reports and Guidelines. Available online at: http://www.go-ship.org/HydroMan.html. DOI: http://dx.doi.org/10.25607/OBP-555

Grasshoff, K. (1976). Automated chemical analysis (Chapter 13) in Methods of Seawater Analysis. With contribution by Almgreen T., Dawson R., Ehrhardt M., Fonselius S. H., Josefsson B., Koroleff F., Kremling K. Weinheim, New York: Verlag Chemie.

Grasshoff, K., Kremling K., Ehrhardt, M. et al. (1999). Methods of Seawater Analysis. Third, Completely Revised and Extended Edition. WILEY-VCH Verlag GmbH, D-69469 Weinheim (Federal Republic of Germany).

Hydes, D.J., Aoyama, M., Aminot, A., Bakker, K., Becker, S., Coverly, S., Daniel, A., Dickson, A.G., Grosso, O., Kerouel, R., Ooijen, J. van, Sato, K., Tanhua, T., Woodward, E.M.S., Zhang, J.Z., (2010). Determination of Dissolved Nutrients (N, P, Si) in Seawater with High Precision and Inter-Comparability Using Gas-Segmented Continuous Flow Analysers, In: GO-SHIP Repeat Hydrography Manual: A Collection of Expert Reports and Guidelines. IOCCP Report No. 14, ICPO Publication Series No 134.

Kimura (2000). Determination of ammonia in seawater using a vaporization membrane permeability method. 7th auto analyzer Study Group, 39-41.

Murphy, J., and Riley, J.P. (1962). Analytica Chimica Acta 27, 31-36.

3.1.3.III. Dissolved inorganic carbon

(a) Bottled-water analysis

(1) Personnel

Akihiko Murata (JAMSTEC) – Principal investigator, Not on board
Masahiro Orui (MWJ)
Yasuhiro Arii (MWJ)
Katsunori Sagishima (MWJ)
Yuta Oda (MWJ)
Nagisa Fujiki (MWJ)

(2) Objective

To clarify vertical distributions of total dissolved inorganic carbon (DIC) in water columns.

(3) Parameter

Total dissolved Inorganic Carbon (DIC)

(4) Instruments and Methods

a. Seawater sampling

Seawater samples were collected by 12 liter Niskin bottles mounted on the CTD/Carousel Water Sampling System. Seawater was sampled in a 250 mL borosilicate glass bottles with ground glass stoppers. A sampling silicone rubber tube with PFA tip was connected to the outlet of Niskin bottle for water sampling. The glass bottles were filled from its bottom gently, without rinsing, and were overflowed for 20 seconds. They were sealed using ground glass stoppers with care not to leave any bubbles in the bottle. Immediately after the water sampling on the deck, the glass bottles were carried to the laboratory for the addition of saturated solution of mercury (II) chloride ($HgCl_2$). Small volume (3 mL) of the sample (1 % of the bottle volume) was removed from the bottle and 100 μL of $HgCl_2$ was added. The bottle was then sealed with a ground glass stopper lubricated with Apiezon® Grease M. Finally, the glass stopper was secured with a clip. The samples were stored in a refrigerator at approximately 5 °C until analysis.

b. Seawater analysis

Measurements of DIC were made with total CO2 measuring system (Nihon ANS Inc.). The system comprises of seawater dispensing unit, a CO2 extraction unit, and a coulometer (Model 3000, Nihon ANS Inc.) The seawater dispensing unit has an auto-sampler (6 ports), which dispenses the seawater from a glass bottle to a pipette of nominal 15 mL volume. The pipette was

kept at 20.00 °C ± 0.05 °C by a water jacket, in which water circulated through a thermostatic water bath. The CO2 dissolved in a seawater sample is extracted in a stripping chamber of the CO2 extraction unit by adding 10 % phosphoric acid solution. The stripping chamber is made approx. 25 cm long and has a fine frit at the bottom. First, a constant volume of acid is added to the stripping chamber from its bottom by pressurizing an acid bottle with nitrogen gas (99.9999 %). Second, a seawater sample kept in a pipette is introduced to the stripping chamber by the same method. The seawater and phosphoric acid are stirred by the nitrogen bubbles through a fine frit at the bottom of the stripping chamber. The stripped CO2 is carried to the coulometer through two electric dehumidifiers (kept at 2 °C) and a chemical desiccant (magnesium perchlorate) by the nitrogen gas (flow rate of 140 mL min^{-1}). Measurements of system blank (phosphoric acid blank), 1.5 % CO2 standard gas in a nitrogen base, and seawater samples (6 samples) were programmed to repeat. The variation of our own made JAMSTEC DIC reference material was used to correct the signal drift results from chemical alternation of coulometer solutions. The values of DIC were set to the assigned value of CRM (batch 209, 2060.05 ± 0.27 μmol kg^{-1}) provided by Prof. Dickson, Scripps Institution of Oceanography, Univ. of California.

(5) Observation log

Seawater samples were collected at 41 stations.

(6) Preliminary results

The repeatability was estimated to be provisionally 1.12 μmol kg^{-1} (n=54), if outliers are excluded.

(7) Data archives

These data obtained in this cruise will be submitted to the Data Management Group (DMG) of JAMSTEC, and will be opened to the public via “Data Research System for Whole Cruise Information in JAMSTEC (DARWIN)” in JAMSTEC web site.

<http://www.godac.jamstec.go.jp/darwin/e>

(b) Underway DIC

(1) Personnel

Akihiko Murata (JAMSTEC) – Principal investigator, Not on board
Yuanxin Zhang (JAMSTEC)
Nagisa Fujiki (MWJ)
Masahiro Orui (MWJ)

(2) Objective

To elucidate spatial variations of total dissolved inorganic carbon (DIC) concentration in sea surface water.

(3) Parameter

Total Dissolved Inorganic Carbon (DIC)

(4) Instruments and Methods

Surface seawater was continuously collected from 5th September to 2nd October 2021 (UTC) during this cruise. Surface seawater was taken from an intake placed at the approximately 4.5 m below the sea surface by a pump, and was filled in a 250 mL glass bottle (SCHOTT DURAN) from the bottom, without rinsing, and overflowed for more than 2 times the amount. Before the analysis, the samples were put in the water bath kept about 20°C for one hour. Measurements of DIC were made with total CO_2 measuring system (Nihon ANS Inc.). The system was comprised of seawater dispensing unit, a CO_2 extraction unit, and a coulometer (Model 3000A, Nihon ANS Inc.). The seawater dispensing unit has an auto-sampler (6 ports), which dispenses the seawater from a glass bottle to a pipette of nominal 15 mL volume. The pipette was kept at 20.00 °C ± 0.05 °C by a water jacket, in which water circulated through a thermostatic water bath. The CO_2 dissolved in a seawater sample is extracted in a stripping chamber of the CO_2 extraction unit by adding 10 % phosphoric acid solution. The stripping chamber is made approx. 25 cm long and has a fine frit at the bottom. First, the certain amount of acid is taken to the constant volume tube from an acid bottle and transferred to the stripping chamber from its bottom by nitrogen gas (99.9999 %). Second, a seawater sample kept in a pipette is introduced to the stripping chamber by the same method as that for an acid. The seawater and phosphoric acid are stirred by the nitrogen bubbles through a fine frit at the bottom of the stripping chamber. The stripped CO_2 is carried to the coulometer through two electric dehumidifiers (kept at 2 °C) and a chemical desiccant (Magnesium perchlorate) by the nitrogen gas (flow rate of 140 mL min^{-1}). Measurements of approx.1.5 % CO_2 standard gas in a nitrogen base, system blank (phosphoric

acid blank), and seawater samples (6 samples) were programmed to repeat. CO_2 standard gas and reference material produced by JAMSTEC (batch Q41, 2034.9 ± 2.9 μmol kg^{-1}) were used to correct the signal drift results from chemical alternation of coulometer solutions. The coulometer solutions were renewed every about 2 days. The values of DIC were set to the assigned value of CRM (batch 209, 2060.05 ± 0.27 μmol kg^{-1}) provided by Prof. Dickson, Scripps Institution of Oceanography, Univ. of California.

(5) Observation log

The cruise track during underway DIC observation is shown in Figure 3.1.3.III-1.

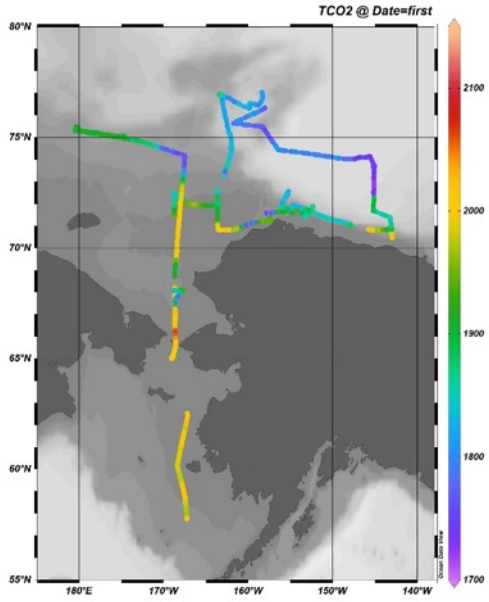

Figure 3.1.3.III-1. Cruise track where underway DIC was measured during the cruise. Concentrations of DIC were shown in color.

(6) Results

Temporal variations of DIC in surface water are shown in Figure 4.3.2-2, together with those of salinity.

(7) Date archives

These data obtained in this cruise will be submitted to the Data Management Group (DMG) of JAMSTEC, and will be opened to the public via “Data Research System for Whole Cruise Information in JAMSTEC (DARWIN)” in JAMSTEC web site.

<http://www.godac.jamstec.go.jp/darwin/e>

3.1.3.IV Alkalinity

(a) Total Alkalinity

(1) Personnel

Akihiko Murata (JAMSTEC) – Principal investigator, Not on board

Nagisa Fujiki (MWJ)

Yasuhiro Arii (MWJ)

Katsunori Sagishima (MWJ)

Masahiro Orui (MWJ)

Yuta Oda (MWJ)

(2) Objective

To survey influences of sea ice melting water and river input on carbonate system properties.

(3) Parameters

Total alkalinity (TA)

(4) Instruments and Methods

a. Seawater sampling

On this cruise, we analyzed TA in seawater collected for DIC. See the section on DIC for water sampling.

b. Seawater analysis

The total alkalinity was measured using a spectrophotometric system (Nihon ANS, Inc.) using a scheme of Yao and Byrne (1998). The calibrated volume of sample seawater (ca. 42 mL) was transferred from a sample bottle into the titration cell with its light path length of 4 cm long via dispensing unit. The TA is calculated by measuring two sets of absorbance at three wavelengths (730, 616 and 444) nm with the spectrometer (TM-UV/VIS C10082CAH, HAMAMATSU). One is the absorbance of seawater sample before injecting an acid with indicator solution (bromocresol green sodium) and another is the one after the injection. To mix the acidified-indicator solution with seawater sufficiently, the mixed solution is circulated in a circulation line by a peristaltic pump for 5 minutes. Nitrogen bubbles were introduced into the titration cell for degassing CO_2 from the mixed solution sufficiently. The TA is calculated based on the following equation:

$$TA = (-[H^+]_T V_{SA} + M_A V_A)/V_S,$$

where M_A is the molarity of the acid titrant added to the seawater sample, $[H^+]_T$ is the total excess

hydrogen ion concentration in the seawater, and V_S, V_A and V_{SA} are the initial seawater volume, the added acid titrant volume, and the combined seawater plus acid titrant volume, respectively. $[H^+]_T$ is calculated from the measured absorbances based on the following equation (Yao and Byrne, 1998):

$$pH_T = -\log[H^+]_T = 4.2699 + 0.002578(35 - S) + \log((R - 0.00131)/(2.3148 - 0.1299R)) - \log(1 - 0.001005S),$$

where S is the sample salinity, and R is the absorbance ratio calculated as:

$$R = (A_{616} - A_{730})/(A_{444} - A_{730}),$$

where A_i is the absorbance at wavelength *i* nm.
Values of TA were corrected and reported based on certified reference material provided by Prof. Dickson, Scripps Institution of Oceanography, Univ. of California (batch 209, 2210.40 ± 0.16 μmol kg^{-1}).

(5) Observation log
Seawater samples for TA were collected at 41 stations.

(6) Preliminary results
The repeatability of this system was provisionally 1.3 μmol kg^{-1} (n = 52), which was calculated from replicate samples after excluding outliers.

(7) Date archives
These data obtained in this cruise will be submitted to the Data Management Group (DMG) of JAMSTEC, and will be opened to the public via "Data Research System for Whole Cruise Information in JAMSTEC (DARWIN)" in JAMSTEC web site.
<http://www.godac.jamstec.go.jp/darwin/e>

(b) Organic Alkalinity

(1) Personnel
Akihiko Murata (JAMSTEC) – Principal investigator, Not on board
Ryan Woosley (MIT)

Jiyoung Moon (MIT)
Zhaohui Alex Wang (WHOI)
Masahiro Orui (MWJ)
Nagisa Fujiki (MWJ)

(2) Objective

To quantify non-negligible amounts of organic alkalinity that can interfere with the measurement of total alkalinity.

(3) Sampling

Seawater samples were collected at given layers of 12 CTD stations (Table 3.1.3.IV-1). The seawater samples were taken from the Niskin bottle with a plastic drawing tube (PFA tubing connected to silicone rubber tubing) connected from the Niskin drain into the 250 ml borosilicate glass bottle. The glass bottle was filled with seawater smoothly from the bottom following a rinse with a seawater of 2 full, bottle volumes. The glass bottle was closed by a stopper, which was fitted to the bottle mouth gravimetrically without additional force. At the chemical laboratory on the R/V Mirai, a headspace of approx. 1% of the bottle volume was made by removing seawater using a plastic pipette. A saturated mercuric chloride of 100 µl was added to poison seawater samples. The glass bottle was sealed with a greased ground glass stopper and the clip was secured.

Table 3.1.3.IV-1. List of sampling

LATITUDE	LONGITUDE	Niskin Bottle No.
65.0006	-169.0806	surface
65.0006	-169.0806	35
65.0006	-169.0806	1
66.1697	-168.6668	surface
66.1697	-168.6668	35
66.1697	-168.6668	1
67.6596	-168.6688	surface
67.6596	-168.6688	35
67.6596	-168.6688	1
70.5007	-168.7547	surface
70.5007	-168.7547	35

70.5007	-168.7547	1
72.5001	-168.7505	surface
72.5001	-168.7505	35
72.5001	-168.7505	1
71.9005	-163.6419	surface
71.9005	-163.6419	35
71.9005	-163.6419	1
71.6597	-155.0213	surface
71.6597	-155.0213	35
71.6597	-155.0213	1
70.8493	-143.0531	surface
70.8493	-143.0531	36
70.8493	-143.0531	4
70.8493	-143.0531	1
73.1662	-145.1636	surface
73.1662	-145.1636	36
73.1662	-145.1636	30
73.1662	-145.1636	28
73.1662	-145.1636	26
73.1662	-145.1636	22
73.1662	-145.1636	21
73.1662	-145.1636	19
73.1662	-145.1636	18
73.1662	-145.1636	17
73.1662	-145.1636	16
73.1662	-145.1636	1
74.3604	-154.4983	surface
74.3604	-154.4983	36
74.3604	-154.4983	13
74.3604	-154.4983	1
77.0399	-158.3693	surface
77.0399	-158.3693	36
77.0399	-158.3693	33
77.0399	-158.3693	30
77.0399	-158.3693	28
77.0399	-158.3693	26

77.0399	-158.3693	24
77.0399	-158.3693	23
77.0399	-158.3693	22
77.0399	-158.3693	21
77.0399	-158.3693	20
77.0399	-158.3693	1
75.3285	179.4858	surface
75.3285	179.4858	33
75.3285	179.4858	32
75.3285	179.4858	30
75.3285	179.4858	29
75.3285	179.4858	28
75.3285	179.4858	27
75.3285	179.4858	26
75.3285	179.4858	24
75.3285	179.4858	21
75.3285	179.4858	18
75.3285	179.4858	1
74.1797	-167.5103	surface
74.1797	-167.5103	36
74.1797	-167.5103	31
74.1797	-167.5103	30
74.1797	-167.5103	29
74.1797	-167.5103	28
74.1797	-167.5103	27
74.1797	-167.5103	26
74.1797	-167.5103	25
74.1797	-167.5103	24
74.1797	-167.5103	22
74.1797	-167.5103	1
68.1	-167.6666	surface
68.1	-167.6666	36
68.1	-167.6666	1

3.1.3.V. Continuous measurement of pCO_2 and pCH_4

(1) Personnel

Akihiko Murata (JAMSTEC) – Principal investigator, Not on board
Yuta Oda (MWJ)
Masahiro Orui (MWJ)
Nagisa Fujiki (MWJ)

(2) Objective

To survey spatial distributions of surface seawater pCO_2 in the western Arctic Ocean.

(3) Parameters

Partial pressures of CO_2 (pCO_2) and CH_4 (pCH_4)

(4) Methods, Apparatus and Performance

Atmospheric and surface seawater pCO_2 and pCH_4 were measured with a system having the off-axis integrated-cavity output spectroscopy gas analyzer (Off-Axis ICOS; 911-0011, Los Gatos Research). Standard gases were measured every about 4 hours, and atmospheric air taken from the bow of the ship (approx.13 m above the sea level) were measured every about 3 hours. Seawater was taken from an intake placed at the approximately 4.5 m below the sea surface and introduced into the equilibrator at the flow rate of (4 - 5) L min^{-1} by a pump. The equilibrated air was circulated in a closed loop by a pump at flow rate of (0.6 - 0.7) L min^{-1} through two electric cooling units, a starling cooler, and the Off-Axis ICOS.

(5) Preliminary result

Distributions of atmospheric and surface seawater CO_2 were shown in Figure 3.1.3.V-1, along with those of sea surface temperature (SST). Distributions of atmospheric and surface seawater CH_4 were displayed in Figure 3.1.3.V-2, along with those of SST.

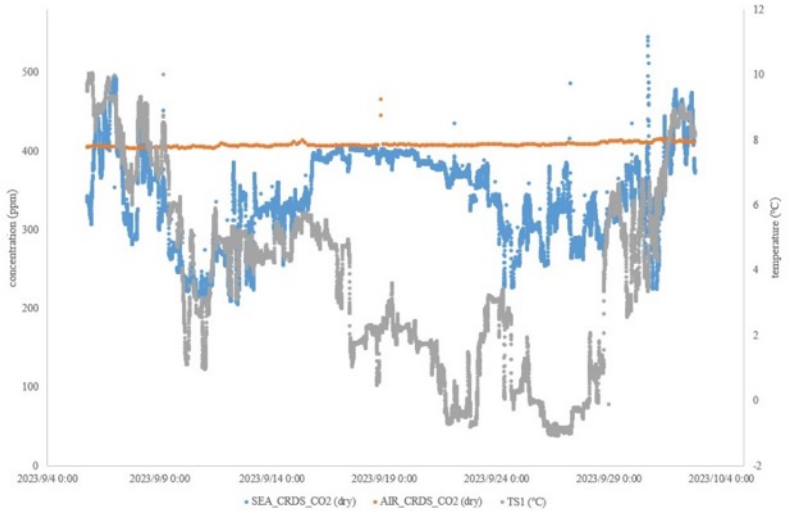

Figure 3.1.3.V-1. Distributions of atmospheric (orange) and surface seawater CO_2 (blue), and SST (grey) as a function of observation time.

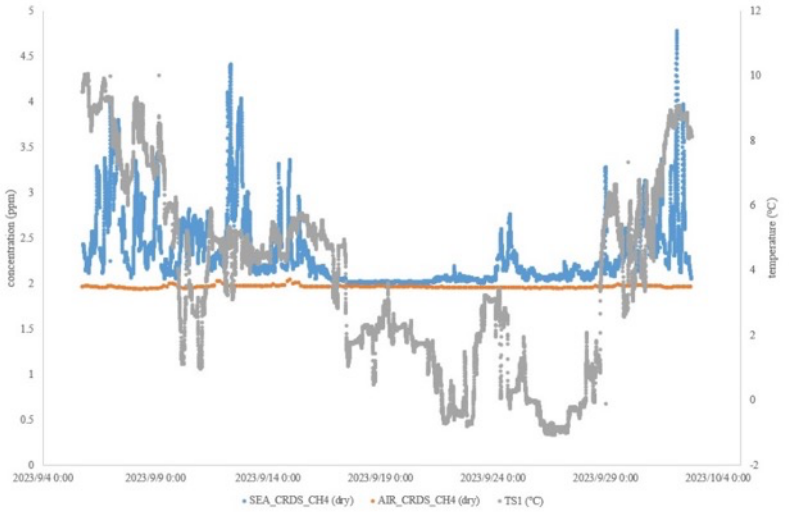

Figure 3.1.3.V-2. Distributions of atmospheric (orange) and surface seawater CH_4 (blue), and SST (grey) as a function of observation time.

(6) Date archives

These data obtained in this cruise will be submitted to the Data Management Group (DMG) of JAMSTEC, and will be opened to the public via “Data Research System for Whole Cruise Information in JAMSTEC (DARWIN)” in JAMSTEC web site.

<http://www.godac.jamstec.go.jp/darwin/e>

3.1.3.VI. Chlorophyll-a

(1) Responsible personnel

Amane Fujiwara (JAMSTEC): Principal Investigator
Yuri Fukai (JAMSTEC):
Hosomi Hosoda (JAMSTEC):

(2) Purpose, background

Phytoplankton biomass in the ocean can be roughly expressed by photosynthetic pigment, chlorophyll-a concentration. The ecological function of phytoplankton can also be characterized by the cell size. To investigate the spatial distribution of phytoplankton biomass and size structure in the Arctic Ocean, we routinely measured the horizontal and vertical distribution of bulk and size-fractionated chl-a concentration.

(3) Methods, instruments

We collected samples for bulk chlorophyll *a* (chl-*a*) concentration from 7 to 9 depths between the surface and ~100 m depth including a chl-*a* maximum layer, and size-fractionated chl-*a* from the surface and a chl-*a* maximum layers. The chl-*a* maximum layer was determined by a fluorometer (Seapoint Sensors, Inc.) attached to the CTD system prior to the water sampling.

Seawater samples for total chl-*a* were vacuum-filtrated (< 0.015 MPa) through the 25mm-diameter ADVANTEC GF-75 filter. Seawater samples for size-fractionated chl-*a* were passed through 20 μm pore-size nylon filter (47 mm in diameter), 2μm pore-size polyester membrane filter (47 mm in diameter), and ADVANTEC GF-75 (25 mm in diameter).

Each filter sample was immediately soaked in 7 ml of N,N-dimethylformamide (DMF, Wako Pure Chemical Industries Ltd.) in a polypropylene tube (Suzuki and Ishimaru, 1990). The tubes were stored at -20 °C under dark condition to extract chl-*a* at least for 24 hours.

Chl-*a* concentrations were measured onboard by a fluorometer (10-AU, TURNER DESIGNS) following the method of Welschmeyer (1994). The 10-AU fluorometer was calibrated against a pure chl-*a* (Sigma-Aldrich Co., LLC) prior to the analysis.

(4) Results

As the preliminary result, the horizontal distribution of chl-a concentration at surface and chl-a maximum layers are plotted in Figure 3.1.3.VI-1. Chl-a concentration showed the typical horizontal pattern of the western Arctic Ocean during the MR23-06C cruise; higher concentration in the shallow shelf and lower in the northern basin area. The horizontal distribution of chl-a size structure (fractional contribution to chla biomass) is also plotted in Figure 3.1.3.VI-2. Phytoplankton size structure also showed the typical pattern; the proportion

of larger cells covaried with chl-a concentration.

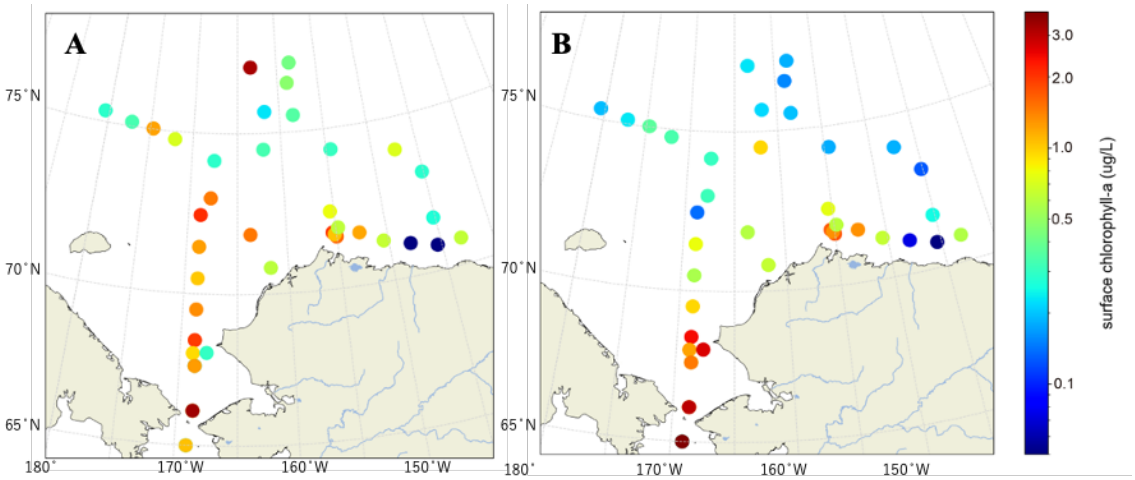

Figure 3.1.3.VI-1. The horizontal distribution of chl-*a* concentration at (A) surface and (B) chl-a maximum layer

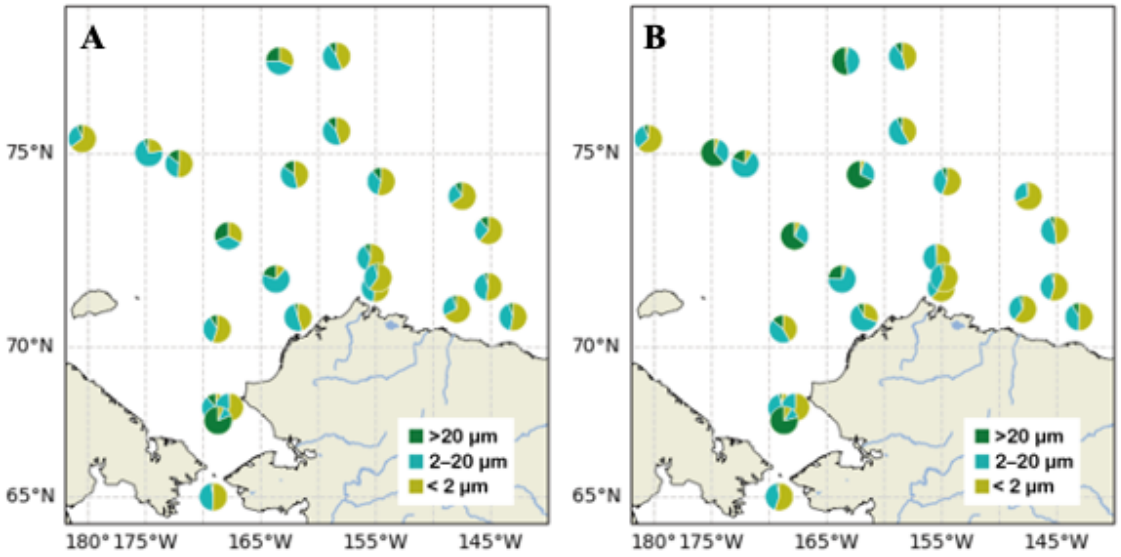

Figure 3.1.3.VI-2. The horizontal distribution of chl-*a* size composition at (A) surface and (B) chl-a maximum layer

(5) Reference

Welschmeyer, N. A. (1994). Fluorometric analysis of chlorophyll a in the presence of chlorophyll b and pheopigments. *Limnology and Oceanography*, *39*(8), 1985–1992. https://doi.org/10.4319/lo.1994.39.8.1985

Suzuki, R., & Ishimaru, T. (1990). An improved method for the determination of phytoplankton

chlorophyll using N, N-dimethylformamide. *Journal of Oceanography*, *46*(4), 190–194. https://doi.org/10.1007/BF02125580

3.1.3.VII. ^{18}O

(1) Responsible personnel

Mariko Hatta (JAMSTEC): Principal Investigator

Amane Fujiwara(JAMSTEC):

Manami Tozawa (Hokkaido University)

Daiki Nomura (Hokkaido University)

(2) Purpose, background

Oxygen isotope of seawater ($\delta^{18}O$) is a useful tracer to distinguish freshwater sources in seawater between sea ice meltwater and meteoric water. It also provides information about how much sea ice has been formed from seawater (brine content). During the cruise of MR23-06C, seawater samples for analysis of $\delta^{18}O$ were routinely collected at the CTD/water sampling stations. The data will be used to quantify changes in biogeochemical properties (such as nutrients and carbonate parameters) due to dilution by sea ice meltwater, mixing with river runoff, or/and to formation of sea ice..

(3) Methods, instruments

Seawater samples were collected from Niskin bottles into glass bottles. $\delta^{18}O$ samples were collected into glass vials (15-20mL) and sealed well without any additional air bubbles. Obtained samples will be determined at a shore-based laboratory by a subcontractor. Samples will be determined by an isotope ratio mass spectrometer (Thermo Scientific Delta V Advantage) equipped with an inlet system including an autosampler (NAKANO ELECTRONICS INC.). Samples will be determined together with a reference CO_2 gas ($\delta^{18}O$ vs VSMOW = 27.88‰, Lot. SKS) and several pre-determined seawaters (DOW3, AGW, SLW4, VSMOW = -0.072, -18.58, - 9.62‰, respectively). The general analytical procedure is as follows: (1) Pipet 2 mL of the water sample into a dedicated sample bottle (25 mL) and then put them in the equilibrator at a constant temperature (18°C) and then turn on the infiltrator. The twenty-four samples are prepared as a set at the same time. (2) Open the valve connected to the rotary pump and exhaust the gas phase in the sample bottle. (3) Close the valve connected to the rotary pump, open the valve connected to the cylinder gas (carbon dioxide gas), and then introduce the equilibrium gas into the sample bottle. The gas introduction step is conducted at the same time for all sample bottles together. (4) After introducing the specified volume, the individual valves connected to each sample bottle are closed simultaneously. (5) The sample bottles are placed in a constant

temperature bath for 12 hours. (6) After the equilibration reaction time, the program automatically introduces equilibrated gas into the mass spectrometer sample introduction container and then measures the stable isotope ratio. (7) The reference gas and sample gas are determined six times each. (8) To maintain the precision, the internal standard deviation of the average value of 6 measurements should be 0.05‰ or less. If there is any issue, rerun those samples. (9) Calculate the oxygen-stable isotope ratio

3.1.3.VIII Iodine-129/Uranium-236

(1) Responsible personnel

Yuichiro Kumamoto (JAMSTEC): Principal Investigator

Amane Fujiwara (JAMSTEC)

(2) Purpose, background

In order to investigate the water circulation and ventilation process in the Bering Sea and Arctic Ocean, seawater samples were collected for measurements of iodine-129 (^{129}I) and uranium-236 (^{236}U).

(3) Methods, instruments

Surface seawater samples were collected from continuous pumped-up water from ~4-m depth or using a bucket. We also collected seawater samples vertically at five stations from the sea surface to near the bottom layer at several stations. The sampling stations for ^{129}I and ^{236}U are summarized in Table .1.3.VIII-1 and 3.1.3.VIII-2, respectively. The seawater samples were collected into a 1-L plastic bottle for ^{129}I and a 5-L plastic container for ^{236}U after a two-time rinsing. The total numbers of the seawater samples for ^{129}I and ^{236}U are 88 and 56, respectively.

^{129}I in the seawater sample is extracted using solvent extraction with carrier iodine added. The sample is precipitated as silver iodide and ^{129}I/^{127}I is measured using accelerator mass spectrometry at the MALT (Micro Analysis Laboratory, Tandem accelerator), The University of Tokyo. 5mL aliquot of the sample is measured for ^{127}I by ICP-MS.

^{236}U in the seawater sample is co-precipitated with Fe hydroxide and purified by UTEVA® resin. The purified sample is co-precipitated as uranium oxide with 1.5 mg Fe hydroxide and ^{236}U/^{238}U is also measured using accelerator mass spectrometry at MALT. 5mL aliquot of the sample is measured for ^{238}U by ICP-MS.

(4) Data archives

These data obtained in this cruise will be submitted to the Data Management Group of JAMSTEC, and will be opened to the public via “Data Research System for Whole Cruise Information in JAMSTEC (DARWIN)” in JAMSTEC web site. <http://www.godac.jamstec.go.jp/darwin/e>

Table 3.1.3.VIII-1: Sampling stations for ^{129}I.

No.	Station ID	sampled date	time		latitude	longitude	remarks
			start	end	deg-N	deg-E	
1	-	2023/9/8	2:43	2:43	65.5731	-168.6039	surface
2	St04	2023/9/9	1:12	1:12	68.5020	-168.7513	surface
3	St06	2023/9/9	18:53	18:53	70.7475	-168.7474	surface
4	St08	2023/9/10	4:39	4:39	72.5005	-168.7514	surface
5	XCTD02	2023/9/12	7:19	7:19	71.2347	-157.3033	surface
6	St14	2023/9/13	-	-	72.4678	-155.3975	vertical
7	St17	2023/9/15	4:00	4:00	71.3113	-150.4755	surface
8	St21	2023/9/17	5:47	5:47	71.6899	-145.1993	surface
9	St22	2023/9/18	-	-	73.1662	-145.1636	vertical
10	St25	2023/9/20	-	-	74.3604	-154.4983	vertical
11	St29	2023/9/21	20:06	20:06	77.0366	-158.3739	surface
12	St31	2023/9/23	-	-	76.9505	-163.3101	vertical
13	St32	2023/9/23	-	-	74.5155	-162.0287	vertical
14	St34	2023/9/25	16:29	16:29	74.7669	-172.0632	surface
15	St35	2023/9/26	4:48	4:48	75.1297	-177.2285	surface
16	St36	2023/9/27	0:45	0:45	75.3285	179.4858	surface
17	St38	2023/9/28	6:35	6:35	74.1797	-167.5103	surface

Table 3.1.3.VIII-2: Sampling stations for ^{236}U.

No.	Station ID	sampled date	time		latitude	longitude	remarks
			start	end	deg-N	deg-E	
1	-	2023/9/8	2:41	2:42	65.5673	-168.6076	surface
2	St04	2023/9/9	1:10	1:12	68.5021	-168.7513	surface
3	St06	2023/9/9	18:50	18:51	70.7374	-168.7474	surface
4	St08	2023/9/10	4:36	4:38	72.5007	-168.7532	surface
5	XCTD02	2023/9/12	7:17	7:19	71.2342	-157.3231	surface
6	St14	2023/9/13	-	-	72.4678	-155.3975	vertical
7	St31	2023/9/23	-	-	76.9505	-163.3101	vertical
8	St32	2023/9/23	-	-	74.5155	-162.0287	vertical
9	St34	2023/9/25	16:29	16:29	74.7669	-172.0632	surface
10	St35	2023/9/26	4:48	4:48	75.1297	-177.2285	surface
11	St36	2023/9/27	0:45	0:45	75.3285	179.4858	surface
12	St38	2023/9/28	6:35	6:35	74.1797	-167.5103	surface

3.1.3.IX Underway Surface Monitoring

(a) Basic biogeochemical analyses

(1) Personnel

Amane Fujiwara (JAMSTEC): Principal Investigator
Masahiro Orui(MWJ) : Operation leader
Nakamura (MWJ)
Shintaro Amikura (MWJ)

(2) Objective

Our purpose is to obtain temperature, salinity, dissolved oxygen, fluorescence, turbidity, refractive index density and total dissolved gas pressure data continuously in near-sea surface water.

(3) Parameters

Temperature
Salinity
Dissolved oxygen
Fluorescence
Turbidity
Total dissolved gas pressure
Refractive index density

(4) Instruments and Methods

The Continuous Sea Surface Water Monitoring System (Marine Works Japan Co. Ltd.) has six sensors and automatically measures temperature, salinity, dissolved oxygen, fluorescence, turbidity, total dissolved gas pressure and refractive index density in near-sea surface water every one minute. This system is located in the “sea surface monitoring laboratory” and connected to shipboard LAN-system. Measured data, time, and location of the ship were stored in a data management PC. Sea water was continuously pumped up to the laboratory from an intake placed at the approximately 4.5 m below the sea surface and flowed into the system through a vinyl-chloride pipe. The flow rate of the surface seawater was adjusted to 10 dm^3 min^{-1}.

a. Instruments

Software

Seamoni Ver.1.2.0

Sensors

Specifications of the each sensor in this system are listed below.

Temperature and Conductivity sensor

Model:	SBE-45, SEA-BIRD ELECTRONICS, INC.
Serial number:	4552788-0264
Measurement range:	Temperature -5 ºC - +35 ºC
	Conductivity 0 S m^{-1} - 7 S m^{-1}
Initial accuracy:	Temperature 0.002 ºC
	Conductivity 0.0003 S m^{-1}
Typical stability (per month):	Temperature 0.0002 ºC
	Conductivity 0.0003 S m^{-1}
Resolution:	Temperature 0.0001 ˚C
	Conductivity 0.00001 S m^{-1}

Bottom of ship thermometer

Model:	SBE 38, SEA-BIRD ELECTRONICS, INC.
Serial number:	3852788-0457
Measurement range:	-5 ºC - +35 ºC
Initial accuracy:	±0.001 ºC
Typical stability (per 6 month):	0.001 ºC
Resolution:	0.00025 ºC

Dissolved oxygen sensor

Model:	RINKO II, JFE ADVANTECH CO. LTD.
Serial number:	0035
Measuring range:	0 – 200%
Resolution:	0.001 mg L^{-1} - 0.004 mg L^{-1} (25 ºC)
Accuracy:	Saturation ± 2 % F.S. (non-linear) (1 atm, 25 ºC)

Fluorescence & Turbidity sensor

Model:	C3, TURNER DESIGNS
Serial number:	2300707
Measuring range:	Chlorophyll in vivo 0 µg L^{-1} – 500 µg L^{-1}
Minimum Detection Limit:	Chlorophyll in vivo 0.03 µg L^{-1}

Measuring range: Turbidity 0 NTU - 1500 NTU
Minimum Detection Limit: Turbidity 0.05 NTU

Total dissolved gas pressure sensor

Model: HGTD-Pro, PRO OCEANUS
Serial number: 36-296-10
Temperature range: -2 °C - 50 °C
Resolution: 0.0001 %
Accuracy: 0.01 % (Temperature Compensated)
Sensor Drift: 0.02 % per year max (0.001 % typical)

(5) Observation log

Periods of measurement, maintenance, and problems during this cruise are listed in Table 3.1.3.IX-1.

Table 3.1.3.IX-1. Events list of the Sea surface water monitoring during MR23-06C

System Date [UTC]	System Time [UTC]	Events	Remarks
2023/08/26	8:03	Start data logging	
2023/09/02 2023/09/05	23:40 – 17:50	All the measurements stopped.	Pump stopped
2023/09/09	03:09–03:31	Filter Cleaning.	-
2023/09/17	03:15–03:35	Filter Cleaning.	-
2023/09/22	01:23	Filter Cleaning.	-
2023/09/30	00:19–00:49	Filter Cleaning..	-
2023/10/02	22:37	All the measurements stopped and End data logging	Pump stopped

We took the surface water samples from this system once a day to compare and correct sensor data with bottle data of salinity, dissolved oxygen, and chlorophyll a. The results are shown in Fig. 3.1.3.IX-2. All the salinity samples were analyzed by the Model 8400B “AUTOSAL” manufactured by Guildline Instruments Ltd. (see 3.1.2.V), and dissolve oxygen samples were analyzed by Winkler method (see 3.1.3.I), chlorophyll *a* were analyzed by 10-AU manufactured by Turner Designs. (see 3.1.3.VI).

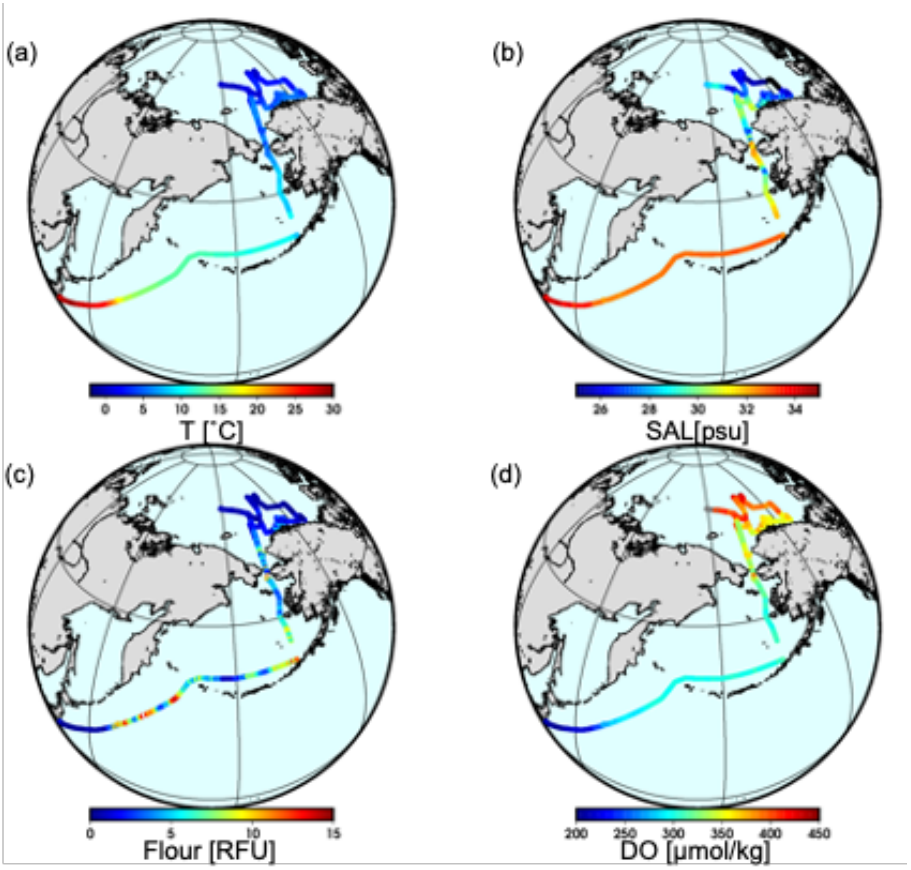

Figure 3.1.3.IX-1 Spatial and temporal distribution of (a) temperature, (b) salinity, (c) fluorescence, and (d) dissolved oxygen concentration in MR23-06C cruise.

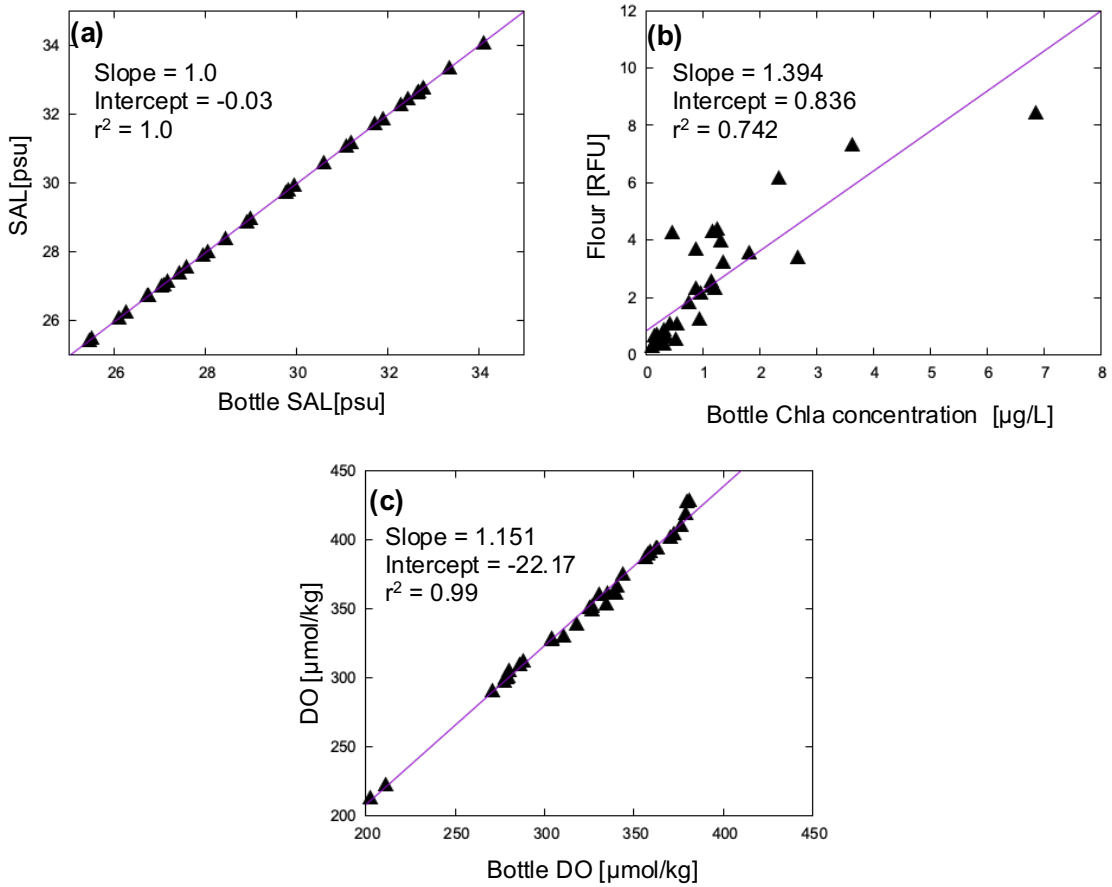

Figure 3.1.3.IX-2 (a) Correlation of salinity between sensor and bottle measured data, (b) fluorescence sensor data and bottle chlorophyll-a concentration, and (c) dissolved oxygen between the sensor and bottle measured data.

(6) Data archives

These data obtained in this cruise will be submitted to the Data Management Group (DMG) of JAMSTEC, and will opened to the public via "Data Research System for Whole Cruise Information in JAMSTEC (DARWIN)" in JAMSTEC web site.

http://www.godac.jamstec.go.jp/darwin/e

(b) Silicate and phosphate

(1) Responsible personnel

Mariko Hatta JAMSTEC

(2) Purpose, background

(2-1)Establish the shipboard system using a programmable flow injection system and identify potential trouble and establish the troubleshooting protocol:

- Purpose: The primary purpose of this study is to develop a compact and automated microfluidic analyzer for nutrient analysis. This innovative system is designed to meet specific criteria for efficient, unsupervised operation, including durability, minimal reagent consumption, and computer-controlled manipulations. In essence, it aims to create a state-of-the-art tool for analyzing nutrients in ocean samples with a focus on practicality and precision.
- Background: The background provides essential context for the study:.*Current Knowledge Gap:* It is established that there's a significant gap in our understanding of ocean biogeochemical data. This knowledge gap is attributed to the complexity and intricacy of the analytical procedures involved in both at-sea and on-land sample analysis.

(2-2) Identify the water mass characteristics with shipboard silicate and phosphate data with the other physical parameters (i.e. Temperature, salinity, oxygen) obtained from the underway surface water monitoring system:

- Purpose: This goal aims to collect and analyze data related to water mass characteristics. It mentions specific parameters such as silicate and phosphate concentrations along with temperature, salinity, and oxygen levels. The purpose is to understand the composition and characteristics of the water masses the ship encounters during its journey.
- Background: ***Arctic Ocean Significance***: The study highlights the significance of the Arctic Ocean, which experiences dynamic changes in freshwater influx due to factors such as sea ice melt and river inputs. These changes have substantial effects on the surface ocean. ***Continental Shelves:*** The Arctic Ocean's unique geographical characteristics, notably its extensive continental shelves, play a vital role in the transport

of geochemical substances from the continental boundary to the Arctic interior. These processes are influenced by climate change, making it increasingly important to understand the Arctic's geochemical cycles.

In summary, the study aims to address the existing knowledge gap by developing an advanced microfluidic analyzer that facilitates nutrient analysis in ocean samples and expands the database. This innovation is particularly important given the intricate nature of existing analytical procedures and the unique environmental changes occurring in the Arctic Ocean. Understanding the geochemical cycles in the Arctic region has broad implications, making this research significant in the context of oceanography and environmental science.

(3) Activities (observation, sampling, development)

The activities described in this section involve the process of collecting and analyzing seawater samples for real-time determination of Silicate (SiO2) and phosphate (PO4) using a programmable flow injection technique. Here's a breakdown of the activities:

1. Seawater Sample Collection: Samples were aspirated into the analysis system using an underway water sampling pump system, waters were collected approximately at 4.5m depth.
2. Real-Time Analysis: The collected seawater samples are then subjected to real-time analysis. The analysis focuses on two key parameters: Silicate (SiO2) and phosphate (PO4).
3. Programmable Flow Injection Technique: The analysis technique being employed is the programmable flow injection technique. This technique involves the controlled injection of samples and reagents into a flowing stream. It allows for precise and automated measurements and is valuable for continuous monitoring.

(4) Methods, instruments

(4-1) Instrumentation

The instrument, miniSIA-2 (Global FIA, Fox Island, WA, USA), comprises two high precision, synchronously refilling milliGAT pumps, two thermostated holding coils, a 6-port LOV (model COV-MANI-6, constructed from polymethyl methacrylate, Perspex®) furnished with a module for an external flow cell (Figure 3.1.3.IX-3). All tubing connections, downstream from the milliGAT pumps including the holding coils (volume 1000 μL), were made with 0.8 mm I.D. polytetrafluoroethylene (PTFE). The holding coils were thermostated at 40C temperature for all

silicate and phosphate analysis. The tubing between the carrier stream reservoirs and the milliGAT pump was made from 1.6 mm I.D. PTFE tubing to minimize degassing under reduced pressure at higher aspiration flow rates. A spectrophotometer (Flame, Ocean Insight, Orlando, FL, USA) and a light source were connected to the flow cells by using optical fibers with 500-µm silica cores encased in 0.8 mm I.D. green PEEK tubing. The end of each fiber exposed to the liquid was cemented with epoxy, cut square, and polished. An Ocean Optics Tungsten Halogen (HL-2000, Ocean Insight, Orlando, FL, USA) light source was used. All assay steps were computer-controlled using commercially available software (FloZF, GlobalFIA, Fox island, WA, USA). The Linear Light Path (LLP) flow cell was purchased from Global FIA. The outlet of the LLP flow cell, was fitted with a 40-psi flow restrictor (GlobalFIA, Fox Island, WA, USA), which, by elevating the pressure within the flow path, efficiently prevented the formation of microbubbles from spontaneous outgassing.

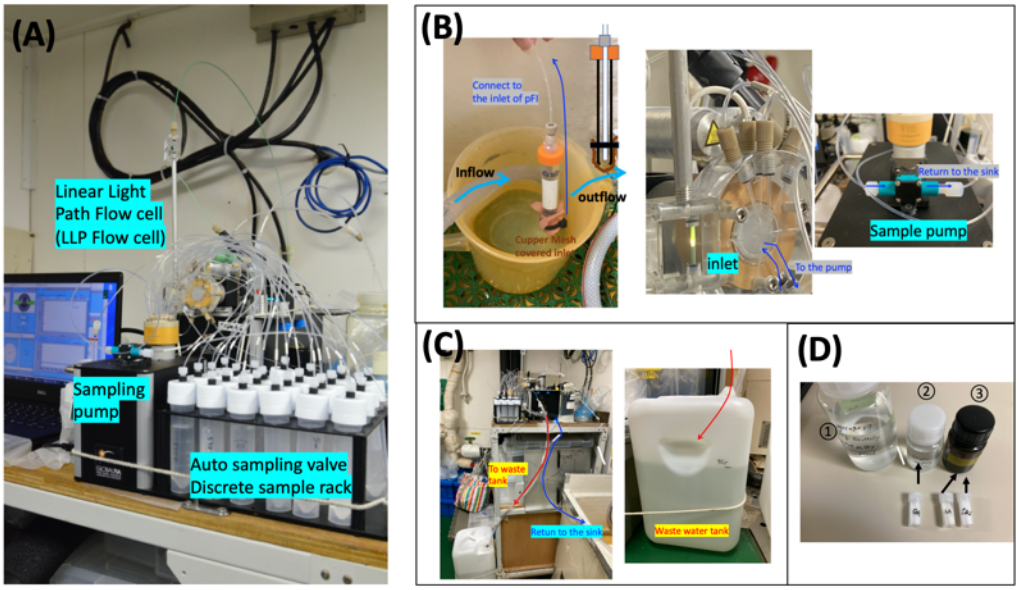

Figure 3.1.3.IX-3. Shipboard analytical system for continuous silicate determination using the programmable flow injection technique. (A) the mini-SIA2 system and the autosampler. (B) Newly established sampling inlet. (C) The waste water drains system (D) Preparation for the reagents for the Silicate analysis during the cruise.

Remarks:

- **Flow Cell Length:** This year, a flow cell with a length of 10 centimeters was utilized. The flow cell is a key component of the analysis system and is used to pass the seawater samples through for analysis.
- **Sample Collection Frequency:** Surface water samples were collected approximately every 10 minutes. This frequent sampling interval allows for more detailed temporal

resolution in the data.

- **Sample Aspiration:** Samples were aspirated into the analysis system using a sample pump for a duration of 20 seconds. Aspiration is the process of drawing the seawater samples into the system for analysis.
- **Temperature Adjustment:** After aspiration, the samples were homogenized to adjust their temperature to room temperature, which is about 25 degrees Celsius. Maintaining a consistent temperature is important for accurate and reproducible analysis, but the room temperature changes significantly during the analysis time or date. Thus, the heating coil has been adjusted to 40C during this cruise to meet the constant determination throughout the cruise.
- **Return of Flushed Surface Samples:** Samples that weren't analyzed, which are referred to as "flushed surface samples". Since they were not mixed with any reagent, these samples were directly returned to the sink, indicating that they were not retained after analysis.
- **Waste Handling:** Any waste samples and reagents generated during the analysis process were drained into a waste tank. These waste materials were stored in the waste tank until the end of the cruise. Proper waste management is crucial for environmental and safety reasons.

(4-2) Analytical methodology

The detailed the methodology using programmable flow injection technique was published in Hatta et al. (2021). The detailed of each reagent and standards were made as follow:

Carrier solution: MilliQ water.
Certified reference materials (KANSO) have been analyzed as a standard solution for this cruise (see Table 3.1.3.IX-2).

Table 3.1.3.IX-2. The certified reference materials

CRMs	Reported silicate value	Reported phosphate value
CK	0.73±0.08	0.048±0.012
CQ	2.20±0.07	0.030±0.009
CR	14.0±0.3	0.394±0.014
CO	34.72±0.16	1.177±0.014
CN	152.7±0.8	2.94±0.03

Silicate analysis:

The acidified molybdate reagent was prepared by dissolving 2 g of ammonium molybdate tetrahydrate crystalline in 500 mL of acidified MilliQ water (2.5 mL of conc. sulfuric acid was added). This solution was stable for 2 months. The mixed solution of ascorbic acid and SDS solution was prepared by dissolving 4 g of L (+)-ascorbic acid in 200 mL of MilliQ water, and then 4 g of solid of ultrapure sodium dodecyl sulfate was added into this ascorbic acid solution, and then 4 g of solid of oxalic acid was added into this mixture.

Phosphate analysis:

The acidified molybdate reagent was prepared by dissolving 2 g of ammonium molybdate tetrahydrate crystalline in 200 mL of acidified MilliQ water (75 mL of conc. sulfuric acid was added to 1L). 0.5g of Ksb was diluted into 50mL of MilliQ water, and then spiked into the molybdate solution. The mixed solution of ascorbic acid and SDS solution was prepared by dissolving 4 g of L (+)-ascorbic acid in 200 mL of MilliQ water, and then 4 g of solid of ultrapure sodium dodecyl sulfate was added into this ascorbic acid solution. All of those reagents were top-upped if they needed.

(5) Results, Future Plans, Lists (samples, observation equipment, deployment & recovery), Local field map (dive tracks, sampling points, survey lines), etc

Results:

- During the cruise, the surface samples for continuous determination were collected every 10 minutes. A total of 1193 samples were determined over 410 hours during this cruise.
- The significant issue was detected while the phosphate determination was operated along the silicate measurement.

Future Plans:

- Recalculate surface silicate values during the cruise.
- Further analysis and interpretation of the entire dataset to provide a comprehensive view of silicate (and phosphate concentrations) in the study area.
- Investigation of the factors influencing the observed silicate anomalies, such as riverine inputs and water mass dynamics.
- Comparisons and validations with other data sources and cruises to refine the understanding of the spatiotemporal distribution of silicate in the region.

- Refining the analytical methodology, especially investigating the issue of the phosphate analysis.
- Continued monitoring and data collection to build on the insights gained during this cruise and contribute to a better understanding of oceanographic processes in the Arctic Ocean.

(6) References

Hatta et al., 2021. Programmable flow injection in batch mode: Determination of nutrients in seawater by using a single, salinity-independent calibration line, obtained with standards prepared in distilled water, Talanta. https://doi.org/10.1016/j.talanta.2021.122354.

(7) Data archives

These data obtained in this cruise will be submitted to the Data Management Group (DMG) of JAMSTEC, and will opened to the public via “Data Research System for Whole Cruise Information in JAMSTEC (DARWIN)” in JAMSTEC web site.

http://www.godac.jamstec.go.jp/darwin/e

© Fluorometric observation of phytoplankton

(1) Personnel

Amane Fujiwara (JAMSTEC) -Principal Investigator

Yuri Fukai (JAMSTEC)

(2) Objective

Our purpose is to obtain surface continuous multi-spectrally excited fluorescence of phytoplankton along the cruise track, which is useful to infer phytoplankton taxonomic composition optically with high spatial resolution.

(3) Parameters

Multi-spectral excitation/emission fluorescence

(4) Instruments and Methods

Horizontal distribution of multi-spectral excitation/emission fluorescence was measured using a *Multi-Exciter* instrument (JFE-Advantech Inc.). *Multi-Exciter* detects fluorescence signals from 630 to 1000 nm which are excited at 9 bands (375, 400, 420, 435, 470, 505, 525, 570, and 590 nm). The *Multi-Exciter* was attached to the continuous surface water monitoring system and measured the spectral fluorescence of surface water every 15 minutes along the cruise track. 15 HPLC samples were also taken from continuous surface water monitoring system to compare the fluorometric signals and phytoplankton pigment composition. Details for the measurement of pigment samples were described in 3.1.3.X.

(5) Preliminary result

Figure 3.1.3.IX-4 shows the underway fluoresceine signal excited at 470 nm along the cruise track.

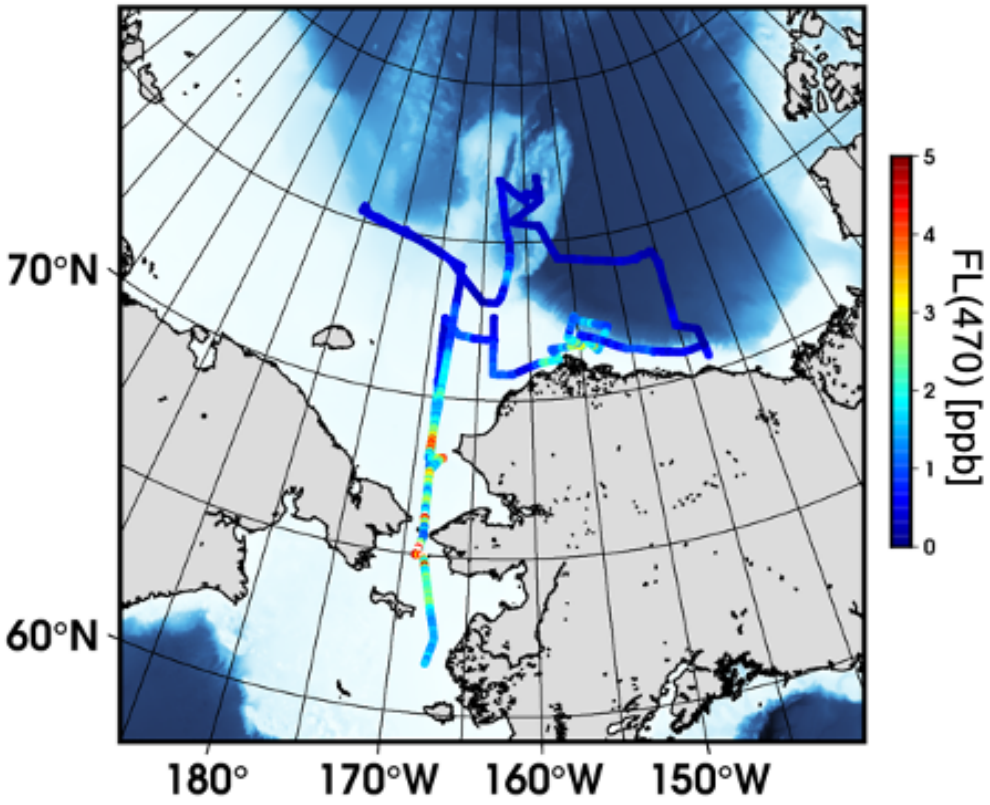

Figure 3.1.3.IX-4. Spatial and temporal distribution of the excited fluorescence at 470nm that is an indicator of chlorophyll-a concentration.

(6) Data archives

These data obtained in this cruise will be submitted to the Data Management Group (DMG) of JAMSTEC, and will opened to the public via "Data Research System for Whole Cruise Information in JAMSTEC (DARWIN)" in JAMSTEC web site.

http://www.godac.jamstec.go.jp/darwin/e

3.1.3.X. Bio-optical observations

(1) Personnel

Amane Fujiwara (JAMSTEC) -Principal Investigator
Yuri Fukai (JAMSTEC)
Manami Tozawa (Hokkaido University)
Daiki Nomura (Hokkaido University)

(2) Objectives

The objective of these observations is to develop and evaluate ocean color algorithms to estimate phytoplankton community composition and algal size using optical properties of seawater as well as investigating in-situ phytoplankton community structure and in-water optical properties. Results from these investigations will be applied to satellite remote sensing and used to clarify the responses of phytoplankton to the recent climate change in the western Arctic Ocean.

(3) Parameters

A. Surface and underwater spectral radiance and irradiance
B. Phytoplankton pigments and absorption coefficient

(4) Instruments and methods

A) Surface and underwater spectral radiance and irradiance

Underwater spectral downwelling planar irradiance, $E_d(\lambda, z)$ [μW cm^{-2} nm^{-1}], and upwelling radiance, $L_u(\lambda, z)$ [μW cm^{-2} nm^{-1} str^{-1}], at 17 wavelengths over the spectral range 380 – 765 nm were measured using a C-OPS spectroradiometer (Biospherical Instrument Inc.). The C-OPS was deployed in free-fall mode up to ~100 m deep at a distance from the stern of the ship to avoid her shadows. Downwelling irradiance incident upon the sea surface $E_d(\lambda, z = 0+)$ was also monitored by a reference sensor with the same specifications as the underwater sensor. Before each deployment of the instrument, 30 seconds of averaged dark values were recorded. Underwater photosynthetically available radiation (PAR) was also calculated by converting the $E_d(\lambda, z)$ to quantum units, $E_{d,q}(\lambda, z)$ [μmol photons m^{-2} s^{-1}], and integrating the $E_{d,q}(\lambda, z)$ from 395 to 710 nm.

B) Seawater samples for phytoplankton pigments were collected from the sea surface and other depths using Niskin-X bottles on the CTD/R. 1 – 4 L of water samples were filtered onto a glass fiber filter (GF/F, 47 mm) and stored in liquid nitrogen. Pigment concentrations will be analyzed on land using high-performance liquid chromatography (HPLC) (Agilent Technologies 1300 series) following the method of van Heukelem and Thomas (2001) after the cruise.

Seawater samples for absorption coefficient measurement were collected from the sea surface. For measurements of the spectral absorption coefficient of particles, particles in 1-4 liter(s) of water sample were concentrated on a glass fiber filter (Whatman GF/F, 25 mm). Filter samples were stored in liquid nitrogen. The optical density (OD) of particles on the filter pad will be measured on land with a spectrophotometer following the method of Stramski et al. (2015), and then, the absorption coefficient of particles ($a_p(\lambda)$), detritus ($a_d(\lambda)$), and phytoplankton ($a_{ph}(\lambda)$) were determined. For measurements of the spectral absorption coefficient of CDOM ($a_{CDOM}(\lambda)$), ~300 ml of water sample was filtrated through a 0.2 μm Nuclepore filter (Whatman, 47 mm). Filtered water samples were stored in a refrigerator until analysis on land. $a_{CDOM}(\lambda)$ will also be measured using a spectrophotometer following the protocol of the IOCCG (International Ocean Colour Coordinating Group) CDOM working group (https://ioccg.org/wp-content/uploads/2019/10/cdom_abs_protocol_public_draft-19oct-2019-sm.pdf).

(5) Station list and sampling location

Table 3.1.3.X-1. Number of instrument deployments or discrete water samples collected for each parameter on the cruise.

Instrument	***Number of stations***
C-OPS	12
Parameter	***Number of samples***
$a_p(\lambda)$, $a_d(\lambda)$, $a_{ph}(\lambda)$,	16
$a_{CDOM}(\lambda)$	20
Phytoplankton pigments (HPLC)	24

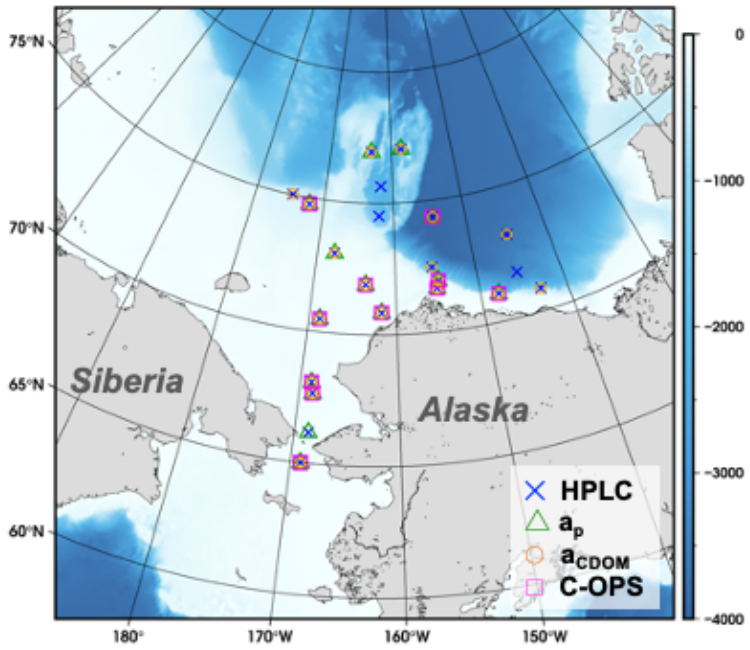

Figure 3.1.3.X-1. Sampling locations of the bio-optical observations. Blue crosses, green triangles, orange circles, and magenta squares indicate the sites where samples/data for HPLC, particulate- and CDOM-absorption coefficients, and in-water radiance/irradiance were collected, respectively.

(6) Reference cited

Stramski, D., R. A. Reynolds, S. Kaczmarek, J. Uitz and G. Zheng. 2015. Correction of pathlength amplification in the filter-pad technique for measurements of particulate absorption coefficient in the visible spectral region. *Appl. Opt.*, 54, 6763-6782. doi: 10.1364/AO.54.006763.

Van Heukelem, L, Thomas C. S. 2001. Computer-assisted high-performance liquid chromatography method development with applications to the isolation and analysis of phytoplankton pigments. *J Chromatogr A*, 910, 31–49.

(7) Data archives

These data obtained in this cruise will be submitted to the Data Management Group of JAMSTEC, and will be opened to the public via “Data Research System for Whole Cruise Information in JAMSTEC (DARWIN)” in JAMSTEC web site.

<http://www.godac.jamstec.go.jp/darwin/e>

3.1.3.XI. Phytoplankton incubation

(1) Personnel

Amane Fujiwara (JAMSTEC) -Principal Investigator
Yuri Fukai (JAMSTEC)
Kohei Matsuno (Hokkaido University)

(2) Background and objectives

Diatoms play critical roles in Arctic marine ecosystems, contributing significantly to the food web and biogeochemical cycles. These roles are particularly sensitive to environmental dynamics. Diatoms can persist for extended periods even after settling on the dark seafloor. Under favorable conditions, such as sufficient light and nutrients facilitated by physical forces, they can resume photosynthesis. For example, seafloor sediment can become suspended and entrained within sea ice during the freezing season. Upon ice melt, this sediment is released into the upper ocean. On the other hand, during the ice-free season, atmospheric turbulence can enhance water column convection, lifting suspended sediment to the near surface. This phenomenon is particularly prevalent in shallow shelf regions. Given the high-seeding potential of diatoms and sediment cycling dynamics, we hypothesized that diatoms within sediment play important roles in initiating both spring and fall phytoplankton blooms. To evaluate the hypothesis and aim of understanding the seeding potential of phytoplankton cells in sediments, we conducted phytoplankton incubation experiments simulating (a) spring phytoplankton bloom using melted sediment-laden sea ice, and (b) fall phytoplankton bloom adding seafloor sediment, respectively.

(3) Parameters

Total chlorophyll-a, size-fractionated chlorophyll-a, phytoplankton pigments, phytoplankton composition (microscopy and DNA), the maximum quantum yield of photochemistry in photosystem II (i.e., F_v/F_m), nutrients (NO_3, NO_2, NH_4, PO_4, $Si(OH)_4$), photosynthetic active radiation, temperature, copepod feeding activity (clearance rate and ingestion rate; Dagg et al., 2006), gut pigments of copepod

(4) Instruments and methods

(a) Spring phytoplankton bloom experiment

Before the cruise, we collected sea ice core samples from the landfast ice at Utquiagvik, Alaska, for the spring bloom simulating experiment. During the cruise, the water for the incubation experiment was collected at a depth of 200m at station 17, where the Pacific Winter Water layer occupies, because the water properties are thought to be similar to pre-spring bloom conditions.

The sampled seawater was filtered through a 0.2 μm pore-sized capsule filter to remove suspended particles and 9-L of filtered water was divided into 8 acid-rinsed polycarbonate tanks. The 8 different ice core samples were melted at 1 ˚C and 1-L of melt-water was added and mixed with filtered seawater. This ice-mixed water was incubated for 12 days under light conditions equivalent to mid-July at 72˚N and the temperature was controlled at 1˚C (Photo 3.1.3.XIII-1). We took samples for total- and size-fractionated chlorophyll-a concentration, phytoplankton pigments, light microscopy, and nutrient concentrations to monitor temporal changes of phytoplankton biomass, community compositions, and nutrients for each experiment (see table for sampling schedule).

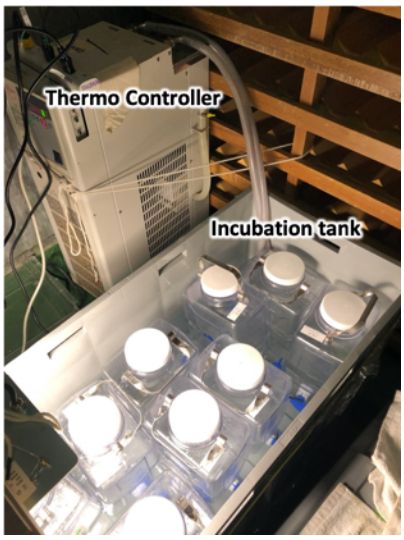

Photo 3.1.3.XIII-1 Incubation system to simulate spring phytoplankton bloom for the Arctic Ocean.

(b) Fall phytoplankton bloom experiment

We collected seawater for incubation from 5 m, sub-surface chlorophyll-a maximum (SCM) layer (23 m), and near-bottom layer (32.9 m) using acid-cleaned Niskin-X samplers equipped on a CTD-CMS at 70.5°N, 168.75°W. The bottom surface sediment was also collected at the same station using a multiple corer system (ASHURA) (see 3.1.3.XIIII for detail sampling). The seawater from 5 m and SCM was collected through 200 μm mesh to remove large zooplankton. The near-bottom seawater was filtered using a filter capsule with 0.2 μm pore size before adding sediments. Then, some sediment-added near-bottom seawater was filtered, and the rest was unfiltered. Using these, we prepared two treatments as follows:

Treatment 1 (surf+SCM): 5m + SCM + filtered sediment-added near-bottom seawater

Treatment 2 (surf+SCM+sediment): 5m + SCM + unfiltered sediment-added near-bottom

seawater

Sediment concentration in the treatment 2 was adjusted to 0.5 cm^3 L^{-1}. Each treatment was prepared in triplicate.

Using an on-deck incubator, the phytoplankton incubation continued for eight days at the actual sea surface temperature and light environments. We monitored the phytoplankton parameters listed above, as Table 3.1.3.XI-1indicated.

From day 8 to 10, after the phytoplankton incubation, we conducted a zooplankton feeding experiment. Five *Calanus glacialis* (C5 stage), collected by an 80 cm ring net (see 3.4 for details) in the Chukchi shelf, were added into a plastic container with five liters of the phytoplankton culture incubated in each treatment. At the same time, we incubated phytoplankton culture as a control. We took samples for total and size chlorophyll-a, DNA, phytoplankton pigments, and light microscopy on days 8 and 10 to calculate the clearance and ingestion rates following Dagg et al., 2006. In addition, the gut pigment and the total length of *Calanus glacialis* were measured on day 10. A part of the antenna of *Calanus glacialis* was stored in ethanol to analyze individuals.

Table 3.1.3.XI-1: Sampling frequency of each parameter for the phytoplankton incubation

Day	0	2	4	6	8
Nutrients	○	○	○	○	○
F_v/F_m	○	○	○	○	○
Total chl.a	○	○	○	○	○
Size chl.a	○				○
Pigments	○				○
Light microscopy	○				○
DNA	○				○

(5) Preliminary results

The time course of total chlorophyll-a during the spring experiment is show in Figure 3.1.3.XI-1, and the time course of total chlorophyll-a, F_v/F_m, and nutrients during the fall bloom experiment are shown in Figures 3.1.3.XI-2 and 3.1.3.XI-3.

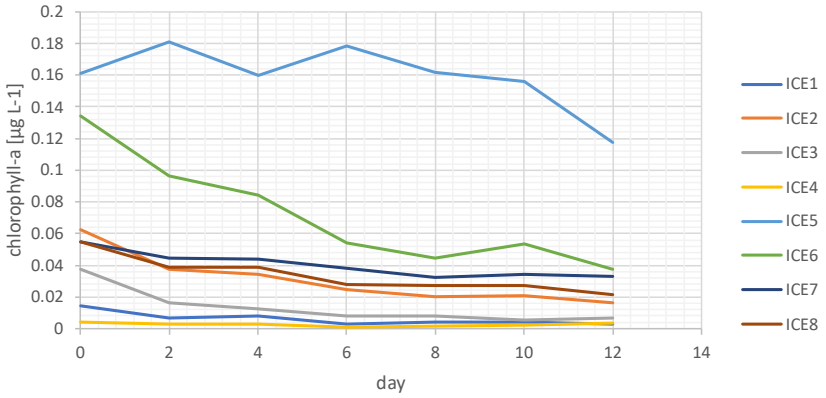

Figure 3.1.3.XI-1: (a) Time course of total chlorophyll-a during the period of the fall bloom experiment.

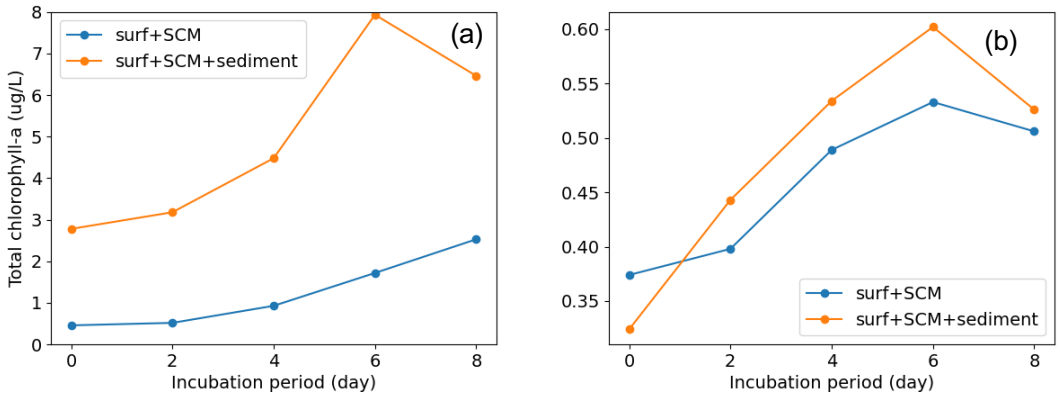

Figure 3.1.3.XI-2: (a) Time course of total chlorophyll-a and (b) Time course of F_v/F_m during the period of the fall bloom experiment.

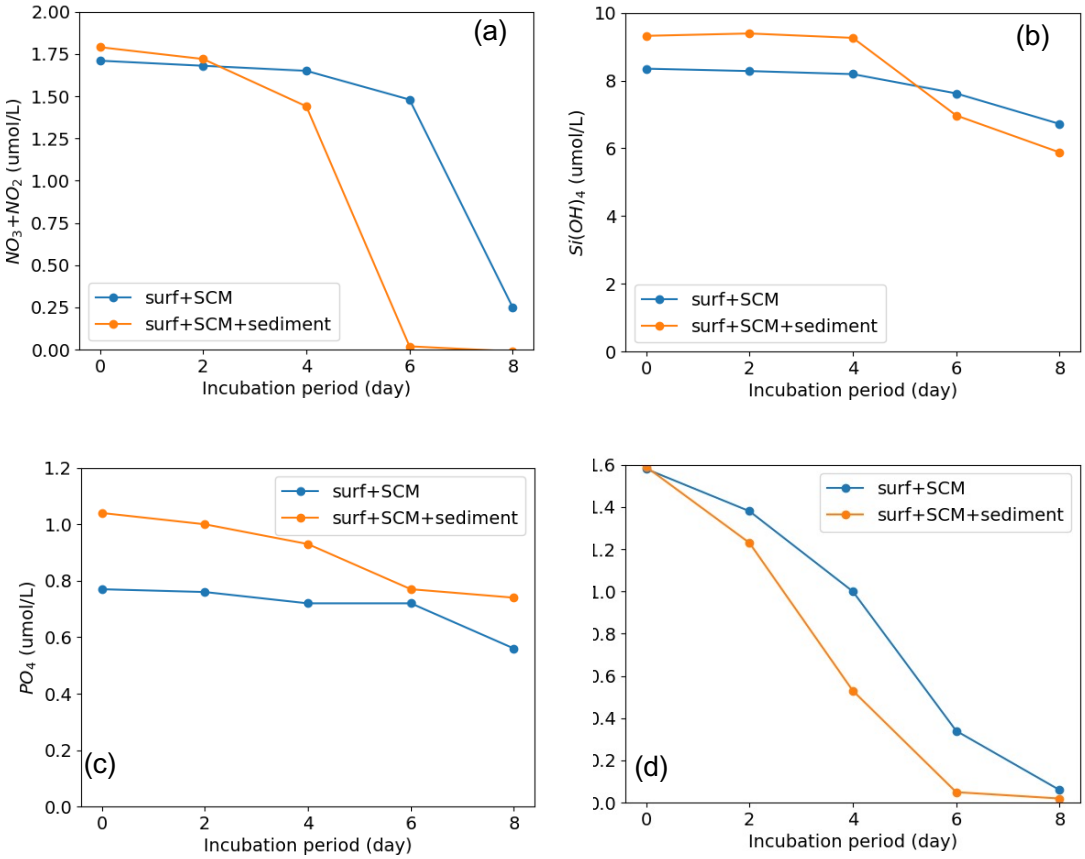

Figure 3.1.3.XI-3: Time course of nutrients. (a) NO_3+NO_2, (b) NH_4, (c) PO_4, (d) $Si(OH)_4$

(6) References

Dagg, M.J., H. Liu, A.C. Thomas (2006) Effects of mesoscale phytoplankton variability on the copepods *Neocalanus flemingeri* and *N. plumchrus* in the coastal Gulf of Alaska, *Deep-Sea Research I*, 53, 321–332.

(7) Data archives

These data obtained in this cruise will be submitted to the Data Management Group of JAMSTEC, and will be opened to the public via "Data Research System for Whole Cruise Information in JAMSTEC (DARWIN)" in JAMSTEC web site.

<http://www.godac.jamstec.go.jp/darwin/e>

3.1.3.XII Trace Metal

(1) Responsible personnel

Mariko Hatta　JAMSTEC

(2) Purpose, background

The three purposes involved in this project related to this shipboard activity and analysis of seawater samples, specifically focusing on aluminum concentration in the Arctic Ocean. Here's a breakdown of each purpose:

1. Establish the shipboard Aluminum system using a programmable flow injection system and identify potential trouble and establish the troubleshooting protocol:

- Purpose: The primary objective here is to set up a shipboard system for monitoring aluminum concentrations in the Arctic Ocean, which is known for its complexity and the challenges it poses for instrumentation. The goal is to create an analytical system that is user-friendly and suitable for shipboard use, eliminating the need for labor-intensive and complicated processes. This system should also avoid the pre-concentration step, which can be challenging in the Arctic Ocean's conditions. Additionally, it aims to anticipate potential technical issues and establish troubleshooting procedures to ensure the reliability of data collection. The simplified system using a programmable flow injection system can streamline the analysis of aluminum concentrations in seawater, making it more accessible and efficient for research purposes in the challenging Arctic environment. It addresses the need for a more practical and user-friendly approach to studying aluminum concentrations in this unique and sensitive ecosystem.
- Background: Aluminum is an important element in oceanography studies as it can serve as a tracer for various ocean processes. The specific objective is to monitor aluminum concentrations in the Arctic Ocean. However, historical instrumentation on board is labor-intensive and complicated to handle at sea, and shore-based determination also requires special instrumentation together with the significant background value issue.

2. Collect seawater samples via Niskin-X bottles attached with a Kevlar cable and with a regular rosette system, to identify any specific contamination:

- Purpose: This purpose involves the collection of seawater samples using specialized Niskin-X bottles attached with Kevlar cables, as well as a regular rosette system. The goal is to examine these samples for any potential contamination.

- Background: Collecting “trace-metal clean” seawater samples is a fundamental but critical activity in the trace metal chemistry in the ocean. The use of Niskin-X bottles and Kevlar cables ensures that samples can be collected at specific depths without contamination. The regular rosette system has potential contamination from its metal cable or settings but likely collects samples from various depths more efficiently. The objective here is to ensure the integrity of the collected samples and assess whether any contamination may affect the analysis of aluminum concentrations from the regular rosette sampling system. Collect seawater samples via Niskin-X bottles attached with a Kevlar cable and with a regular rosette system, to identify any specific contamination.

3. Characterize the water masses with dissolved Aluminum concentration and expand the database in the Arctic Ocean:

- Purpose: This purpose focuses on characterizing different water masses in the Arctic Ocean by analyzing their dissolved aluminum concentrations. Additionally, there's a goal to contribute to and expand the existing database of aluminum concentration data.
- Background: The Arctic Ocean's water masses can vary in their chemical composition, and dissolved aluminum concentration is one parameter used to characterize these variations. Expanding the database of aluminum concentration data in this region contributes to a better understanding of the Arctic Ocean's dynamics and can aid in research related to ocean circulation, biogeochemistry, and environmental changes.

In summary, these purposes represent a comprehensive effort to establish an analytical system, collect seawater samples with minimal contamination, and contribute to the understanding of the Arctic Ocean's water masses through the analysis of dissolved aluminum concentrations. These activities are essential for oceanography research and environmental monitoring in the Arctic region.

(3) Activities (observation, sampling, development)

Seawater samples were collected from the following stations, shown in the map (Figure 3.1.3.XII-1):

Regular rosette system: Stations 2, 3, 7, 8, 9, 10, 11, 12, 13, 14 (NBC), 15, 16, 17, 20, 21, 23, 25, 27, 29, 31, 32 (NAP), 34, 35, 36, 37, 38, Total 26 stations.

Clean-sampling system: Stations 23, 32, 34, 35, total 4 stations.

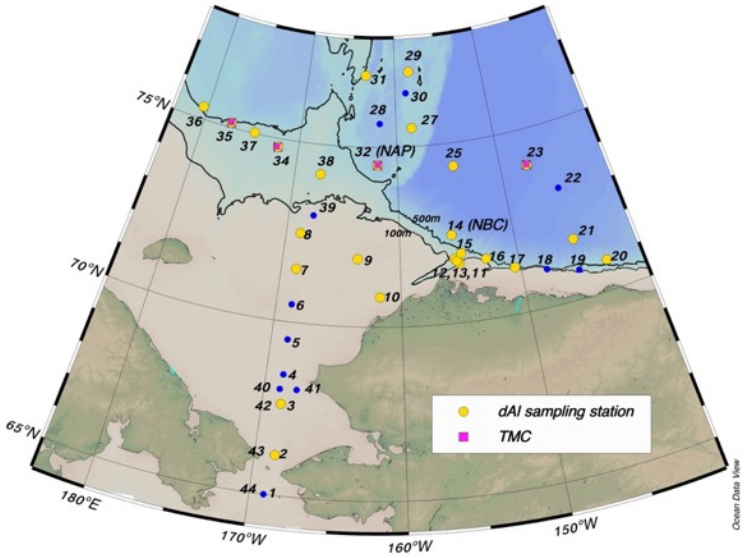

Figure 3.1.3.XII-1. Sampling location during MR23-06C. Blue dots are all of the CTD stations, and yellow circles are the stations to collect dissolved Aluminium samples.

Targeting Parameters

- Conductivity, Temperature, Depth, Turbidity, Chlorophyll, DO from a portable RINKO-Profiler
- Depth from a portable depth sensor
- Salinity
- Nutrients (NH_4, NO_3, NO_2, PO_4, SiO_2)
- Dissolved trace metals (Fe, Al etc.)
- Total trace metal (Fe, Al etc.)

The ranges and accuracies of parameters measured by the RINKO-Profiler (ASTD152, S/N:0659) are as follows:

Parameter	Range	Accuracy
Conductivity	0.5 ~ 70 [mS/cm]	+/- 0.01 [mS/cm]
Temperature	-3 ~ 45 [deg-C]	+/- 0.01 [deg-C]
Depth	0 ~ 600 [m]	+/- 0.3 [%] FS
Turbidity	0 ~ 1000 [FTU]	+/- 0.3 [FTU] or +/- 2 [%]
Chlorophyll	0 ~ 400 [ppb]	+/- 1 [%] FS
DO	0 ~ 200 [%]	+/- 2 [%] FS

The calibration data sheet (Date: 2020-07-10):

Parameter.	Actual.	Measured.	Deff.	Accuracy
Temp.[deg-C]	12.655	12.654.	-0.001	+/- 0.008 [deg-C]
Cond. [ms/cm]	40.607	40.607	0.000	+/- 0.008 [mS/cm]
TURB. [FTU]	172.68	172.61	-0.07	+/- 3.11 [FTU]
Chl. [ppb].	75.22.	77.22.	2.00	+/- 4.00 [ppb]
Depth [MPa].	4.500=447.68 (m)	447.67	-0.01	+/- 2.50 [m]
DO [%].	99.04	98.92.	-0.12.	+/- 1.00 [%]

The collected seawater samples were subjected to acidification using 100 μL of 20% trace metal clean hydrochloric acid spiked into a 100 mL sample. Subsequently, the determination of dissolved aluminum content was carried out using the newly established protocol, employing the programmable flow injection technique in conjunction with a PMT detector.

(4) Methods, instruments

(4-1) Trace metal clean sampling system

The sampling process was executed with the use of individual Niskin-X bottles directly attached to a Kevlar cable. To ensure secure attachment, vinyl tape was wrapped around the Kevlar cable, and each Niskin sampling bottle was affixed using stainless pins designed to fit the cable. This meticulous attachment method was employed to minimize any potential damage to the Kevlar cable during the mounting of Niskin bottles.

At the lowermost part of the cable, a weight system consisting of two sets of 20 kg weights, combined by a rope, was attached, along with a portable RINKO profiler, using a shackle. These weights served the crucial purpose of providing negative buoyancy for the Kevlar line. To mitigate the risk of equipment-induced contamination, the deepest Niskin bottle was positioned at least 1 meter away from the profiler and weights.

The shallower sampling depths were located at points exceeding 20 meters. The standard approach of manually suspending individual Teflon-coated Niskin bottles on the Kevlar cable was employed. This time-tested method, in use for over three decades (as outlined by Bruland et al., 1979), proved effective.

Each Niskin bottle was equipped with an internally recording depth sensor (JFA Advantech) to

accurately capture the sampling depth. The techniques and data used for verifying depth should be comprehensively documented in the cruise metadata.

The cable was lowered and rolled up at a controlled speed of less than 0.5 meters per second during the sampling process. Samples were collected at specific locations as follow:

.Station	Target Depth (m)	Sample	RINKO
23	20,50,100,300,400	Y	Y
32	100,150,220,300,400	Y	Y
34	100,125,175,200,250	Y	Y
35	100,125,175,200	Y	Y

(4-2) Niskin-X bottle

In this cruise, the Niskin-X bottles were meticulously prepared to maintain the integrity of the samples. Here's a step-by-step summary of the preparation and handling process:

1. Before the cruise commenced, the Niskin-X bottles were coated with Teflon, and all the O-rings were replaced with Viton ones that had been pre-acid washed. No acid made contact with the external surfaces of the bottles, especially the nylon components.
2. At the start of this cruise, each bottle was cleaned according to the GEOTRACES cookbook protocol, ensuring thorough decontamination. The cleaning process involved the following steps:
   a. Each bottle was filled with a 5% detergent solution and left for one day.
   b. Bottles were rinsed ten times with deionized ultra-high purity water (Milli-Q water) until there were no traces of detergent.
   c. Bottles were filled with 0.1M HCl (analytical grade) for two days and then emptied through the spigot to rinse.
   d. Bottles were rinsed five times with deionized ultra-high purity water (Milli-Q water).
   e. Bottles were filled with ultra-high purity water (Milli-Q water) for two days.
   f. After discarding the Milli-Q water, bottles were filled with ultra-high purity water (Milli-Q water) until ready for use.
3. Following the cleaning process, the Niskin bottles were transferred to a clean booth (located in WET2 lab), where they were prepared for sampling. Each bottle was covered with big plastic bags, and a Teflon-coated messenger was added when required. These preparations were completed in a WET 2 lab.
4. The Niskin bottles, equipped with depth sensors (JFA Advantech), were arranged inside

the clean sampling booth. The plastic bags covering the bottles were removed right before attaching them to the Kevlar cable.

5. During the deployment, two different sizes of Niskin bottles were used based on the specific cast requirements.
6. Once the Kevlar cable reached the target depth, a Teflon-coated messenger was released, and a brief waiting period of approximately 1 minute (or 3 mins, depending on the depth) allowed the last bottle to be tripped.
7. After completing the cast, each Niskin bottle was transferred to the clean booth for the sampling process. A custom-built Niskin bottle cart (an updated version) was used to carefully transport the sampling bottles, which were then hung on the sampling rack located in a clean sampling booth. This process was facilitated by personnel, typically a helper, who received the bottles through a door in the WET2 lab.
8. The sampling rack itself was specifically constructed for this activity, ensuring secure handling and storage of the Niskin bottles during the entire sampling operation. This meticulous approach in bottle preparation and handling was crucial for maintaining the integrity of the collected samples and ensuring the reliability of the data obtained during the cruise.

(4-3) Sub-sampling in the clean booth

The following samples were collected within a HEPA filtered temporal clean booth.

Parameter	Filtered[y/n]	Analysis on the board[y/n]	Stored samples[y/n]
Salinity	n	n	y
Nutrients	n	y	n
Dissolved Al	y	y	n
Dissolved Fe	y	n	y

The handling and preparation of samples for various analyses, including salinity, nutrients, and dissolved metals (Aluminum and Iron) involved several meticulous steps:

Salinity/nutrient Samples:

- Salinity and nutrient samples were transferred directly from the Niskin bottles to individual subsampling bottles.
- Samples for salinity were stored for later analysis, and nutrient measurements were carried out on the RV Mirai using shipboard protocols established by MWJ.

Dissolved Aluminum and Iron Samples:

- Samples for dissolved metal analysis, including Aluminum, were filtered through 0.2 μm Acropak filters.
- Dissolved Aluminum samples were directly collected in acid-clean PMP (perfluoropolymer) bottles. Prior to the cruise, these bottles were pre-cleaned with 1M HCl.
- Dissolved Iron samples were stored in pre-cleaned 100 mL PFA (perfluoroalkoxy) bottles. These bottles were cleaned using the GEOTRACES cookbook protocols in a shore-based laboratory.

The cleaning process for both types of bottles was as follows:

1. Bottles were soaked for one day in an alkaline detergent.
2. Rinsed ten times with ultra-high purity water (Milli-Q water) until no traces of detergent remained.
3. Soaked in a 6 M reagent-grade HCl bath for more than one day.
4. Rinsed five times with ultra-high purity water (Milli-Q water).
5. Filled with 1M nitric acid (analytical grade) and heated to 80°C for 5 hours in a heated oven. Each bottle was packed with a plastic bag containing Milli-Q water in case of any spills.
6. Rinsed five times with ultra-high purity water (Milli-Q water) inside an ISO Class-5 laminar flow hood.
7. Filled the bottles with ultra-high purity water (Milli-Q water) and heated them at 80°C for 5 hours in a heated oven. Each bottle was again packed with a plastic bag containing Milli-Q water as a precaution.
8. Rinsed five times with ultra-high purity water (Milli-Q water) inside an ISO Class-5 laminar flow hood.
9. The cleaned bottles were packed in sets of six within double bags until they were ready for use.

These rigorous cleaning and preparation procedures were essential to ensure the integrity of the collected samples and to prevent any contamination during subsequent analysis. The specific steps were designed to meet the high purity standards required for accurate dissolved metal measurements in the samples.

(4-4) Shipboard dissolved Al measurement

(4-4-1) Instrumentation

The instrument, miniSIA-2 (Global FIA, Fox Island, WA, USA), comprises two high precision,

synchronously refilling milliGAT pumps, two thermostated holding coils, a 6-port LOV (model COV-MANI-6, constructed from polymethyl methacrylate, Perspex®) furnished with a module for an fluoroecence flow cell (Figure 3.1.3.XII-2). All tubing connections, downstream from the milliGAT pumps including the holding coils (volume 1000 µL), were made with 0.8 mm I.D. polytetrafluoroethylene (PTFE). The holding coils were thermostated at 50C for all aluminium analysis. The tubing between the carrier stream reservoirs and the milliGAT pump was made from 1.6 mm I.D. PTFE tubing to minimize degassing under reduced pressure at higher aspiration flow rates. Photon counter for fluorescence measurement with filter holder mounted for easy access (Global FIA, Fox Island, WA, USA) with a high intensity LED with filter holder mounted encased in 0.8 mm I.D. black tubing. The end of each fiber exposed to the liquid was cemented with epoxy, cut square, and polished. All assay steps were computer-controlled using commercially available software (FloZF, GlobalFIA, Fox island, WA, USA). The outlet of the flow cell was fitted with a 40-psi flow restrictor (GlobalFIA, Fox Island, WA, USA), which, by elevating the pressure within the flow path, efficiently prevented the formation of microbubbles from spontaneous outgassing.

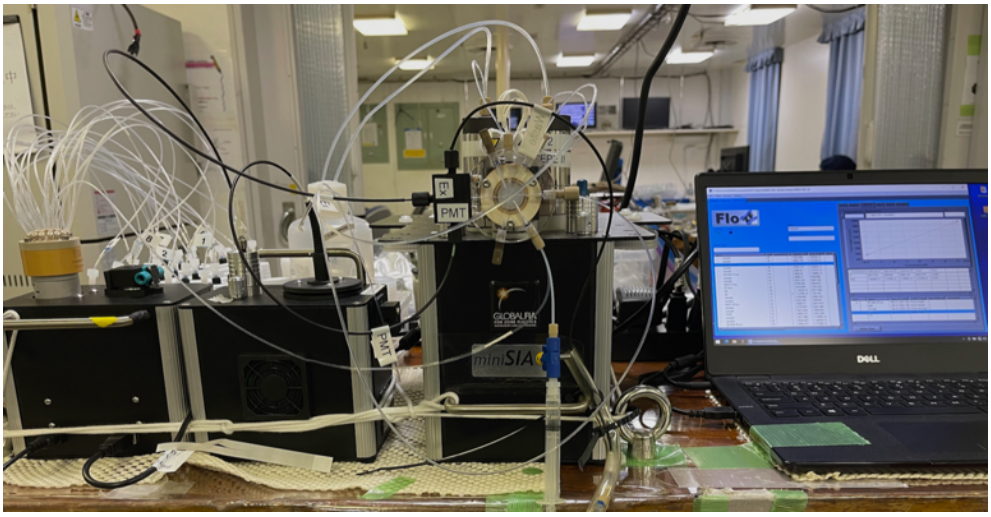

Figure 3.1.3.XII-2. Shipboard analytical system for dissolved Aluminium determination using the programmable flow injection technique.

(4-4-2) Analytical methodology

Methodology (pFI-Al) using Programmable Flow Injection Technique:

1. Carrier Solution:

The carrier solution used in the analysis is MilliQ water, which is known for its high purity and suitability for analytical purposes.

2. Stock Aluminum Standard Solution:

A stock Aluminum standard solution with a concentration of 100.1 mg/L was purchased. This stock solution was then diluted with acidified MilliQ water (pH 1) to create a primary stock solution with a concentration of 3.7 µM.

3. Working Standards:
Working standards with different concentrations were prepared using the primary stock solution and filtered seawater solution or with MilliQ water. The working standards created include:
0 nM (control or blank), 11.08 nM, 22.09 nM
4. Reaction Reagent:
Dissolve 0.05g of Lumogalion in 30 mL of MilliQ water to create Lumogalion stock solution. Combine 1 mL of the Lumogalion solution with 100 mL of a 2M ammonium acetate buffer solution at a pH of 6.

5. Brij Solution:
The Brij solution was stored in a 60°C oven to maintain a liquid form.
To create the 5% Brij solution, dissolve 17.5 mL of Brij solution and scale it up to a total volume of 200 mL with MilliQ water.

(5) Results, Future Plans, Lists (samples, observation equipment, deployment & recovery), Local field map (dive tracks, sampling points, survey lines), etc

Results:

- During the cruise, a total of 416 seawater samples were collected and analyzed using the developed method.
- The detection limit of this method was approximately 1-2 nM, indicating its sensitivity to low concentrations of Aluminum in seawater.
- Preliminary vertical profiles of dissolved Aluminum (dAl) were generated, and a subset of these profiles is shown in Figure 3.1.3.XII-3.
- The dAl values increased with depth, and a significant dAl anomaly was observed at the surface, suggesting a strong influence from riverine input.
- Subsurface waters exhibited lower dAl values and were characterized as "winter water" based on Danielson et al.'s classification (2020).
- Higher dAl values were associated with the presence of Atlantic waters.
- Figure 3.1.3.XII-4 displays the dAl values at station 20, and there is a close agreement with data from a previous cruise (MR22-06C Station 16) that used a flow injection system for determination.

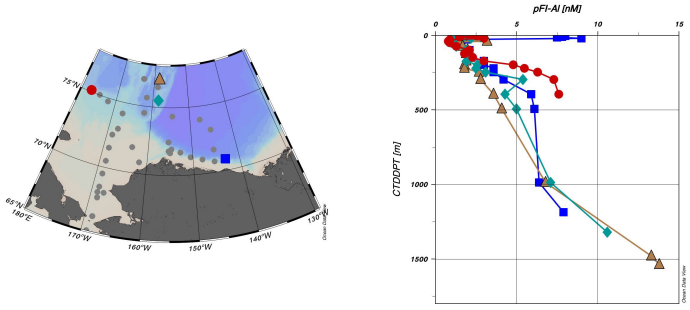

Figure 3.1.3.XII-3. Vertical profiles of dissolved Al during MR23-05C.

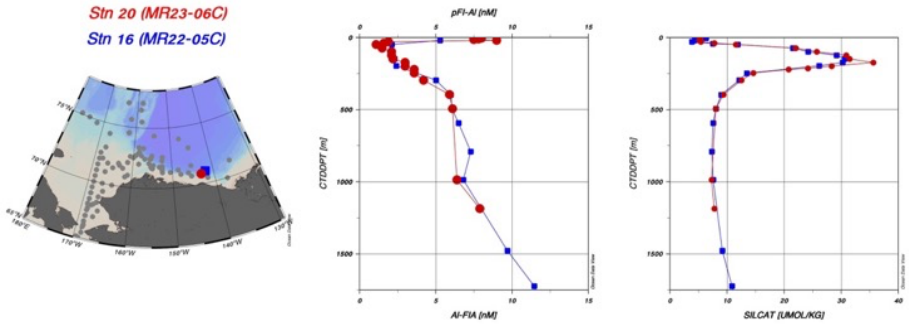

Figure 3.1.3.XII-4. The vertical profiles of dissolved Aluminium during the MR23-06C and MR22-06C. The sample of MR22-05C was determined using a flow injection analysis (Resing and Measures, 1994).

Future Plans:

- Further analysis and interpretation of the entire dataset to provide a comprehensive view of dissolved Aluminum concentrations in the study area.
- Investigation of the factors influencing the observed dAl anomalies, such as riverine inputs and water mass dynamics.
- Comparisons and validations with other data sources and cruises to refine the understanding of the spatiotemporal distribution of dAl in the region.
- Refining the analytical methodology and enhancing the detection limits for more precise measurements in future research.
- Continued monitoring and data collection to build on the insights gained during this cruise and contribute to a better understanding of oceanographic processes in the Arctic Ocean.

(6) References

Danielson, S. L., Ahkinga, O., Ashjian, C., Basyuk, E., Cooper, L. W., Eisner, L., et al. (2020). Manifestation and consequences of Arctic amplification in the Bering and Chukchi Seas. Deep Sea Res.

Resing and Measures (1994). Fluorometric Determination of AI in Seawater by Flow Injection Analysis with In-line Preconcentration, Anal. Chem., 66, 4105-4111.

(7) Data archives

These data obtained in this cruise will be submitted to the Data Management Group (DMG) of JAMSTEC, and will opened to the public via “Data Research System for Whole Cruise Information in JAMSTEC (DARWIN)” in JAMSTEC web site.

http://www.godac.jamstec.go.jp/darwin/e

3.1.3.XIII. Sediment sampling

(1) Personnel

Amane Fujiwara (JAMSTEC) -Principal Investigator
Yuri Fukai (JAMSTEC)
Satoshi Kimura (JAMSTEC)
Kohei Matsuno (Hokkaido University)

(2) Objectives

Sediment sampling was conducted to reveal the microalgal biomass and the spatial distribution of diatom communities in sediments of the Pacific Arctic shelf.

(3) Parameters

Chlorophyll-a concentration
Diatom cell number

(4) Instruments and methods

Multiple corer system (Ashura) used in this cruise consists of the main body (60 kg weight) and three acryl corer attachments. The core barrel is 60 cm long and has a 7.4 cm inner diameter. At the beginning of the multiple corer system going down, the speed of wire out was set to be 0.5 m s^{-1}. Wire out was stopped at a depth of about 5–10 m above the seafloor, and the core system was left to stand for 30 seconds to reduce any pendulum motion of the system. After stabilizing the multiple corer system, the wire was stored at a speed of 0.3 m s^{-1} while carefully watching a tension meter. After confirmation of the multiple corer system touching the bottom, the wire continued until bowing. The rewinding of the wire was started at a dead slow speed (0.3 m s^{-1}), and then the winch wire was wound up at 0.5 m s^{-1}.

Sediment sampling by the multiple corer system was conducted at ten stations in the Chukchi shelf (Table 3.1.3.XIII-1). Surface sediment subsamples for chlorophyll-a and diatom cell analyses were collected from the sediment cores using a spatula. A part of the sediment (1 cm^3) was soaked immediately in 7 mL of *N,N*-dimethylformamide (DMF, Wako Pure Chemical Industries Ltd.) and stored at -20 °C in the dark for at least 24 hours to extract chlorophyll-a. Chlorophyll-a concentrations were measured by a fluorometer (10-AU, TURNER DESIGNS) following the method of Welschmeyer (1994). Before the analysis, the 10-AU fluorometer was calibrated against pure chlorophyll-a (Sigma-Aldrich Co., LLC). The rest of the sediment has been stored in a refrigerator until further diatom cell analysis on land.

Table 3.1.3.XIII-1: Sediment sampling location

Station No.	Date (UTC)	Latitude (°N)	Longitude (°W)	Bottom depth (m)
3	2023/9/8	67.66	168.67	49
5	20203/9/9	69.38	168.75	51
6	20203/9/9	70.50	168.76	38
9	2023/9/10	71.90	163.64	41
10	2023/9/11	70.84	161.72	44
11	2023/9/12	71.66	155.02	97
39	2023/9/28	73.03	167.76	66
40	2023/9/29	68.08	168.87	58
41	2023/9/30	68.10	167.67	52
44	2023/9/30	65.00	169.07	50

(5) Preliminary results and Future plans

Figure 3.1.3.XIII-1 shows chlorophyll-a concentrations in sediments as preliminary results. Diatom cells in sediments will be estimated using the most probable number (MPN) method (Imai et al., 1984) in the shore laboratory.

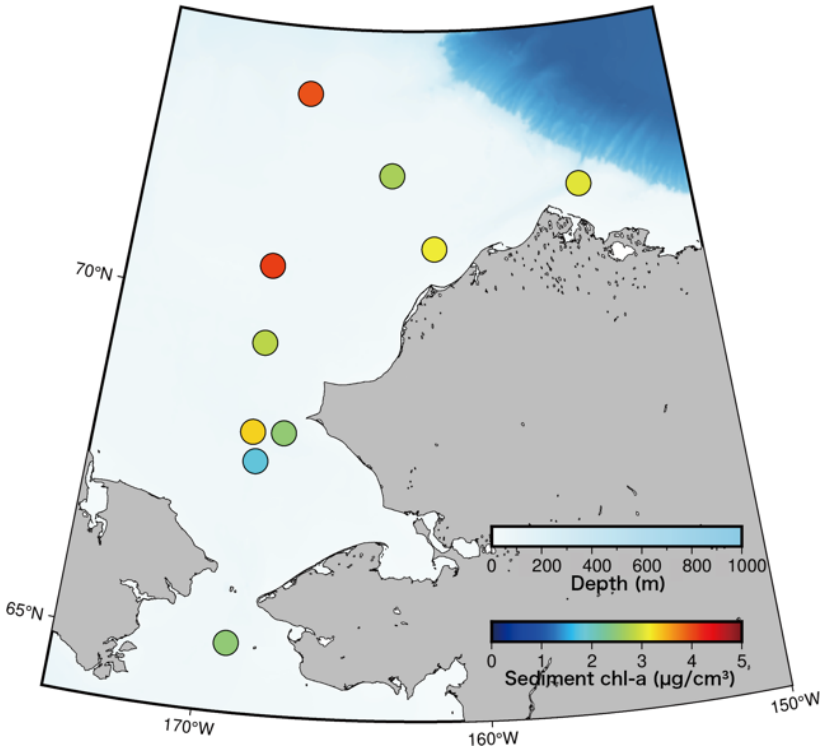

Figure 3.1.3.XIII-1: Chlorophyll-a concentration in the surface sediments

(6) References

Welschmeyer, N. A. (1994), Fluorometric analysis of chlorophyll a in the presence of chlorophyll b and pheopigments. *Limnol. Oceanogr.* 39, 1985–1992.

Imai, I., Itoh, K., & Anraku, M. (1984). Extinction dilution method for enumeration of dormant cells of Red Tide organisms in marine sediments. *Bulletin of Plankton Society of Japan*, 312, 123–124.

(7) Data archives

These data obtained in this cruise will be submitted to the Data Management Group (DMG) of JAMSTEC, and will opened to the public via "Data Research System for Whole Cruise Information in JAMSTEC (DARWIN)" in JAMSTEC web site.

http://www.godac.jamstec.go.jp/darwin/e

3.1.4. Geological observations

3.1.4.I. Sea bottom topography measurements

(1) Responsible Personnel

Amane Fujiwara	JAMSTEC -PI
Ryo Oyama	NME (Nippon Marine Enterprises, Ltd.)
Kazuho Yoshida	NME
Satomi Ogawa	NME
Yohei Sugimoto	NME
Yoichi Inoue	MIRAI Crew

(2) Purpose, background

R/V MIRAI is equipped with the Multi Beam Echo Sounding system (MBES). The objective of MBES is collecting continuous bathymetric data along ship track to make a contribution to geological and geophysical studies.

(3) Activities

Observation period: 25 Aug. 2023 - 28 Sep. 2023

(4) Methods, instruments

The MBES system “SEABEAM 3012 (L3 Communications ELAC Nautik, Germany)” on R/V MIRAI was used for measuring depth of water during this cruise. To get accurate sound velocity of water column for ray-path correction of acoustic multibeam, we used Surface Sound Velocimeter (SSV) data to get the sea surface (6.62m) sound velocity, and the deeper depth sound velocity profiles were calculated by temperature and salinity profiles from CTD, XCTD and Argo float data by the equation in Del Grosso (1974)

In addition, the water column image analyzer (WCI: one of the function with SEABEAM 3012) was operated in the arctic ocean area. This equipment can collect the water column image data of backscattering signal from the transducer to the seafloor.

Table 3.1.4.I-1 shows system configuration and performance of SEABEAM 3012.

Table 3.1.4.I-1: SEABEAM 3012 System configuration and performance

Frequency:	12 kHz
Transmit beam width:	2.0 degree

Transmit power:	4 kW
Transmit pulse length:	2 to 20 msec.
Receive beam width:	1.6 degree
Depth range:	50 to 11,000 m
Number of beams:	301 beams (Spacing mode: Equi-angle)
Beam spacing:	1.5 % of water depth (Spacing mode: Equi-distance)
Swath width:	60 to 150 degrees
Depth accuracy:	< 1 % of water depth (average across the swath)

(5) Results, Future Plans, Lists

i) Results

The results will be published after primary processing.

ii) Data archives

These data obtained in this cruise will be submitted to the Data Management Group of JAMSTEC, and will be opened to the public via “Data Research System for Whole Cruise Information in JAMSTEC (DARWIN)” in JAMSTEC web site.

< http://www.godac.jamstec.go.jp/darwin/e >

iii) Remarks (Times in UTC)

The following periods, MBES data acquisition was suspended.

00:00 03 Sep. 2023 - 12:31 12 Sep. 2023 (called at Dutch Harbor & shallow water)
08:12 13 Sep. 2023 - 08:21 13 Sep. 2023 (system maintenance)
14:00 13 Sep. 2023 - 14:14 13 Sep. 2023 (ANS system operation)
15:24 13 Sep. 2023 - 16:10 13 Sep. 2023 (ANS system operation)
10:25 14 Sep. 2023 - 13:25 14 Sep. 2023 (shallow water)
07:27 15 Sep. 2023 - 14:02 15 Sep. 2023 (shallow water)
09:19 16 Sep. 2023 - 10:37 16 Sep. 2023 (shallow water)
01:01 19 Sep. 2023 - 01:19 19 Sep. 2023 (system maintenance)
23:10 21 Sep. 2023 - 23:17 21 Sep. 2023 (system maintenance)
23:10 21 Sep. 2023 - 23:17 21 Sep. 2023 (system maintenance)
19:09 23 Sep. 2023 - 19:25 23 Sep. 2023 (ANS system operation)
22:48 24 Sep. 2023 - 21:56 21 Sep. 2023 (system maintenance)
16:38 26 Sep. 2023 - 16:47 26 Sep. 2023 (system maintenance)

3.1.4.II. Sea surface gravity measurements

(1) Responsible personnel

Amane Fujiwara	JAMSTEC -PI
Ryo Oyama	NME (Nippon Marine Enterprises, Ltd.)
Kazuho Yoshida	NME
Satomi Ogawa	NME
Yohei Sugimoto	NME
Yoichi Inoue	MIRAI Crew

(2) Purpose, background

The local gravity is an important parameter in geophysics and geodesy. The gravity data were collected during this cruise.

(3) Activities

Observation period: 25 Aug. 2023 - 04 Oct. 2023

(4) Methods, Instruments

i) Parameters

Relative Gravity [CU: Counter Unit]

[mGal] = (coefl: 0.9946) * [CU]

ii) Methods, Instruments

The relative gravity using LaCoste and Romberg air-sea gravity meter S-116 (Micro-g LaCoste, LLC) was measured during the cruise. To convert the relative gravity to absolute one, we measured gravity, usingthe portable gravity meter (Scintrex gravity meter CG-5), at Shimizu port as the reference points.

(5) Results, Future plans, Lists

i) Results

Absolute gravity table is shown in Table 3.1.4.II-1.

Table 3.1.4.II-1: Absolute gravity table of the MR23-06C cruise

No.	Date m/d	UTC	Port	Absolute Gravity [mGal]	Sea Level [cm]	Ship Draft [cm]	Gravity at Sensor *1 [mGal]	S-116 Gravity [mGal]
#1	8/24 12001.74	07:05	Shimizu(Okitsu)	979729.49	201	658	979730.39	
#2*2	11/9	-	Shimizu	-	-	-	-	-

*1: Gravity at Sensor = Absolute Gravity + Sea Level*0.3086/100 + (Draft-530)/100*0.2222
*2: The scheduled date and port of the end of the next cruise.

ii) Data archives

These data obtained in this cruise will be submitted to the Data Management Group of JAMSTEC, and will be opened to the public via “Data Research System for Whole Cruise Information in JAMSTEC (DARWIN)” in JAMSTEC web site.

<http://www.godac.jamstec.go.jp/darwin/e>

iii) Remarks

The following period, Navigation data (latitude, longitude, speed over ground and course over ground) had been invalid due to suspending input of GNSS NMEA. These navigation data were replaced to correct value which were complemented from other GNSS NMEA data.

01:14UTC 27 Aug. 2023 - 03:04UTC 27 Aug. 2023

3.1.4.III. Surface magnetic field measurement

(1) Responsible personnel

Amane Fujiwara	JAMSTEC -PI
Ryo Oyama	NME (Nippon Marine Enterprises, Ltd.)
Kazuho Yoshida	NME
Satomi Ogawa	NME
Yohei Sugimoto	NME
Yoichi Inoue	MIRAI Crew

(2) Purpose, background

Measurement of magnetic force on the sea is required for the geophysical investigations of marine magnetic anomaly caused by magnetization in upper crustal structure. We measured geomagnetic field using a three-component magnetometer during this cruise.

(3) Activities

Observation period: 25 Aug. 2023 - 04 Oct. 2023

(4) Methods, instruments

i) Parameters

Three components of a magnetic field vector on-board, Hx, Hy, Hz [nT]

Hx : A magnetic field component in the bow/stern direction on the vessel horizontal plane. “To bow” is positive.

Hy : A magnetic field component in the port/starboard direction on the vessel horizontal plane. “To starboard” is positive.

Hz : A perpendicular magnetic field component to the vessel horizontal plane. “upward” is positive.

ii) Methods, instruments

A shipboard three-components magnetometer system (SFG2018, Tierra Tecnica) is equipped on-board R/V MIRAI. Three-axes flux-gate sensors with ring-cored coils are fixed on the fore mast. Outputs from the sensors are digitized by a 20-bit A/D converter (1 nT/LSB) and sampled at 8 times per second. Yaw (heading), Pitch and Roll are measured by the Inertial Navigation Unit (INU) for controlling attitude of a Doppler radar. Ship's position, speed over ground (Differential GNSS) and gyro data are taken from LAN every second.

The relation between a magnetic-field vector observed on-board, $\mathbf{H}_{\mathrm{ob}}$, (in the ship's fixed coordinate system) and the geomagnetic field vector, $\mathbf{F}$, (in the Earth's fixed coordinate

system) is expressed as:

$$\mathbf{H}_{\mathrm{ob}} = \tilde{\mathbf{A}}\,\tilde{\mathbf{R}}\,\tilde{\mathbf{P}}\,\tilde{\mathbf{Y}}\,\mathbf{F} + \mathbf{H}_{\mathrm{p}} \qquad \text{(a)}$$

where $\tilde{\mathbf{R}}$, $\tilde{\mathbf{P}}$ and $\tilde{\mathbf{Y}}$ are the matrices of rotation due to roll, pitch and heading of a ship, respectively. $\tilde{\mathbf{A}}$ is a 3 x 3 matrix which represents magnetic susceptibility of the ship, and $\mathbf{H}_{\mathrm{p}}$ is a magnetic field vector produced by a permanent magnetic moment of the ship's body. Rearrangement of Eq. (a) makes

$$\tilde{\mathbf{B}}\,\mathbf{H}_{\mathrm{ob}} + \mathbf{H}_{bp} = \tilde{\mathbf{R}}\,\tilde{\mathbf{P}}\,\tilde{\mathbf{Y}}\,\mathbf{F} \quad \text{(b)}$$

where $\tilde{\mathbf{B}} = \tilde{\mathbf{A}}^{-1}$, and $\mathbf{H}_{bp} = -\tilde{\mathbf{B}}\,\mathbf{H}_{\mathrm{p}}$. The magnetic field, $\mathbf{F}$, can be obtained by measuring, $\tilde{\mathbf{R}}$, $\tilde{\mathbf{P}}$, $\tilde{\mathbf{Y}}$ and $\mathbf{H}_{\mathbf{ob}}$, if $\tilde{\mathbf{B}}$ and $\mathbf{H}_{bp}$ are known. Twelve constants in $\tilde{\mathbf{B}}$ and $\mathbf{H}_{\mathbf{bp}}$ can be determined by measuring variation of $\mathbf{H}_{\mathbf{ob}}$ with , $\tilde{\mathbf{R}}$, $\tilde{\mathbf{P}}$, and, $\tilde{\mathbf{Y}}$ at a place where the geomagnetic field, $\mathbf{F}$, is known.

(5) Results, Future Plans, Lists

i) Results

The results will be published after the primary processing.

ii) Data archives

These data obtained in this cruise will be submitted to the Data Management Group of JAMSTEC, and will be opened to the public via “Data Research System for Whole Cruise Information in JAMSTEC (DARWIN)” in JAMSTEC web site.

<http://www.godac.jamstec.go.jp/darwin/e>

iii) Remarks

a) For calibration of the ship’s magnetic effect, “figure-eight” turns (a pair of clockwise and anti-clockwise rotation) were held at the following periods and positions.

20:14UTC 31 Aug. 2023 - 20:36UTC 31 Aug. 2023 (53-47N, 177-06E)
01:33UTC 18 Sep. 2023 - 01:55UTC 18 Sep. 2023 (73-11N, 145-10W)
06:03UTC 26 Sep. 2023 - 06:25UTC 26 Sep. 2023 (75-08N, 177-18W)

b) The following periods, navigation data (speed over ground, gyro, longitude, latitude, and sea depth) were invalid.

01:23:03UTC 22 Sep. 2023 - 01:23:10UTC 22 Sep. 2023
00:38:46UTC 28 Sep. 2023 - 00:39:23UTC 28 Sep. 2023

3.1.5 Reception experiment of GPS augmentation data by Quasi-Zenith Satellite

Evaluation of performance of the DFMC SBAS from QZSS

(1) Personnel

Toru Takahashi (ENRI)

Amane Fujiwara (JAMSTEC)

(2) Objectives

The aviation and maritime activities in the Arctic are growing with the recession of the Arctic sea ice. A model study suggested that the Global Navigation Satellite System (GNSS), which operates with the augmentation system such as the Satellite-based augmentation systems (SBAS) and Advanced Receiver Autonomous Integrity Monitoring (ARAIM), is effective for the navigation of aviation and maritime in the Arctic because of poor infrastructures (Reid et al., 2016). However, the current L1 SBAS broadcasts augmentation messages from geostationary (GEO) satellites, which are not available practically in the polar region at a latitude of 72 degrees or higher.

The Dual Frequency Multi Constellation Satellite Based Augmentation System (DFMC SBAS) has been standardization by the International Civil Aviation Organization (ICAO). Broadcasting augmentation messages from the Inclined Geosynchronous Orbit (IGSO) satellite is considered to be included in the future updates. The Electronic Navigation Research Institute (ENRI) developed the DFMC SBAS prototype based on the draft standards (Kitamura et al., 2018), and test messages are broadcasted from the Japanese Quasi-Zenith Satellite System (QZSS).

In the polar region, an auroral activity often generates the irregularity ionospheric plasma density and the ionospheric electric filed is intensified simultaneously. The carrier phase of the GNSS signal is fluctuated by the auroral activity. Since the fluctuation sometimes causes the loss of lock on GNSS signals, the impact the auroral activity on the GNSS carrier phase should be investigated.

The main objective of this study is to evaluate the performance DFMC SBAS broadcasted from Japanese QZSS in the Arctic and high latitude regions. To test the DFMC SBAS in the Arctic, we installed the GNSS antenna, GNSS receivers, and DFMC SBAS receivers to oceanographic research vessel MIRAI.

(3) Activities (observation, sampling, development)

Signals from GNSS satellites and DFMC SBAS messages transmitted from the QZSS are recorded by GNSS receivers installed in MIRAI. Performance (accuracy and integrity) of the DFMC SBAS from QZSS is evaluated in the on-board environment in the Arctic region.

i. GNSS Receiver

A JAVAD DELTA receiver recorded signals from GPS, Galileo, GLONASS, BeiDou, and QZSS at the frequency of L1, L2, and L5 bands. The receiver recorded the observation message, including the pseudorange and carrier phase, with a sampling rate of 1 Hz. The navigation message, including the satellite obit information

ii. DFMC SBAS Message receivers

To obtain DFMC SBAS messages, a Furuno prototype DFMC SBAS receiver and CORE Cohac receivers were installed. The DFMC SBAS messages were generated by Electronic Navigation Research Institute (ENRI) and broadcasted from QZS02 and OZS04 satellites with a frequency of 1 Hz.

iii. Scintillation receiver

The GNSS signals are sometimes fluctuated by a combination of the ionospheric irregularity and electric field. The fluctuation is called scintillation and becomes a cause of the loss-of-lock GNSS signal. Since we need to receive the carrier phase with high and precise sampling to observe the scintillation, the Septentrio PolaRx5S, which records the GNSS signals with a sampling rate of 50

iv. GNSS Antenna

The GNSS antenna used was a Trimble GA830 capable of receiving L1, L2, and L5 bands. The antenna was designed for maritime and cold weather specification.

(4) Activities (observation, sampling, development)

The GNSS signals successfully received by JAVAD DELTA and Septentrio PolaRx5S. Figure 1 shows the time series of the solution of precise point positioning. The DFMC SBAS message was also recorded by the Furuno prototype receiver and CORE Cohac, but the messages were not sometime recorded. This was likely to be caused by the ionospheric scintillation or visibility of the satellite.

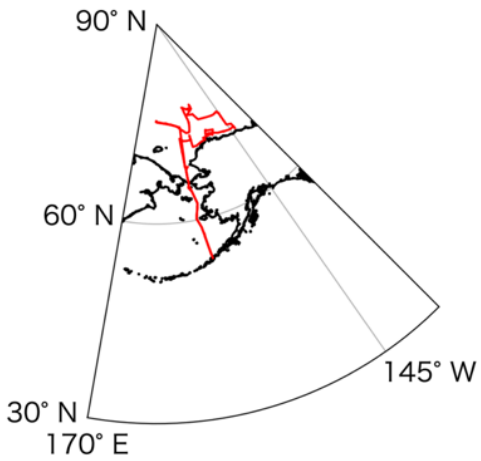

Figure 3.1.5-1. Time series of solution of precise point positioning

(5) References

Kitamura, M., Aso, T., & Sakai, T. (2018) Wide Area Augmentation Performance of DFMC SBAS Using Global Monitoring Stations, The 16th IAIN World Congress 2018.

Reid, T., Walter, T., Blanch, J., & Enge, P. (2016) GNSS Integrity in The Arctic. NAVIGATION, 63: 469– 492. doi: 10.1002/navi.169.

(6) Data archives

These data obtained in this cruise will be submitted to the Data Management Group of JAMSTEC, and will be opened to the public via “Data Research System for Whole Cruise Information in JAMSTEC (DARWIN)” in JAMSTEC web site.

<http://www.godac.jamstec.go.jp/darwin/e>

3.2. Development of under-ice observation system

(1) Personel

Shojiro Ishibashi (JAMSTEC) – System Integrator (Not on board)
Kiyotaka Tanaka (JAMSTEC) – Operation Leader and System Engineer
Makoto Sugesawa (JAMSTEC) – System Engineer and Operator
Satoshi Kimura (JAMSTEC) – Scientific adviser and Operator
Hiroshi Yoshida (JAMSTEC) – System adviser
Satomi Ogawa (Nippon Marine Enterprises, Ltd.; NME) – Operator
Mariko Hatta (JAMTEC) – Operation supporter
Amane Fujiwara (JAMSTEC) – Operation supporter
Kazuho Yoshida (NME) – Tether handler
Ryo Oyama (NME) – Tether handler
Kazuho Yoshida (NME) – Tether handler
Yohei Sugimoto (NME) – Tether handler
Yosaku Maeda (JAMSTEC) – Engineer (Not on board)
Hiroshi Matsumoto (JAMSTEC) – Engineer (Not on board)

(2) Objective

The under-the-ice drone named COMAI (Fig. 3.2-1) is a middle size autonomous underwater vehicle (AUV) for observations under the ice in the Arctic. The drone will autonomously cruise and observe environment under the ice in coverage area of 15 km. A completion of fully autonomous operation under ice is more complex than operation in open sea because of two big breakthrough items. One is positioning and the other is emergency recovery. In high latitude area, performance of a magnetic compass or an inertial navigation system is degraded. The degradation causes increase of navigation error. In the third trial we repeat evaluations of the navigation system and try under ice observations. The test items are followings:

1） evaluation of the navigation system in high latitude area,
2） cruising tests using acoustic remote control mode and autonomous control mode, and
3） observation under the ice.

All tests were carried out with a thin tether including optical fiber cable because the recovery functions are not yet evaluated in this season’s trial

Figure 3.2-1. A recovery scene of COMAI.

(3) Instruments and Methods

The drone is a platform of observation sensors under sea-ice. It will autonomously cruises and surveys under sea- ice without a tether cable (At this time a tether cable is used in all trials). Specifications of the drone is listed in Table 3.1. The maximum cruising range designed is about 30 km or endurance is about 16 hours (at cruising speed of 1 kt). The drone utilizes a hybrid navigation system consisting of a MEMS inertial measurement unit, a magnetic compass and a Doppler velocity log (DVL). The navigation system block diagram is shown in Fig. 3.2-2. The drone has four operation modes: 1) an untethered remotely operated vehicle mode (UROV) , 2) an acoustical ROV mode (AROV), 3) a radio wave ROV mode (RROV), and 4) an autonomous underwater vehicle (AUV) mode. In the AUV mode, three cruising patterns (heading-depth control, way-point control, and way-line control) are selectable. It has a special cruising mode named “escape mode” in addition to them. The mode automatically controls the drone to go to a preprogramed position after completion of an autonomous mission. This enables the drone to escape from ice covered area to open sea area. If one of the navigation devices is down, the drone automatically changes the control mode to the heading-depth control with an acoustical super short baseline navigation toward an acoustic light house pre-deployed as shown in Fig. 3.2-3.

The drone system consists of major three parts: a vehicle body, a ship-side console, and an acoustic system. Its body is made from aluminum and covered with an FRP fairing cover. The ship-side console provides a graphical user interface of the drone system for operation and maintenance. The acoustic system consists of an acoustical communication modem/ locator and an acoustic pinger for the acoustical lighthouse.

Table 3.2-1: Specifications of COMAI.

Items	Specifications	Remarks
Size	2.3 x 0.6 x 0.7 m	
Weight	330 kg	in air
Depth rating	300 m	
Cruising speed	2 kt	3 kt max.
Cruising range	30 km	
Power	Li-ion battery （5.7 kWh）	
Actuators	Horizontal thrusters (100 W) x 2 Vertical thruster (100 W) x 1 Rudders	
Scientific payloads	CTD (conductivity, temperature, depth) sensor Turbidity and chlorophyll meter Snap shot camera Multi beam sonar	 installed on top side installed on top side

COMAI is equipped with scientifical sensors: a CTD sensor (miniCTD, Valeport), a turbidity and chlorophyll meter (ECO FLUNTU, WET Labs), a snap shot camera (2592 x 1944 pixels, F2.2) with LED strobe lights, and a 260 kHz multi beam sonar (837B Delta T, IMAGENEX). The camera and the multi beam sonar are mounted on top side of the body because of ice bottom observations. All data obtained are automatically logged in a drone internal memory and a hard disk of the personal computer of the ship-side console (if ROV mode).

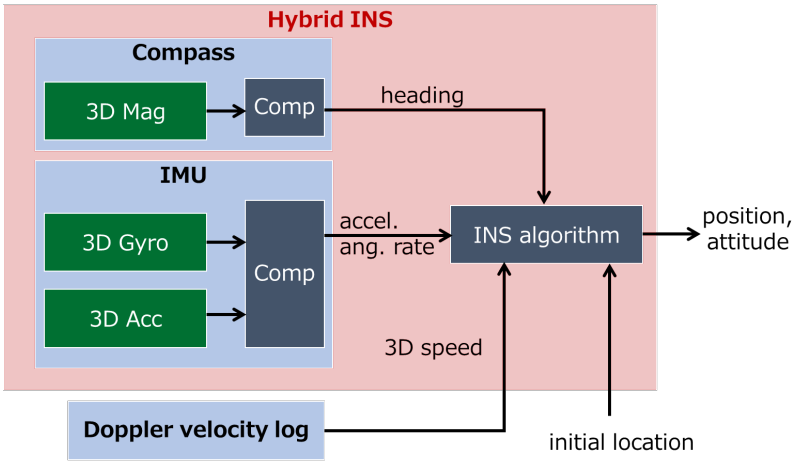

Figure 3.2-2 Block diagram of the hybrid navigation system.

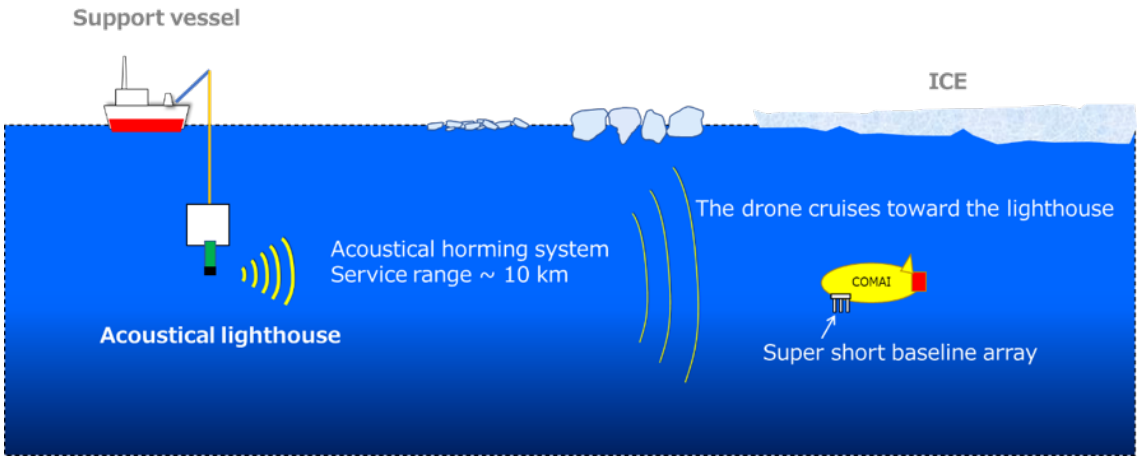

Figure 3.2-3. A working image of the heading-depth control with the acoustical super short baseline navigation in the escape mode.

(4) Test log

Location		Date (JST)	Time(JST)		water depth	Dive #	Test Items	Descriptions
Lat.	Lon.		Start	End				
70.82567	-161.7167	12-Sep-23	3:03	4:08	44.8 m	1	#1	INS performance test
73.16433	-145.166	18-Sep-23	2:46	4:53	3600 m	2	#3	Acoustical remote control test with AUV mode
73.08667	-164.8553	25-Sep-23	7:27	7:53	69 m	3	#3	DVL performance test
75.44967	179.649	27-Sep-23	5:05	7:27	852 m	4	#4	Observation and measurement test

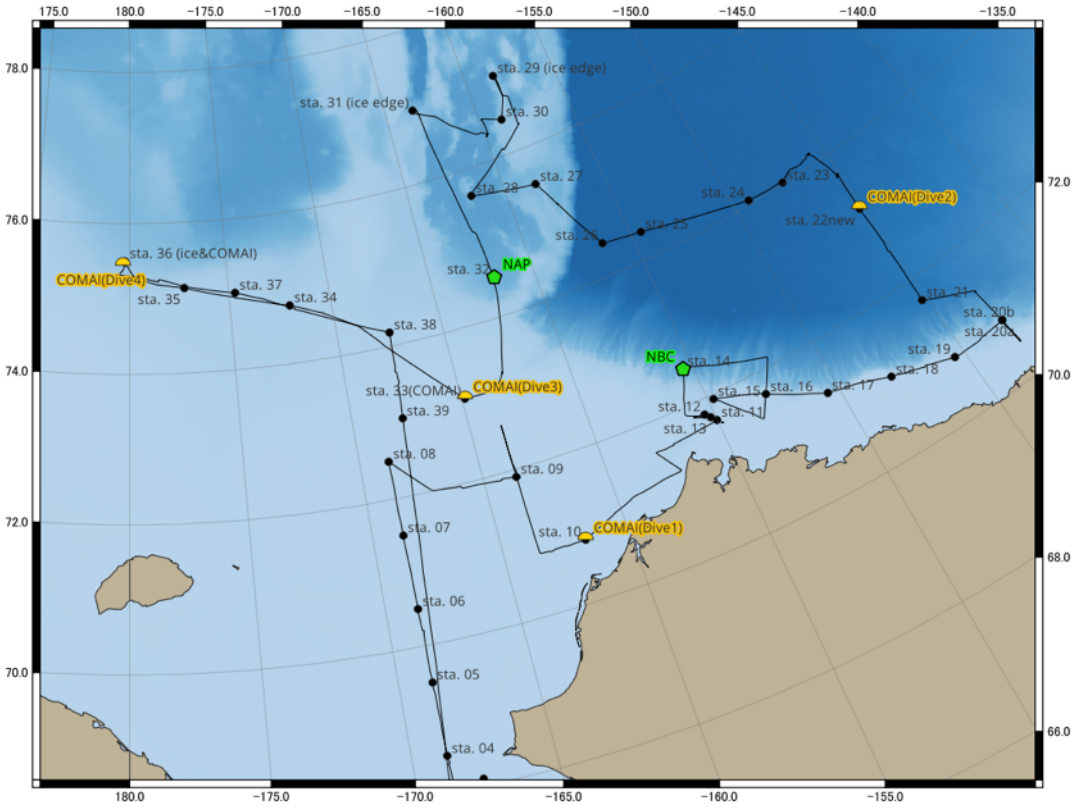

Figure 3.2-4. Map of the test points. Yellow highlighted words show the diving numbers

(5) Preliminary results

1) Navigation performance

Fig. 3.2-5 a) and b) show tracks of the drone measured with the hybrid navigation system (closed circle) and tracks of the support ship in the dives #1 and #3, respectively. In the dive #1, the DVL-INS hybrid system used the water tracking mode. On the other hand, in the dive #3, the bottom tracking mode is used. Obviously the bottom tracking mode makes small position errors. At the present stage, COMAI should be used in shallow water zone where bottom reference tracking is available. Another position data however shows the case which the INS compensated water reference tracking data does not make large errors in short period (tens of minutes). We need to recognize this reason to improve the navigation system.

(a)

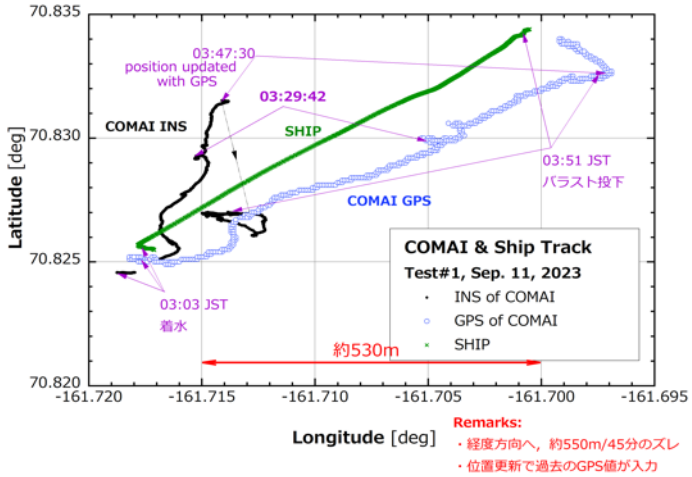

(b)

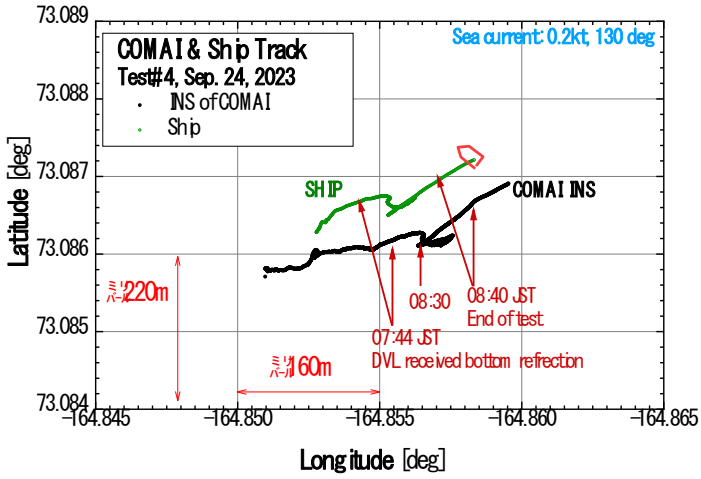

Figure 3.2-5. The drone tracks in the Dive #1 and #3. (a) Comparative experiments of vehicle positions measured with the GPS and the INS of COMAI in Dive #1. In this dive, the DVL is used in water reference tracking mode. (b) The INS is compensated with data of bottom reference tracking with the DVL in Dive #3, Test #4.

2) Observation performance

We tried under ice observation but never achieved. COMAI had cruised around sea-ice pieces and obtained some physical data as shown in Figure 3.2-6 and 3.2-7. In the figure, black lines or dots denotes vehicle descending and pink lines or dots ascending.

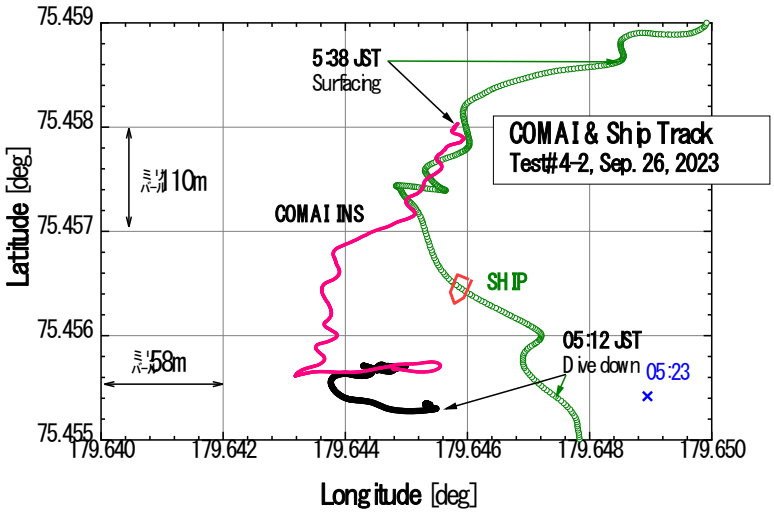

Figure 3.2-6　COMAI track in the dive #4

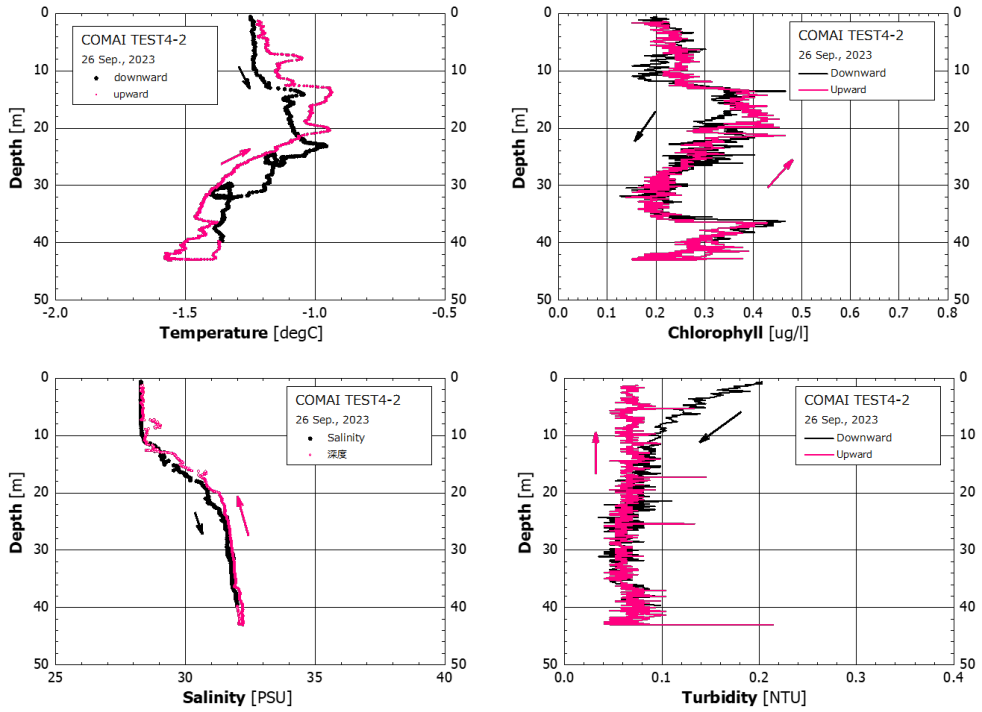

Figure 3.2-7　Depth vs. temperature, salinity, chlorophyll, and turbidity measured in the dive #4.

(6) Data archives

These data obtained in this cruise will be submitted to the Data Management Group (DMG) of JAMSTEC, and will be opened to the public via “Data Research System for Whole Cruise Information in JAMSTEC (DARWIN)” in JAMSTEC web site.

http://www.godac.jamstec.go.jp/darwin/e

3.3 Quantification of the microplastic inventory in the waters of the western Arctic Ocean and microplastic influx from the Pacific Ocean

(1) Responsible personnel:

Takahito Ikenoue, JAMSTEC -PI, not onboard

Zhao Shiye, JAMSTEC, onboard

(2) Purpose, background

The Arctic Ocean on the Pacific side is one of the potential accumulation areas of plastic debris from the Pacific Ocean due to the Pacific water inflow through the Bering Strait. However, quantitative data on microplastics (MPs) have been reported mainly for the Arctic Ocean on the Atlantic side, and the data on MPs in the Arctic Ocean on the Pacific side are very limited (Ikenoue et al., 2022). The Arctic Ocean on the Pacific side has already been subjected to multiple environmental stresses, such as increased surface water temperatures, ocean acidification, and stratification enhancement, due to global warming and the resulting sea ice melting in the Arctic Ocean (Harada, 2016). Therefore, the influx of MPs and attached microbial communities (Plastisphere) from the Pacific Ocean may further increase environmental stresses on marine ecosystems (Bergmann et al., 2022), and it is an urgent task to quantitatively clarify the current status of MPs pollution in the Arctic Ocean on the Pacific side.

In order to predict the future impact of marine microplastic pollution on marine ecosystems and biogeochemical cycles in the Arctic Ocean, we will collect neuston net samples and filtered seawater samples at multiple depths in the Arctic Ocean on the Pacific side, and clarify the followings:

- Inventory of MPs in the Arctic Ocean on the Pacific side (Especially, the Canada Basin and East Siberian Sea)
- Abundance of MPs entering the Arctic Ocean from the Pacific Ocean (Bering Strait)
- Composition of plastisphere present in or entering the Arctic Ocean
- Changes of plastic particles due to the photodegradation

(3) Activities (observation, sampling, development)

- Floating plastic particles collection
- eDNA samples of plastic associated microorganisms
- Water-column Microplastics sampling
- Changes of plastic particles due to the photodegradation

(4) Methods, instruments

- **Floating plastic particles collection:** Floating microplastic samples were collected using a neuston net with a perpendicular mouth opening of 75 cm height and 100 cm width, equipped with a 333 μm mesh opening net with a collecting mesh bag at the cod-end. The net without cod-end was rinsed from the outside with running seawater prior to use. At each station, the net was towed three times at ca. 1-1.5 knots for 20 min from the starboard side (Fig. 3.3-1a). A flow meter was installed at the net mouth to estimate the volume of water filtered during each tow. The collected samples were fixed with ca. 2-3% formalin and stored at room temperature until analysis.
- **eDNA samples of plastic associated microorganisms**: Upon the neuston net on deck, particles in the cod end net were picked out to account for the genomic characteristics of microbial community colonized on the surface. Each particle was placed into a Cyrovial with 2 ml RNAlater for further analysis. Meanwhile, Two 2-L surface seawater at each neuston net station, collected by the bucket, were filtered with the Sterivex filter for free-living microbes. All the eDNA samples were frozen until further analysis.
- **Water-column Microplastics sampling:** In-situ pumps (WTS-LV, McLane Research) were tethered to a single A-frame wire (Fig. 3.3-1b) to collect the water-column plastic particles. The Seawater was directed through a series of filters of the pump: The samples passed through 15-μm filter disks. All pump samplings were programmed to run for 3.0 hours at each depth resulting in ca. 300-500 L seawater filtered. The collected filters were wrapped with an aluminum foil and stored frozen until analysis.
- **Changes of plastic particles due to the photodegradation:** Plastic particles in the glass bottles with sterile seawater are incubated in a 6-L glass container filled with the surface seawater (Fig. 3.3-1c). The samples will be exposed to the air on the deck. At predetermined time points, plastic particles are saved for further analysis in the lab.

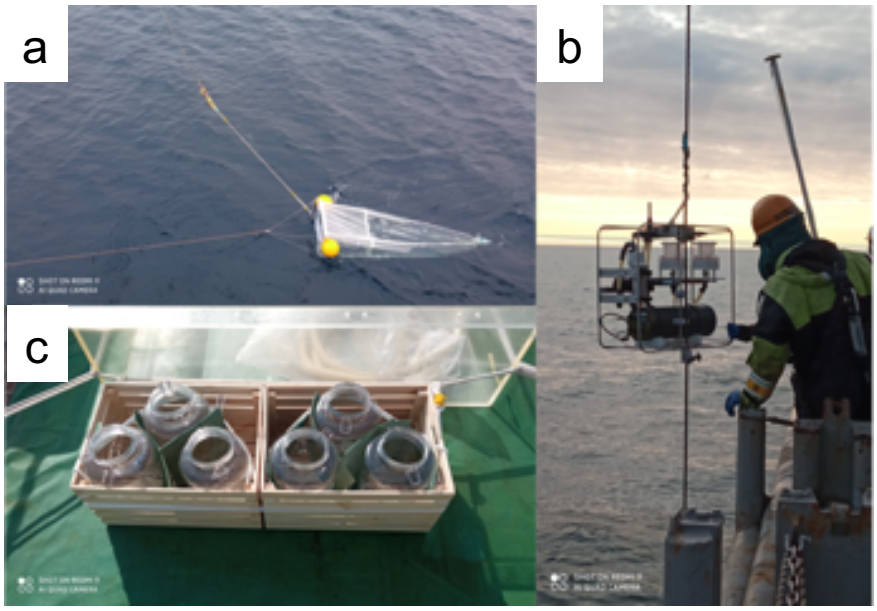

Fig.3.3-1**:** Sampling and experimental methods utilized in this project (a, Neuston Net; b, In-situ Pump; c, Glass containers used for photodegradation incubation).

(5) Results

- **Neuston-net samples and plastic e-DNA samples:** A total of 32 surface net tows were carried out at 17 sampling stations between 65°N-77°N and 179°E - 147°W, in the Pacific section of the Arctic Ocean. 40 different particles were saved at 14 sampling stations for microbiome analysis (Fig. 3.3-2).
- **Water-column Microplastics sampling:** Subsurface water samplings were carried out at 4 stations with two in-situ pumps (WTS-LV, McLane Research). At each station, particle samples at the surface and near-floor layers were collected.
- **Changes of plastic particles due to the photodegradation:** In total, 24 particle samples were harvested after one, two and three-week experiment.

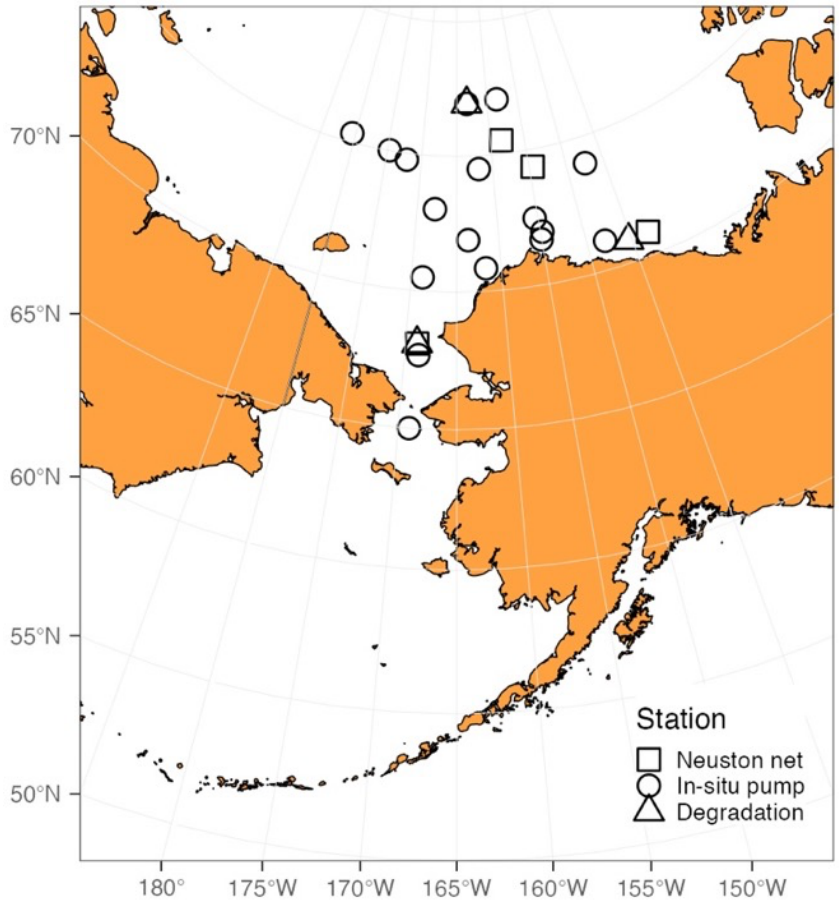

Fig.3.3-2: Sampling locations of Neuston nets, In-situ pump and Photodegradation experiments.

(6) References

Ikenoue T., Nakajima R., Fujiwara A. et al. Horizontal distribution of surface microplastic concentrations and water-column microplastic inventories in the Chukchi Sea, western Arctic Ocean, Sci. Total Environ. 855, 159564 (2023).

Bergmann, M., Collard, F., Fabres, J. et al. Plastic pollution in the Arctic. Nat. Rev. Earth. Environ. 3, 323–337 (2022).

(7) Data archives

These data obtained in this cruise will be submitted to the Data Management Group (DMG) of JAMSTEC, and will be opened to the public via “Data Research System for Whole Cruise Information in JAMSTEC (DARWIN)” in JAMSTEC web site.

http://www.godac.jamstec.go.jp/darwin/e

3.4. Changes in clouds and aerosols over the ice-free Arctic Ocean

3.4.1. GPS Radiosonde

(1) Responsible personnel

Jun Inoue	NIPR/ SOKENDAI
Kazutoshi Sato	NIPR/ SOKENDAI
Kazu Takahashi	SOKENDAI
Ryo Oyama	NME
Kazuho Yoshida	NME
Satomi Ogawa	NME
Yohei Sugimoto	NME

(2) Purpose, background

To understand the thermodynamic structure of the boundary layer, as well as the characteristics of migratory cyclones and anticyclones, GPS radiosonde observations were performed from 00 UTC 08 September 2023 to 00 UTC 29 September 2023. The data obtained will be used mainly for studies of clouds, validation both of reanalysis data and of satellite analyses, as well as data assimilation. The data were also used during the cruise for briefing information with regard to drone flights.

(3) Activities (observation, sampling, development)

We observed vertical profiles of atmospheric (Temperature, Humidity, Pressure, Wind speed and direction).

(4) Methods, instruments

The Vaisala RS41-SGP was used for 00 and 12 UTC launches launches. The observing frequency over the Arctic Ocean (north of the Bering Strait) was twice times per day (00 and 12 UTC). The software (MW41 Vaisala Sounding System; version 2.11.0), processor (SPS311), GPS antenna (GA20), UHF antenna (RB21) and balloon launcher (ASAP) used were all from Vaisala Oyj. Prior to launch, the humidity, air temperature and pressure sensors were calibrated using the calibrator system (RI41 and PTB330, Vaisala). In cases when the wind relative to the ship was not appropriate for launch, the handy launch method was selected. For every launch, a Totex 200 g balloon was used. Several simultaneous observations were replaced with CPS sondes during the

night (e.g., 12 UTC). Most data were entered into the Global Telecommunication System (GTS) though the Japan Meteorological Agency immediately after each observation and thus were available for use in operational weather forecasts.

Table 3.4.1-1 summarizes the log of the GPS radiosonde observations. Raw data were recorded in binary format during ascent. ASCII data were converted from raw data.

(5) Preliminary results

The locations of all radiosonde observations performed during the cruise are shown in Figure 3.4.1-1. A time–height cross-section of observed air temperature and wind during the cruise is shown in Figure 3.4.1-2. The Radiosonde observation was made for 3 weeks, 8-29 September. Additionally, we observed three cyclone events on this cruise.

During 12-13 September, Radiosonde observations were conducted with the cyclone. During this period, we observed southerly winds which are associated with low-pressure systems. These winds transport heat from the Pacific Ocean to the Arctic Ocean. This results in that the tropopause height was recorded at 10,500 m. After the cyclone passed away, the height decreased to 9,500 m. During 17-20 September, the conditions were similar to the conditions during 12-13 September.

During 26-28 September, conditions were characterized by the southerly winds associated with a low-pressure system. However, the tropopause height was less than 10,000 m. The temperature was lower than other results on this cruise at all altitudes. These winds came from the southwest and passed over Siberia. These conditions were different from the other two events.

Table 3.4.1-1: GPS radiosonde launch log with surface observations.

ID	Date	Latitude	Longitude	Psfc	Tsfc	RHsfc	WD	Wsp
	YYYYMMDDHH	degN	degW	hPa	degC	%	deg	m/s
RS001	2023090800	65.06442	169.04793	1017.81	4.00	84	337	15.5
RS002	2023090812	66.82290	168.66345	1018.06	4.90	78	7	12.7
RS003	2023090900	68.34372	168.73263	1017.82	4.70	84	40	8.3
RS004	2023090912	70.17555	168.70664	1014.73	4.50	95	90	7.9
RS005	2023091000	71.50187	168.75389	1012.12	3.50	98	80	8.2
RS006	2023091012	71.97425	166.16017	1008.31	1.40	98	87	13.0
RS007	2023091100	72.58829	163.65265	1005.71	0.70	100	66	9.0

RS008	2023091112	70.82935	162.69718	1000.85	3.80	100	41	4.7
RS009	2023091200	70.84540	161.70326	997.66	3.50	99	49	4.7
RS010	2023091300	71.78285	155.56559	997.36	3.60	100	265	7.2
RS011	2023091400	72.46602	155.38328	1000.94	3.00	95	275	10.1
RS012	2023091412	71.53761	153.57325	1003.33	2.40	99	107	1.8
RS013	2023091500	71.69071	152.70638	1000.96	5.00	96	105	7.2
RS014	2023091512	71.05521	147.89274	995.07	4.00	99	64	11.7
RS015	2023091600	70.81653	145.41703	993.56	3.40	97	44	8.0
RS016	2023091612	70.73917	143.06993	994.86	2.90	98	313	6.1
RS017	2023091700	71.32649	143.22821	996.04	0.80	98	61	2.8
RS018	2023091800	73.16519	145.16636	1001.81	-1.40	98	56	7.9
RS019	2023091812	73.67677	145.18852	1003.50	-1.70	98	57	11.1
RS020	2023091900	74.01398	147.46557	1004.41	-0.60	97	53	13.8
RS021	2023091918	74.35977	154.50096	1009.90	1.30	91	57	11.7
RS022	2023092000	74.36037	154.49867	1010.60	0.70	93	56	12.6
RS023	2023092006	74.43505	156.41878	1012.09	-0.20	95	44	12.0
RS024	2023092012	75.11551	157.65979	1013.68	-0.70	89	40	12.9
RS025	2023092100	75.50041	158.38440	1010.99	-1.10	91	24	13.0
RS026	2023092112	76.07203	159.48234	1007.09	-1.40	93	34	15.0
RS027	2023092200	77.02300	158.36911	1002.60	-1.70	95	34	9.6
RS028	2023092300	76.95014	163.31161	1002.20	-1.50	98	23	9.4
RS029	2023092312	75.24472	162.32236	1002.31	-0.80	95	359	5.6
RS030	2023092400	74.51448	162.01923	1004.91	0.20	90	357	4.0
RS031	2023092412	73.28255	162.95033	1009.09	-0.70	98	273	3.7
RS032	2023092500	73.08650	164.85458	1012.28	-1.50	98	283	2.2
RS033	2023092512	74.57621	170.32259	1012.18	-1.50	86	91	0.9
RS034	2023092600	74.94070	174.50049	1008.48	-2.10	98	337	6.1
RS035	2023092612	75.29292	179.78866	1007.27	-4.60	92	292	2.9
RS036	2023092700	75.41742	179.70796(degE)	1001.79	-3.50	87	175	9.0
RS037	2023092706	75.22857	178.63125	1001.10	-2.80	82	190	10.0
RS038	2023092712	75.02119	174.67938	1002.20	-2.10	87	192	10.8
RS039	2023092800	74.72787	171.90396	1002.51	-0.70	92	172	8.3
RS040	2023092812	73.55966	167.58786	1002.12	0.90	96	133	9.4
RS041	2023092900	72.01883	168.01648	1003.04	3.60	64	264	5.4

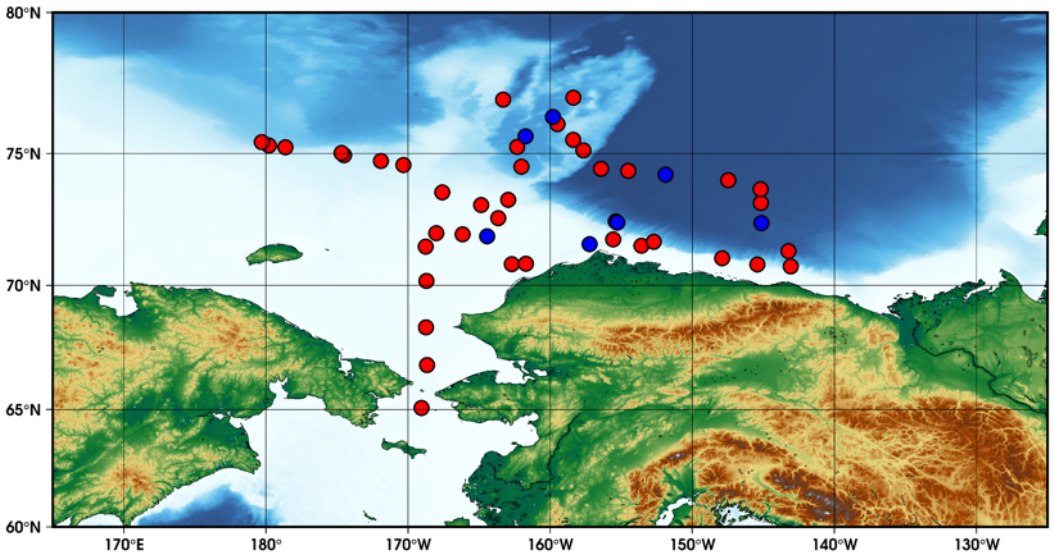

Figure 3.4.1-1: A cruise map with GPS sonde measurement points (red marks) and CPS sonde measurement points (blue marks, see in 3.4.2)

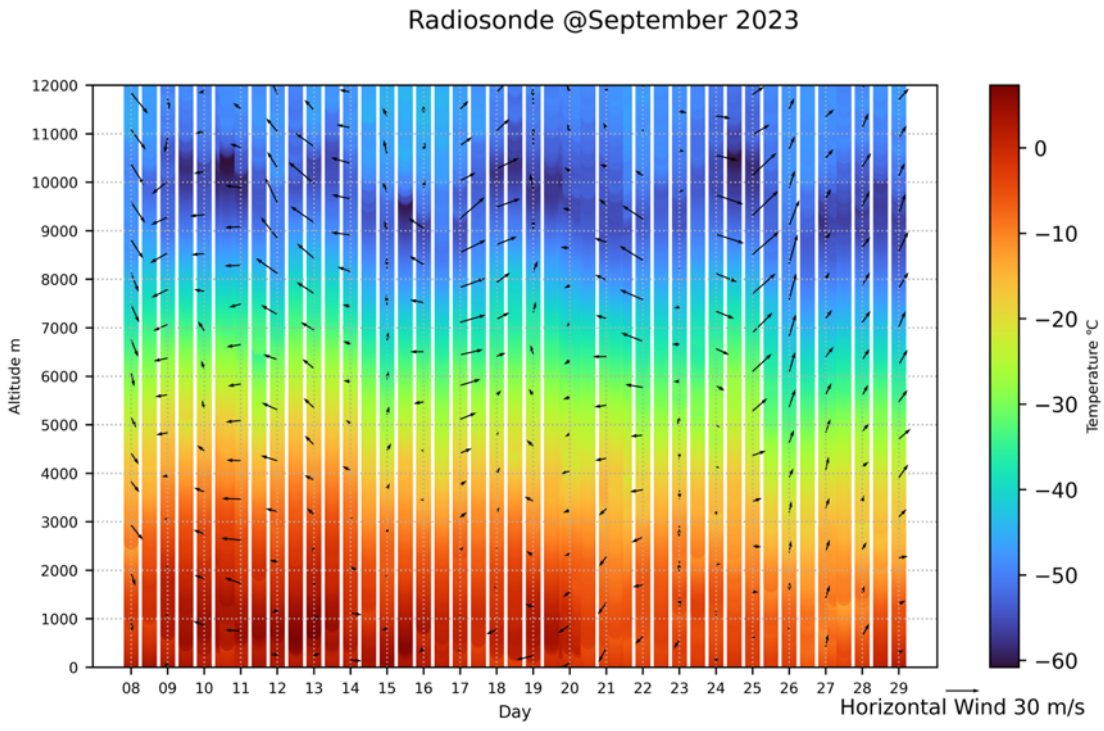

Figure 3.4.1-2: A time–height cross section of observed air temperature (color) and wind (vector) during the cruise

3.4.2. Cloud Particle Sensor sonde

(1) Responsible personnel

Jun INOUE	NIPR/SOKENDAI
Kazutoshi SATO	NIPR/SOKENDAI
Kazu TAKAHASHI	SOKENDAI
Ryo OYAMA	NME
Kazuho YOSHIDA	NME
Satomi OGAWA	NME
Yohei SUGIMOTO	NME

(2) Purpose, background

To understand the vertical profiles of Arctic cloud, we conducted Cloud Particle Sensor (CPS) sonde observations over the Arctic Ocean and the Bering Sea. The CPS sonde, developed by the Japanese Meisei Electric Co., Ltd. (Meisei), measures vertical distributions of cloud particles (number density, size and phase (i.e., water cloud or ice cloud)) in addition to meteorological elements (i.e., temperature, relative humidity, height, wind direction and wind speed). This was the inaugural trial of cloud particle observations over the Arctic Ocean in October during the R/V Mirai cruise.

(3) Activities (observation, sampling, development)

Overall, 7 CPS sondes were launched during 10–22 September 2023. The CPS sonde observed parameters below:

Cloud particles (number of densities, Particle size and Output signal voltage)
Wind speed and direction
Pressure
Temperature
Relative Humidity

See Table 3.4.2-1 “CPS sonde launch log with surface observation”.

(4) Methods, instruments

We used the CPS sonde which comprises a CPS sonde and a GPS radiosonde transmitter (RS-11G, Meisei). The CPS sonde was connected to a 300 g balloon (Totex TA-300), parachute and Vaisala radiosonde. We used the Meisei standard GPS sonde ground system (RD-08AC), software (MGPS-R) and 400 MHz antenna.

(5) Preliminary results

Figure 3.4.2-1 shows the track of the R/V Mirai during MR23-06C and the locations of the CPS sonde launches over the Arctic Ocean. Figures 3.4.2-2–3.4.2-8 show vertical profiles of temperature and relative humidity obtained by the RS-11G GPS radiosondes and the number of particles, degree of polarization and P output obtained by the CPS sondes.

Table 3.4.2-1: CPS sonde launch log with surface observations.

No.	Date (YYYYMMDD) Time (HH:MM) UTC	Lat (degN) Lon (degW)	Psfc (hPa)	Tsfc (ºC)	RHsfc (%)	WDsfc (deg) WSsfc (m/s)
01	20230910 15:00	71.90 164.43	1007.0	1.1	98	82 11.5
02	20230912 12:00	71.60 157.22	996.4	3.0	100	354 4.4
03	20230913 12:00	72.42 155.28	999.5	2.8	100	276 7.6
04	20230917 12:00	72.40 145.13	998.5	0.4	91	42 7.4
05	20230919 12:00	74.22 151.88	1007.9	1.0	93	68 11.4
06	20230921 06:00	75.63 161.73	1010.5	-0.8	88	32 11.5
07	20230922 12:00	76.33 159.80	1000.2	-1.4	96	31 7.5

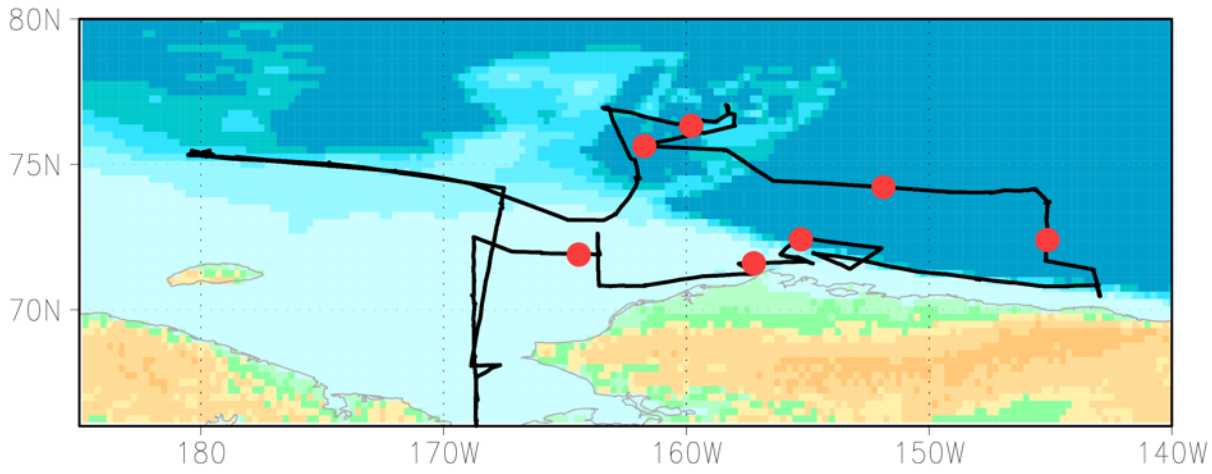

Figure 3.4.2-1: A cruise map with the CPS sonde measurement points (red marks).

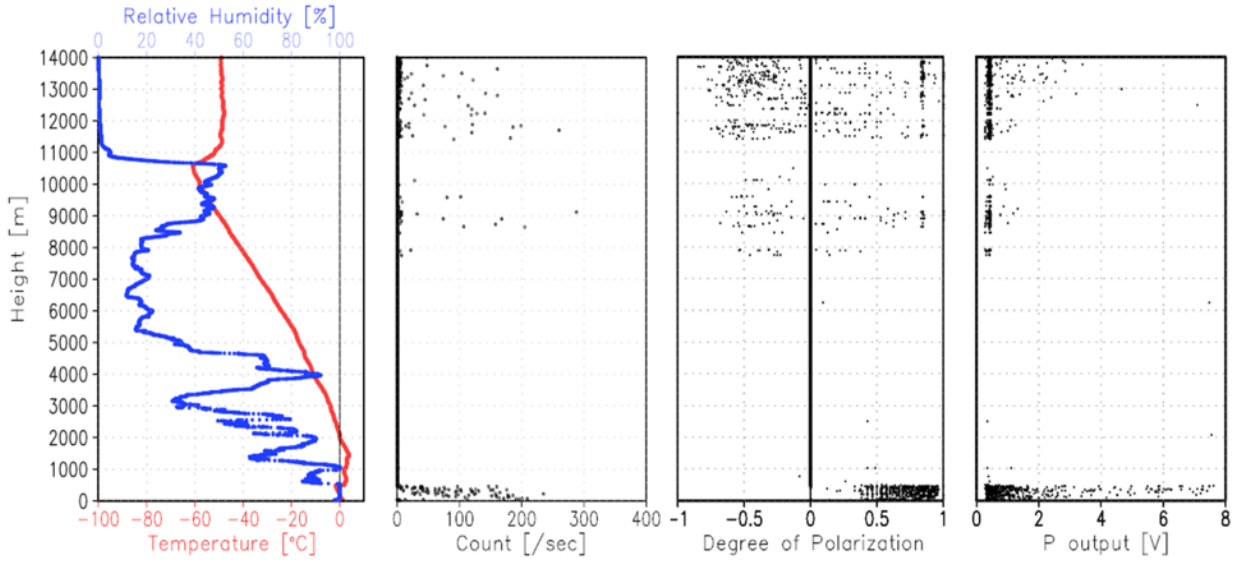

Figure 3.4.2-2: Vertical profiles of temperature (red) and humidity (blue) obtained by RS-11G radiosonde, and number of particles, degree of polarization and P output obtained by CPS sonde for No.1 launch (10 September).

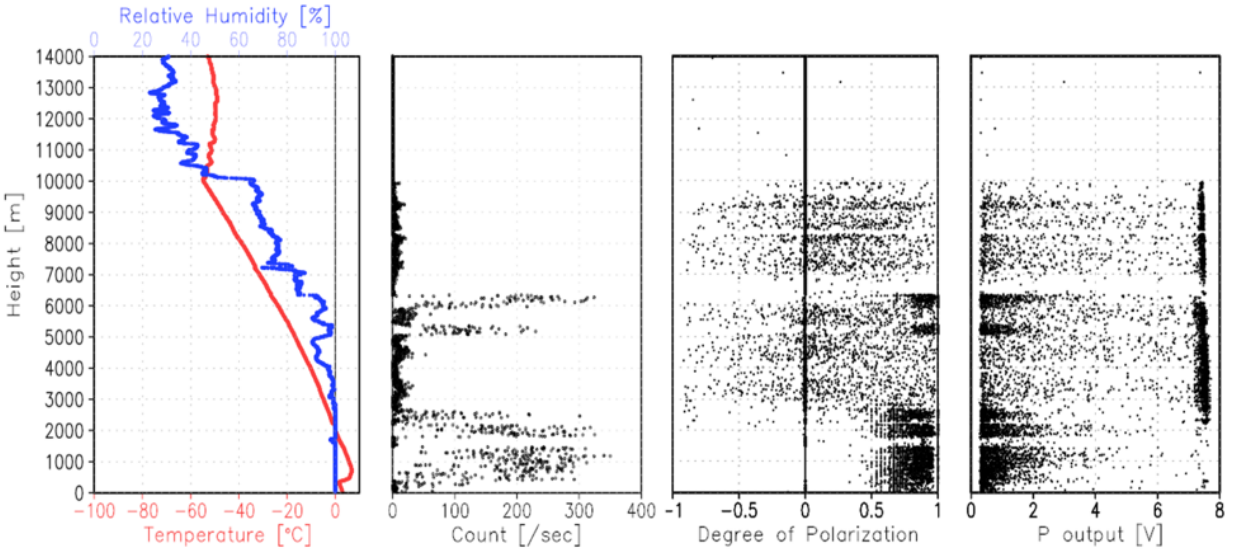

Figure 3.4.2-3: Same as in Figure 3.4.2-2, but for No.2 launch (12 September).

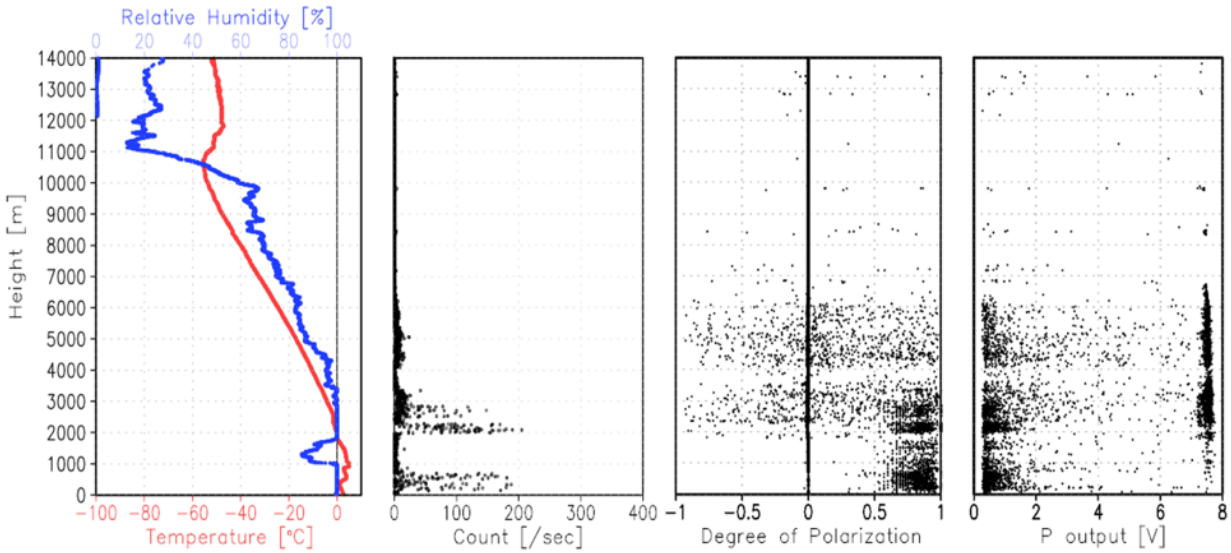

Figure 3.4.2-4: Same as in Figure 3.4.2-2, but for No.3 launch (13 September).

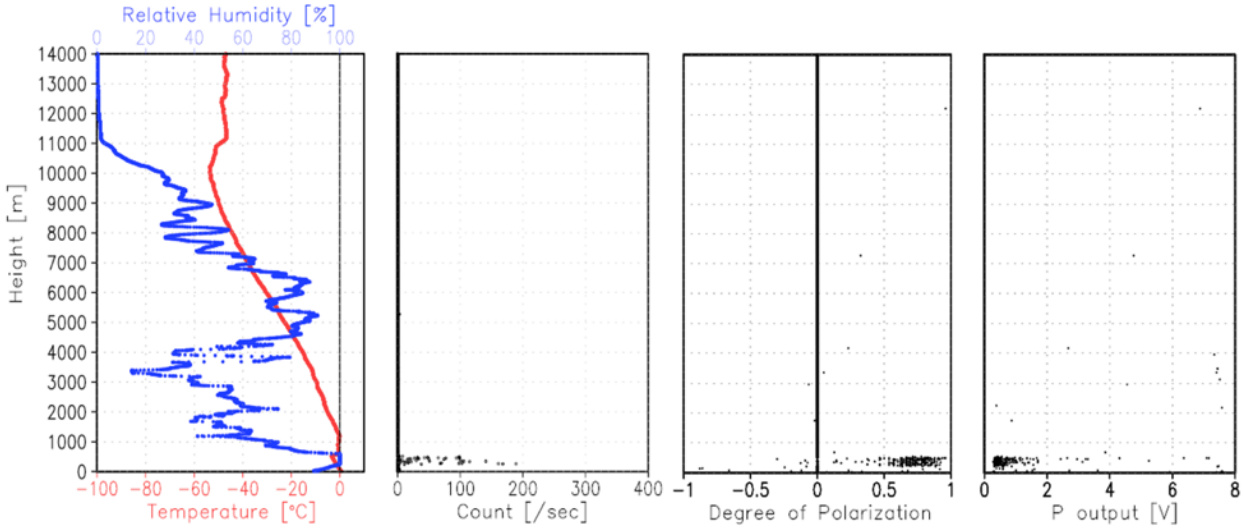

Figure 3.4.2-5: Same as in Figure 3.4.2-2, but for No.4 launch (17 September).

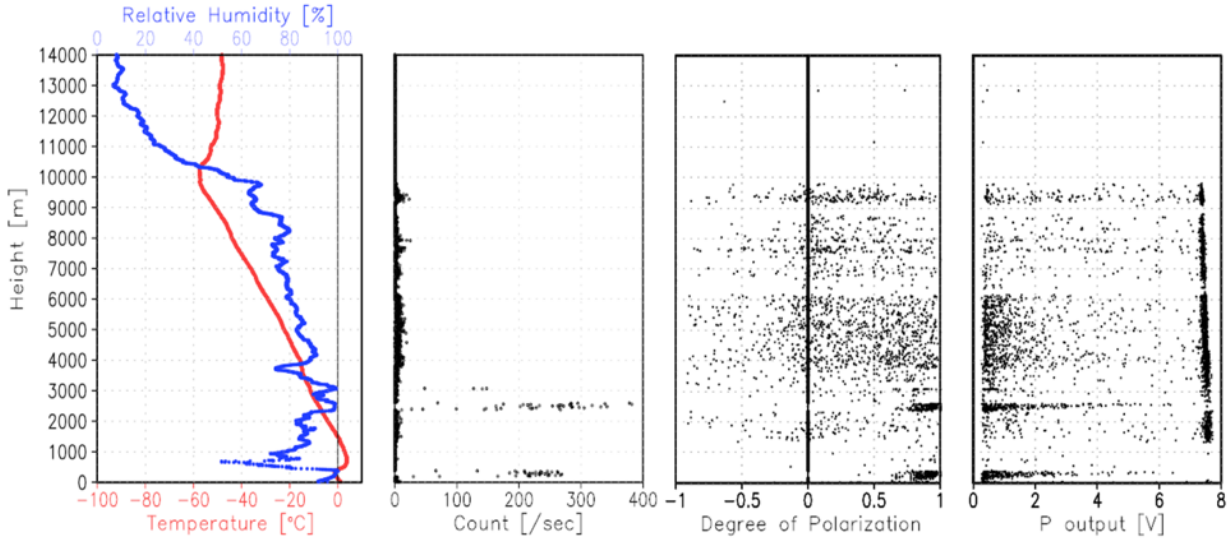

Figure 3.4.2-6: Same as in Figure 3.4.2-2, but for No.5 launch (19 September).

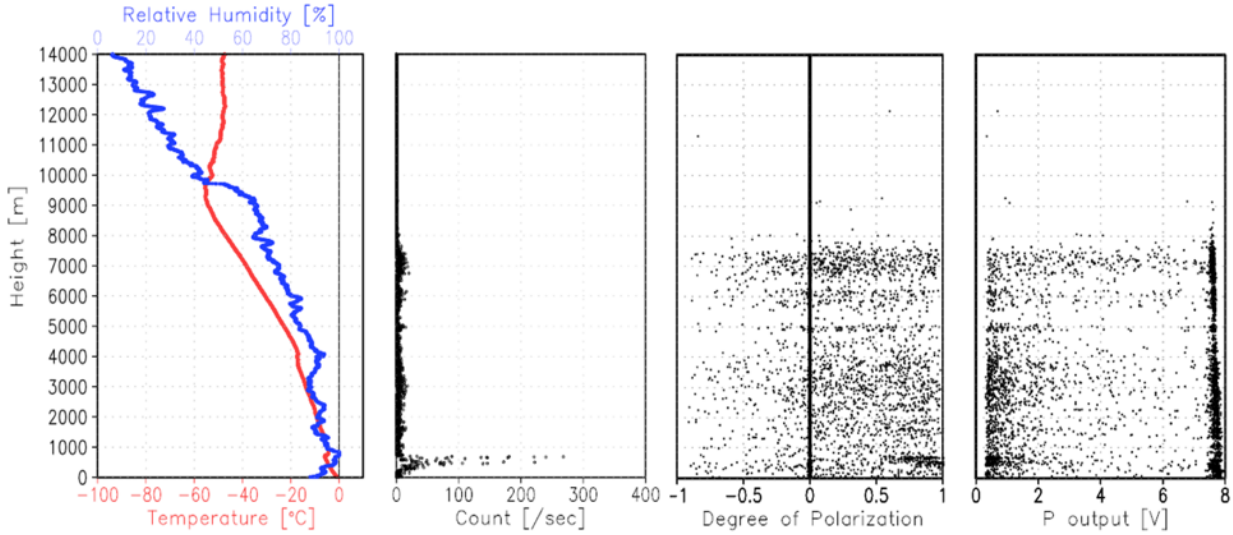

Figure 3.4.2-7: Same as in Figure 3.4.2-2, but for No.6 launch (21 September).

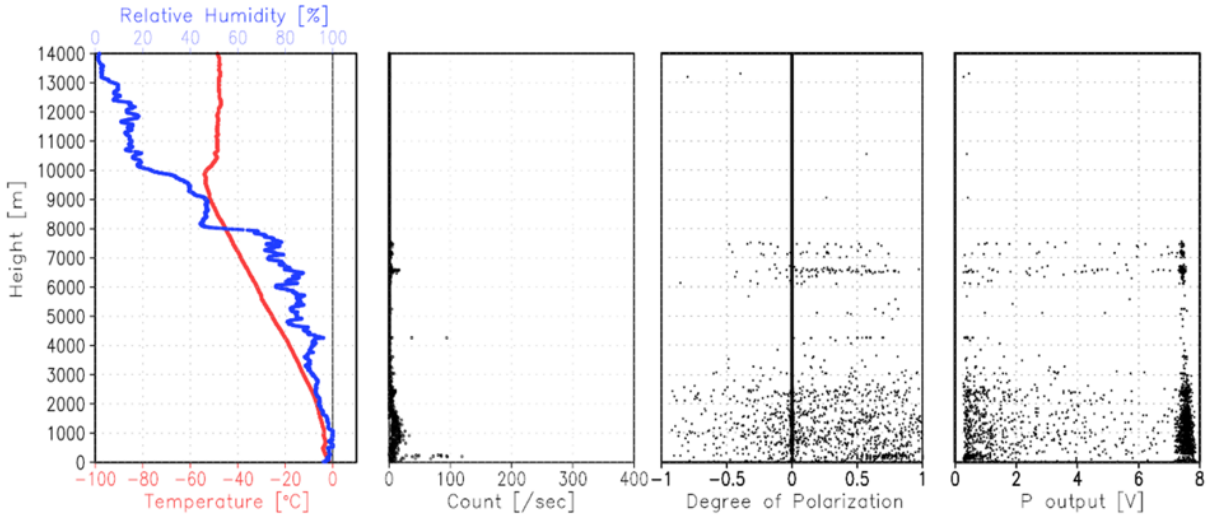

Figure 3.4.2-8: Same as in Figure 3.4.2-2, but for No.7 launch (22 September).

3.4.3. Drones

(1) Personnel

Jun INOUE	NIPR/SOKENDAI
Kazutoshi SATO	NIPR/SOKENDAI
Kazu TAKAHASHI	SOKENDAI
Tsubasa KODAIRA	The University of Tokyo

(2) Purpose, background

The objectives of this observation approach were to obtain meteorological profiles.

(3) Activities (observation, sampling, development)

To monitor the vertical structures of atmosphere and aerosols, we conducted vertical profiling using small meteorological sensors onboard drone. The status of the Global Navigation Satellite System (GPS & GLONASS), radio waves (2.4 GHz) and gyrocompass were fundamental for stable and safe drone operations.

(4) Methods, instruments

Two types of drones were used (i.e., DJI Mavic2 Enterprise Dual and ACSL SOTEN). An iMet-XQ2 (hereafter, XQ2) (International Met Systems, Inc.: weight 60 g), which was the primary meteorological sensor, was installed on the right front arm of drone with a radiation shield. The XQ2 can record air temperature, relative humidity, air pressure, and GPS position at 1-s intervals with quality equivalent to that of a radiosonde. The radiation shield reduces the effect of radiation from the sun and that of other infrared radiation from the atmosphere and the body of the drone. Additionally, the shape of the shield also reduces the chance of direct accretion of cloud droplets and precipitation on the probe. The secondary meteorological sensor (M5Stack, BME688), installed on the left rear arm, was used to measure the same meteorological parameters as measured by XQ2 but from the opposite side of the drone. The environmental wind speed and direction were observed using two hot-wire anemometers (Hortplan, HWS-19-ONE: weight 1 g) installed in a self-designed cylinder (height: 13 cm above the body of the drone) generated using a 3D printer. Additionally, an aerosol counter (Sensirion, SPS30: weight 26 g) was used to monitor the particle size distribution in the 0.3–10 μm range. The details of SPS30 were shown in 3.4.6. The onboard microcomputers (M5Stack, M5StickCPlus, and ATOM lite) gathered the data from the secondary meteorological sensor (rear sensor), wind sensors, and particle counter, processed them at 1-s intervals, and transmitted them to the land station via the 920 MHz Lora module (ES920LR3). The system battery (450 mAh lipobattery) was independent of drone, enabling it to operate for at least 30 min.

(5) Preliminary results

During the Arctic cruise in 2023, 27 vertical profiles of atmosphere up to a maximum height of 1000 m were conducted from end-August to end-September 2023 (Fig. 3.4.3-1). Table 3.4.3 presents the flight summary. Figure 3.4.3-2 shows the example of vertical profiles up to about

1100m of air temperature, relative humidity, wind speed, wind direction and aerosols number (flight #009). We successfully obtained vertical profiles of atmosphere using drones except for five flights (#010, #015, #016, #017, #026).

(6) Remarks

Flights (#010 & #026) did not provide data because the small meteorological instruments have some technical errors. ASCL SOTEN crushed into ocean owing to unknown mechanical errors (flight #016). The iMet-XQ2, which was used for flight #015, was installed on crushed ASCL SOTEN for flight #016. Therefore, there is no iMet-XQ2 data for flight #015. During flights #015-#017 and #025, small sea ices were observed near the sea ice edge. To compare vertical profiles of atmospheric parameters by drone with that by radiosonde, three flights (#014, #018, #020) have been conducted after radio sonde launch.

Table 3.4.3-1: Flight summary

No.	mm/dd	Takeoff (SMT)	Landing (SMT)	Lat (˚N)	Lon (˚W)	Max Altitude (m)	Purpose of flight Remarks (station number, other issues)
001	08/31	09:22	09:30	53-46	177-08E	500	Test flight (No station number)
002	09/08	09:27	09:35	67-39	168-39	500	St.03
003	09/09	17:08	17:16	68-30	168-45	500	St.04
004	09/11	08:02	08:15	70-49	161-42	900	St.10
005	09/11	14:33	14:42	70-50	161-42	300	St.10 (Dripping on drone)
006	09/12	13:25	13:36	71-48	155-23	800	St.12 (Dripping on drone)
007	09/12	17:30	17:44	71-44	155-11	1000	St.13 (Dripping on drone)
008	09/13	13:18	13:26	72-28	155-23	500	St.14 (Dripping on drone and BME sensor)
009	09/14	08:26	08:40	71-56	154-46	1100	St.15
010	09/14	14:56	15:10	71-41	152-43	1100	St.16 (No observation data except for iMet-XQ2 data)
011	09/14	19:43	19:52	71-18	150-28	600	St.17 (Dripping on drone)
012	09/16	19:59	20:12	71-41	145-12	1000	St.21 (Dripping on drone)
013	09/17	08:09	08:22	73-09	145-09	1050	St.22 (Dripping on drone)
014	09/18	15:30	15:43	73-09	145-09	1000	St.22 (Dripping on drone, Radio sonde time)
015	09/22	12:39	12:51	76-57	163-25	700	St.31 (Icing on drone, No iMet-XQ2 data)
016	09/22	13:03	--:--	76-57	163-25	-	St.31 Crushed drone (No observation data)
017	09/22	13:12	13:19	76-57	163-25	80	St.31 Sea ice monitoring at 7, 50, 80m altitude
018	09/22	15:33	15:43	76-56	163-21	700	St.31 (Radio sonde time)
019	09/23	12:43	12:56	74-30	161-56	1000	St.32 (Dripping on drone, smoke from ship)
020	09/23	15:32	15:46	74-30	162-01	1050	St.32 (Dripping on drone, Radio sonde time)
021	09/24	08:02	08:17	73-10	163-10	1100	St.33 (Night time)
022	09/24	12:30	12:43	73-05	164-51	1050	St.33
023	09/25	11:08	11:21	74-45	172-03	1000	St.34
024	09/26	19:00	19:12	75-07	177-13	1000	St.35
025	09/26	10:27	10:30	75-28	179-38E	400	St.36 (Icing on drone, auto landing due to several mechanical error)
026	09/28	09:33	09:40	73-01	167-45	800	St.39 (iMet-XQ2 relatively humidity data error)
027	09/29	14:36	14:49	68-04	168-51	800	St.40

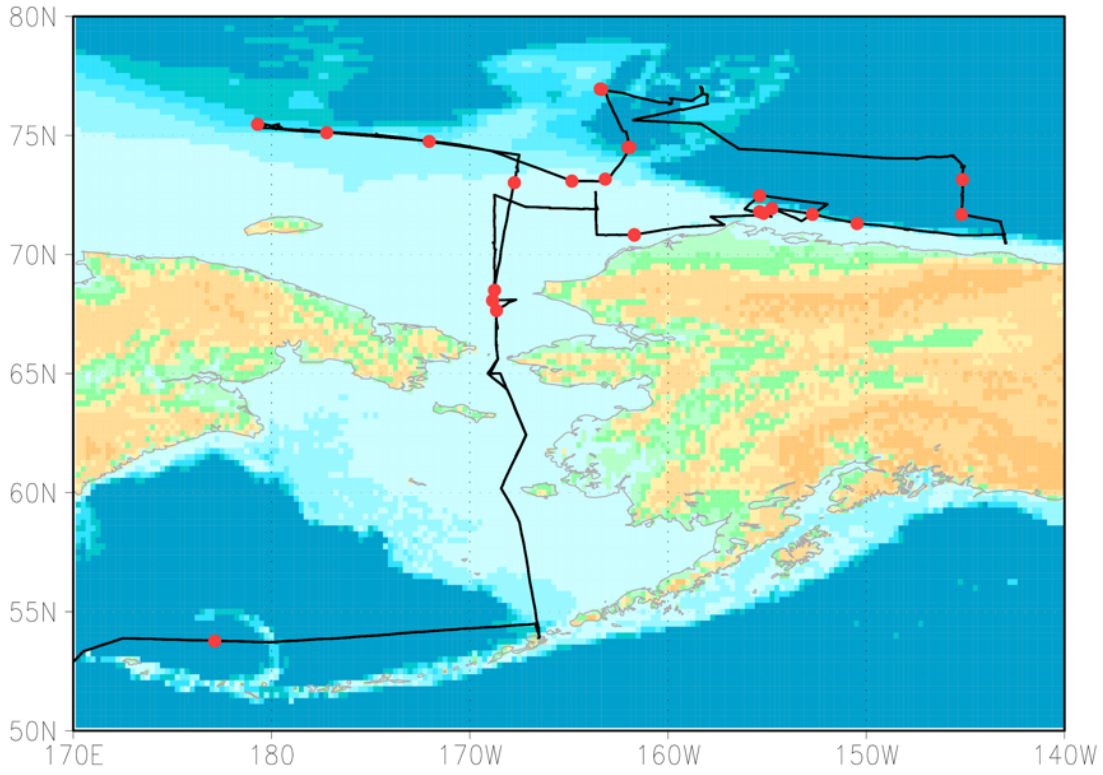

Figure 3.4.3-1: A cruise map with drone measurement points (red marks).

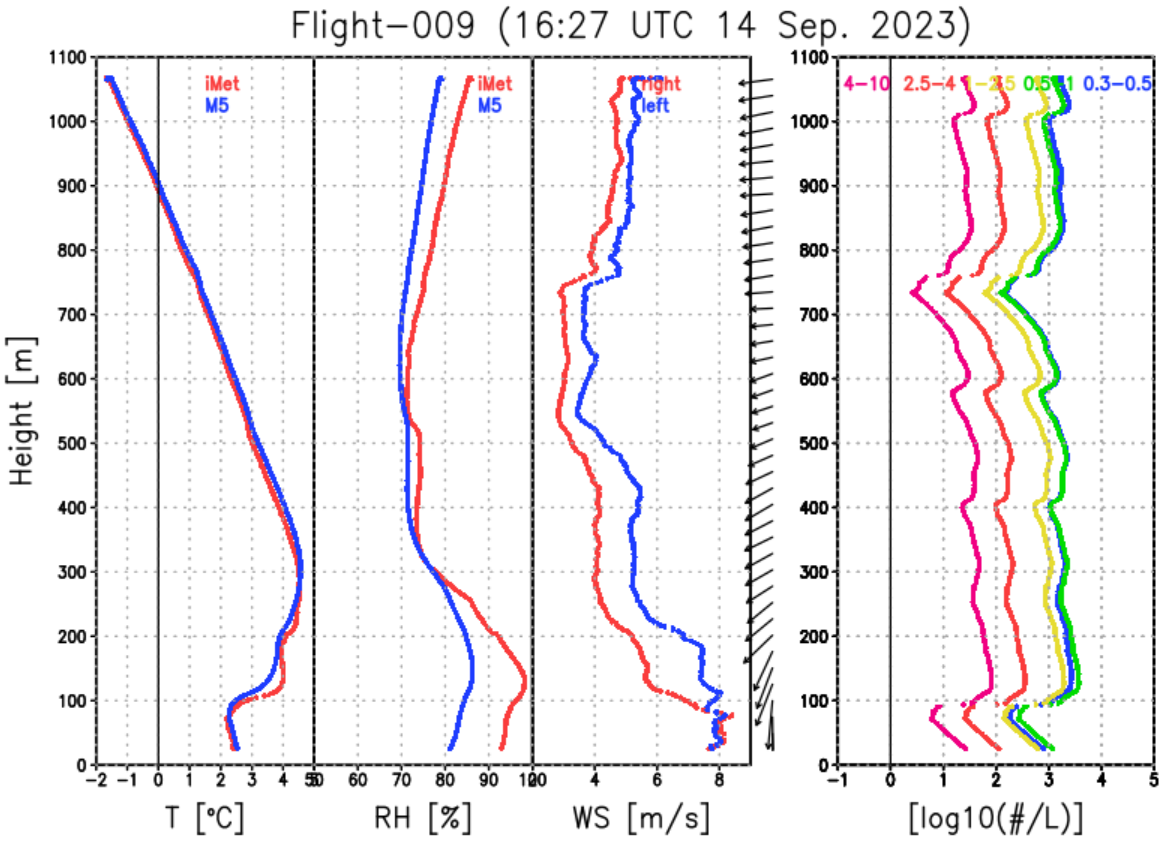

Figure 3.4.3-2: Examples of icing flight profiles on flight #009: (a) air temperature, (b) relative humidity, (c) mean wind speed and from the two onboard anemometers, (d) particle number concentrations. Red and blue lines in (a) and (b) indicate the values from the upstream sensor (iMet-XQ2) and downstream sensor (M5stack Env II), respectively. The number concentrations detected by the particle counter (SPS30) are shown in (d), with different colors displayed by different particle size ranges (unit: μm), as identified in the legend in the figure.

3.4.4. Microwave radiometer

(1) Personnel

Jun INOUE	NIPR/SOKENDAI	
Kazutoshi SATO	NIPR/SOKENDAI	
Kazu TAKAHASHI	SOKENDAI	
Masaki KATSUMATA	JAMSTEC	(not on board)
Akira KUWANO-YOSHIDA	Kyoto Univ.	(not on board)
Masahiro MINOWA	Furuno Electric Co., Ltd.	(not on board)

(2) Purpose, background

The objectives of this observation approach were to retrieve the total column integrated water vapor, and the vertical profiles of water vapor and temperature.

(3) Activities (observation, sampling, development)

To obtaine the total column integrated water vapor, and the vertical profiles of water vapor and temperature, the Microwave radiometer on ship was operated continuously.

(4) Methods, instruments

Two microwave radiometers (hereafter MWR; manufactured by Furuno Electric Co., Ltd.) are used. The MWRs received natural microwave within the angle of 20 deg. from zenith. One of the MWRs for the water vapor observes at the frequencies around 22 GHz, to retrieve the column integrated water vapor (or precipitable water), and the vertical profile of the water vapor. The other MWR measures at the frequencies around 55 GHz to retrieve vertical profile of the air temperature.

The observation was made approximately every 20 seconds except when periodic auto-calibration was on-going (once in several minutes). The rain sensor is equipped to identify the period of rainfall.

In addition to the MWRs, the whole sky camera was installed beside the MWR. This is to monitor cloud cover, which also affects the microwave signals. The camera obtained the whole-sky image every 2 minutes.

Both instruments were installed at the top of the roof of aft wheelhouse, as in Fig. 3.4.4-1. The data were continuously obtained all through the cruise period.

(5) Preliminary results

The data have been obtained all through the cruise. The further analyses for the water vapor (column-integrated amount and vertical profile), the air temperature (vertical profile), etc., will be carried out after the cruise.

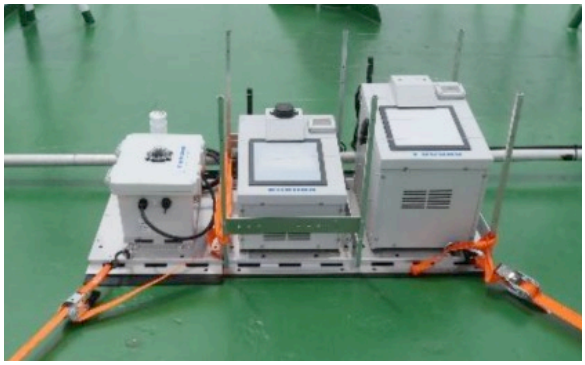

Figure 3.4.4-1: Outlook of the instruments installed at the roof of the aft wheelhouse; the microwave radiometer for the air temperature (right), microwave radiometer for the water vapor (middle), and the whole-sky camera (left).

3.4.5. Lidar ceilometer

(1) Responsible personnel

Jun Inoue	NIPR/SOKENDAI
Kazutoshi Sato	NIPR/SOKENDAI
Kazu Takahashi	SOKENDAI
Ryo Oyama	NME
Kazuho Yoshida	NME
Satomi Ogawa	NME
Yohei Sugimoto	NME

(2) Purpose, background

Information on cloud base height and liquid water amount around cloud base is important for comprehension of the process of cloud formation. During this cruise, cloud base height was measured using a lidar ceilometer (CL61, Vaisala, Finland).

(3) Activities (observation, sampling, development)

The lidar ceilometer observed parameters below:

1. Cloud base height up to five layers (unit: m).
2. Backscatter profile (parallel- and polarized component of the backscattered light, attenuated volume backscatter coefficient), linear depolarization ratio of the backscatter volume
3. Estimated cloud amount (unit: oktas) and height (unit: m).

The attenuated backscatter of the light by each particle on the path through the atmosphere consists of parallel-polarized ($P\ POL$) and cross-polarized ($XPOL$) attenuated backscatter profiles. The sum of $P\ POL$ and $XPOL$ is the total attenuated backscatter profile (ABS:m−1 sr−1). The depolarization ratio (LDR) is the ratio of $XPOL$ and $P\ POL$ ($XPOL/P\ POL$), which identifies the cloud phase and precipitation. The typical LDR ranges are ∼0 (droplets), 0.01–0.2 (rain), 0.1–0.2 (dust), 0.2–0.4 (snow), and >0.3 (ice crystals) (Vaisala, 2021).

The ceilometer was operated continuously during Arctic cruise.

(4) Methods, instruments

We measured cloud base height and the backscatter profile using a ceilometer (CL61, Vaisala, Finland) throughout this cruise.

Major parameters for the measurement configuration are as follows;

Laser source: Indium Gallium Arsenide (InGaAs) Diode Laser
Transmitting center wavelength: 910.55 nm
Transmitting average power: 30 mW
Repetition rate: 9.5 kHz

Detector: Silicon avalanche photodiode (APD)
Measurement range: 0 ~ 15.4 km
Resolution: 4.8 meter
Sampling rate: 5 sec

Cloud base height and the backscatter profile in the archive dataset were recorded with resolution of 4.8 m.

(5) Preliminary results

Figure 3.4.5-1 shows the time series of cloud base height over Arctic region (north part of 66ºN) measured by the CL61. The low-level cloud with base height below 0.5km dominated during Arctic cruise. After 19 September 2023, multilayer clouds and relatively high-level cloud (base height above 0.5km) were observed by the CL61. To compare detected cloud base height from CL61 with that from previous model (CL51), the time series of cloud base height for 1st layer cloud over Arctic region from CL61 and CL51 is shown in Fig. 3.4.5-2. Although the temporal change in cloud base height by the CL61 is almost similar to that by the CL51, the difference in cloud base height between the CL61 and CL51 were found when the CL61 detected cloud with base height exceeding 0.5km. Additionally, we make scatter plot of first layer cloud base-height from CL61 and CL51 (Fig. 3.4.5-3). The cloud base height by the CL61 is higher than that by the CL51.

(6) Reference

Vaisala, 2021. Technical description vaisala lidar ceilometer CL61. pp. 1–43.

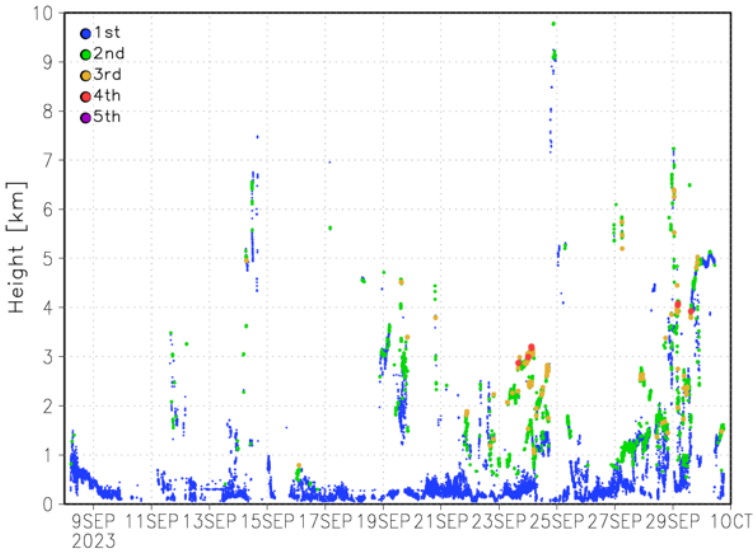

Figure 3.4.5-1: Time series of cloud base height for five layers over Arctic (north part of 66ºN) from the CL61.

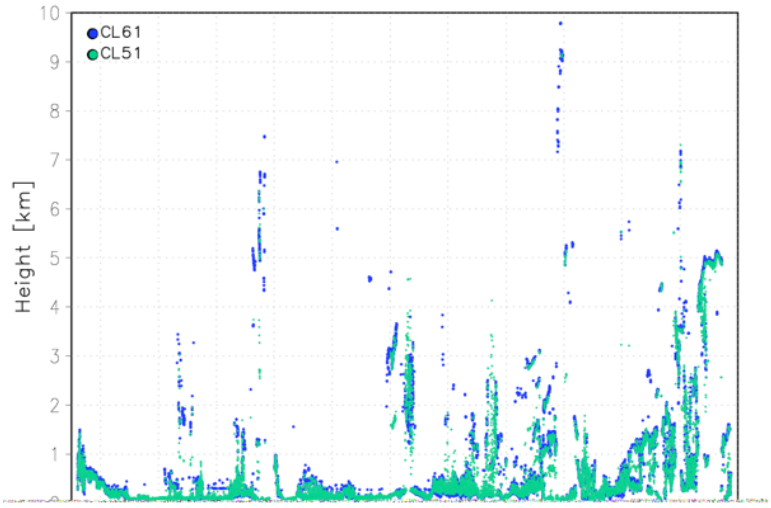

Figure 3.4.5-2: Time series of cloud base heights over Arctic (north part of 66ºN) from the CL61 and CL51.

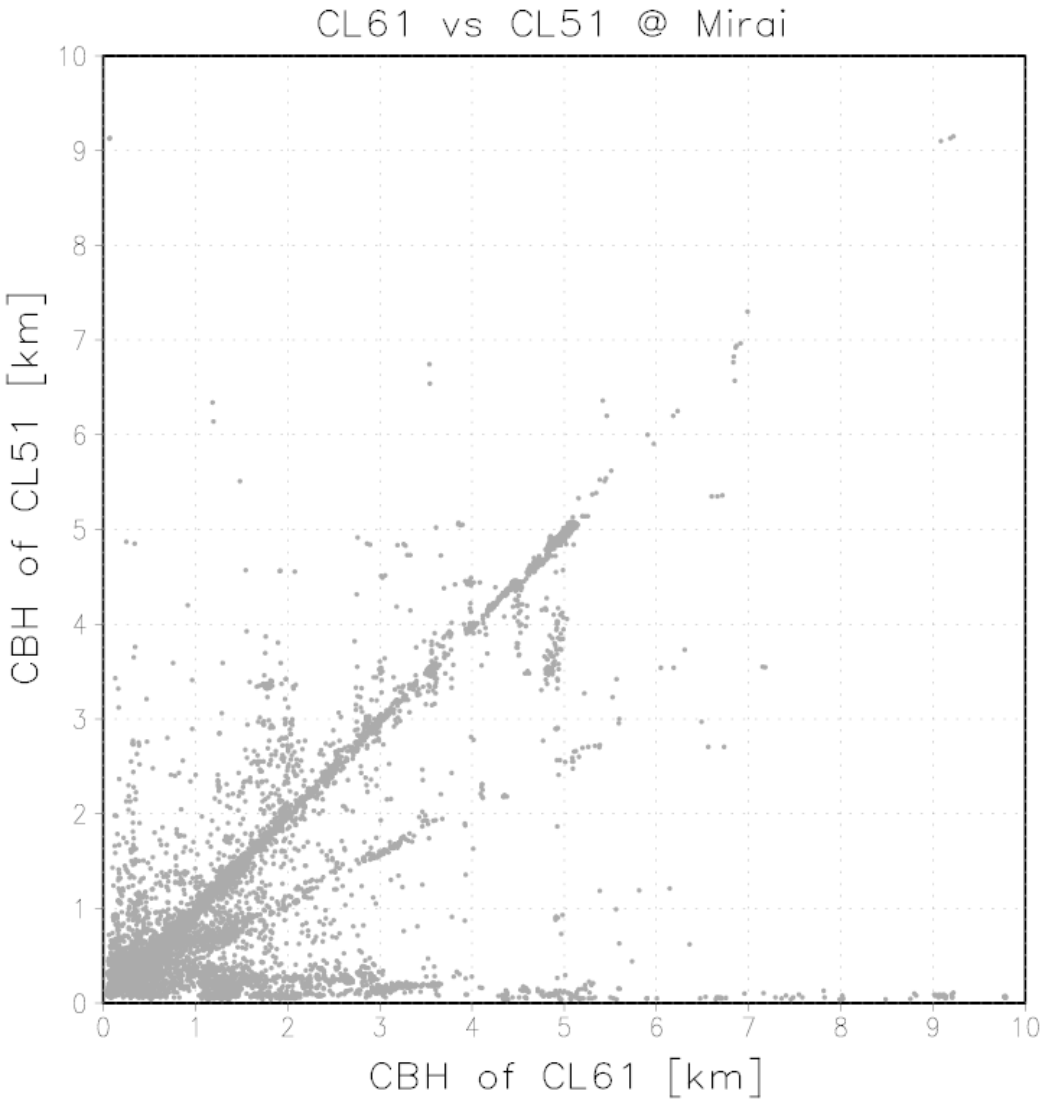

Figure 3.4.5-3: Scatter plot of detected cloud base height (CBH) for first layer cloud over Arctic region (north part of 66ºN) by the CL61 and CL51.

3.4.6. Surface aerosol observations：

(1) Responsible personnel

Jun Inoue	NIPR/SOKENDAI	- onboard
Kazutoshi Sato	NIPR/SOKENDAI	- onboard
Kazu Takahashi	SOKENDAI	- onboard

(2) Purpose, background

- To investigate roles of aerosols in the marine atmosphere in relation to the cloud formation
- To investigate the relationship between sea state and aerosol characteristics

(3) Activities (observation, sampling, development)

The surface aerosol observations obtained parameters below:

• Particle size distribution

• Gas resistance of Volatile Organic Compounds (VOCs) in the air mass

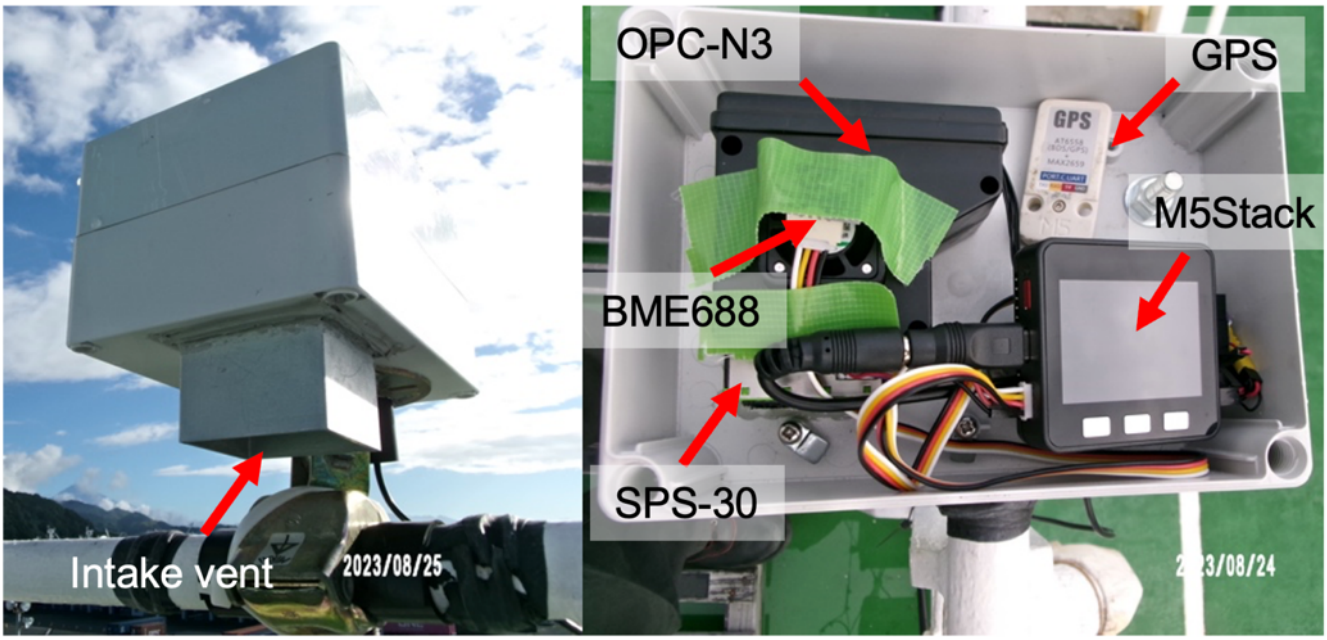

Figure 3.4.6-1: Outside and inside of the aerosol counter box.

(4) Methods, instruments

All sensors were stored a box installed at the compass deck as shown in Figure 3.4.6-1. A microSD card in a microcomputer (M5Stack Basic, M5Stack, Inc.) recorded the aerosol number concentration, VOCs information, ambient meteorological environment in the box, and GPS position. The data was manually retrieved every day if the wind speed was not strong. The measurement was made from 25 August 2023 to 2 October 2023.

(4-1) Particle size distribution

The number concentration of aerosols was measured by two optical particle counters every minute (SPS-30, Sensirion, Inc.; OPC-N3, Alphasense, Inc.). SPS-30 has five bins (0.3−0.5, 0.5−1, 1−2.5, 2.5−4, 4−10 μm). The larger particle bins > 2.5μm were empirically estimated as the three smaller bins based on manufacturer statistics because of the low sampling flow rate (0.3−0.35 L/min). The data was an instantaneous value measured in a second. OPS-N3 has 24 bins in the range of 0.35−40μm and is sampled in 30 sec at an average rate of 0.2 L/min. Although each bin data was recorded, the same size range of SPS-30 was calculated in the microcomputer in the box.

(4-2) Gas resistance of VOCs at the sea surface

Marine-origin VOCs are considered the source of marine aerosols. BME688 (Bosch, Inc.) is a gas scanner measuring the sum of VOCs/contaminants in the surrounding air with air pressure, temperature, and relative humidity measurements. The sensor provides gas resistance values of the target heater profile, which consists of ten selective heater temperature steps with identical sampling periods. In this cruise, the cycle of target temperature and sampling period was continued in a second, which was the same configuration of the BME688 on the drone. The heater profile is shown in Table 3.4.6-1. The unit of resistance was Ω and recorded in $\log_{10}(\Omega)$. Note that this sensor under this configuration did not provide any exact value of VOCs, but some indications of VOC variabilities originated from atmospheric or oceanic states. The air temperature and relative humidity from BME688 might have warm and dry biases because of the effect of heating on the gas scanner.

Table 3.4.6-1: BME688 gas scan cycle.

Profile order	T1	T2	T3	T4	T5	T6	T7	T8	T9	T10
Temperature (˚C)	320	250	200	150	200	200	250	320	370	350
Period (μ sec)	25	10	50	75	25	25	50	50	25	50

(4-3) Gas resistance of VOCs in the upper atmosphere and surface ocean.

To obtain the end member of air mass in the atmospheric boundary layer and air-sea interface, the BME688 also measured the upper atmosphere by a drone up to 1100m at maximum (see section 3-4-3), and the air in the thermal cup fill in the intake seawater (Figure 3.4.6-2). The intake seawater (4.5-m depth) was also experimentally investigated using the same configuration of BME688 at several points along the cruise track, including CTD stations (Table 3.4.6.2). 150 ml of seawater was filled into a thermal cup, and the lid with BME688 attached to the back was closed. A microcomputer (M5StickCPlus, M5Stack, Inc.) recorded the air in the cup for 30min. The 5-minute length data when the air temperature in the cup stabilized was archived for analysis.

Figure 3.4.6-2: The BME688 measurements of a drone and intake seawater.

The BME688 measurements of the intake seawater are shown in Table 3.4.6-2.

Table 3.4.6-2: Log of BME688 for seawater.

No.	Date & Time (UTC)	Lat (°N)	Lon (°E)	Remarks
001	2023/08/26 01:05	36.86	143.57	
002	2023/08/26 22:15	39.47	147.85	
003	2023/08/27 08:30	40.92	150.56	
004	2023/08/27 21:01	42.69	153.52	
005	2023/08/28 02:13	43.43	154.82	
006	2023/08/28 06:41	44.08	155.91	
007	2023/08/28 10:57	44.73	156.69	
008	2023/08/28 18:46	45.71	158.60	
009	2023/08/29 03:16	46.91	160.66	
010	2023/08/29 07:31	47.46	161.59	
011	2023/08/29 18:46	48.99	164.32	
012	2023/08/29 23:22	49.62	165.46	
013	2023/08/30 02:55	50.08	166.30	
014	2023/08/30 07:04	50.61	167.29	
015	2023/08/30 17:30	52.19	169.28	
016	2023/08/31 00:00	53.34	170.52	
017	2023/08/31 05:26	53.82	172.28	
018	2023/08/31 16:30	53.80	176.38	
019	2023/08/31 20:11	53.78	177.12	CTD test
020	2023/09/01 06:07	53.77	-179.78	
021	2023/09/01 15:27	53.89	-176.61	
022	2023/09/01 21:33	54.01	-174.56	
023	2023/09/02 04:55	54.16	-172.30	
024	2023/09/02 14:30	54.33	-169.36	
025	2023/09/02 21:00	54.45	-167.34	
026	2023/09/04 22:38	53.98	-166.53	
027	2023/09/05 17:25	56.89	-167.06	
028	2023/09/05 23:26	58.01	-167.32	
029	2023/09/06 03:41	58.78	-167.51	
030	2023/09/06 16:00	60.80	-168.09	
031	2023/09/06 20:31	61.59	-167.63	
032	2023/09/07 02:28	62.58	-167.24	
033	2023/09/07 14:22	64.46	-168.29	
034	2023/09/07 20:55	65.00	-169.08	sta.01
035	2023/09/08 03:51	65.77	-168.61	
036	2023/09/08 15:40	67.64	-168.66	sta. 03
037	2023/09/09 00:21	68.50	-168.75	sta. 04
038	2023/09/09 15:54	70.50	-168.76	sta. 06
039	2023/09/09 22:32	71.50	-168.76	sta. 07
040	2023/09/10 04:40	72.50	-168.75	sta. 08
041	2023/09/10 16:12	71.90	-163.64	sta. 09
042	2023/09/10 23:55	72.62	-163.66	wave buoy
043	2023/09/11 20:27	70.84	-161.84	sta. 10
044	2023/09/12 03:40	71.12	-59.55	
045	2023/09/12 14:59	71.66	-155.04	sta. 11
046	2023/09/12 20:20	71.77	-155.30	sta. 12
047	2023/09/12 23:52	71.74	-155.20	sta. 13
048	2023/09/13 19:42	72.47	-155.41	sta. 14
049	2023/09/14 15:07	71.96	-154.77	sta. 15
050	2023/09/14 21:32	71.69	-152.73	sta. 16
051	2023/09/15 03:18	71.32	-150.51	sta. 17
052	2023/09/15 15:16	71.06	-148.01	sta. 18
053	2023/09/15 22:06	70.82	-145.42	sta. 19
054	2023/09/16 03:42	70.85	-143.06	sta.20a
055	2023/09/17 03:07	71.68	-145.18	sta. 21
056	2023/09/17 22:55	73.65	-146.17	sta.22
057	2023/09/18 22:20	74.01	-147.46	sta. 23
058	2023/09/19 20:37	74.36	-154.49	sta. 25
059	2023/09/20 15:57	75.50	-158.38	sta. 27
060	2023/09/21 04:30	75.64	-161.75	sta. 28
061	2023/09/21 19:39	77.04	-158.37	sta. 29
062	2023/09/22 02:48	76.46	-158.82	sta. 30
063	2023/09/23 01:40	76.95	-163.29	sta. 31
064	2023/09/23 17:20	74.52	-161.97	sta. 32 (NAP)
065	2023/09/24 21:49	73.99	-164.86	sta. 33
066	2023/09/25 15:19	74.78	-172.01	sta. 34
067	2023/09/26 03:52	75.13	-177.30	sta. 35
068	2023/09/26 22:39	75.47	179.68	sta. 36
069	2023/09/27 15:28	75.04	-174.69	sta. 37
070	2023/09/28 14:37	73.06	-167.77	sta. 39
071	2023/09/29 21:45	68.078	-168.87	sta. 40
072	2023/09/30 16:25	66.17	-168.66	sta. 43
073	2023/10/01 19:14	62.33	-167.21	

(5) Preliminary results

Figure 3.4.6-3 shows the time series of the number concentration of aerosols (1−2.5μm in SPS-30), relative humidity, gas resistance, T5 extracting of the effect of air temperature and humidity, and wind speeds. The increase in the number of concentrations was found in the periods under high wind speeds (e.g., 6−8 September and 19−22 September), under high relative humidity (i.e., fog) (12−16 September), and under the tailwind situation (red lines in wind speeds) when the effect of the funnel smoke was significant. VOC resistance at each target temperature deviated partly due to the temporal variabilities in relative humidity and air temperature (not shown). The spikes in the resistance time series came from the ship funnel effect, suggesting that higher VOC air mass has lower resistance. The residual component of

each target temperature was calculated by extracting the effect of relative humidity and air temperature using multiple regression. The example of time series of the residual term (T5') has a weak negative correlation with surface wind speed, suggesting that more VOCs are supplied into the atmosphere under lower wind speeds. Analyzing seawater's temporal and spatial variability, the air-sea transfer of VOCs and cloud-aerosol interaction would be well understood.

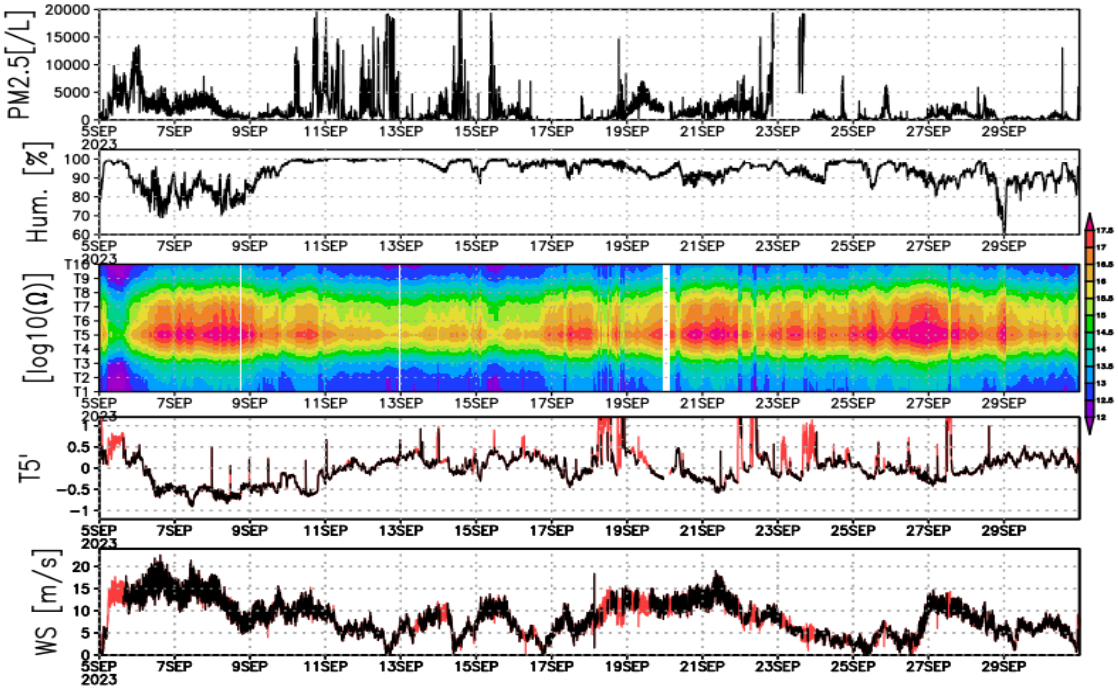

Figure 3.4.6-3: Time series of particle counts (1−2.5μm), relative humidity, gas resistance from T1 to T10, recusal T5 extracting the effect of air temperature and relative humidity, and wind speeds. Red lines in the last two bottom figures indicate the tailwind condition (relative wind direction between 80-280˚).

3.4.7. C-band Weather Radar

(1) Responsible personnel

Jun Inoue	NIPR/SOKENDAI
Kazutoshi Sato	NIPR/SOKENDAI
Kazu Takahashi	SOKENDAI
Ryo Oyama	NME
Kazuho Yoshida	NME
Satomi Ogawa	NME
Yohei Sugimoto	NME

(2) Purpose, background

Low-level clouds over the Arctic Ocean, which usually dominate during early winter, have a key role in the sea/ice surface heat budget. In addition, cyclones that modify the sea-ice distribution are also very important with regard to comprehension of air–ice–sea interaction. To capture the broad-scale characteristics of cloud–precipitation systems and their temporal and spatial evolutions over the Arctic Ocean, the three-dimensional radar echo structure and wind field of rain/snow clouds were derived based on C-band Doppler radar observations.

(3) Activities (observation, sampling, development)

The C-band Doppler weather radar observed the three-dimensional radar echo structure and wind field of rain/snow clouds.

The following lists the radar variables that are converted from the power and the phase of the backscattered signal of vertically and horizontally polarized channels:

Radar reflectivity:	Z
Doppler velocity:	Vr
Spectrum width of Doppler velocity:	SW
Differential reflectivity:	ZDR
Differential propagation phase:	ΦDP
Specific differential phase:	KDP
Co-polar correlation coefficients:	ρHV

The radar was operated continuously from 12:00 UTC on 24 August to 08:00 UTC on 4 October.

(4) Methods, instruments

The basic specifications of the C-band Doppler weather radar installed onboard the R/V Mirai are as follows:

Frequency:	5370 MHz (C-band)
Polarimetry:	Horizontal and vertical (simultaneously transmitted and received)
Transmitter:	Solid-state transmitter
Pulse Configuration:	Using pulse-compression

Output Power: 6 kW (H) + 6 kW (V)
Antenna Diameter: 4 meter
Beam Width: 1.0 degrees
INU (Inertial Navigation Unit): PHINS (IXBLUE S.A.S.)

The antenna is controlled to point in the commanded ground-relative direction by controlling the azimuth and elevation to cancel the ship attitude (i.e., roll, pitch and yaw) detected by the INU. The Doppler velocity is also corrected by subtracting the ship motion in the beam direction.

As part of routine maintenance, the internal parameters of the radar were checked and calibrated at the beginning and end of the cruise, whereas the following parameters were checked on a daily basis: (1) frequency, (2) peak output power and (3) pulse width.

During the cruise, the radar was operated in two modes, as shown in Tables 3.4.7-1 and 3.4.7-2. The radar was operated typically by repeating a volume scan with 17 plan position indicators (PPIs) at 6-min intervals. A dual pulse repetition frequency (PRF) mode with typical maximum range of 100 km was used for the volume scan. A surveillance PPI scan was performed every 30 min in a single PRF mode with maximum range of 300 km. Range height indicator (RHI) scans were operated whenever necessary to determine vertical structures in certain azimuth directions. On the return leg from the Arctic Ocean, vertical point scans were added and performed to collect data for ZDR calibration.

(5) Preliminary results

The radar operated continuously from 26 August to 3 October. During the M23-06C cruise, several precipitation systems that passed near the track of the R/V Mirai were captured by the C-band weather radar.

(6) Remarks (Times in UTC)

1. During the following periods, data acquisition was suspended because of maintenance.
   22:30 02 Sep. 2023 - 17:00 05 Sep. 2023 (Called at the Dutch Harbor port)
   17:06 07 Sep. 2023 - 17:29 07 Sep. 2023 (System maintenance)
   17:34 07 Sep. 2023 - 17:36 07 Sep. 2023 (System maintenance)
   21:22 07 Sep. 2023 - 22:06 07 Sep. 2023 (System maintenance)
   14:00 14 Sep. 2023 - 14:36 14 Sep. 2023 (System maintenance)
   14:42 14 Sep. 2023 - 14:54 14 Sep. 2023 (System maintenance)
   15:46 14 Sep. 2023 - 15:59 14 Sep. 2023 (System maintenance)
   21:10 14 Sep. 2023 - 21:30 14 Sep. 2023 (System maintenance)
   06:40 15 Sep. 2023 - 06:54 15 Sep. 2023 (System maintenance)
   23:34 01 Oct. 2023 - 23:42 01 Oct. 2023 (System maintenance)

2. The following period, some of ingest data and raw products in a scan were not acquired due to trouble of the radar data processor. For more information, refer to "NoDataList" files which are attached to the dataset.
   18:36 05 Sep. 2023 - 06:54 15 Sep. 2023

3. Re-unfolding correction of Doppler velocity was not used during this cruise.

Table 3.4.7-1: Parameters for scan strategy

	Surveillance PPI Scan	Volume Scan						RHI Scan
Repeated Cycle (min.)	30	6						6
Times in One Cycle	1	1						3
Pulse Width (long / short, in microsec)	200 / 2	64 / 1		32 / 1		32 / 1		32 / 1
Scan Speed (deg/sec)	18	18		24		36		9 (in el.)
PRF(s) (Hz)	400	dual PRF (ray alternative)						1250
		667	833	938	1250	1333	2000	
Pulses / Ray	16	26	33	27	34	37	55	32
Ray Spacing (deg.)	0.7	0.7		0.7		1.0		0.23
Azimuth	Full Circle							Optional
Bin Spacing (m)	150							
Max. Range (km)	300	150		100		60		100
Elevation Angle(s) (deg.)	0.5	0.5		1.0, 1.8, 2.6, 3.4, 4.2, 5.1, 6.2, 7.6, 9.7, 12.2 15.2		18.7, 23.0, 27.9, 33.5, 40.0		-0.2 to 60.0

(7) Data archives

These data obtained in this cruise will be submitted to the Data Management Group (DMG) of JAMSTEC, and will be opened to the public via “Data Research System for Whole Cruise Information in JAMSTEC (DARWIN)” in JAMSTEC web site.

http://www.godac.jamstec.go.jp/darwin/e

3.5. Possibility of the expanding distribution in plankton and fishes associated with sea ice reduction in the Pacific sector of the Arctic Ocean

3.5.1. Zooplankton

(1) Personnel

Kohei Matsuno (Hokkaido University) - Principal Investigator

Tatsuya Kawakami (Hokkaido University)

(2) Objectives

The goals of this study are following:

1) Clarifying spatial distribution of mesozooplankton communities
2) Evaluation physiological conditions (stable isotope and fatty acids) of the Pacific and Arctic zooplankton
3) Comparison population structure and fatty acids of dominant copepod *Calanus glacialis/marshallae* between different populations examined by haplotype analysis

(3) Parameters

Mesozooplankton abundance

Stable isotope

Fatty acids

Haplotypes of *Calanus glacialis/marshallae*

(4) Sampling and treatment

(4-1) Plankton net sampling

Zooplankton samples were collected by vertical hauls of a Quad-NORPAC net at 37 stations in the Pacific Arctic Ocean. Quad-NORPAC net (mesh sizes: 335, 150 and two 63 μm with large cod-end, mouth diameter: 45 cm) was towed between surface and 150 m depth or bottom -7 m (stations where the bottom shallower than 150 m) at all stations (Fig. 3.5-1 and Table 3.5-1). At seven stations, additional casts were performed between surface and 200 m depth for comparison with Korean Polar Research Institute's data set and samples (Fig. 3.5-1 and Table 3.5-1). The volume of water filtered through the net was estimated from the reading of a flow-meter mounted in the mouth ring. The zooplankton samples collected by the NORPAC net with 335 and 150 μm mesh were immediately fixed with 5% buffered formalin for zooplankton community structure analysis. Samples collected with 63 μm mesh were used for evaluation of the zooplankton physiological parameters (stable isotope and fatty acids composition). After the sorting, the remaining sub-samples were fixed with 99.5% ethanol as backup samples for haplotype analysis of *Calanus glacialis*.

80 cm ring net (mesh: 335 μm, mouth diameter: 80 cm) was towed between surface and 300-

500 m or bottom -7 m at 20 stations (Fig. 3.5-1 and Table 3.5-2). Fresh samples were used for evaluation of the zooplankton physiological parameters (stable isotope and lipid composition). After the sorting, the remaining sub-samples were divided with a Motoda box splitter, and fixed with 99.5% ethanol as backup samples.

(4-2) On-board treatment

We immediately added with 10% soda water (CO_2 water) into samples collected by 63 μm NORPAC or 335 μm ring net after net sampling. We sorted with all zooplankton at species level as many as possible for copepods, euphausiids, chaetognaths, appendicularians, amphipods and siphonophora. One specimen was transferred into a small plastic case (3 mL), and stored in –80°C for fatty acid composition analysis (by Dr. Yasuhiro Ando in Hokkaido University). Using another specimen of same species in the lipid analysis, we also transferred several specimens into a glass bial bin (6 mL), and dried at 60ºC in an oven for measuring stable isotope (by Dr. Maki Noguchi in JAMSTEC). For *C. glacialis/marshallae*, we measured prosome length with an eye-piece micrometer under a stereo microscope, and cut their antenules by needles. The antenules were preserved in a 1.5 mL plastic tube filled with 99% ethanol for haplotype (16s rRNA) analysis (by Dr. Junya Hirai in The University of Tokyo). Remaining body was treated same procedure for fatty acids sample as written above.

(5) Station list

Table 3.5-1: Data on plankton samples collected by vertical hauls with a Quad-NORPAC net.

Station no.	Position Lat. (N)	Position Lon.	S.M.T. Date	S.M.T. Hour	Length of wire (m)	Angle of wire (°)	Depth estimated by wire angle (m)	Mesh size (μm)	Flowmeter No.	Flowmeter Reading	Estimated volume of water filtered (m^3)	Remark
1	65 0	169 4.82 W	7 Sep.	13:45 - 13:49	42	4	42	335	3996	588	8.97	
								150	4361	480	7.32	
								63				1)
								63				1)
2	66 10.12	168 39.99 W	7 Sep.	22:14 - 22:19	48	2	48	335	3996	585	8.92	4)
								150	4361	490	7.48	
								63				1)
								63				1)
3	67 39.95	168 39.87 W	8 Sep.	11:22 - 11:25	42	8	42	335	3996	434	6.62	
								150	4361	373	5.69	
								63				1)
								63				1)
4	68 30.02	168 44.98 W	8 Sep.	16:17 - 16:19	46	1	46	335	3996	456	6.95	
								150	4361	446	6.81	
								63				2)
								63				2)
5	69 30.03	168 44.98 W	8 Sep.	23:26 - 23:31	44	2	44	335	3996	436	6.65	
								150	4361	415	6.33	
								63				2)
								63				2)
6	70 30.09	168 45.16 W	9 Sep.	9:00 - 9:03	31	10	31	335	3996	378	5.76	
								150	4361	360	5.49	
								63				2)
								63				2)
7	71 30.04	168 45.4 W	9 Sep.	14:39 - 14:43	41	3	41	335	3996	461	7.03	
								150	4361	447	6.82	
								63				2)
								63				2)
8	72 30.01	168 44.89 W	9 Sep.	21:21 - 21:25	51	1	51	335	3996	513	7.82	
								150	4361	462	7.05	
								63				1)
								63				1)
9	71 54.01	163 38.29 W	10 Sep.	9:22 - 9:25	34	1	34	335	3996	391	5.96	
								150	4361	292	4.46	
								63				1)
								63				1)
10	70 50.59	161 42.8 W	11 Sep.	14:18 - 14:21	37	7	37	335	3996	429	6.54	
								150	4361	349	5.33	
								63				1)
								63				1)
13	71 44.10	155 11.9 W	12 Sep.	17:00 - 17:08	151	8	150	335	3996	1515	23.10	
								150	4361	1478	22.55	
								63				1)
								63				1)
14	72 28.21	155 24.27 W	13 Sep.	12:12 - 12:18	150	1	150	335	3996	1533	23.38	
								150	4361	1532	23.38	
								63				1)
								63				1)
15	71 56.32	154 46.39 W	14 Sep.	9:25 - 9:32	150	1	150	335	3996	1363	20.79	
								150	4361	1339	20.43	
								63				2)
								63				2)
16	71 41.5	152 43.72 W	14 Sep.	13:36 - 13:43	151	5	150	335	3996	1383	21.09	
								150	4361	1350	20.60	
								63				1)
								63				1)
17	71 18.68	150 28.46 W	14 Sep.	20:38 - 20:45	151	1	151	335	3996	1455	22.19	
								150	4361	1370	20.91	
								63				2)
								63				2)
18	71 3.89	147 56.59 W	15 Sep.	8:12 - 8:15	77	10	76	335	3996	781	11.91	
								150	4361	758	11.57	
								63				2)
								63				2)
19	70 49.00	145 24.99 W	15 Sep.	15:00 - 15:08	150	3	150	335	3996	1465	22.34	
								150	4361	1491	22.75	
								63				2)
								63				2)

S.M.T. is UTC-8h
1) Samples was used for experiments on board
2) Experiment, remaining was preserved in ethanol
3) High wave and strong wind
4) Medusa abundant
5) Phytoplankton abundant

Table 3-5-1: (Continued).

Station no.	Position Lat. (N)	Position Lon.	S.M.T. Date	S.M.T. Hour	Length of wire (m)	Angle of wire (°)	Depth estimated by wire angle (m)	Mesh size (μm)	Flowmeter No.	Flowmeter Reading	Estimated volume of water filtered (m^3)	Remark
20	70 50.84	143 3.32 W	15 Sep.	19:30 - 19:37	150	2	150	335	3996	1415	21.58	
								150	4361	1411	21.53	
								63				1)
								63				1)
21	71 41.39	145 12 W	16 Sep.	20:16 - 20:24	151	6	150	335	3996	1470	22.42	
								150	4361	1440	21.97	
								63				1)
								63				1)
23	74 1.16	147 28.58 W	18 Sep.	16:43 - 16:52	150	1	150	335	3996	1571	23.96	
								150	4361	1600	24.42	
								63				1)
								63				1)
25	74 21.59	154 30.06 W	19 Sep.	14:12 - 14:21	156	16	150	335	3996	1666	25.41	
								150	4361	1558	23.77	
								63				1)
								63				1)
27	75 29.99	158 22.94 W	20 Sep.	14:49 - 14:58	152	10	150	335	3996	1848	28.18	3)
								150	4361	1752	26.73	3)
								63				1)
								63				1)
27	75 29.99	158 22.94 W	20 Sep.	15:02 - 15:14	200	2	200	335	3996	2126	32.42	3)
								150	4361	1929	29.44	3)
								63				1)
								63				1)
28	75 38.53	161 44.95 W	20 Sep.	20:32 - 20:40	150	4	150	335	3996	1530	23.33	
								150	4361	1499	22.87	
								63				1)
								63				1)
28	75 38.53	161 44.95 W	20 Sep.	20:45 - 20:57	200	1	200	335	3996	1975	30.12	
								150	4361	1892	28.87	
								63				2)
								63				2)
29	77 2.19	158 22.43 W	21 Sep.	12:07 - 12:14	150	1	150	335	3996	1406	21.44	
								150	4361	1392	21.24	
								63				1)
								63				1)
30	76 27.62	158 49.18 W	21 Sep.	20:32 - 20:39	150	1	150	335	3996	1459	22.25	
								150	4361	1435	21.90	
								63				2)
								63				2)
30	76 27.62	158 49.18 W	21 Sep.	20:45 - 20:54	201	5	200	335	3996	1845	28.14	
								150	4361	1832	27.96	
								63				1)
								63				1)
31	76 56.96	163 21.79 W	22 Sep.	14:15 - 14:22	151	5	150	335	3996	1382	21.08	
								150	4361	1363	20.80	
								63				1)
								63				1)
31	76 56.96	163 21.79 W	22 Sep.	14:27 - 14:36	200	1	200	335	3996	1849	28.20	
								150	4361	1805	27.54	
								63				1)
								63				1)
32	74 30.71	161 59.91 W	23 Sep.	14:38 - 14:46	150	1	150	335	3996	1508	23.00	
								150	4361	1310	19.99	
								63				1)
								63				1)
34	74 45.99	172 3.65 W	25 Sep.	10:19 - 10:27	150	1	150	335	3996	1382	21.08	
								150	4361	1316	20.08	
								63				1)
								63				1)
34	74 45.99	172 3.65 W	25 Sep.	10:32 - 10:42	200	4	200	335	3996	1805	27.53	
								150	4361	1763	26.90	
								63				1)
								63				1)

S.M.T. is UTC-8h

1) Samples was used for experiments on board

2) Experiment, remaining was preserved in ethanol

3) High wave and strong wind

4) Medusa abundant

5) Phytoplankton abundant

Table 3-5-1: (Continued).

Station no.	Position Lat. (N)		Position Lon.		S.M.T. Date	S.M.T. Hour	Length of wire (m)	Angle of wire (°)	Depth estimated by wire angle (m)	Mesh size (μm)	Flowmeter No.	Flowmeter Reading	Estimated volume of water filtered (m^3)	Remark
35	75	7.78	177	13.75 W	25 Sep.	20:07 - 20:14	156	16	150	335	3996	1410	21.50	
										150	4361	1324	20.20	
										63				1)
										63				1)
35	75	7.78	177	13.75 W	25 Sep.	20:21 - 20:31	201	5	200	335	3996	1823	27.80	
										150	4361	1727	26.35	
										63				2)
										63				2)
36	75	19.68	179	29.21 E	26 Sep.	17:26 - 17:33	150	4	150	335	3996	1508	23.00	
										150	4361	1465	22.36	
										63				1)
										63				1)
37	75	1.11	174	41.19 W	27 Sep.	9:05 - 9:16	150	4	150	335	3996	2012	30.68	3)
										150	4361	1910	29.15	3)
										63				1)
										63				1)
37	75	1.11	174	41.19 W	27 Sep.	9:23 - 9:39	200	4	200	335	3996	2895	44.15	3)
										150	4361	2534	38.67	3)
										63				2)
										63				2)
38	74	10.78	167	30.59 W	27 Sep.	23:33 - 23:40	150	1	150	335	3996	1376	20.98	
										150	4361	1287	19.64	
										63				2)
										63				2)
39	73	1.75	167	45.52 W	28 Sep.	8:29 - 8:34	59	18	56	335	3996	605	9.23	
										150	4361	530	8.09	
										63				2)
										63				2)
40	68	4.58	168	51.96 W	29 Sep.	14:21 - 14:24	51	1	51	335	3996	499	7.61	4)
										150	4361	475	7.25	4)
										63				2)
										63				2)
42	67	39.69	168	39.94 W	29 Sep.	22:22 - 22:25	42	2	42	335	3996	395	6.02	
										150	4361	370	5.65	
										63				2)
										63				2)
43	66	10.2	168	39.85 W	30 Sep.	8:28 - 8:31	48	2	48	335	3996	458	6.98	5)
										150	4361	280	4.27	5)
										63				2)
										63				2)
44	65	0.02	169	4.77 W	30 Sep.	16:15 - 16:18	43	6	43	335	3996	400	6.10	
										150	4361	366	5.58	
										63				2)
										63				2)

S.M.T. is UTC-8h

1) Samples was used for experiments on board

2) Experiment, remaining was preserved in ethanol

3) High wave and strong wind

4) Medusa abundant

5) Phytoplankton abundant

Table 3.5-2: Data on plankton samples collected by vertical hauls with a ring net. GG54: 0.335 mm mesh size.

Station no.	Position			S.M.T.		Length of wire (m)	Angle of wire (°)	Depth estimated by wire angle (m)	Kind of cloth	Remark
	Lat. (N)	Lon.		Date	Hour					
3	67-39.951	168-39.87	W	8 Sep.	11:30	42	6	42	GG54	Experiment, remaining in ethanol
6	70-30.09	168-45.16	W	9 Sep.	9:06	31	5	31	GG54	Experiment
8	72-30.01	168-44.89	W	9 Sep.	21:30	51	1	51	GG54	Experiment, remaining in ethanol
9	71-54.01	163-38.29	W	10 Sep.	9:22	34	2	34	GG54	Experiment, remaining in ethanol
10	70-50.59	161-42.80	W	11 Sep.	14:24	37	4	37	GG54	Experiment, remaining in ethanol
13	71-44.10	155-11.90	W	12 Sep.	17:13	280	3	280	GG54	Experiment, remaining in ethanol
14	72-28.21	155-24.27	W	13 Sep.	12:25	300	2	300	GG54	Experiment, remaining in ethanol, 1/2 Alix 1/2 Hokkaido Univ.
16	71-41.50	152-43.72	W	14 Sep.	13:49	180	1	180	GG54	Experiment, remaining in ethanol
18	71-3.89	147-56.59	W	15 Sep.	8:20	75	1	75	GG54	Cloged by large medusa
20	70-50.84	143-3.32	W	15 Sep.	19:42	300	1	300	GG54	Experiment, remaining in ethanol, 1/2 Alix 1/2 Hokkaido Univ.
21	71-41.39	145-12.00	W	16 Sep.	20:28	300	1	300	GG54	Experiment, remaining in ethanol
23	74-1.16	147-28.58	W	18 Sep.	16:56	300	1	300	GG54	Experiment, remaining in ethanol, 1/2 Alix 1/2 Hokkaido Univ.
25	74-21.59	154-30.06	W	19 Sep.	14:12	300	10	295	GG54	Experiment, remaining in ethanol, 1/2 Alix 1/2 Hokkaido Univ.
27	75-29.99	158-22.94	W	20 Sep.	15:35	300	10	295	GG54	Experiment, remaining in ethanol
29	77-2.19	158-22.43	W	21 Sep.	12:18	300	1	300	GG54	Experiment, remaining in ethanol
31	76-56.96	163-21.79	W	22 Sep.	14:41	500	9	494	GG54	Experiment, remaining in ethanol, 1/2 Alix 1/2 Hokkaido Univ.
32	74-30.71	161-59.91	W	23 Sep.	14:51	300	3	300	GG54	Experiment, remaining in ethanol
34	74-45.99	172-3.65	W	25 Sep.	10:47	300	2	300	GG54	Experiment, remaining in ethanol, 1/2 Alix 1/2 Hokkaido Univ.
36	75-19.68	179-29.21	E	26 Sep.	17:39	300	1	300	GG54	Experiment, remaining in ethanol, 1/2 Alix 1/2 Hokkaido Univ.
37	75-1.11	174-41.19	W	27 Sep.	9:44	260	6	259	GG54	Experiment, remaining in ethanol

S.M.T. is UTC-8h

(6) Preliminary results

As a preliminary results, we present following items.

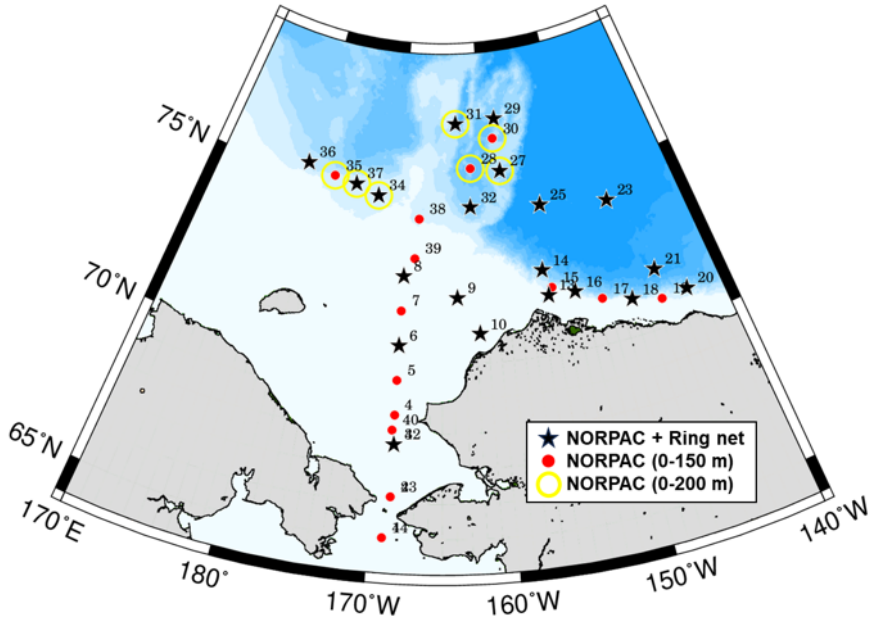

Fig. 3.5-1. Location of the sampling stations in the Pacific Arctic Ocean from 7 to 30 September in 2023.

(7) Data archives

These data obtained in this cruise will be submitted to the Data Management Group of JAMSTEC, and will be opened to the public via “Data Research System for Whole Cruise Information in JAMSTEC (DARWIN)” in JAMSTEC web site.
<http://www.godac.jamstec.go.jp/darwin/e>

3.5.2. Phytoplankton

(1) Personnel

Kohei Matsuno (Hokkaido University) - Principal Investigator
Tatsuya Kawakami (Hokkaido University)

(2) Objective

The goals of this study are following:

1) Clarifying spatial distribution of phytoplankton and microprotist assemblages by a multispectral excitation–emission fluorometer (MFL) and a microscopy
2) Evaluating photosynthetic activity by a pulse-amplitude modulated fluorometer
3) Clarifying spatial distribution of ice-algae biomarkers in sediment

(3) Parameters

Phytoplankton community in cell number
Fluorescence by phytoplankton taxon
Fv/Fm
alpha
ETRm
IP^{25}

(4) Sampling and treatment

(4-1) Surface monitoring

We took surface water samples from underway system once a day for examining cell density and photosynthetic activity from north Pacific Ocean to Bering Sea. The water sample was fixed by glutaraldehyde (1% final concentration), and another fresh water kept in a dark bottle. Using the fresh water, maximum photochemical efficiency (Fv/Fm) was measured using a pulse-amplitude modulated fluorometer (Water-PAM; Walz, Effeltrich, Germany) in sediment preservation room (3-5ºC). After light-acclimatation in the dark bottle over 15 minutes, samples (4 mL) were placed in a quartz cuvette. Fv/Fm of each sample was determined by red LED with a peak illumination at 650 nm. The initial fluorescence (Fv) was measured by applying a weak measuring light, and

a saturating pulse was applied to determine the maximum fluorescence (Fm). Then, the samples in the measuring cuvette were light-acclimated for 15 minutes by turning off the internal actinic light source of the PAM fluorometer. After the acclimation, rapid light curve was obtained by illuminating the samples for 10 s before each ΔF/Fm measurement at each of a series of eight irradiances that increased in steps from 136 to 2122 μmol photons m^{-2} s^{-1}.

(4-2) Niskin sampler and bucket

Sea water samples (1 L) were collected from surface, chlorophyll *a* maximum layer (SCM) and bottom -5 m (where bottom depth was < 200 m) by bucket and Niskin water sampler at 38 stations (Fig. 3-5-2, Table 3-5-3). The water samples were fixed by glutaraldehyde (1% final concentration) for microscopic analysis. In the land laboratory, the samples will be concentrated to 20 mL with a syphon, and microprotists will be enumerated and identified under an inverted microscopy. Additionally, seawater sample (4 mL) was used for measuring photosynthetic activity (see detail method in above section). A MFL was attached on the CTD frame to measure the vertical profile of phytoplankton taxonomic composition where the bottom depth was < 500 m.

(4-3) Sediment sampling

Sea bottom sediments were collected by a multiple corer system (Ashura) at 11 stations in the Pacific Arctic Ocean (Fig. 3.5-2., Table 3.5-4). Surface sediment (0-1 cm) were cut and preserved in dark and cool (~4ºC) condition for examining ice-algae biomarker (by Dr. Takuto Ando in Akita University).

(5) Station list

Table 3.5-3: Data on water samples collected by Niskin water sampler and bucket. Circle indicate MFL was attached on the CTD frame.

St.	Date	Latitude (°N)		Longitude			Sampling depth (m)	MFL
1	7 Sep.	65	0	169	4.82	W	0, 25, 44	○
2	7 Sep.	66	10.12	168	39.99	W	0, 25, 49	○
3	8 Sep.	67	39.95	168	39.87	W	0, 23, 44	○
4	8 Sep.	68	30.02	168	44.98	W	0, 21, 47.9	○
5	8 Sep.	69	30.03	168	44.98	W	0, 16, 46	○
6	9 Sep.	70	30.09	168	45.16	W	0, 23, 32.9	○
7	9 Sep.	71	30.04	168	45.4	W	0, 25, 43	○
8	9 Sep.	72	30.01	168	44.89	W	0, 27, 53.3	○
9	10 Sep.	71	54.01	163	38.29	W	0, 18, 35	○
10	11 Sep.	70	50.59	161	42.8	W	0, 26, 38	○
13	12 Sep.	71	44.10	155	11.9	W	0, 8	
14	13 Sep.	72	28.21	155	24.27	W	0, 15	
15	14 Sep.	71	56.32	154	46.39	W	0, 15	
16	14 Sep.	71	41.5	152	43.72	W	0, 7	
17	14 Sep.	71	18.68	150	28.46	W	0, 15	
18	15 Sep.	71	3.89	147	56.59	W	0, 16	
19	15 Sep.	70	49.00	145	24.99	W	0, 15	
20	15 Sep.	70	50.84	143	3.32	W	0, 16	
21	16 Sep.	71	41.39	145	12	W	0, 20	
22	17 Sep.	73	9.85	145	9.94	W	0, 70	
23	18 Sep.	74	1.16	147	28.58	W	0, 25	
25	19 Sep.	74	21.59	154	30.06	W	0, 60	
27	20 Sep.	75	29.99	158	22.94	W	0, 55	
28	20 Sep.	75	38.53	161	44.95	W	0, 38	
29	21 Sep.	77	2.19	158	22.43	W	0, 45	
30	21 Sep.	76	27.62	158	49.18	W	0, 38	
31	22 Sep.	76	56.96	163	21.79	W	0, 30	
32	23 Sep.	74	30.71	161	59.91	W	0, 37	
34	25 Sep.	74	45.99	172	3.65	W	0, 23	
35	25 Sep.	75	7.78	177	13.75	W	0, 30	
36	26 Sep.	75	19.68	179	29.21	E	0, 20	
37	27 Sep.	75	1.11	174	41.19	W	0, 25	
38	27 Sep.	74	10.78	167	30.59	W	0, 24.4	○
39	28 Sep.	73	1.75	167	45.52	W	0, 18	○
40	29 Sep.	68	4.58	168	51.96	W	0, 14	○
42	29 Sep.	67	39.69	168	39.94	W	0, 18	○
43	30 Sep.	66	10.2	168	39.83	W	0. 15	○
44	30 Sep.	65	0.12	169	4.11	W	0, 5	○

Table 3.5-4: Station list of sediments samples collected with Multiple corer system (Ashura) at 12 stations in the Pacific Arctic Ocean during September 2023.

St.	Date	Latitude (°N)	Longitude (°W)	Bottom depth (m)	Sampling depth (cm)
3	8 Sep.	67-39.95	168-39.87	49.6	0-1
5	8 Sep.	69-30.03	168-44.98	51	0-1
6	9 Sep.	70-30.09	168-45.16	38.8	0-1
7	9 Sep.	71-30.04	168-45.4	48.7	0-1
9	10 Sep.	71-54.01	163-38.29	40.6	0-1
10	11 Sep.	70-50.59	161-42.8	44.2	0-1
11	12 Sep.	71-39.60	155-1.31	99	0-1
39	28 Sep.	73-1.75	167-45.52	66	0-1
40	29 Sep.	68-4.58	168-51.96	58	0-1
41	29 Sep.	68-6	167-40.02	48	0-1
44	30 Sep.	65-0.12	169-4.11	50	0-1

(6) Preliminary results

As a preliminary results, we present following items.

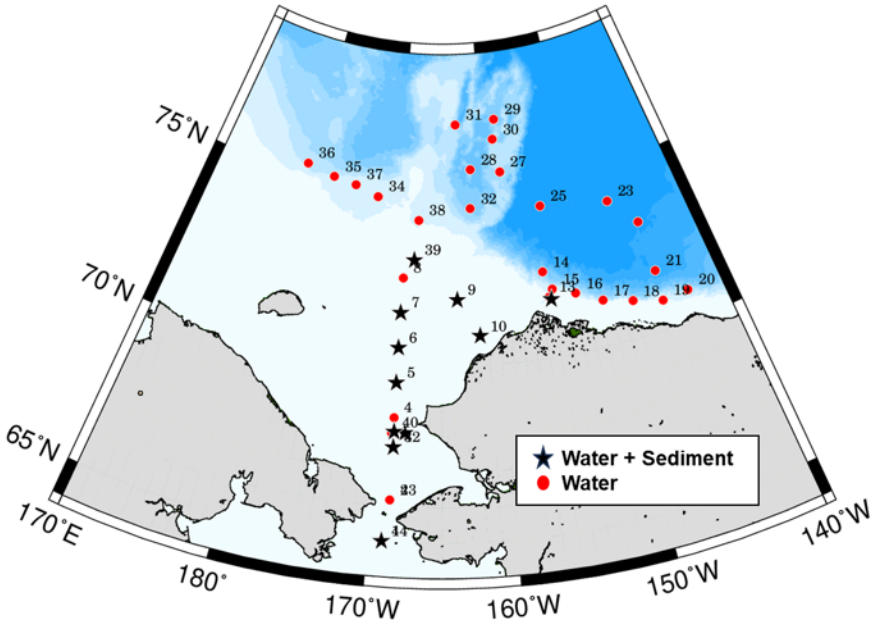

Fig. 3.5-2. Location of water (surface and sub-surface chlorophyl maximum) and sediment sampling stations in the Pacific Arctic Ocean.

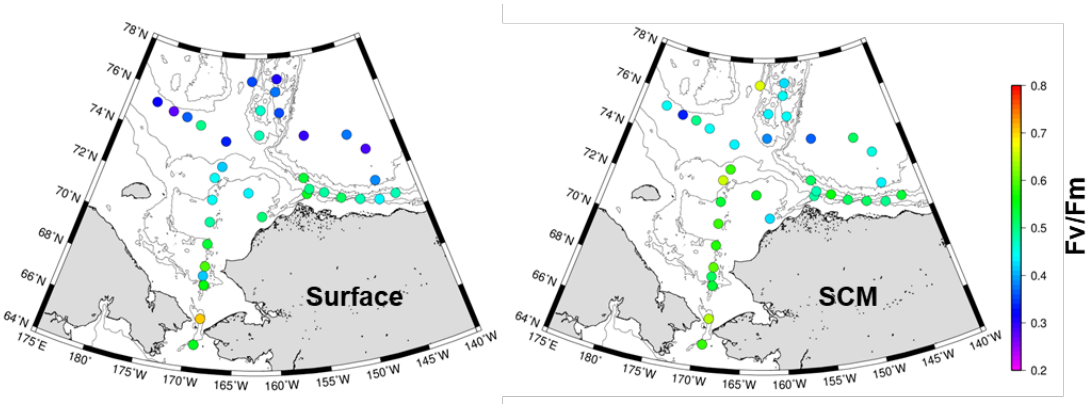

Fig. 3.5-3. Spatial distribution of the maximum photochemical efficiency (Fv/Fm) at the surface and the sub-surface chlorophyll-*a* maximum layer (SCM).

(7) Data archives

These data obtained in this cruise will be submitted to the Data Management Group of JAMSTEC, and will be opened to the public via "Data Research System for Whole Cruise Information in JAMSTEC (DARWIN)" in JAMSTEC web site.
<http://www.godac.jamstec.go.jp/darwin/e>

3.5.3. Fish

(1) Personnel

Kohei Matsuno (Hokkaido University) - Principal Investigator
Tatsuya Kawakami (Hokkaido University)

(2) Objectives

The goals of this study are following:

1) To clarify the spatial distribution of common fish species in the Arctic region and its relationship with the oceanographic environment.
2) To reveal a linkage between fish and plankton by combining the results from eDNA detection and plankton survey.
3) To reveal latitudinal transition in pelagic fish community across the temperate zone to the Pacific Arctic.

(3) Parameters

Environmental DNA

(4) Instruments and methods

(4.1) eDNA collection from seawater

To estimate the spatial distribution of fish in the Pacific Arctic, eDNA samples were obtained from the northern Bering Sea, Chukchi Sea, and Canada Basin by filtration of seawater (Fig. 3-5-4, Table 3-5-5). Depths for water collection were basically determined as 5 m and bottom layer at stations on the Chukchi Sea shelf (about 50 m depth) and 5 m, 30 m, and 150 m at stations on the Shelf slope and the Canada basin (about 50 m depth). When the bottom depth was shallower than 150 m, bottom layer was determined as the deepest layer for eDNA sampling. The bottom layer was defined as being 5 m or 10 m above the sea floor. These sampling depths covered the Pacific summer water and the Pacific winter water and corresponded with the net towing depth of plankton sampling. Additionally, eDNA samples were collected from seawater from the layer deeper than 200 m in the Chukchi Sea shelf and in the Canada Basin. These samples were intended to evaluate the vertical distribution of fish in the central Arctic.

In the Arctic region, seawater was collected using 12 L Niskin bottles mounted on the CTD/Carousel Water Sampling System from multiple depths. In a few stations, seawater continuously pumped up from about 5 m depth for the underway sea-surface monitoring was used for eDNA sampling instead of seawater collected by a Niskin sampler. For each water sample, a clean, plastic tank or foldable plastic bag was filled with 5 L of collected seawater. At each site and depth, the 5 L of water sample was filtered through a 0.45 μm pore size cartridge filters (Sterivex HV, Millipore, Billerica, MA, USA) in two or three replicates using a peristaltic tubing pump (Masterflex 07528-10, Cole-Parmer, IL, USA) at a flow rate of 100 ml/min. Filtration was halted when the 5L of water was completely filtered or clogging became severe. After filtration, the filters were filled with 2.0 ml of RNA*later* and then stored at −20 °C.

Along the track between the Japanese coast and the Bering Sea, the pumped-up seawater was collected and filtered for eDNA sampling (Fig. 3-5-4, Table 3-5-5). Water collection and filtration was conducted in the same manner described above. However, in this case, filtration was performed using a syringe filter with 5 μm pore size (Minisart NML, Sartorius, Goettingen, Germany) in four replicates. After filtration, the filters were filled with about 0.4 ml of RNA*later* and then stored at −20 °C.

To prevent cross-contaminations, all equipment used for eDNA sampling was soaked in a 2% bleach solution (approximately 0.12% NaOCl) for at least 30 min and subsequently rinsed three times with Milli-Q water. The workspace was decontaminated using bleach disinfectant spray (approximately 0.1% NaOCl). For each water collection and filtration, disposable gloves and masks were used. Further, 500 mL of Milli-Q water was also filtered as a negative control for every 5 sites to check for cross-contamination during the filtration process.

(5) Station list

Table 3.5-5. List of sampling stations where eDNA sample was collected.

Site (CTD Station)	Date (UTC)	Latitude	Longitude	Bottom depth (m)	Sampling depth (m)	Water collection procedure
NP01	25-Aug	36° 36.58 N	143° 12.08 E	7598	4.5	Pumped-up seawater
NP02	27-Aug	40° 36.54 N	149° 59.27 E	5363	4.5	Pumped-up seawater
NP03	28-Aug	43° 51.47 N	155° 31.15 E	5448	4.5	Pumped-up seawater
NP04	29-Aug	47° 0.25 N	160° 48.95 E	5361	4.5	Pumped-up seawater
NP05	30-Aug	50° 13.39 N	166° 33.98 E	4864	4.5	Pumped-up seawater
BS01	31-Aug	53° 36.65 N	171° 30.03 E	3218	4.5	Pumped-up seawater
BS02	1-Sep	53° 44.48 N	178° 52.34 E	2858	4.5	Pumped-up seawater
BS03	2-Sep	54° 5.38 N	173° 31.45 W	3641	4.5	Pumped-up seawater
BS04	2-Sep	54° 29.57 N	166° 38.68 W	483	4.5	Pumped-up seawater
BS05	5-Sep	58° 6.28 N	167° 20.48 W	63.7	4.5	Pumped-up seawater
BS06	6-Sep	62° 10.31 N	167° 17.99 W	28.1	4.5	Pumped-up seawater
St01	7-Sep	65° 0.04 N	169° 4.78 W	49.5	5, 44	Niskin water sampler
St02	8-Sep	66° 10.16 N	168° 40.02 W	55.1	5, 50	Niskin water sampler
St03	8-Sep	67° 39.9 N	168° 39.87 W	49.7	5, 44	Niskin water sampler
St04	9-Sep	68° 30.08 N	168° 45 W	53.3	5, 48	Niskin water sampler
St05	9-Sep	69° 22.93 N	168° 44.98 W	51.7	5, 46	Niskin water sampler
St06	9-Sep	70° 30.03 N	168° 45.33 W	38.8	5, 33	Niskin water sampler
St07	9-Sep	71° 30.11 N	168° 45.37 W	48.7	5, 43	Niskin water sampler
St08	10-Sep	72° 28.26 N	168° 45.53 W	59.1	5, 53.3	Niskin water sampler
St09	10-Sep	71° 54.02 N	163° 38.38 W	40.6	5, 35	Niskin water sampler
St10	11-Sep	70° 50.47 N	161° 43 W	44.2	5, 39	Niskin water sampler
St13	13-Sep	71° 46.23 N	155° 18.83 W	303	5, 30, 150, 298	Niskin water sampler
St14	13-Sep	72° 28.34 N	155° 24.34 W	1985	5, 30, 150, 400, 1966	Niskin water sampler
St15	14-Sep	71° 56.42 N	154° 46.46 W	496	5, 30, 150, 486	Niskin water sampler
St16	14-Sep	71° 41.42 N	152° 43.22 W	209	5, 30, 204	Niskin water sampler
St17	15-Sep	71° 18.92 N	150° 30.6 W	365	5, 30, 150, 360	Niskin water sampler
St18	15-Sep	71° 3.89 N	147° 56.56 W	81	5, 30, 72	Niskin water sampler
St19	15-Sep	70° 49.16 N	145° 28.01 W	180	5, 30, 170	Niskin water sampler
St20	16-Sep	70° 50.88 N	143° 3.51 W	1191	5, 30, 150, 400, 1187	Niskin water sampler
St21	17-Sep	71° 41.32 N	145° 12.23 W	3333	5, 30, 150, 400, 3307	Niskin water sampler
St22	18-Sep	73° 9.85 N	145° 9.94 W	3601	5, 30, 150	Niskin water sampler
St23	18-Sep	74° 1.14 N	147° 26.86 W	3775	5, 30, 150	Pumped-up seawater/ Niskin water sampler
St25	19-Sep	74° 21.6 N	154° 29.94 W	3851	5, 30, 150, 400, 3307	Niskin water sampler
St27	20-Sep	75° 29.96 N	158° 22.81 W	1334	5, 30, 150, 400, 1320	Niskin water sampler
St28	21-Sep	75° 38.57 N	161° 44.92 W	877	5, 30, 150	Niskin water sampler
St29	21-Sep	77° 2.03 N	158° 22.09 W	1564	5, 30, 150, 400, 1539	Niskin water sampler
St30	22-Sep	76° 27.22 N	158° 48.19 W	1508	5, 30, 150, 400, 1380	Niskin water sampler
St31	22-Sep	76° 57.18 N	163° 26.8 W	1331	5, 30, 150, 400, 1981	Niskin water sampler
St32	23-Sep	74° 30.5 N	161° 56.53 W	1664	5, 30, 150, 400, 1627	Niskin water sampler
St34	25-Sep	74° 45.98 N	172° 3.76 W	324	5, 30, 150, 314	Niskin water sampler
St35	26-Sep	75° 7.79 N	177° 13.91 W	407	5, 30, 150, 396	Niskin water sampler
St36	27-Sep	75° 21.05 N	179° 32.11 E	650	5, 30, 150, 590	Pumped-up seawater/ Niskin water sampler
St37	27-Sep	75° 1.11 N	174° 40.89 W	282	5, 30, 150, 280	Niskin water sampler
St38	28-Sep	74° 11.39 N	167° 33.66 W	247	5, 30, 150, 242	Niskin water sampler
St39	28-Sep	73° 1.75 N	167° 45.52 W	66.3	5, 30, 60	Niskin water sampler
St40	29-Sep	68° 4.54 N	168° 51.93 W	59	5, 30, 52	Niskin water sampler
St41	30-Sep	68° 6.03 N	167° 40.05 W	52.4	5, 30, 47	Niskin water sampler
St42	30-Sep	67° 40.69 N	168° 38.33 W	49.5	5, 30, 44	Niskin water sampler
St43	30-Sep	66° 10.2 N	168° 39.83 W	55	5, 30, 50	Niskin water sampler
St44	1-Oct	65° 0.12 N	169° 4.11 W	49.8	5, 30, 44	Niskin water sampler

(6) Preliminary results

During the cruise, eDNA samples were obtained from a total of 50 stations including 39 stations in the Arctic (Fig. 3.5-4, Table 3.5-5). In the Arctic region, eDNA samples were collected concurrently with the plankton sample. These samples will be the subject of metabarcoding analysis to clarify the reginal differences in species composition and distributional shift of fish in the Arctic. Quantitative PCR (qPCR) will also be used for species-specific detection of eDNA of common Arctic fishes (e.g., salmons, cods, flatfishes) to track their distribution and to estimate their abundance. Integrating the eDNA data and distribution of planktons can describe inter-species network (e.g., food web) and it is expected to reveal the Arctic ecosystem change.

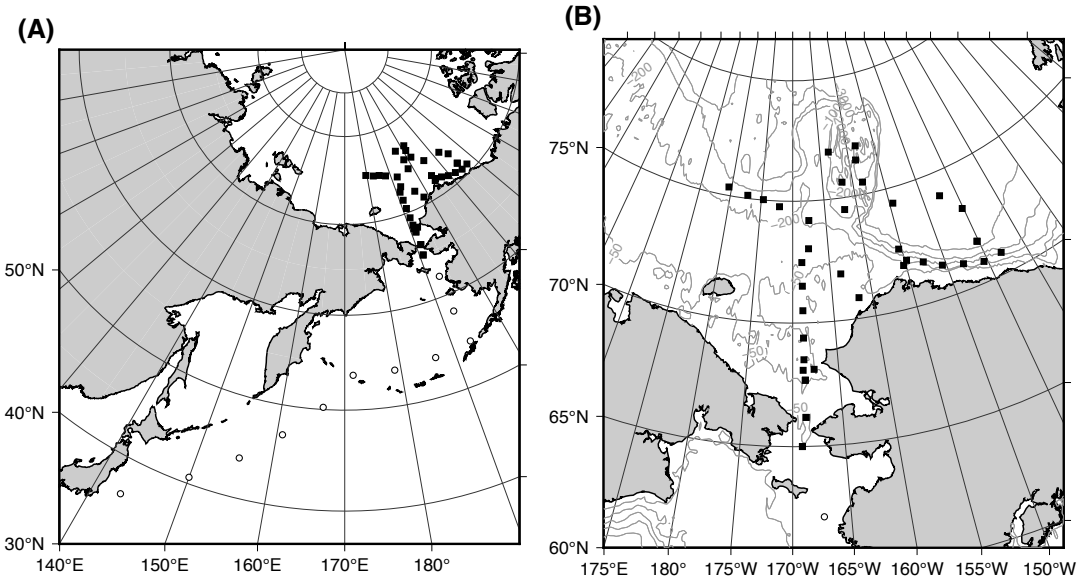

Fig. 3.5-4. Map showing the stations where eDNA samples were collected. (A) Locations of the sampling stations during the whole cruise. (B) Locations of the sampling stations in the Arctic region. eDNA collection was performed using a 0.45 μm pore size cartridge filters (black squares) or a 5 μm syringe filters (white circles).

(7) Data archives

These data obtained in this cruise will be submitted to the Data Management Group of JAMSTEC, and will be opened to the public via “Data Research System for Whole Cruise Information in JAMSTEC (DARWIN)” in JAMSTEC web site.

<http://www.godac.jamstec.go.jp/darwin/e>

3.6 Observation of air-sea-wave-ice interaction over the Pacific Arctic Region

(1) Responsible personnel

Tsubasa Kodaira (Principal Investigator, The University of Tokyo)
Takuji Waseda (The University of Tokyo, not on board)
Takehiko Nose (The University of Tokyo, not on board)
Xingkun Kun (The University of Tokyo, not on board)
Tomotaka Katsuno (The University of Tokyo, not on board)
Masafumi Kimizuka (Tokyo Metropolitan College of Industrial Technology, Tokyo, Japan, not on board)
Yusuke Kawaguchi (The University of Tokyo, not on board)

(2) Purpose, background

The sustained satellite observation since 1979 has revealed a significant reduction in the extent of Arctic sea ice. This reduction signifies the expansion of ice-free open water areas where the wind wave growth can be enhanced. Within the Marginal Ice Zone (MIZ), where the waves and sea ice strongly interact with each other, the distribution of sea ice often exhibits heterogeneity, which leads to interactions among the atmosphere, ocean, waves, and sea ice. The primary objective of our research is to investigate the air-sea-wave-ice interactions to improve the prediction of sea ice distribution within the MIZ and, by extension, improve the forecasting of the Arctic environment. During this research expedition, considerable attention was dedicated to the examination of the roles played by surface waves and oceanic eddies near the sea ice covered areas as well as MIZ.

We deployed multiple drifting-type wave buoys. These buoys were strategically placed to investigate the propagation of ocean surface waves beneath the Arctic sea ice and to observe how these waves develop within areas covered by sea ice under the influence of wind. Anticipated outcomes include the determination of the attenuation rate of surface waves as they traverse beneath the Arctic sea ice and the elucidation of the fetch law within the presence of sea ice.

In addition to wave research, we conducted an intensive deployment of multiple ocean surface drifters near the sea ice to observe and estimate the lateral turbulent diffusion coefficient within the MIZ, focusing on oceanic eddies. Concurrently, we maintained continuous measurements of the atmosphere, ocean, waves, and sea ice through the use of instruments aboard the research vessel R/V Mirai.

The data collected during this expedition also serves a valuable purpose in the evaluation of numerical model predictions concerning waves and ocean currents, thereby advancing

our ability to simulate and forecast the intricate dynamics of the Arctic environment.

(3) Activities (observation, sampling, development)

The following activities are conducted during this cruise.

- Deployments of the drifting wave buoys
- Deployments of the ocean surface drifter with drogue and wave sensor
- Measurements of waves by ship-board instruments
- Visual observation of waves and sea ice
- Measurements of ship motion by ship-board instruments
- Measurements of temperature and salinity vertical profile by XCTD

(4) Methods, instruments

A) Drifting type wave buoy Spotter

Spotter is a compact and solar-powered wave buoy, developed by Sofar Technologies, Inc. Directional wave spectra are estimated onboard and sent via Iridium satellite communication hourly. Statistical wave parameters such as significant wave height, peak wave period, peak wave direction, peak wave directional spread, mean wave period, mean wave direction, mean wave directional spread. Wind speed, and wind direction are also estimated based on the wave spectra. In addition to the wave parameters, GPS location and sea surface temperature are also measured and sent. In this cruise, We have deployed two Spotter wave buoys near the Barrow Canyon and over the Canada Basin, respectively (see, Figure 3.6-4 and Table 3.6-1).

B) Drifting type wave bouy XFZ

XFZ-V2 is a compact and battery-powered wave buoy, developed by our group. Frequency wave spectra are estimated onboard and sent via Iridium satellite communication hourly. Based on the spectra, statistical wave parameters such as significant wave height and mean wave period can be also calculated. GPS locations are also measured and sent. In this cruise, We have deployed seven XFZ wave buoys in the northern part of the Chukchi Sea, near the Barrow Canyon, and near the Chukchi Borderland (see, Figure 3.6-4 and Table 3.6-1).

C) Wave sensing ocean surface Drifter (Wave Drifter)

Wave Drifter is a compact and battery-powered ocean surface drifter, developed by our group. Wave Drifter consists of the surface float and the drogue. The same sensing system with XFZ was installed with a larger amount of battery. One Wave Drifter was deployed near the Mackenzie river mouth, one Wave Drifter was deployed he most west point during

the cruise, and seven Wave Drifter were deployed near sea ice over the Canada Basin (see, Figure 3.6-4 and Table 3.6-1).

D) Microwave wave gauge (JRC)

Microwave wave gauge (SJM-001), produced by Japan Radio Co. Ltd., was installed at the bow of R/V Mirai to obtain a continuous and detailed wave data along the ship trajectory (Figure 3.6-1). The sensor radiates microwave signal to the water surface and receive the reflected signal. Ba sed on the Doppler shift between the transmitted and the reflected microwaves, relative velocity of the water surface is measured and subsequently water surface displacement is estimated. The accelerometer and the gyro sensor are mounted on the sensor and used to remove the signal caused by ship motion. The absolute displacement of the water surface is obtained after the correction. The data is obtained at 10 Hz frequency, and spectral analysis for noise removal is conducted for every 20 minutes record.

Figure 3.6-1 Microwave wave gauge installed at the bow.

E) X-band radar wave analysis system (JRC)

X-band radar wave analysis system (NJZ-1882), produced by Japan Radio Co. Ltd., was installed at the bridge to obtain a continuous and detailed wave data along the ship trajectory (Figure 3.6-2). The signal from X-band radar (MR) installed in R/V Mirai is used for the wave analysis. Bulk wave parameters such as significant wave height, wave period, wave lengeth, and wave direction were calculated and recorded. The calibration data for the wave height were obtained in the previous cruises and they were used in this cruise. Analyzed radar image and two dimensional wave spectra were also recorded.

Figure 3.6-2 X-band wave analysis system installed in the bridge.

F) Inertial Measurement Unit (IMU)

Five IMU based ship motion measurement devices were placed multiple points in R/V Mirai. Three devices are placed near the bow, center, and near the stern along the main axis of R/V Mirai. The other two are placed starboard side and the portside near the center of the ship. The IMU was placed to set the sensor x-axis parallel to the R/V Mirai's ship axis. The IMU measures 3-axis acceleration and 3-axis gyration at 16Hz. The measurement periods were from 20230904 to 20230909, and from 20230916 to 20230929.

G) Network Camera

Two cameras (AXIS M2026-LE Mk II) were installed on the compass deck to record the visual images of the forward direction of the ship and starboard side of the ship, respectively (Figure 3.6-3). They are connected to a recorder (AXIS S3008, 2TB) placed indoor. The resolution of the recorded movie is 1920 x 960 and the frame rate is 30 fps. The measurement periods of the two cameras were from 20230904 to 20231002, and from 20230918 to 20231002, respectively.

Figure 3.6-3 Network cameras installed on the compass deck.

H) XCTD

Vertical profiles of sea water temperature and salinity were measured by XCTD-1 probes manufactured by Tsurumi-Seiki Co. (TSK). The electric signal from the probe was converted by MK-150N (TSK), and was recorded by AL-12B software (Ver.1.1.4, TSK). We launched three probes by using the automatic launcher. The XCTD observation log is shown in Table 3.6-2.

(5) Results

A) Drifting type wave buoys

Preliminary results of trajectories of the deployed drifting buoys and the time series of bulk wave statistics are shown in Figure 3.6-4 and Figure 3.6-5, respectively.

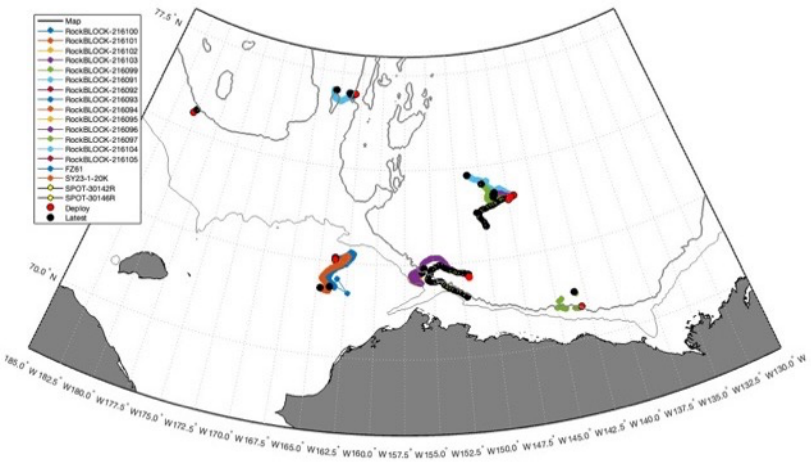

Figure 3.6-4 Map showing trajectories of deployed wave buoys. Points with white edges

indicate the locations where the buoys were deployed.

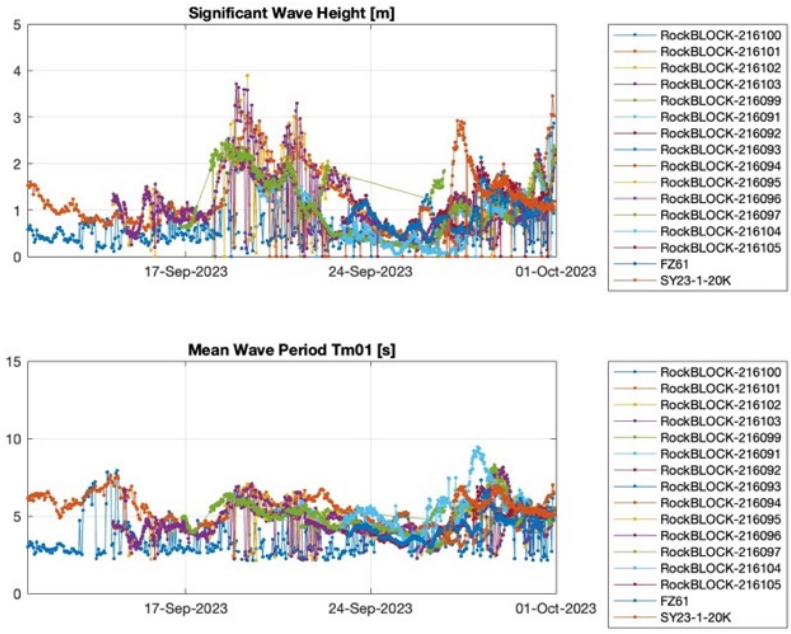

Figure 3.6-5 Timeseries of significant wave height and mean wave period measured by the deployed wave buoys.

B) Microwave wave gauge and X-band radar wave analysis system

Preliminary results of the time series of wave statistics based on the microwave wave gauge and X-band radar wave analysis system are shown in Figure 3.6-6.

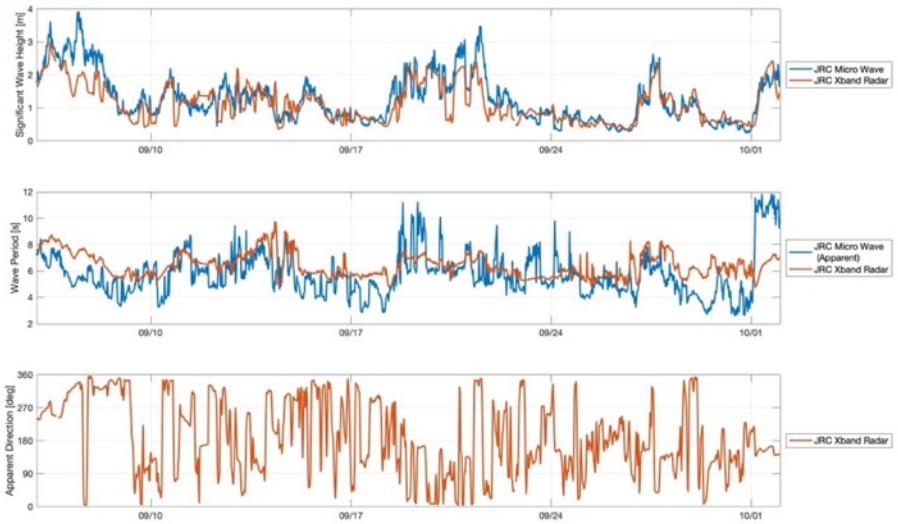

Figure 3.6-6 Timeseries of significant wave height, wave period, and apparent wave direction

measured by Microwave wave gauge and X-band radar wave analysis system on board R/V Mirai.

C) Ship motion

Preliminary results of the sample time series of acceleration for 3 sensor axes, pitch, roll, and heading from the five IMUs installed to R/V Mirai are shown in Figure 3.6-7.

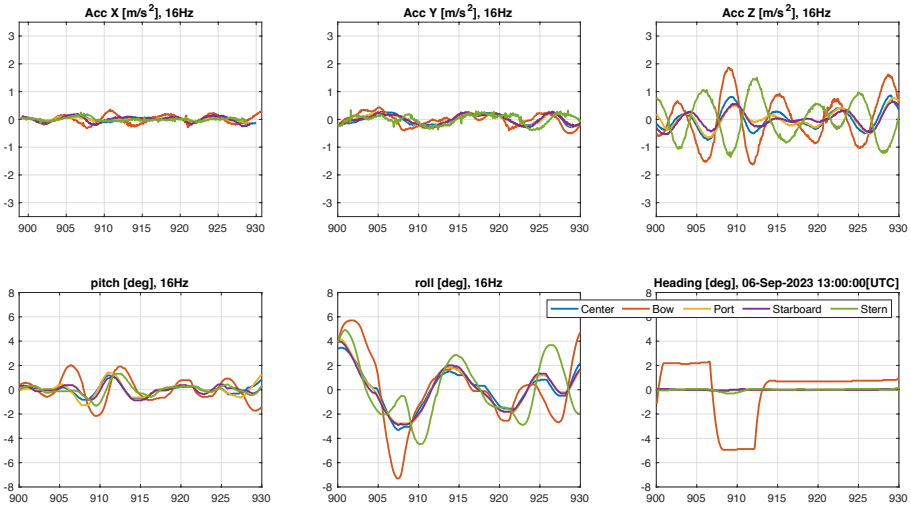

Figure 3.6-7 Sample timeseries of acceleration for 3 sensor axes, pitch, roll, and heading from five IMUs installed to R/V Mirai.

D) Network Camera

Sample pictures of the network cameras are shown in Figure 3.6-8.

Figure 3.6-8 Sample images of the network cameras.

Table 3.6-1: List of drifting buoy deployment locations

Date [YYYY/MM/DD]	Time [hh:mm]	Deployment Position		Drifting Bouy		
		Latitude [deg]	Longitude [deg]	XFZ	Drifter	Spotter
2023/09/11	00:08	72.61579 N	163.64978 W	216100	-	-
2023/09/11	00:38	72.56598 N	163.64536 W	216101	-	-
2023/09/14	05:53	72.10908 N	151.96579 W	-	-	30142R
2023/09/14	05:53	72.10891 N	151.9659 W	216102	-	-
2023/09/14	05:54	72.10874 N	151.966 W	216103	-	-
2023/09/16	20:23	70.85218 N	143.06518 W	-	216099	-
2023/09/18	20:09	74.10204 N	146.93251 W	-	216091	-
2023/09/18	21:02	74.06135 N	147.1797 W	-	216092	-
2023/09/18	21:05	74.06148 N	147.19029 W	-	216093	-
2023/09/18	21:24	74.06013 N	147.18332 W	-	-	30146R
2023/09/18	21:26	74.06193 N	147.18372 W	-	216094	-
2023/09/18	21:27	74.06224 N	147.18376 W	-	216095	-
2023/09/18	21:30	74.06383 N	147.18316 W	-	216096	-
2023/09/18	22:09	74.0186 N	147.45109 W	-	216097	-
2023/09/22	20:52	76.95428 N	163.43686 W	216104	-	-
2023/09/22	22:10	76.94906 N	163.36464 W	216105	-	-
2023/09/23	02:10	76.53664 N	158.65906 W	213458	-	-

2023/09/26	18:10	75.46714 N	180.37368 E	-	210405	-

Table 3.6-2: List of XCTD measurements

Station No.	Date [YYYY/MM/DD]	Time [hh:mm]	Latitude [deg]	Longitude [deg]	Depth [m]
WaveBuoy1	2023/09/11	00:14	72-36.7486 N	163-38.6729 W	53
X040	2023/09/18	20:03	74-06.2133 N	146-55.0620 W	3767
X041	2023/09/18	21:27	74-03.7403 N	147-11.0261 W	3772

(6) Data archives

These data obtained in this cruise will be submitted to the Data Management Group (DMG) of JAMSTEC, and will be opened to the public via “Data Research System for Whole Cruise Information in JAMSTEC (DARWIN)” in JAMSTEC web site.

http://www.godac.jamstec.go.jp/darwin/e

3.7 Investigating the physical and ecophysiological basis of fall phytoplankton blooms in the Chukchi and Beaufort seas

(1) Responsible personnel

Colin Kremer (University of Connecticut) – Principal Investigator, Not on board

Hannah Larson (University of Connecticut)

Atsushi Matsuoka (University of New Hampshire) – Not on board

(2) Objectives

- Examine the effects of biotic and abiotic stressors on natural phytoplankton communities
- Expand Arctic phytoplankton community data and increase Arctic strains in culture collections
- Ground-truth bio-optical properties to support remote sensing models of the Pacific Arctic Ocean

(3) Activities

(3-1) Mesocosm incubation studying the effects of biotic and abiotic stressors on phytoplankton community

(3-1a) Instruments and Methods

Mesocosm experiments were conducted twice with seawater sampled from 10m depth at Stations 3 (Mesocosm 1) and 28 (Mesocosm 2), representing a southern highly productive entrance to the Western Arctic Ocean and a northern region of low productivity, respectively. 130 L seawater was filtered through 200μm nylon mesh to remove larger debris and zooplankton and homogenized into two 50L carboy and two 20L containers, later combined in a 50L carboy. Each 50L container had 2L subsampled for DNA analysis and was then further divided into eight 5L polyethylene cubes, creating a total of 24 containers. Eight treatments in triplicate were created representing a factorial study of three factors: High Temperature (HT) versus Low, or in-situ, Temperature (LT); High Light (HL) versus Low Light (LL); and Present Invader (PI) versus Absent Invader (AI).

Upon subdividing into 5L containers, each cube was supplemented with additional nutrients to ensure that phytoplankton growth was not nutrient limited over the course of the experiment. Cubes undergoing the invasion treatment received an additional inoculation of southern phytoplankton imitating the invasion of new species. *Emiliania huxleyi* (NCMA1742), also known as E. hux, was inoculated in Mesocosm 1 and a mixed community from Mesocosm 1 likely containing both southern Arctic phytoplankton and E. hux was inoculated into Mesocosm 2.

Incubation tanks were set up on deck to manipulate both temperature and light. One incubation tank was set to the in-situ temperature of the collected water (6C and 2C,

respectively) while the other tank was maintained at an increased temperature (13C and 7C, respectively). Each incubation tank had two HOBO loggers installed on the surface of the water to measure light and temperature levels every 15 minutes throughout the entire study.
The temperature controlled incubation tanks on deck experienced additional stress when ambient temperatures became too warm or went below 0C, causing them to occasionally deviate from desired temperature. The temperature controlling system experienced challenges throughout the experiment, resulting in highly fluctuating temperatures and a period of time in the first experiment when the temperatures in both tanks reached unhealthy levels for phytoplankton survival, reaching as high as 19C warmer than the set temperature.
Each incubation tank was covered in shade cloth reducing light in the tanks to ~45% of ambient light. Half of each tank was further reduced by an additional layer of shade cloth, letting in ~10% of ambient light. HOBO loggers were positioned in each incubation tank such that each logger recorded either the High Light or Low Light conditions within the same temperature tank.
Mesocosms were incubated for 9 days and periodically sampled for fluorescence and community composition. Raw fluorescence values were read every day for each cube and processed with a fluoremeter (10-AU, TURNER DESIGNS). Samples for measuring community composition were collected periodically throughout incubations and preserved with glutaraldehyde for later taxonomic identification and enumeration. At the culmination of each incubation experiment, each cube was also sampled to preserve DNA and to make live culture collections. DNA was collected on a 0.22µm MCE (mixed cellulose esters) membrane and stored in -80C for later 16s and 18s analysis. Treatments showing phytoplankton growth were sampled for later cell isolation in order to create and maintain live culture collections (allowing us to subsequently study species growing in the experiments in the laboratory). Sampling frequencies for each parameter for each incubation are listed below.

Table 3.7-1– 1: Frequency of sampling for different measures collected during Mesocosm 1, using water collection from Station 3. DNA samples from Day 0 were only collected from the 50L homogenized containers, not individual cubes.

Day	0	1	2	3	4	5	6	7	8	9
Fluorescence	o	o	o	o	o	o	o	o	o	o
Community Composition	o		o		o					o
DNA	o*									o
Live Water										o

Table 3.7-1–2: Sampling frequency of different parameters sampled during Mesocosm 2, using water collection from Station 28. DNA sample from Day 0 was only collected from 50L homogenized containers, not individual cubes.

Day	0	1	2	3	4	5	6	7	8	9
Fluorescence	o	o	o	o	o	o	o	o	o	o
Community Composition	o		o			o				o
DNA	o*									o
Live Water										o

(3-1b) Preliminary Results and Future Plans

Changes in raw fluorescence over the course of the nine day incubation show a qualitative difference in phytoplankton growth between different treatments. Robust statistical analyses have not yet been conducted. We present Figures 3.7-1 and 3.7-2 as preliminary results from the two mesocosm experiments.

Community composition and DNA samples will be analyzed to determine success and/or effects of the invasion treatments as well as which other resident species grew well under different biotic and abiotic conditions.

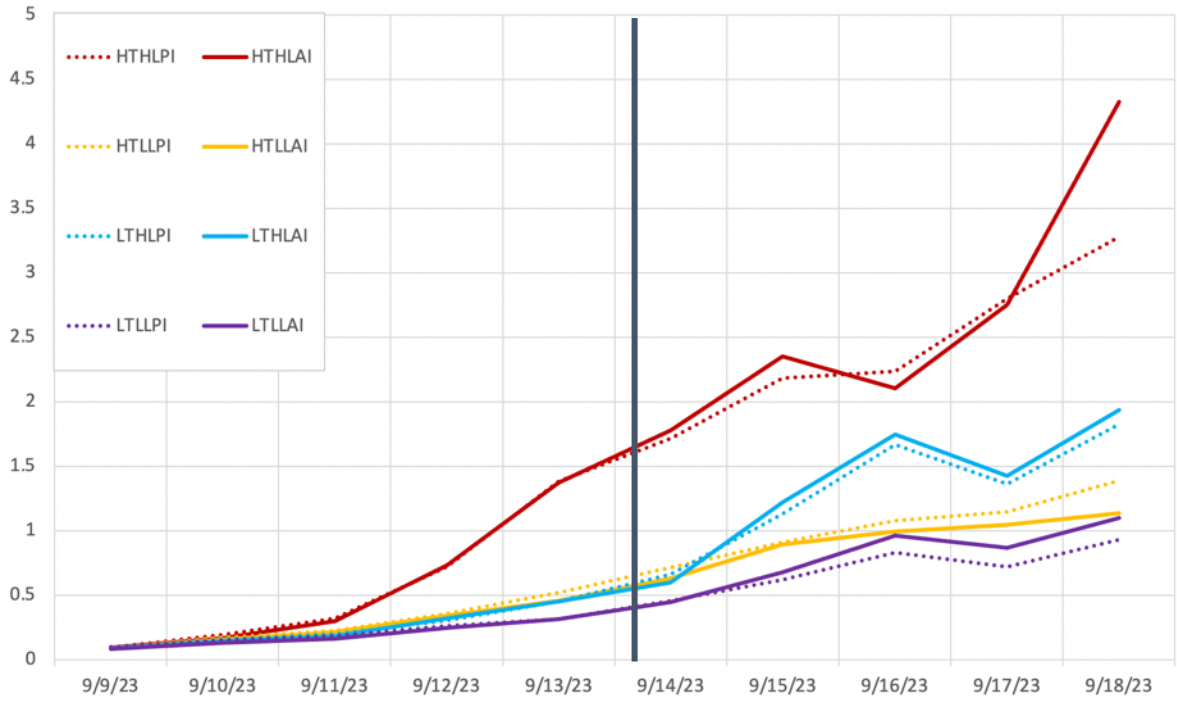

Figure 3.7-1: Raw fluorescence for each of the eight treatments, averaged over three replicates, from Mesocosm 1. A vertical gray line marks where temperature conditions for the incubation

tanks stopped approximating the desired temperatures.

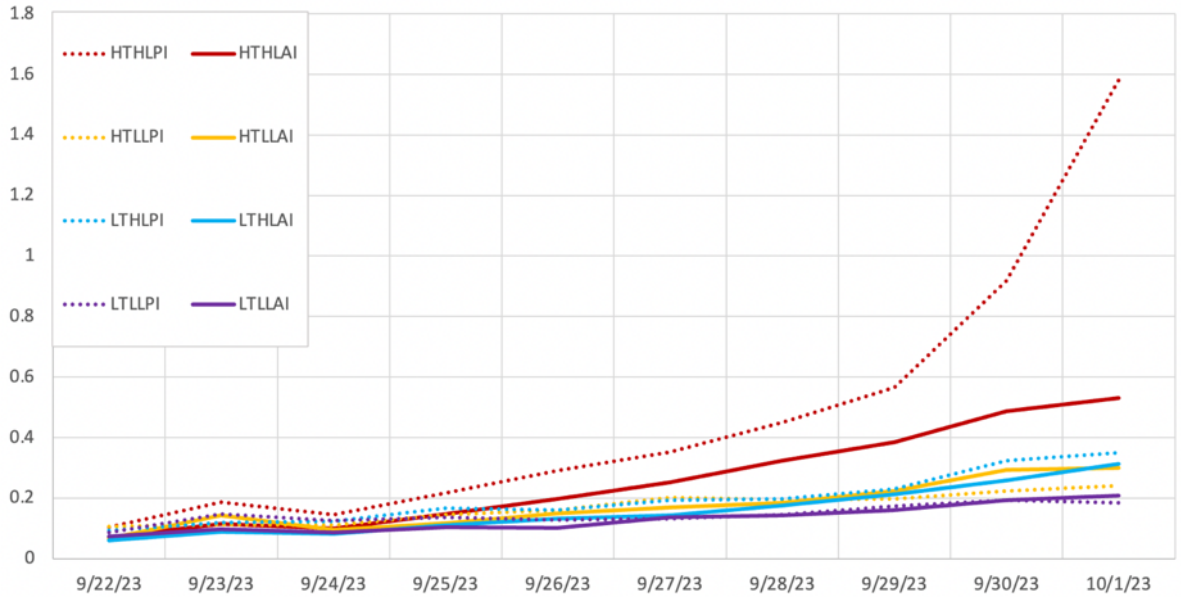

Figure 3.7-2: Raw fluorescence for each of the eight treatments, averaged over three replicates, from Mesocosm 2.

We present the below temperature plots for each of the two incubation experiments as additional explanation for some of the trends observed in the fluorescence plots. Environmental data plots for Mesocosm 1 temperature (Fig. 3.7-3) and light (Fig. 3.7-4) are presented below to demonstrate changes in temperature over the course of the experiment and day/night light cycles. Environmental data plots for Mesocosm 2 temperature (Fig. 3.7-5) and light (3.7-6) are similarly presented, with more daily fluctuations in temperature but shallower temperature changes overall.

Figure 3.7.3-1b – 3: Temperature data for Mesocosm 1. The High Temp tank temperature controller was set to 12C and Low Temp was set at 6C.

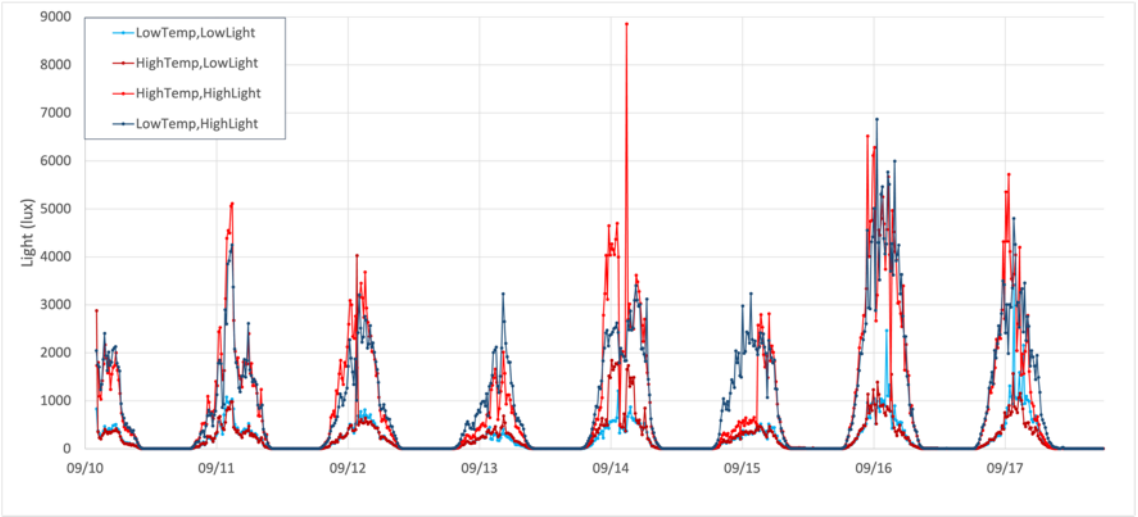

Figure 3.7-3: Light data for Mesocosm 1.

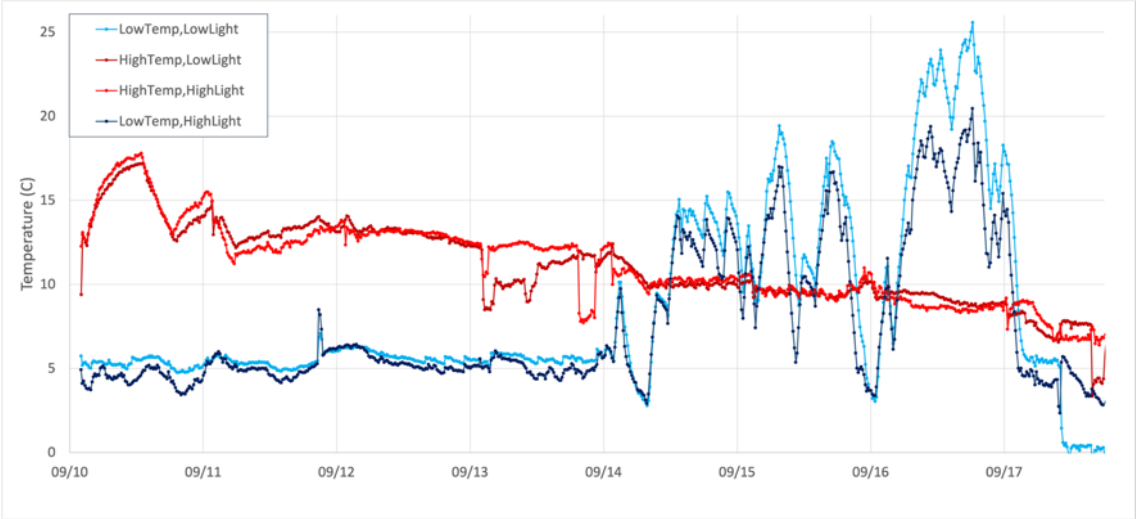

Figure 3.7-4: Temperature data for Mesocosm 1. The High Temp tank temperature controller was set to 8˚C and low temp was set to 2˚C.

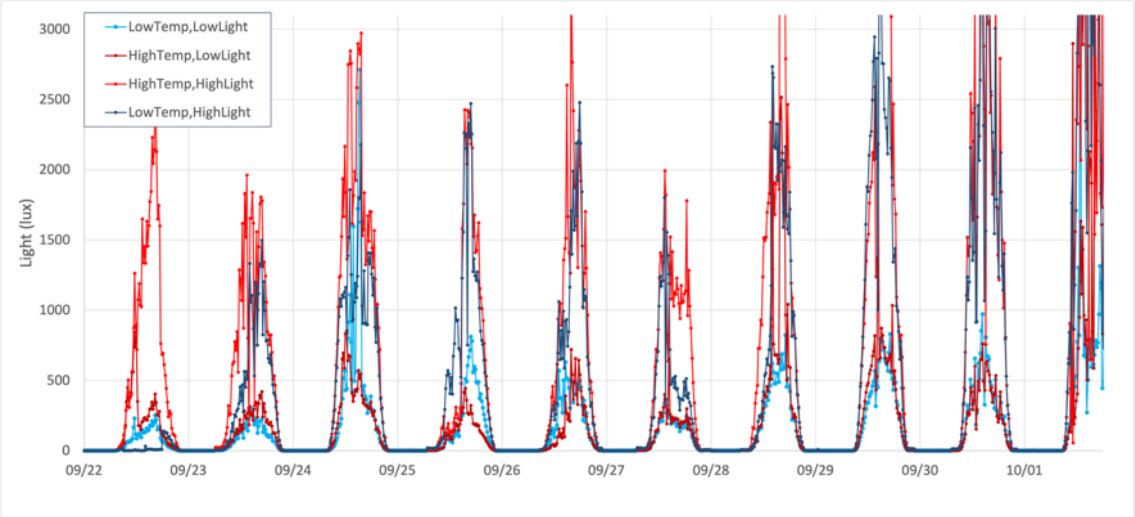

Figure 3.7-5: Light data for Mesocosm 2.

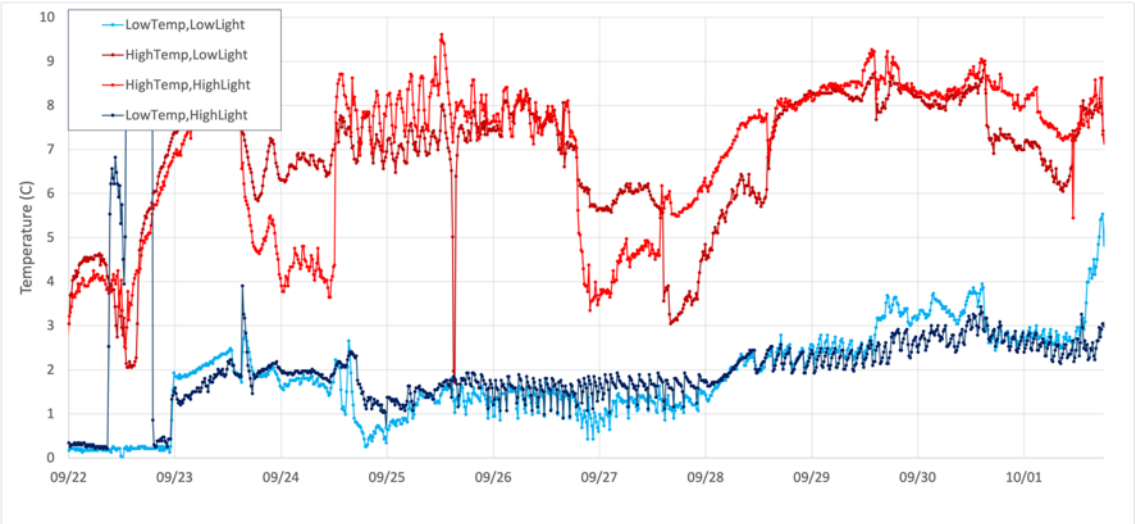

Figure 3.7-6: Temperature data for Mesocosm 2.

(3-2) Bio-optical property assessment

(3-2a) Instruments and Methods

At 12 sites, water samples were collected at SCM (subsurface chlorophyll a maximum), 10m, and either 5m or surface, using a bucket (surface samples) and Niskin water sampler. Collected water was used to take samples of POC (particulate organic carbon), SPM (suspended particulate matter), eDNA, and preserved in glutaraldehyde for later study of community composition, according to the following methods:

- 4L were collected each for POC (particulate organic carbon) and SPM (suspended particulate matter). Samples were filtered onto pre-combusted and pre-weighed (SPM only) GF/F filters. Between 1.5 and 4L of water was filtered for each sample, based on

how much water could be filtered while keeping the filter intact and within a reasonable amount of time (<~12 hours). Filters were dried in a drying oven at 55C for >1hr and stored at room temperature for later analysis.

- 2L of water was filtered on a 0.22µm MCE (mixed cellulose esters) membrane and stored in -80C for later 16s and 18s analysis.
- 40ml was filtered through a 300µm mesh filter and preserved with glutaraldehyde for later taxonomy and enumeration via laboratory flow cam.

(3-2b) Results and Future Plans

Filters and preserved samples were transported back to a lab for future analysis and will be used to support phytoplankton components in future ecosystem models.

(3-3) Phytoplankton collection for live culturing

At 12 sites, water samples were collected at SCM (subsurface chlorophyll a maximum), 10m, and either 5m or surface, using a bucket (surface samples) and Niskin water sampler. 150ml of water was filtered through a a 300µm mesh filter and stored under cool, illuminated conditions to promote phytoplankton survival and growth. These water samples were then transported back to a lab where individual cells could be isolated into growth media via methods of serial dilution and individual cell picking. We will use a combination of taxonomic identification and genomics to identify different species. These unialgal strains will be maintained in the lab for future laboratory studies of Arctic phytoplankton ecophysiology. We have maintained 261 unialgal stains including many diatom and upwards of 35 possible species.

(4) Sampling List and Map

Table 3.7-2: Bio-optical samples collected at various sampling stations. *5m at St 38 was only sampled for POC

Bio-optical properties						
St.	Date (UTC)	Latitude	Longitude	Sampling depth (m)	SPM water filtered at each depth (L)	POC water filtered at each depth (L)
1	7-Sep	65-0.04 N	169-4.78 W	surface, 10, SCM	1,1.5,1.65	4,4,4
6	9-Sep	70-30.03 N	168-45.33 W	surface, 10, SCM	1.5,1.5,2.3	4,3,3
10	11-Sep	70-50.47 N	161-43 W	5, 10, SCM	4,4,3.5	3,4,3
11	12-Sep	71-39.6 N	155-1.31 W	5, 10, SCM	1.8,2,3.5	1.5,2.1,3.5
20	16-Sep	70-50.88 N	143-3.51 W	5, 10, SCM	4,4,4^	4^,4,4^
23	18-Sep	74-1.14 N	147-26.86 W	5, 10, SCM	4,4,5.5	4,4,4
31	22-Sep	76-57.18 N	163-26.8 W	5, 10, SCM	4,4,4	4,3.3,4
34	25-Sep	74-45.98 N	172-3.76 W	5, 10, SCM	4,4,4	4,4,4
36	26-Sep	75-21.05 N	179-32.11 E	10, SCM	4,4	4,4
38	28-Sep	74-11.39 N	167-33.66 W	5*, 10, SCM	4,4	4,4,4
41	30-Sep	68-6.03 N	167-40.05 W	5, 10, SCM	2.25,3,4	2,2.75,4
42	30-Sep	67-40.69 N	168-38.33 W	5, 10, SCM	3,3,3	2.3,3,3

Table 3.7-3: Parameters of phytoplankton composition collected at different sampling stations

Phytoplankton community parameters					
St.	Date (UTC)	Latitude	Longitude	Sampling depth (m)	Parameters sampled
1	7-Sep	65-0.04 N	169-4.78 W	surface, 10, SCM	eDNA, flow cam, live water
3	8-Sep	67-39.42 N	168-39.95 W	5, 10, SCM	eDNA, flow cam, live water
6	9-Sep	70-30.03 N	168-45.33 W	surface, 10, SCM	eDNA, flow cam, live water
10	11-Sep	70-50.47 N	161-43 W	5, 10, SCM	eDNA, flow cam, live water
11	12-Sep	71-39.6 N	155-1.31 W	5, 10, SCM	eDNA, flow cam, live water
14	13-Sep	72-28.34 N	155-24.34 W	5, 10, SCM	eDNA, flow cam, live water
18	15-Sep	7103.89 N	147.56.56 W	SCM	live water
20	16-Sep	70-50.88 N	143-3.51 W	5, 10, SCM	eDNA, flow cam, live water
23	18-Sep	74-1.14 N	147-26.86 W	5, 10, SCM	eDNA, flow cam, live water
31	22-Sep	76-57.18 N	163-26.8 W	5, 10, SCM	eDNA, flow cam
34	25-Sep	74-45.98 N	172-3.76 W	5, 10, SCM	eDNA, flow cam
36	26-Sep	75-21.05 N	179-32.11 E	10, SCM	eDNA, flow cam
38	28-Sep	74-11.39 N	167-33.66 W	5, 10, SCM	eDNA, flow cam, live water
41	30-Sep	68-6.03 N	167-40.05 W	5, 10, SCM	eDNA, flow cam, live water
42	30-Sep	67-40.69 N	168-38.33 W	5, 10, SCM	eDNA, flow cam, live water

(5) Results and Future Plans

We present a map of sampling locations as preliminary results. We will finish processing the remaining DNA, phytoplankton community, and bio-optical property samples brought back to the lab. The SPM and POC samples will be used to inform remote sensing models of phytoplankton and primary production in the Arctic. Our goal is also to use many of the new unialgal phytoplankton strains to conduct further lab-based studies on the effects of various biotic and abiotic stressors on population and community dynamics of different Arctic phytoplankton. We will use fluorescence results from the mesocosm experiment in conjunction with community compositional data (to be analyzed from preserved samples) to prepare a publication on the effects of biotic and abiotic stressors on Arctic phytoplankton communities.

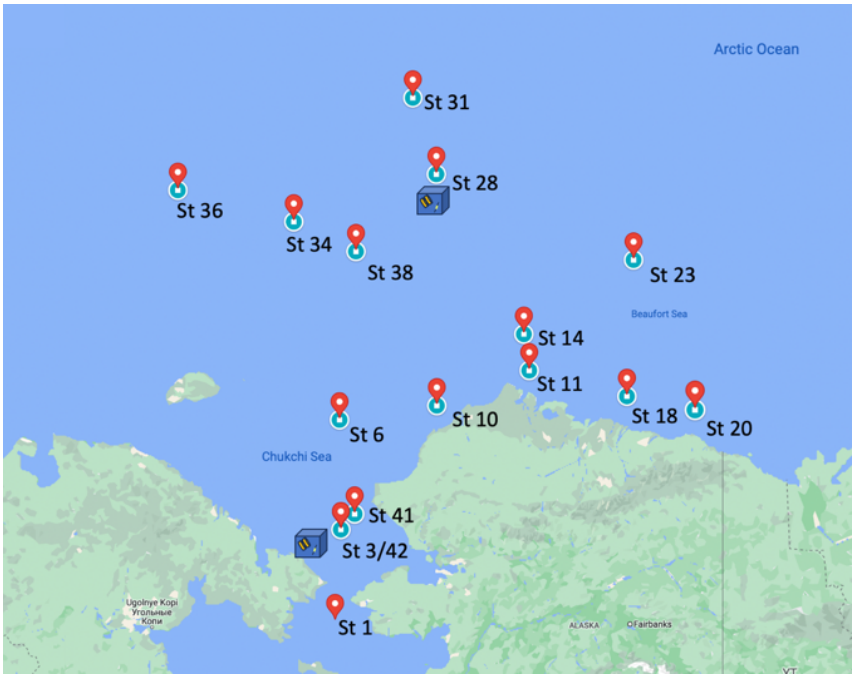

Figure 3.7-7: Location of bio-optical property and phytoplankton community sampling locations (red circles) as well as mesocosm incubation starting points (blue boxes).

(6) Data archives

These data obtained in this cruise will be submitted to the Data Management Group (DMG) of JAMSTEC, and will be opened to the public via “Data Research System for Whole Cruise Information in JAMSTEC (DARWIN)” in JAMSTEC web site.

http://www.godac.jamstec.go.jp/darwin/e

3.8 Nitrogen Fixation in a Changing Arctic Ocean: An Overlooked Source of Nitrogen?

(1) Responsible personnel:

Lisa Winberg von Friesen (University of Copenhagen) -PI, onboard
Stine Zander Hagen (University of Copenhagen), onboard
Lasse Riemann (University of Copenhagen), not onboard
Takuhei Shiozaki (The University of Tokyo), not onboard

(2) Purpose, background

During the last 50 years, the Arctic has warmed more than twice as much as the rest of the world. The continuous thinning and retraction of sea ice increases light availability, which has pronounced effects on primary production potential in the Arctic Ocean, but with nutrient availability - in particular nitrogen (N) – as a key determinant. In fact, the extent of nitrogen limitation in the Arctic Ocean is predicted to regionally intensify. Nitrogen will thus be an increasingly important regulator of primary production in the new Arctic. Accurate determination of sources of nitrogen to the Arctic Ocean is, therefore, a critical prerequisite for predictions of primary production and carbon sequestration in the Arctic Ocean during the era of climate change.

The scientific goals of this project are to quantify biological nitrogen fixation in the Beaufort, Chukchi, and northern Bering seas, and address how dissolved and particulate organic matter (DOM and POM) influence (photo)heterotrophic nitrogen fixation. Arctic regions are under-sampled for nitrogen fixation, the local environmental regulation of nitrogen fixation in the Pacific Arctic unknown, and prediction of future nitrogen biogeochemistry in this part of the Arctic ocean is speculative (Shiozaki et al., 2017; Sipler et al., 2017; von Friesen and Riemann, 2020).

(3) Activities (observation, sampling, development)

In total 34 stations were sampled (standard depths: 5, 20, 50, 100, 500, B-5 m). At 34 of those stations a vertical profile of DNA and RNA was collected. At 16 stations a vertical profile of nitrogen fixation and primary production rates was collected through 24 h bottle incubations with stable isotope tracers. At 32 stations DOC amendment and POM removal experiments were performed to investigate its impact on nitrogen fixation. At two locations (Chukchi and Bering shelf) sediment resuspension experiments were performed. Three stations in the Bering Strait area were sampled twice with approximately three weeks in between.

(4) Methods, instruments

The objective is to quantify nitrogen fixation and to identify the active diazotrophs and their regulation. nitrogen fixation and primary production are determined using $^{15}N_2$ and $NaH^{13}CO_3$ incorporation, respectively. Present and active diazotrophs are identified using *nifH* amplicon Illumina sequencing of bulk DNA. Experiments were carried out onboard to determine the relative importance of cyanobacterial and heterotrophic nitrogen fixation and evaluate the regulating role of DOM and POM. Water from different water masses were exposed to a range of different DOM amendments to determine potential carbon limitation of nitrogen fixation for heterotrophic or photoheterotrophic diazotrophs, respectively. Water from 5, 20, 50, 100, 500 and/or B-5 was incubated for 24 h in an on-deck water tank with continuously flowing surface water to mimic in situ temperatures. Bottles were individually shaded depending on the depth of origin. Additionally, pilot experiments of the influence by sediment resuspension on nitrogen fixation at Arctic shallow shelves were carried out.

Parameters: DNA, RNA, bacterial abundance, nitrogen fixation, primary production, dissolved organic carbon (DOC), coloured dissolved organic matter (cDOM), lignin

(5) Future Plans

Samples will be processed at the University of Copenhagen, Technological University of Denmark and Tokyo University during 2023-2024. Participation in this cruise was funded through the early career researcher call of JAMSTEC 2022.

(6) References

Shiozaki, T., Fujiwara, A., Ijichi, M., Harada, N., Nishino, S., Nishi, S., et al. (2018). Diazotroph community structure and the role of nitrogen fixation in the nitrogen cycle in the Chukchi Sea (western Arctic Ocean). Limnology and Oceanography, 63(5), 2191–2205. https://doi.org/10.1002/lno.10933

Sipler, R. E., Baer, S. E., Connelly, T. L., Frischer, M. E., Roberts, Q. N., Yager, P. L., & Bronk, D. A. (2017). Chemical and photophysiological impact of terrestrially‐derived dissolved organic matter on nitrate uptake in the coastal western Arctic. Limnology and Oceanography, 62(5), 1881–1894. https://doi.org/10.1002/lno.10541

Von Friesen, L. W., & Riemann, L. (2020). Nitrogen Fixation in a Changing Arctic Ocean: An Overlooked Source of Nitrogen? Frontiers in Microbiology, 11, 596426. https://doi.org/10.3389/fmicb.2020.596426

(7) Data archives

These data obtained in this cruise will be submitted to the Data Management Group (DMG)

of JAMSTEC, and will be opened to the public via “Data Research System for Whole Cruise Information in JAMSTEC (DARWIN)” in JAMSTEC web site.
http://www.godac.jamstec.go.jp/darwin/e

3.9. Exploring microplankton interactions and their functional roles in a changing Arctic

(1) Personnel:

Eva Lopes (Faculty of Sciences of University of Porto, Interdisciplinary Centre of Marine and Environmental Research, onboard) -PI,

(2) Background/Purpose

Analysing the change in the redistribution of plankton microbial communities and their functions within the changing Arctic Ocean will be of great relevance since they form a web of highly diverse species and functions that quickly react to change, dictating shifts on ocean primary production and consequently on ecosystem sustainability. This campaign will represent a step forward in generating new knowledge regarding microplankton responses to already demonstrated climate change driving forces in one of the most difficult regions to sample. During this campaign, the Arctic Ocean prokaryotic and unicellular eukaryotic communities will be analysed from a community dynamics and ecological perspective. First by understanding how planktonic prokaryotic and unicellular eukaryotic communities interplay with each other and secondly by investigating the dynamics between viruses and their microplankton hosts. The main goals of this campaign are:

1. Discover the key interconnections (taxonomical and functional) between prokaryotic and unicellular eukaryotic communities in the Arctic Ocean, by studying its dynamic interaction in field surveys.
2. Understand the influence of viruses in controlling the taxonomic and functional (N cycle pathways) interactions between the prokaryotes and unicellular eukaryotic communities.
3. Evaluate the environmental differences between the Pacific and Arctic water masses (focusing mainly on temperature and nitrogen availability) and its influence on the interactive dynamics between planktonic prokaryotes, unicellular eukaryotes, and viruses.

(3) Parameters

Genomics (microbial DNA)

(4) Instruments and Methods

In order to analyse the marine microbial communities, seawater samples were collected across the Pacific-Arctic Ocean, with some specific locations. Such as the Bering Strait, Chucki Sea, Barrow Canyon, and Canada Basin (Table 3.9-1). Two different depth layers were used on board: Surface Chlorophyll Maximum (SCM; n = 58) and Bottom (n = 58). The Bottom layer was defined as being 5 m (B-5) or 10 m (B-10) above the sea floor, depending on the station depth.

Table 3.9-3. Geospatial description of samples collected onboard R/V Mirai (SCM: Surface Chlorophyll Maximum).

Station	CAST	Latitude	Longitude	Sampling Day	Collection Instrument	Depth Classification
S01	1	65.0006	-169.081	07/09/2023	Niskin Bottle	Bottom; SCM
S02	1	66.1697	-168.667	07/09/2023	Niskin Bottle	Bottom; SCM
S03	2	67.6649	-168.665	08/09/2023	Niskin Bottle	Bottom; SCM
S03		67.6649	-168.665	08/09/2023	Ashura	Bottom
S04	1	68.5017	-168.751	08/09/2023	Niskin Bottle	Bottom; SCM
S05	1	69.5001	-168.749	08/09/2023	Niskin Bottle	Bottom; SCM
S05		69.5001	-168.749	08/09/2023	Ashura	Bottom
S06	1	70.5007	-168.755	09/09/2023	Niskin Bottle	Bottom; SCM
S08	1	72.5001	-168.751	09/09/2023	Niskin Bottle	Bottom; SCM
S09		71.9005	-163.642	10/09/2023	Ashura	Bottom
S10	1	70.8415	-161.716	11/09/2023	Niskin Bottle	Bottom; SCM
S10		70.8415	-161.716	11/09/2023	Ashura	Bottom
S11		71.6597	-155.021	12/09/2023	Ashura	Bottom
S13	1	71.735	-155.199	12/09/2023	Niskin Bottle	Atlantic Water; Remnant Winter Water
S14	2	72.4678	-155.398	13/09/2023	Niskin Bottle	Bottom; SCM
S15	1	71.9393	-154.773	14/06/2023	Niskin Bottle	Bottom; SCM
S16	1	71.6902	-152.716	14/06/2023	Niskin Bottle	Bottom; SCM
S18	1	71.0652	-147.941	15/09/2023	Niskin Bottle	Bottom; SCM
S20	2	70.849	-143.054	15/09/2023	Niskin Bottle	Bottom; SCM
S22	1	73.1662	-145.164	17/09/2023	Niskin Bottle	Bottom; SCM
S23	1	74.0138	-147.462	18/09/2023	Niskin Bottle	Bottom; SCM
S25	1	74.3599	-154.501	19/09/2023	Niskin Bottle	Bottom; SCM
S27	1	75.5	-158.377	20/09/2023	Niskin Bottle	Bottom; SCM

S29	2	77.0363	-158.374	21/09/2023	Niskin Bottle	Bottom; SCM
S30	1	76.4597	-158.822	21/09/2023	Niskin Bottle	Bottom; SCM
S31	2	76.9505	-163.31	22/09/2023	Niskin Bottle	Bottom; SCM
S32	2	74.5155	-162.029	23/09/2023	Niskin Bottle	Bottom; SCM
S34	1	74.7669	-172.063	25/09/2023	Niskin Bottle	Bottom; SCM
S36	1	75.3285	179.4858	26/09/2023	Niskin Bottle	Bottom; SCM
S37	1	75.0182	-174.676	27/09/2023	Niskin Bottle	Bottom; SCM
S38	1	74.1797	-167.51	27/09/2023	Niskin Bottle	Bottom; SCM
S39	1	73.0285	-167.758	28/09/2023	Niskin Bottle	Bottom; SCM
S39		73.0285	-167.758	28/09/2023	Ashura	Bottom
S40	1	68.0756	-168.867	29/09/2023	Niskin Bottle	Bottom; SCM
S40		68.0756	-168.867	29/09/2023	Ashura	Bottom
S41	1	68.1	-167.667	29/09/2023	Niskin Bottle	Bottom; SCM
S43	1	66.17	-168.664	30/09/2023	Niskin Bottle	Bottom; SCM
S44		66.17	-168.664	30/09/2023	Ashura	Bottom

Along the cruise, seawater samples were collected using 12 L Niskin bottles on a CTD/Rosette multi-sampler, between the 7th and 30th of September 2023. Every water sample was collected on a 10 L plastic and foldable container and rinsed three times. Regarding the filtration, a peristaltic pump (JIHUMP; BT-100CA) was used. To prevent contamination, the filtration tubes were cleaned with 2 L of sample water. The seawater samples, were then, filtered through a 0.22 µm pore size Sterivex filter (SVGV010RS, Merck Millipore, Portugal). Each station and each depth had duplicated samples. Filtration was stopped when the water volume was finished or when the Sterivex filters were strongly clogged. Once the filtration was complete, the filters were stored on board at -80 °C, until further genomic (16S and 18S) and metagenomic analysis. These samples were collected with the purpose of observing the dynamics of the microbial communities across the water column in the Arctic Ocean.

In the Barrow Canyon area, a microcosmos experiment was performed, where the Pacification phenomenon was reproduced. The aim was to mix surface waters, collected at 100m, with bottom waters, collected at 300m. The aim is to analyse which interactions between the communities change during the period of 48 hours of incubation. Water collected at 100m was classified as "Remnant Winter Water" and water collected at 300m was classified as "Atlantic Water". The seawater samples, were then, filtered through a 0.2 µM polycarbonate membrane filter (Merck Millipore, Portugal). When the filtration was finished, 4 mL of DNA/RNA Shield was added to the cryotube where the filter was. The samples were stored on board at -80 °C. For each sample, a respective nutrient sample was also taken and stored on board at -20 °C. The main intention of this experiment was to observe how the microbial communities will change due to the progressive intensification of the Pacific and Arctic water connectivity, considering the heat transport.

Across the Chukchi Sea line, opportunistic sampling occurred. Sediment samples were collected from a multiple core sampler, Ashura, and the joint water was filtered through a 0.22 µm pore size Sterivex filter (SVGV010RS, Merck Millipore, Portugal). A total of fourteen samples were collected and stored on board at -80 °C, until further genomic and metagenomic analysis. These samples were collected with the purpose of comparing the microbial communities differences between the sediments and water, with a special focus on diatoms.

(6) Preliminary results

During this cruise, genomics samples were collected from a total of thirty-three stations (Fig. 3.9-1). These samples will be the subject of genomic (16S and 18S) and metagenomic analyses, to understand how prokaryotes and unicellular eukaryotes interact between with each other, and

eventually, how virus influences these communities. A comparison between the microbial communities of the Pacific-Arctic and Atlantic-Arctic will also be performed.

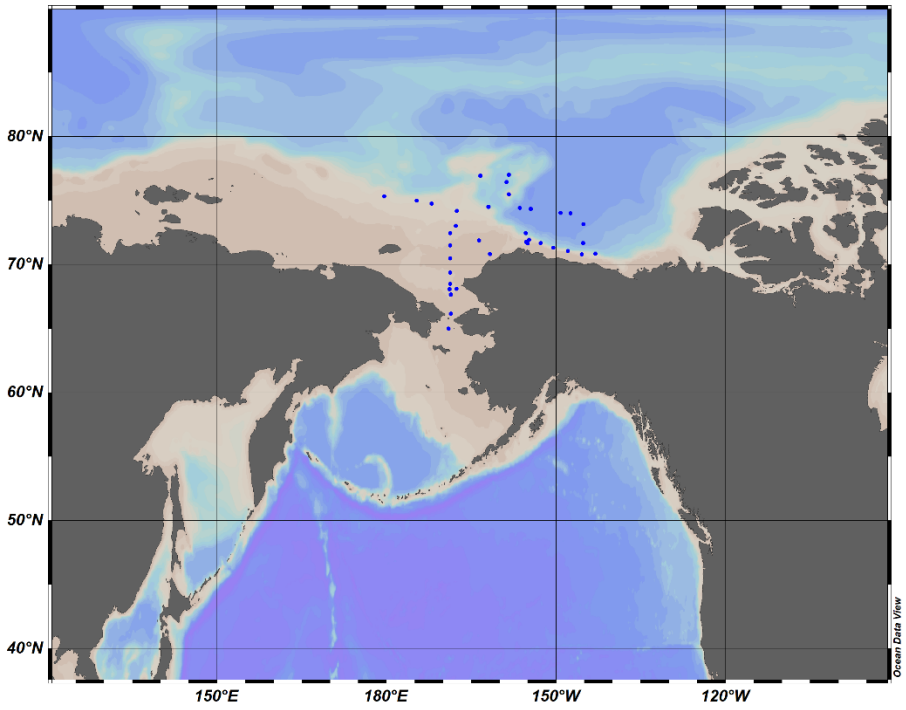

Figure 3.9-9: Map of the sampling area and sampling sites.

(7) Data archives

The data obtained in this cruise will be submitted to the Data Management Group of JAMSTEC and will be opened to the public via the “Data Research System for Whole Cruise Information in JAMSTEC (DARWIN)” on the JAMSTEC website.

3.10. Determining the contribution of siphonophores to mesopelagic backscatter in the Arctic

(1) Responsible personnel

Alix Rommel (Scottish Ocean Institute, University of St Andrews) -PI on board

Andrew Brierley (Scottish Ocean Institute, University of St Andrews), not on board

(2) Purpose and background

The scientific purpose of this proposal is to investigate the deep scattering layer (DSL) in the Arctic using underway acoustic data in concert with paired observations from a lowered echosounder and stereo camera. This will provide invaluable insights into the gelatinous community of the Arctic, a woefully under-sampled group (Proud et al., 2019), and eventually lead to more accurate fish biomass estimates. As well as providing new acoustic data, this research will also potentially yield important results regarding the Arctic Ocean in a changing climate. Inhabitants of the mesopelagic zone provide many ecosystem services (St. John et al., 2016): Many members of the mesopelagic community partake in dial vertical migration, spending the day at depths and ascending to the surface at night. Through this migration, the mesopelagic community plays an important role in the biogeochemical cycling processes of the earth, including the biological carbon pump. Though the idea of using lowered echosounders in conjunction with cameras to study the organisms inhabiting the DSL and their target strengths is not new (Backus & Barnes, 1957), it has only relatively recently been possible to implement this method successfully (Ermolchev & Zaferman, 2003; Thorvaldsen, 2018). This method enables the use of higher frequencies at short range (high-frequency observations from ship-mounted echosounder are not possible because high frequency sound is attenuated rapidly by sea water (Simmonds et al., 2005)) as well as visual confirmation of the organisms responsible for the backscatter observed with the lowered echosounder, which is especially valuable in the absence of catch data. This method also enables the determination of target strengths (the proportion of sound at a given frequency backscattered by a target species), which is the critical parameter for scaling echo intensity to biomass.

(3) Activities

Unfortunately, our instruments shipped to Dutch Harbor did not arrive in time for the departure of the MR23-06C cruise, and the planned survey could not be conducted. Instead, acoustic data from the shipboard ADCP (see 3.1.2.III) and MBES (see 3.1.4.I), as well as zooplankton net samples and environmental DNA data (see 3.4), will be shared by JAMSTEC and Hokkaido University.

(4) References

Backus, R. H., & Barnes, H. (1957). Television-echo sounder observations of midwater sound scatteres. Deep Sea Research (1953), 4, 116–119. https://doi.org/10.1016/0146-6313(56)90041-7

Ermolchev, V. A., & Zaferman, M. L. (2003). Results of experiments on the video-acoustic estimation of fish target strength in situ. ICES Journal of Marine Science, 60(3), 544–547. https://doi.org/10.1016/S1054-3139(03)00049-3

Proud, R., Handegard, N. O., Kloser, R., Cox, M., & Brierley, A. S. (2019). From siphonophores to deep scattering layers: Uncertainty ranges for the estimation of global mesopelagic fish biomass. https://doi.org/10.1093/icesjms/fsy037

Simmonds, E. J., MacLennan, D. N., & MacLennan, D. N. (2005). Fisheries acoustics: Theory and practice (2nd ed). Blackwell Science.

St. John, M. A., Borja, A., Chust, G., Heath, M., Grigorov, I., Mariani, P., Martin, A. P., & Santos, R. S. (2016). A Dark Hole in Our Understanding of Marine Ecosystems and Their Services: Perspectives from the Mesopelagic Community. Frontiers in Marine Science, 3. https://www.frontiersin.org/articles/10.3389/fmars.2016.00031

Thorvaldsen, K. G. (2018). Improved density measurements of mesopelagic fish and the presence of physonect siphonophores in sound scattering layers, measured with multifrequency acoustics and a stereo camera mounted on a lowered probe [Master thesis, The University of Bergen]. https://bora.uib.no/bora-xmlui/handle/1956/18753

3.11 Better understanding of climate-driven changes of biogeochemical dynamics in the western Arctic Ocean

(1) Responsible personnel

Zhangxian Ouyang (University of Delaware) -PI, not on board

Bo Dong (University of Delaware), onboard

Wei-Jun Cai (University of Delaware), not on board

(2) Objectives

Based on the data collected in previous cruises, we identified the substantial expansion of the subsurface acidified water (Qi et al., 2017). From 1994 to 2010, the aragonite undersaturated water became deeper in the Canada Basin and extended into higher latitude. Our analysis confirms that the atmospheric CO_2 intrusion and sea-ice melt are two dominant drivers for acidification in the stratified and freshened surface waters. Meanwhile, we attributed increased Pacific Winter Water (PWW) inflow as the main cause for intensified acidification in the subsurface Canada Basin as it has an original low pH and Ω_{ar} and as it is further modified by receiving extra respiratory CO_2 addition in the Chukchi Sea Shelf. However, it is challenging to separate and quantify the contributions of Pacific corrosive water, terrestrial organic carbon remineralization and local organic matter respiration to ocean acidification. Therefore, our proposed to sample δ^{13}C-DIC and other biogeochemical parameters to decipher carbon source in different water masses and better understand how acidified-PWW transporting from the Chukchi/Beaufort shelves to the adjacent Canada Basin accelerates the subsurface ocean acidification associated with anthropogenic carbon storage.

δ^{13}C-DIC analysis provides us with a useful tool for identifying the carbon source adding into dissolved inorganic carbon (DIC) pool. The effects of degradation of organic carbon to DIC, drawdown of DIC by primary production and air-sea CO_2 exchange could be distinguished from one another by analyzing the pairs of DIC and δ^{13}C-DIC. In the water column, loss of DIC generally leaves isotopically heavy C, whereas addition of DIC by degradation of organic carbon matters adds isotopically light C. As a result, the relative changes in DIC leaves unique carbon isotopic fingerprints in water. Combined with mass balance mixing model of DIC and δ^{13}C-DIC, the deviations between observed δ^{13}C-DIC and conservative mixed δ^{13}C-DIC ($\Delta\delta^{13}$C-DIC) associated with the deviation in DIC (ΔDIC) become a useful and powerful tool to quantify the contributions of degradation of terrestrial and local organic carbon at the background of corrosive

PWW.

Here, we propose to collect δ^{13}C-DIC samples in 2023 JAMSTEC cruise, extending our study scope in carbon isotopic perspective to a more comprehensive area covering from the Chukchi shelf to the Canada Basin. This approach will provide us with a better understanding of Arctic carbon dynamics, in particular, the carbon flows, exports, and degradation from highly productive shelves to oligotrophic basins, and thus a better ability to predict future changes in the Arctic carbon system, as well as other geophysical and biogeochemical components. In addition, we propose to collect pH samples in parallel with other carbonate parameters (TA and DIC) to ensure at least two of four carbonate parameters (TA, DIC, pH, pCO_2) are available for each water sample. High-precision pH measurement can be valuable for ocean acidification research. It also can be used for carbonate data validation and internal consistency analysis.

(3) Activities (observation, sampling, development)

The water samples of δ^{13}C-DIC and pH were collected on board R/V Mirai from September 4 to October 4, 2023, in the Chukchi Sea, Beaufort Sea, and the adjacent Canada Basin. In total, 688 samples of δ^{13}C-DIC and 690 samples of pH were collected from 41 stations. About 15% duplicates were collected for quality control purpose.

(4) Methods and Instruments

I. Sampling

δ^{13}C-DIC and pH sampling procedure is as the same as the procedure of DIC sampling, described in the book Guide to Best Practices for Ocean CO_2 Measurements (Dickson et al. 2007). First, rinse the sample bottle twice with 30–40 ml of sample seawater from Niskin bottle to remove any dust and particles. Second, fill the bottle smoothly from the bottom using a drawing tube which extends from the Niskin drain to the bottom of the glass sample bottle. It is critical to remove any bubbles from the draw tube before filling. Overflow the water by at least a half, and preferably by a full, bottle volume. Insert the stopper and transport the samples to the onboard lab.

For pH samples, bottles were secured with rubber bands and clamps, and then placed in a dark cooler until being analyzed.

As all δ^{13}C-DIC samples will be brought back to UD's lab, a poison procedure is needed to avoid biological effect. For each bottle, a headspace of ~1% of the bottle volume is left to allow for water expansion (i.e., 1 ml for a 125 ml bottle). This can be achieved by pulling out the stopper and using a pipette to remove excess water (1 ml). Mercuric chloride is added to poison the sample

using a pipette (to poison a 125 ml sample requires 50 µl of saturated mercuric chloride solution). Next, seal the bottle carefully to ensure that it remains gas tight. Wipe the excess water from the ground glass in the bottle neck and apply some grease (not too much) around the ground glass stopper, insert the stopper completely, and twist the stopper to squeeze the air out of the grease to make a good seal. Finally, use a rubber band and a clamp to positively reinforce closure and invert the bottle several times to disperse the mercuric chloride solution thoroughly. The samples should be stored in a cool, dark, location.

II. Sample Analysis

- **pH**

All pH sample were analyzed within 8 hours after collection to avoid pH changes due to biological processes. Samples were measured by an Agilent 8453 spectrophotometer system (Fig. 3.11-1). After water bathed to 25.0 ºC, samples were injected into the flow cell three times for rinsing. At the last injection, the absorbance was measured and recorded as blank. Then, the sample was fully mixed with meta-cresol purple solution (mCP) and injected into the flow cell. The absorbance was measured and recorded at 25ºC. For all samples, we conducted an extra measurement with a second mCP addition for dye perturbation correction (Clayton and Byrne, 1993).

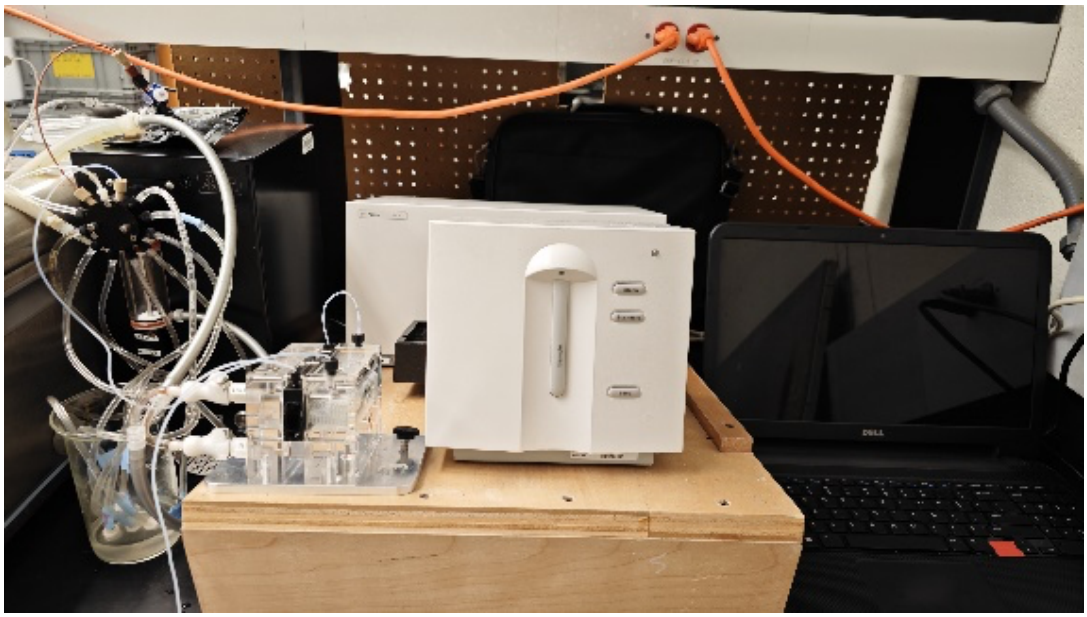

Fig. 3.11-1 Agilent 8453 spectrophotometer system for pH analysis

- **δ^{13}C-DIC**

Analysis of δ^{13}C-DIC samples are conducted using a DIC- δ^{13}C analyzer (Apollo SciTech, USA). Briefly, a CO_2 extraction device and Cavity Ring-Down Spectrometer (CRDS) isotopic detector (G2131-i, Picarro, USA) were coupled to simultaneously measure DIC and δ^{13}C in a 3–4 mL sample over an ~11 min interval, with average precision of 1.5 ± 0.6 μmol kg^{-1} for DIC and 0.05 ± 0.05‰ for δ^{13}C-DIC. We will ensure the accuracy of the analysis by calibrating against 2-3 $NaHCO_3$ internal standard solutions and comparing with selected samples analyzed at the UC Davis Stable Isotope Facility. DIC Certified Reference Materials (CRMs) will also be used for quality control purposes. The instrumentation principles and sample analysis procedure are described in detail in Su et al., (2019) and Deng et al., (2022).

(5) Preliminary Results

- pH precision validation

93 duplicate samples for pH were taken during the cruise. The preliminary results show that the average difference between duplicates ($\overline{\Delta pH}$) was -0.00006, and the standard deviation of differences of all duplicates ($\sigma_{\Delta pH}$) was 0.0009. About 77% samples have a ΔpH within ± 0.001. No clear dependency of ΔpH on pH, depth, measurement wait time, suggesting that if samples were measured promptly (within 8 hours after sampling) and stored with minimal headspace, pH change due to biological activity or air-sample gas exchange during sample analysis was negligible.

- pH accuracy validation

3 bottles of TRIS buffer were measured during Mirai cruise as accuracy checks. 1 bottle was measured on September 6th before the first CTD station for instrument calibration and 2 bottles were during the sample analysis on September 18th. The measurements yielded an average pH value of 8.0893 (8.0935 expected at 25 ºC) with a standard deviation of 0.0026. The difference of -0.0042 shows that the accuracy of pH measured by spectrophotometer meets the GOA-ON weather quality data threshold of 0.02 pH units.

- pH distribution

All pH were reported at 25ºC in the total scale. Our preliminary results showed that, along the central channel Chukchi Sea, pH values were relatively higher in the surface mixed layer compared to the bottom water (Fig. 3.11-2a). The highest pH values appeared in the northern Chukchi Sea (70-72ºN), while the lowest pH values found in the subsurface PWW layer (100-250 m) in the Chukchi Plateau area. Along the shelf break/slope section (Fig. 3.11-2b), one of the most

prominent features of pH distribution is the subsurface-low pH. We noticed that this low-pH layer became even shallower in the northwestern Chukchi shelf slope (170ºW -180ºW) compared to the Baufort Sea slope (140ºW -160ºW)

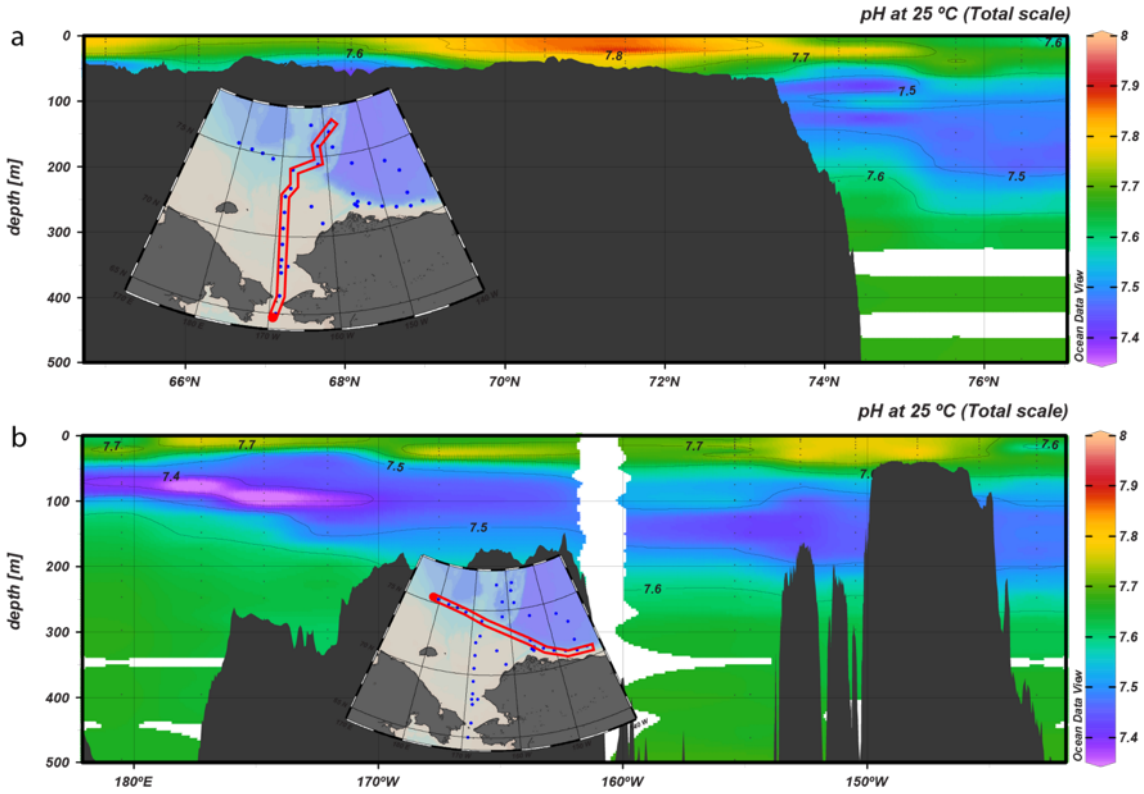

Fig. 3.11-2 pH distributions in the water columns along (a) the central channel on the Chukchi Shelf and Chukchi plateau and (b) shelf slopes from the Chukchi Sea to the Beaufort Sea.

(6) References

Clayton, T.D. and Byrne, R.H., 1993. Spectrophotometric Seawater Ph Measurements - Total Hydrogen-Ion Concentration Scale Calibration of M-Cresol Purple and at-Sea Results. Deep-Sea Research Part I-Oceanographic Research Papers, 40(10): 2115-2129.

Deng, X., Li, Q., Su, J., Liu, C. Y., Atekwana, E., & Cai, W. J. (2022). Performance evaluations and applications of a δ13C-DIC analyzer in seawater and estuarine waters. *Science of The Total Environment*, 833, 155013.

Dickson, A. G., Sabine, C. L., & Christian, J. R. (2007). *Guide to best practices for ocean CO2 measurements*. North Pacific Marine Science Organization.

Qi, D., Chen, L., Chen, B., Gao, Z., Zhong, W., Feely, R. A., ... & Zhan, L. (2017). Increase in acidifying water in the western Arctic Ocean. *Nature Climate Change*, *7*(3), 195-199.

Su, J., Cai, W. J., Hussain, N., Brodeur, J., Chen, B., & Huang, K. (2019). Simultaneous determination of dissolved inorganic carbon (DIC) concentration and stable isotope (δ13C-DIC) by Cavity Ring-Down Spectroscopy: Application to study carbonate dynamics in the Chesapeake Bay. *Marine Chemistry*, *215*, 103689.

(7) Data archive

The data obtained in this cruise will be submitted to the Data Management Group of JAMSTEC, and will be opened to the public via "Data Research System for Whole Cruise Information in JAMSTEC (DARWIN)" in JAMSTEC web site. http://www.godac.jamstec.go.jp/darwin/e.

3.12 Temporal variations of the carbonate chemical components in the Arctic Ocean within summertime

(1) Responsible personnel

Manami Tozawa (Hokkaido University, not on board) -PI
Daiki Nomura (Hokkaido University, not on board)
Akihiko Murata(JAMSTEC, not on board)
Mariko Hatta (JAMSTEC, on board)
Amane Fujiwara (JAMSTEC, on board)

(2) Purpose, background

The Arctic Ocean is an important area for the atmospheric CO_2 absorption, accounting for approximately 10% of the total amount of the oceanic CO_2 absorption even though the Arctic Ocean covers only about 3% of the total ocean area (Bates and Mathis, 2009). Although potential effects of sea ice formation and melting on $CO_2$and biogeochemical cycles in the ocean have previously been discussed (e.g., Vancoppenolle et al., 2013), effects of sea ice freeze and melt processes on CO_2 in surface water and the CO_2 exchange with the atmosphere are still unknown. To clear up temporal variations of the carbon cycle in the Arctic Ocean within summertime, we examine carbonate chemical and corresponding biogeochemical components during the cruise.

(3) Methods and parameter

Samples and data for our research will be shared from the research proposal No.1 (PI: Amane Fujiwara). In particular, we will analyze pCO2, DIC, TA, oxygen isotope, and CDOM data (see 3.1.3 for details).

(4) References

Bates, N., & Mathis, J. (2009). The Arctic Ocean marine carbon cycle: evaluation of air-sea CO2 exchanges, ocean acidification impacts and potential feedbacks. Biogeosciences, 6(11), 2433–2459.

Vancoppenolle, M., Bopp, L., Madec, G., Dunne, J., Ilyina, T., Halloran, P. R., & Steiner, N. (2013). Future Arctic Ocean primary productivity from CMIP5 simulations: Uncertain outcome, but consistent mechanisms. Global Biogeochemical Cycles, 27(3), 605–619. https://doi.org/10.1002/gbc.20055

3.13 Isotope analysis of water vapor

(1) Personnel

Hotaek Park (JAMSTEC, not on board) -PI

(2) Background and objective

The recent retreating Arctic sea-ice can cause larger evaporation from the open sea surface. The evaporated water vapor is likely linked to the terrestrial water cycle as a precipitable water implicating to the atmospheric circulation. In reality, observations identified the increase of autumnal precipitation and the resultant increase of snow depth in the northeastern Siberia. The increased snow enhances the insulation effect on permafrost warming during the winter season, as well as is correlated to the increase in spring peak discharge associated to the snow meltwater. The Siberian major rivers indicated the increasing trends in the spring discharge for the recent decades. Furthermore, the snow-induced permafrost warming can increase the melting of ground ice within the permafrost, combining with the warming air temperature, and thus increasing the connectivity of the melted water to the river discharge. Likewise, these linkages suggest the potential impacts of the declining Arctic sea-ice on the terrestrial hydrologic processes.

Up to now, however, observations and models have provided little quantitative assessment on the declined sea-ice impact on the terrestrial water cycle. The linkage of the evaporated water vapor from the opened Arctic Ocean surface to the terrestrial hydrology is considerably complex over mixing with different source waters in the atmosphere. Isotope is a useful tool to examine the linkage of the Arctic Ocean sourced water to the terrestrial hydrology, tracking the origins of the terrestrial precipitation. Focused on the advantage of stable water isotope, a precipitation isotope observational network was constructed, and conducted the water sampling at the Arctic Ocean and land. The isotope measurement of the atmospheric water vapor on the MIRAI Arctic cruise was included at the observational network activity and has continued since 2019, as a research topic in the ArCS and ArCS II projects.

The observed data likely provide important information for the spatial and temporal variability of the isotopic ratios along the cruise route over the opened Arctic Ocean surface and during the precipitation events. However, the observed records have constraints in identifying the implication of the declined sea ice to the intensified terrestrial water cycle at the global scale. Numerical models are a useful tool to realize the impact of the declining sea ice on the terrestrial hydrology at long-term and global scales. However, the modeling requires the validation of the simulated results against observations. The combination of numerical model simulation and isotope observation makes it possible to explore the relationship of the declining sea ice and the

terrestrial water cycle. This document reports the isotopic properties measured at the R/V MIRAI 2023 Arctic cruise.

(3) Parameters

Isotope ratios of Oxygen and Hydrogen and water vapor concentration

(4) Instrument and method

The isotope of atmosphere water vapor was monitored by a L2130-*i* Isotope and Gas Concentration Analyzer (Picarro, Fig. 3.13-1), which simultaneously provides $\delta^{18}O$ and $\delta^{2}H$ for isotopic H_2O with high-precision measurements, including water vapor concentration for the range of 1000 to 50000 ppm with 1–2 Hz measuring frequency. The observed data are archived on the storage of the spectrometer, operated by windows operational system. Two standard liquids, for example with isotopic values of -0.41/-1.59‰ and -31.20/-245.26‰ for $\delta^{18}O/\delta^{2}H$, are individually injected for 15 minutes every 12-hour, in which the derived linear regression equation is used to calibrate the monitored values by the spectrometer.

Figure 3.13-1. Isotope spectrometer system

(5) Preliminary results

The measured isotopic ratios averaged to hourly time steps exhibit their time-series variability in the Arctic Ocean during the whole cruse period from August 25 to October 3, 2023, including air and sea surface temperature (Fig. 3.13-2), although there were intermittent measurement gaps during the cruise period. The isotopic ratios of $\delta^{18}O/\delta^{2}H$ showed higher values at the initial dates of the cruse as the vessel cruised relatively warm regions. Then, the ratios headed to gradually decreasing direction and recorded the minimum values (i.e., -25.2‰ for $\delta^{18}O$ and -175.8 for $\delta^{2}H$) on Sep. 26, responding to the cold air temperature. During the period from Sep. 16 to Sep. 27 as the vessel stayed over the northern Arctic Ocean, the air temperature recorded 0°C below, and the sea surface temperature also positively decreased consistent with the air temperature, representing the spatial variability of the sea surface heat condition along the vessel cruising routes across north to south and east to west.

The isotopic ratios of $\delta^{18}O/\delta^{2}H$ significantly correlated with air temperature, as identified for the previous years (i.e., 2019–2022). The d-excess (= $-8\times\delta^{18}O + \delta^{2}H$) that is an index representing humidity and temperature conditions of the evaporated sea surface exhibited the largest diurnal variability at the range of approximately 40 ‰, relative to the lower variability of $\delta^{18}O$ and $\delta^{2}H$ (Fig. 3.13-2). The d-excess was correlated to the difference between sea surface and air temperature with larger scattering, as shown in the past cruise data. The water vapor recorded lower isotopic ratios at relatively cold temperature, which resulted in higher d-excess values (Fig. 3.13-2). The larger difference between air and sea surface temperature represents higher atmospheric demand for evaporation, consequently higher evaporation, in which the d-excess practically indicated higher values. This suggests that the measurements had captured the isotopic ratios of water vapor evaporated from the warmer ocean surface.

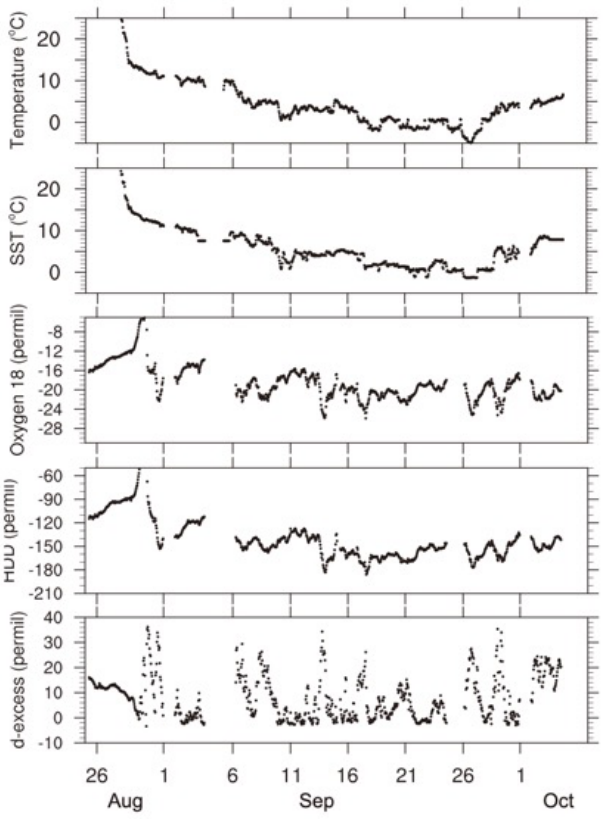

Figure 3.13-2. Time-series variability of air and sea surface temperatures and water isotope variables during MR23-06C cruise period.

The $\delta^{18}O$ and $\delta^{2}H$ ratios indicated significantly high correlation (Fig. 3.13-3). Their relationship yielded the slope of 7.34, compared to the values from 2019 to 2021, while was lower than 2022. The entire slopes, including the past cruises distributed within the ranges of 4.8 and 7.6, which was compared with the values (i.e., 5.75 in Tiksi and 6.0 in Mackenzie delta) obtained at the northernmost terrestrial sites. However,

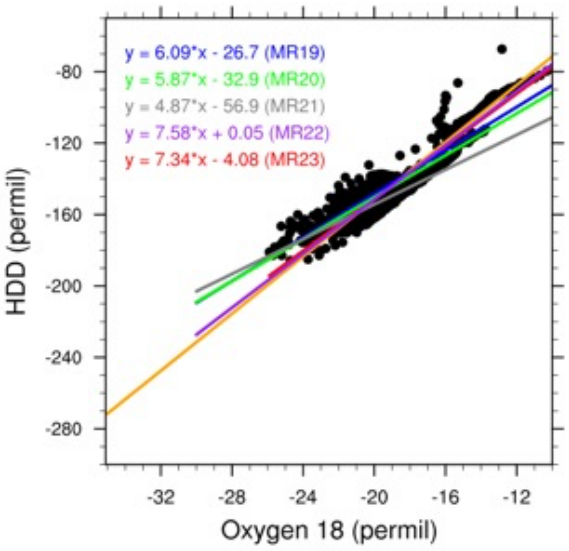

Figure 3.13-3. Relationship between observed hourly oxygen and hydrogen isotope in the whole cruises from 2019 to 2023, including individual linear regression equation.

the slopes derived by the five-year cruise is lower than the value 8 of global meteoric water line (GMWL), which represent the sensitivity of isotope to regional and temporal air temperatures.

(6) Data archive

The data obtained in this cruise will be submitted to the Data Management Group of JAMSTEC, and will be opened to the public via “Data Research System for Whole Cruise Information in JAMSTEC (DARWIN)” in JAMSTEC web site. http://www.godac.jamstec.go.jp/darwin/e.

3.14 Greenhouse gases observation

(1) Personnel

Yasunori Tohjima (NIES, not on board) -PI
Shigeyuki Ishidoya (AIST, not on board)
Amane Fujiwara (JAMSTEC, on board)
Shinji Morimoto (Tohoku Univ. , not on board)
Daisuke Goto (NIPR, not on board)
Prabir Patra (JAMSTEC, not on board)

(2) Background and objective

(2-1) Continuous observations of CO_2, CH_4 and CO mixing ratios

The Arctic region is warming about twice as fast as the global average. Additionally, several studies suggested that the global warming would potentially enhance emissions of the greenhouse gases including CO_2 and CH_4 from the carbon pools in the Arctic permafrost into the atmosphere. The recent accelerated increase rate of the atmospheric CH_4 might be attributed to the enhanced emissions from the Arctic region. Therefor there are growing concerns about feedback mechanism between global warming and the greenhouse gas emissions from the Arctic region. The objective of this study is to detect the increases in the atmospheric greenhouse gas levels associated with the ongoing global warming in the Arctic region in the early stage. The continuous observations of the atmospheric CO_2 and CH_4 mixing ratios during this cruise would allow us to detect the enhanced mixing ratios associated with the regional emissions and to estimate the distribution of the regional emission sources. The atmospheric CO mixing ratios, which were also observed at the same time, can be used as an indicator of the anthropogenic emissions associated with the combustion processes.

Photo 3.14-1. Continuous measurement system of the atmospheric CO_2, CH_4, and CO based on a cavity ring-down spectrometer (CRDS) used during MR23-06C cruise.

(2-2) Discrete flask sampling

In order to clarify spatial variations and air-sea exchanges of the greenhouse gases at northern high latitude, whole air samples were collected into 32 stainless-steel flasks on-board R/V MIRAI (MR23-06C). The collected air samples will be analyzed for the mixing ratios of CO_2, O_2, Ar, CH_4, CO, N_2O and SF_6 and the stable isotope ratios of CO_2 and CH_4.

(3) Parameters

(3-1) Continuous observations of CO_2, CH_4 and CO mixing ratios

Mixing ratios of atmospheric CO_2, CH_4, and CO.

(3-2) Discrete flask sampling

Mixing ratios of atmospheric CO_2, O_2 (O_2/N_2 ratio), Ar (Ar/N_2 ratio), CH_4, CO, N_2O and SF_6, $\delta^{13}C$ and $\delta^{18}O$ of CO_2, $\delta^{13}C$ and δD of CH_4.

(4) Instrument and method

(4-1) Continuous observations of CO_2, CH_4 and CO mixing ratios

Atmospheric CO_2, CH_4, and CO mixing ratios were measured by a wavelength-scanned cavity ring-down spectrometer (WS-CRDS, Picarro, G2401, see Photo 3.14-1). An air intake, capped with an inverted stainless-steel beaker covered with stainless steel mesh, was placed on the right-side of the upper deck. A diaphragm pump (GAST, MOA-P108) was used to draw in the outside air at a flow rate of ~8 L min^{-1}. Water vapor in the sample air was removed to a dew pint of about 2°C and about -35°C by passing it through a thermoelectric dehumidifier (KELK, DH-109) and a Nafion drier (PERMA PURE, PD-50T-24), respectively. Then, the dried sample air was introduced into the WS-CRDS at a flow rate of 100 ml min^{-1}. The WS-CRDS was automatically calibrated every 49 hours by introducing 3 standard airs with known CO_2, CH_4 and CO mixing ratios. The analytical precisions for CO_2, CH_4 and CO mixing ratios are about 0.02 ppm, 0.3 ppb and 3 ppb, respectively.

(4-2) Discrete flask sampling

The air sampling equipment consisted of an air intake, a diaphragm pump (GAST MOA), a Stirling cooler (Twinbird) with a water trap, solenoid valves (CKD), a flow meter and a back pressure valve. Ambient air was pumped using the diaphragm pump from an air intake, dried cryogenically and filled into a 1 L stainless-steel flask at a pressure of 0.27 MPa.

(5) Preliminary results

The continuous observations of CO_2, CH_4 and CO mixing ratios were conducted during the entire cruise. The time series of the atmospheric CH_4, CO_2, and CO mixing ratios observed during the entire cruise are shown in Fig. 3.14-2. Sampling logs of the discrete flask sampling are listed in Table 3.14-1.

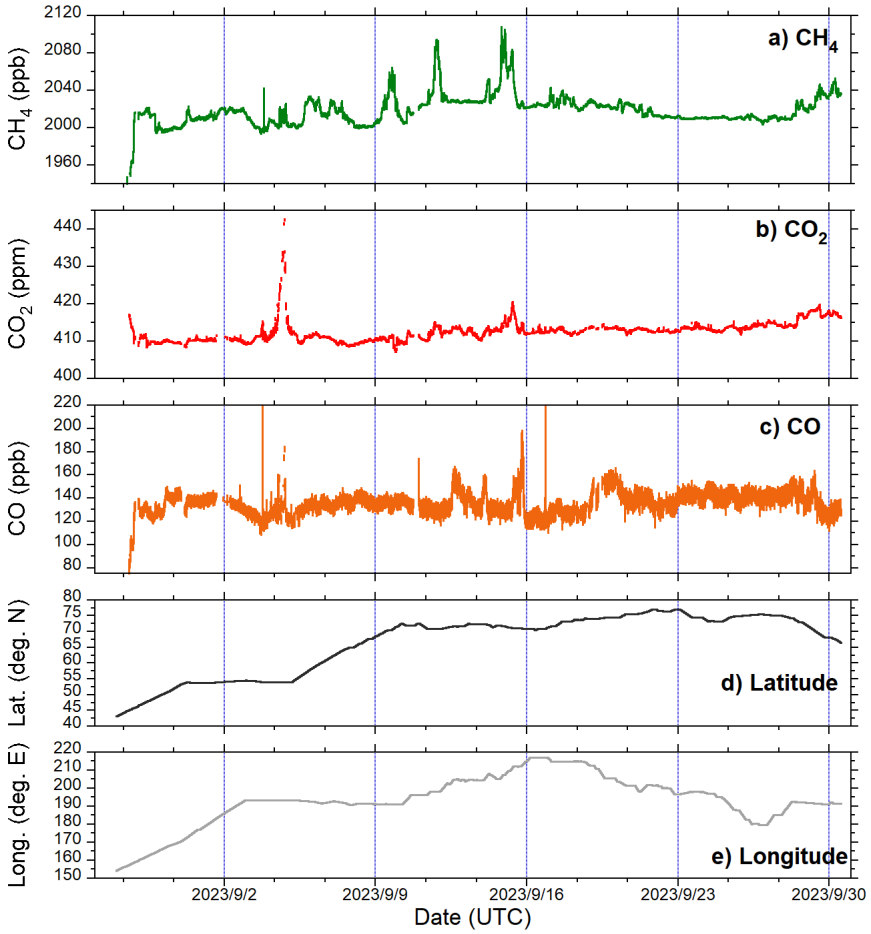

Figure 3.14-2: The time series of the atmospheric (a) CH_4, (b) CO_2, and (c) CO mixing ratios observed during the entire period of MR23-06C cruise. The observation position, (d) latitude and (e) longitude are also plotted in the bottom.

Table 3.14-1 Logs of the discrete flask sampling

Date [UTC]	Time [UTC]	Latitude	Longitude
2023/08/26	23:37	39-39.24753N	148-10.62802E
2023/08/28	9:49	44-31.40637N	156-36.85226E
2023/08/29	0:02	46-28.01068N	159-53.52115E
2023/08/29	23:26	49-37.63721N	165-28.85654E
2023/08/31	0:32	53-23.19166N	170-41.65886E
2023/08/31	22:57	53-45.94241N	177-49.91078E
2023/09/01	22:49	54-01.85162N	174-10.59382W

2023/09/02	22:44	54-28.99999N	166-47.64037W
2023/09/05	21:49	57-42.11055N	167-14.65965W
2023/09/06	21:17	61-43.19581N	167-32.99463W
2023/09/08	1:07	65-17.67974N	168-46.98543W
2023/09/08	21:32	68-02.22797N	168-42.71690W
2023/09/09	21:00	71-10.89107N	168-45.11856W
2023/09/10	23:02	72-34.82730N	163-39.11731W
2023/09/12	0:59	70-54.90316N	161-06.12463W
2023/09/12	22:02	71-48.93109N	155-35.50459W
2023/09/13	22:17	72-28.05550N	155-23.74003W
2023/09/14	23:41	71-39.12731N	152-31.47384W
2023/09/15	23:29	70-48.73992N	145-17.23229W
2023/09/17	1:53	71-34.31429N	144-28.02946W
2023/09/18	2:22	73-15.43358N	145-09.14629W
2023/09/18	23:58	74-00.97089N	147-28.08445W
2023/09/20	3:55	74-24.67122N	155-50.53218W
2023/09/20	23:36	75-29.98530N	158-22.59223W
2023/09/23	1:54	76-57.03615N	163-15.34648W
2023/09/24	2:20	74-31.65636N	162-04.46340W
2023/09/25	5:30	73-51.33071N	167-18.81394W
2023/09/26	6:10	75-08.12225N	177-16.18002W
2023/09/27	2:07	75-19.52961N	179-29.50283E
2023/09/28	4:18	74-20.04839N	168-44.78456W
2023/09/29	0:12	71-47.93366N	168-04.17223W
2023/10/03	1:43	57-33.60451N	167-10.68679W

(6) Data archive

The data obtained in this cruise will be submitted to the Data Management Group of JAMSTEC, and will be opened to the public via “Data Research System for Whole Cruise Information in JAMSTEC (DARWIN)” in JAMSTEC web site. http://www.godac.jamstec.go.jp/darwin/e.

4. Cruise Log

Table 4-1 Cruise Log of MR23-06C

Date [UTC]	Time [UTC]	Station ID	Activities								Remarks
			CTD cast	XCTD	clean optical	zooplankton	sediment	Neuston net	In-situ Pump	Flying Drone	sonde launch	
25-Aug	2:00											Departed the port of Shimizu
26-Aug												Started the monitoring of sea surface water properties
31-Aug				x								Test cast of CTD rosette system and mooring releasers
3-Sep	17:50											Called the port of Dutch Harbour
4-Sep												
5-Sep	2:00											Departed the port of Dutch Harbour
6-Sep												
7-Sep	21:00	sta. 01	x		x	x		x				
8-Sep	0:00	RS001									x	
	6:20	sta. 02	x			x						
	12:00	RS002									x	
	15:20	sta. 03	x		x	x	x	x		x		
9-Sep	0:00	RS003									x	
	0:20	sta. 04	x			x				x		
	6:43	sta. 05	x			x	x					
	12:00	RS004									x	
	15:00	sta. 06	x		x	x	x	x		x		
	22:55	sta. 07	x			x				x		
10-Sep	0:00	RS005									x	
	4:50	sta. 08	x			x						
	12:00	RS006									x	
	15:00	CPS001									x	
	15:30	sta. 09	x		x	x	x	x		x		
11-Sep	0:00	RS007									x	
	0:14	XCTD01		x								Ice Edge site, deployed drifting buoys
	12:00	RS008									x	
	16:00	sta. 10	x		x	x	x	x		x		COMAI Trial
12-Sep	0:00	RS009									x	
	7:35	XCTD02		x								
	7:54	XCTD03		x								
	8:11	XCTD04		x								
	8:29	XCTD05		x								
	8:41	XCTD06		x								
	9:04	XCTD07		x								
	9:21	XCTD08		x								
	9:38	XCTD09		x								
	9:54	XCTD1		x								

		0									
	12:00	CPS002								x	
	15:00	sta. 11	x		x		x	x	x		
	18:51	XCTD1 1		x							
	19:17	XCTD1 2		x							
	19:48	XCTD1 3		x							
	20:17	XCTD1 4		x							
	20:41	sta. 12	x						x		
	22:03	XCTD1 5		x							
	22:27	XCTD1 6		x							
	23:50	sta. 13	x			x			x		
13-Sep	0:00	RS010								x	
	3:38	XCTD1 7		x							
	4:44	XCTD1 8		x							
	5:34	XCTD1 9		x							
	6:28	XCTD2 0		x							
	7:25	XCTD2 1		x							
	12:00	CPS003								x	
	15:00	sta. 14	x		x	x		x	x		Recovered NBC Mooring
14-Sep	0:00	RS011								x	
	5:46	XCTD2 2		x							
	6:45	XCTD2 3		x							
	7:35	XCTD2 4		x							
	9:17	XCTD2 5		x							
	10:08	XCTD2 6		x							
	12:00	RS012								x	
	15:00	sta. 15	x		x	x		x	x		
	19:49	XCTD2 7		x							
	21:40	sta. 16	x			x			x		
15-Sep	0:00	RS013								x	
	1:17	XCTD2 8		x							
	3:35	sta. 17	x			x			x		
	7:05	XCTD2 9		x							
	12:00	RS014								x	
	15:00	sta. 18	x		x	x		x	x		
	19:53	XCTD3 0		x							
	22:08	sta. 19	x			x			x		
16-Sep	0:00	RS015								x	
	1:26	XCTD3 1		x							
	3:30	sta. 20a	x			x					
	8:17	XCTD3 2		x							
	8:52	XCTD3 3		x							

	9:32	XCTD34		x								
	12:00	RS016									x	
	17:00	sta. 20b							x			deployed drifting buoys
	21:50	XCTD35		x								
	23:45	XCTD36		x								
17-Sep	0:00	RS017									x	
	3:16	sta. 21	x			x			x			
	9:43	XCTD37		x								
	12:00	CPS004									x	
	12:34	XCTD38		x								
	16:00	sta. 22	x						x			COMAI Trial
18-Sep	0:00	RS018									x	
	4:48	XCTD39		x								
	12:00	RS019									x	
	20:03	XCTD40										
	21:27	XCTD41										
	22:15	sta. 23	x	x	x		x		x			
19-Sep	0:00	RS020									x	
	5:04	sta. 24	x									
	9:50	XCTD42		x								
	12:00	CPS005									x	
	12:16	XCTD43		x								
	17:00	sta. 25	x			x	x		x	x		
	18:00	RS021									x	
20-Sep	0:00	RS022									x	
	4:40	sta. 26	x									
	6:00	RS023									x	
	12:00	RS024									x	
	17:00	sta. 27	x				x		x	x		
21-Sep	0:00	RS025									x	
	4:30	sta. 28	x				x					
	6:00	CPS006									x	
	12:00	RS026									x	
	19:43	sta. 29	x				x		x		x	Ice Edge Observation
22-Sep	0:00	RS027									x	
	2:42	sta. 30	x				x					
	12:00	CPS006									x	
	20:40	sta. 31	x			x	x		x		x	Ice Edge Observation
23-Sep	0:00	RS028									x	
	12:00	RS029									x	
	17:00	sta. 32	x		x		x		x		x	Deployed NAP Mooring
	14:41	XCTD44										
24-Sep	0:00	RS030									x	
	3:40	XCTD45		x								
	5:41	XCTD46		x								
	7:37	XCTD47		x								
	12:00	RS031									x	
	19:00	sta. 33		x								COMAI Trial
	19:00	XCTD48										
25-Sep	0:00	RS032									x	

	8:46	XCTD49		x								
	11:19	XCTD50		x								
	12:00	RS033									x	
	15:00	sta. 34	x		x		x			x		
26-Sep	0:00	RS034									x	
	3:10	sta. 35	x		x		x			x		
	8:17	XCTD51		x								
	12:00	RS035									x	
	19:10	sta. 36	x			x		x		x		Ice Edge/COMAI trial
27-Sep	0:00	RS036									x	
	6:00	RS037									x	
	9:05	XCTD52		x								
	12:00	RS038									x	
	15:00	sta. 37	x		x		x		x			
	21:08	XCTD53		x								
28-Sep	0:00	RS039									x	
	6:21	sta. 38	x			x						
	10:34	XCTD54		x								
	12:00	RS040									x	
	15:00	sta. 39	x			x	x	x		x		
29-Sep	0:00	RS041									x	
	19:31	sta. 40	x		x	x	x		x	x		
30-Sep	1:35	sta. 41	x				x					
	3:20	XCTD55		x								
	4:10	XCTD56		x								
	4:59	XCTD57		x								
	5:39	sta. 42	x			x						
	15:30	sta. 43	x			x		x				
	23:36	sta. 44	x		x	x	x					
3-Oct												Arrived in Dutch Harbour

5. Notice on using

This cruise report is a preliminary documentation as of the end of the cruise. This report is not necessarily corrected even if there is any inaccurate description (i.e., taxonomic classifications). This report is subject to be revised without notice. Some data in this report may be raw or unprocessed. If you are going to use or refer to the data in this report, it is recommended to ask the Chief Scientist for the latest status. Users of information on this report are requested to submit Publication Report to JAMSTEC. http://www.godac.jamstec.go.jp/darwin/explain/1/e#report
E-mail: submit-rv-cruise@jamstec.go.jp